NACA TM 1365

NATIONAL ADVISORY COMMITTEE FOR AERONAUTICS

TECHNICAL MEMORANDUM 1365

PAPERS ON SHIMMY AND ROLLING BEHAVIOR OF LANDING GEARS

PRESENTED AT STUTTGART CONFERENCE OCT. 16 AND 17, 1941

Translation of "Bericht über die Sitzung Flattern und Rollverhalten von Fahrwerken am 16./17. Oktober 1941 in Stuttgart," Lilienthal-Gesellschaft für Luftfahrtforschung, Bericht 140

NACA

Washington

August 1954

1F

NATIONAL ADVISORY COMMITTEE FOR AERONAUTICS

TECHNICAL MEMORANDUM 1365

PAPERS ON SHIMMY AND ROLLING BEHAVIOR OF LANDING GEARS

PRESENTED AT STUTTGART CONFERENCE OCT. 16 AND 17, 1941

Translation of "Bericht über die Sitzung Flattern und Rollverhalten von Fahrwerken am 16./17. Oktober 1941 in Stuttgart," Lilienthal-Gesellschaft für Luftfahrtforschung, Bericht 140

CONTENTS

APPENDIX

EXPERIENCES IN FLIGHT OPERATION*

By E. Hoffmann

In view of the various problems concerning landing gears which are discussed in the following lectures it might be of interest to look into the question of to what extent landing-gear disorders encroach upon flight operation or readiness-for-action of aircraft, and what causes are, numerically, of particular significance.

Before discussing the numerical values compiled in the following table I must, to permit better understanding, briefly outline the type and extent of the numerical material available: In the reports to be made by field elements of the armed forces distinction is made between reports raising objections and reports relating disorders. The first kind includes all sources of technical error determined after a flight, the second every undesirable deviation of a flight and its cause, regardless whether that cause lies in personnel errors, technical errors, or other shortcomings. Both types of reports deal, therefore, in the technical domain, frequently with the same source of error; practically, however, they differ by the amount of damage done to the airplane. For 80 to 90 percent of all reports of disorders this damage amounts to more than 10 percent, for the majority of all reports of objections to less than 10 percent. The figures compiled in the table have been obtained by evaluation of reports of disorders only and must therefore be regarded (with consideration of what has been said above) as minimum values.

Regarding the amount of evaluated reports it must be pointed out that damages caused by enemy action are not reported. For the rest, one can of course in times of war not expect all disorders which occur to be completely covered by reports. Anyway, one may assume that the material not included in the evaluation would not cause any essential shift in the indicated percentages. In accordance with these presuppositions the calculated values make no claim to absolute accuracy. However, they permit with certainty a satisfactory survey of the extent of disorders which are connected in any way with the design of the landing gear.

---

*"Flugbetriebserfahrungen," Bericht 140 der Lilienthal-Gesellschaft, pp. 3-4.

PROPORTION OF VARIOUS CAUSES OF DISORDERS TO THE TOTAL NUMBER OF DISORDERS ACCORDING TO THE STATUS: FIRST HALF-YEAR 1941

Model	Tail-gear design	Locking device	Of 100 disorders there are due to					
			Technical errors		Operational errors			Landing-gear portion
			On the air frame:	On the landing gear:	Landing-gear operation:	Hard landing:	Veering-off:	
b1	Wheel	Without	18	16	2-3	3-4	13-14	35
b2	Wheel	Without	7-9	5-6	3-4	7	26-27	42
C1	Wheel	Without	20-23	15-16	4-5	6-7	4-5	30
C2	Wheel	With	10-12	9-11	3-4	15	7-8	36
C3	Wheel	With	14	13	1-2	6-7	5-6	26
C4	Wheel	Without	8-9	7-8	---	6-7	7-8	22
C5	Wheel	Without	10-15	9-11	3-4	6-7	5-6	25
C6	Wheel	With	16-20	15-18	1-2	5-6	8	32
B1	Shoe	Without	18	17-18	---	6	3-4	27
B2	Wheel	With	15-16	13-14	7	14	0.6	35
b3	Wheel	With	4-5	3-4	---	7	9	20
b4	Wheel	With	5	4-5	---	3-4	10-11	19
b5	Skid	Without	-----	-----	---	6-7	27-28	34
b6	Wheel	Without	13-14	12-13	5	8-9	2	28
b7	Wheel	Without	6-7	3-4	---	---	10	13
b8	Wheel	Without	4-5	3-4	---	4-5	15-16	24
b9	Skid	Without	12-13	10	---	7-8	27	44
b10	Skid	Without	2-3	1	---	3-4	3-4	9
b11	Shoe	Without	3-4	2	---	6-7	2-3	11
A1	Skid	Without	6	5-6	---	5-6	2-3	14
A2	Skid	Without	8-9	7-8	---	10	2-3	20
A3	Wheel	With	5-6	5-6	---	6-7	3-4	16
A4	Skid	Without	4-5	4-5	---	5-6	2-3	13

Since it is in many cases difficult to distinguish, in evaluating the reports, between cause and effect (for instance whether the tire failure which has occurred caused the veering off (ground looping) or vice versa, whether a failure of the landing gear took place due to leveling off at too high an altitude or due to inadequate strut strength) and since these values therefore depend on personal and thus contestable judgment, we combined in the present numerical table all these causes and could thereby determine a "landing-gear portion" which is independent of this personal judgment. Not included were all landing errors in which contact with the ground was made either too soon (ahead of the landing field) or too late (at the end of the landing field), also nose-overs and ground loops. In part these cases, too, are connected with the landing gear (through braking power) but not directly with the problems discussed here; thus, they had not to be taken into consideration.

A comparison of the two first numerical columns of the table shows that about 80 to 90 percent of all airframe disorders are caused by technical errors in the landing gear. A special group is formed by the tire failures which read their maximum in the models C2 and C5 and cause approximately 5 to 6 percent of all disorders (50 to 60 percent of all airframe disorders). According to a more exact investigation, the damages caused by tire failures are for airplanes with fixed landing gear approximately of an order of magnitude up to 15 percent, for the remaining airplanes with retractable landing gear of an order of magnitude up to 25 percent of all airframe disorders. It is true that the numbers in column 2 do not permit a direct comparison of the efficiency of the landing gear of different models since they are not related to the number of flights performed or airplanes employed. This appears with particular clearness in the models B1 and B2 for which there is a ratio of approximately 1:2 in the number of take-offs.

The column "veering off" presents information on the rolling behavior of the different models. First of all, the low percentages for the models b10 to A4 (training planes exclusively) are striking. The assumption that the number of disorders in this group is about as high as for instance in the group b1 to C1 but is brought down to the low percentage by much more frequent operational errors is not correct. On the contrary, the absolute number of damaged airplanes in this group is so low as to be insignificant for flight operation as well as for replacement. The rolling behavior of these airplanes must therefore be regarded as fully satisfactory. Conditions are different for the models b2, b5, and b9. The model b9 is of little interest because it is old and only few specimens are still in existence, the model b5, being a foreign product, is of no interest at all. The extraordinarily high number of failures of model b2, however, gave rise to a more thorough investigation. It was found that only about 30 percent of all cases of veering-off occurred on take-off (in contrast to customary expectations and explanations, the plane veered off unequivocally (85 percent) to the

right). As a rule, the phenomenon of veering off occurred when the tail was raised up after a rolling distance of 80 to 100 m. 70 percent of the cases of veering-off occurred in landing, toward the end of the landing run, thus with the tail wheel on the ground. Almost always the veering off caused landing-gear failures which brought with them damage of, on the average, 20 percent. It was remarkable that in most cases the tires were not ruined. Since there existed in various plants quite recently the tendency to reduce cost by omitting the locking device for the tail gear in new series, it must be pointed out here that the model b2 also was originally equipped with such a mechanism. Only the economizing on this device caused the sudden increase in veering-off cases. Conversely, the subsequent equipment with a tail-gear locking device of the model A3 which at first also exhibited a strong tendency toward veering-off was highly successful as can be seen also from the numerical table. Furthermore the model C2 was subjected to a partial investigation for a period of 3 months. The numbers of veering-off cases in take-off and in landing showed here, too, the ratio 30:70. The predominant direction of veering-off in take-off was to the left. A few of the cases in landing were initiated by premature disengagement of the tail-gear self-aligning device.

Summarizing one may say that at any rate the rolling properties of at least those models for which not less than 25 percent of all failures can be traced back to veering off must be called unsatisfactory. In view of the required repairing capacity, failures of the order of magnitude shown are not permanently tolerable; since the possibility of corrective measures exists, they are unjustifiable as well.

Violent tail wheel shimmy occurred on model C1 when used on runways; temporarily it greatly reduced employment of that airplane. The frequency of these cases does not appear in the numerical table. They are, however, partly responsible for the relatively high values in columns 1 and 2. The cases of shimmy had the particularly unpleasant effect not only of leading to tail gear failures but also of putting so much stress on the entire fuselage end and the tail surfaces that numerous failures occurred on both structural components. Since subsequent installation of a tail-gear locking device was impossible, a braking mechanism was used as a remedy. For reasons of completeness I should like to mention that tail-wheel shimmy led to difficulties in still another model not enumerated in the table.

Although, for understandable reasons, no absolute numbers could be indicated in this report, the importance of the problems discussed in the following lectures can still be recognized unequivocally from the given percentages. The fact that the landing gear at present participates in the entire number of disorders with a share of on the average 25 percent, shows the importance not only of producing a landing gear possessing rolling stability but also of all further work in the field of landing gears. Improvement of landing gears does not give rise to an

efficiency increase; however, a reduction of the tendency toward disorders effects with certainty increased readiness-for-action, lowers the necessary supply of replacements, and saves, therefore, in the last analysis productive capacity in repairing as well as in manufacture.

Translated by Mary L. Mahler
National Advisory Committee
for Aeronautics

LATERAL GUIDING FORCES ON OBLIQUELY RUNNING AIRPLANE TIRES*

By R. Harling

INTRODUCTION

Determination of lateral stresses on airplane landing gears and calculation of phenomena of shimmy of tail wheels or of forces and moments which determine the directional stability of an airplane rolling on the ground require knowledge of the lateral guiding or cornering forces on the rubber-tired airplane wheel.

Due to lateral flexibility of the tire, the rolling direction is not within the wheel plane during action of lateral forces, a yaw angle of the wheel is created and, consequently, a lateral guiding force on the ground counteracting the lateral force. As already known from measurements of Fromm (ref. 1) on automobile tires, the rubber-tired wheel can produce lateral guiding forces only when it runs at an angle of yaw. With increasing yaw angle, this lateral guiding force first increases, but later approaches the value corresponding to the sliding friction. This variation is affected essentially by the wheel load, lateral rigidity, inflation pressure of the tire, and by the friction coefficient.

For various airplane tires, in particular tail-wheel tires up to the size 630 by 220, the correlation between lateral deformation and lateral force was determined statically, that between yaw angle and lateral guiding force on a rotating steel drum.

MEASUREMENT OF LATERAL DEFORMATION

In the test for determination of the tire deformation, the wheel was held fixed and the ground was, as it were, pulled away from under it. Figure 1 shows the clamped wheel on a small carriage running on ball bearings. Loading of the wheel is accomplished by means of weights acting on a lever arm. By pulling on the carriage with a predetermined force, the tire is deformed. The deformation may be read on a Vernier scale to within an accuracy of 1/10 mm. In order to eliminate effects due to deflection of the clamping device used for the wheel, the path of the wheel axle was determined separately with a dial indicator and subtracted from the deformation path measured. This procedure probably guarantees a reliable determination of the tire deformation.

---

*"Seitenführungskräfte bei Schräglauf von Flugzeugreifen," Bericht 140 der Lilienthal-Gesellschaft, pp. 4-7.

If a force acts on a rubber-tired wheel at rest normal to the wheel plane, the tire is laterally deformed. By plotting the lateral force against the tire deformation, one obtains the characteristic curves of the lateral deformation. Figure 2 shows the characteristic curves for the tire 465 × 165 at various wheel loadings. One can see how the lateral deformation of the tire increases with increasing wheel load.

This phenomenon is in contrast to measurements performed earlier (ref. 2) where lateral deformation of the tire decreased with increasing wheel load. In this test setup, the wheel was pulled tangent to a circular arc with the swivel axle as center. Thereby, there originated probably a moment which influenced the lateral pull and led to the results mentioned.

Lateral deformation is, furthermore, a function of the tire inflation (fig. 3). By increase of the tire inflation pressure, the tire takes on greater lateral rigidity, whereby the lateral deformation decreases. Summarizing, one may say that tire deformation is a function of size and physical properties, load, and tire inflation pressure.

MEASUREMENT OF CORNERING FORCES

For determination of the cornering force, the wheel which is supported in a fork so that it can rotate freely, runs on a steel drum of 1.7 m diameter (fig. 4). Slots provided in the fork make adjustment of different amounts of trail possible as are required, for instance, for investigation of tail-wheel shimmy. The load of the wheel may be varied by interchange of weights. The lateral pull, thus the lateral guiding force of the wheel, is determined directly at the wheel axle with a force-measuring dynamometer.

The test procedure is as follows: the wheel, set at a yaw angle by a steel wire with connected force-measuring dynamometer, is placed on the drum which is already turning. The yaw angle is read on the scale, the lateral guiding force on the dynamometer.

The variation of the lateral guiding force is plotted against the yaw angle for several wheel loads in figure 5. The values for tire size 465 × 165 were taken as an example. With increasing yaw angle, an ever increasing part of the runway and contact surface starts sliding. Consequently, the curve slopes more and more toward the horizontal, which is attained for complete sliding. This representation shows that the lateral guiding force is also very strongly dependent on the friction coefficient; the higher the friction coefficient, the more lateral guiding force can be resisted by the tire.

The tire inflation pressure also affects the lateral guiding force (fig. 6). For angles of yaw up to about 5° or 6°, the curves show a

steeper slope with increasing internal pressure. Transition to the horizontal is solely dependent on the magnitude of the friction coefficient, as mentioned above.

COMPARATIVE TESTS

Comparative tests performed earlier, with a tail wheel 260 × 85 on the steel drum and on the road, showed partly quite good agreement. For the tests, the tail wheel was installed between the rear wheels of an automobile with front-wheel drive (fig. 7). The tail wheel with shock-absorber leg was attached to a lever traversable in the longitudinal plane of the automobile. Loading was accomplished by means of a compression spring. By means of a lever clamped to the shock-absorber leg, the tractive force was transferred to the dynamometer and could be read there. The yaw angle was determined by means of an indicator on a scale. With this tail wheel, tests were performed on roads of various conditions and on wet turf.

Good agreement was found to exist between the results of the tests on the steel drum and on a tar road (fig. 8). The lateral guiding forces there are almost equal. On crushed stone, in contrast, the lateral guiding force is somewhat smaller, which is due to a rolling effect. The tire does not slide on the loose gravel, but rolls on it like on the race of a ball bearing, and can thus not resist as large a lateral guiding force. The friction coefficient of the tire on wet turf is probably so small that the curve, as can be seen here, lies even below the curve of the lateral guiding force on crushed stone.

CALCULATION OF THE LATERAL GUIDING FORCE

A calculation of the lateral guiding force is possible with an equation (ref. 3)

$$S = \mu P \tanh (c_p \psi)$$

known from investigations of automobile tires. This equation contains as determining factors, in addition to the yaw angle ψ, the friction coefficient μ, the wheel load P, and an empirical value c_p. The value c_p was fixed so that good agreement was created between test curve and calculated curve.

In order to obtain an unequivocal confirmation for the correctness of the results found on the steel drum and further data for the calculation of airplane landing gears and of the rolling stability of airplanes, tests with still larger airplane wheels were conducted on a specially built trailer on the Reich automobile express highway.[1]

Translated by Mary L. Mahler
National Advisory Committee
for Aeronautics

REFERENCES

1. Becker, G., Fromm, H., and Maruhn, H.: Schwingungen in Automobillenkungen. Berlin 1931.

2. Dietz, O., and Harling, R.: Seitensteifigkeit und Seitenführung von Flugzeugreifen. Deutsche Luftfahrtforschung, FB 1498, Oct. 29, 1941. (Available in translation as AAF translation ATI No. 18905.)

3. Huber, L.: Die Fahrtrichtungsstabilität des schnellfahrenden Kraftwagens. Dtsch. Kraftf.-Forsch., Heft 44, Berlin 1940.

---

[1]The test results are published in a report of the Zentrale für Wissenschaftliches Berichtswesen über Luftfahrtforschung des Generalluftzeugmeisters.

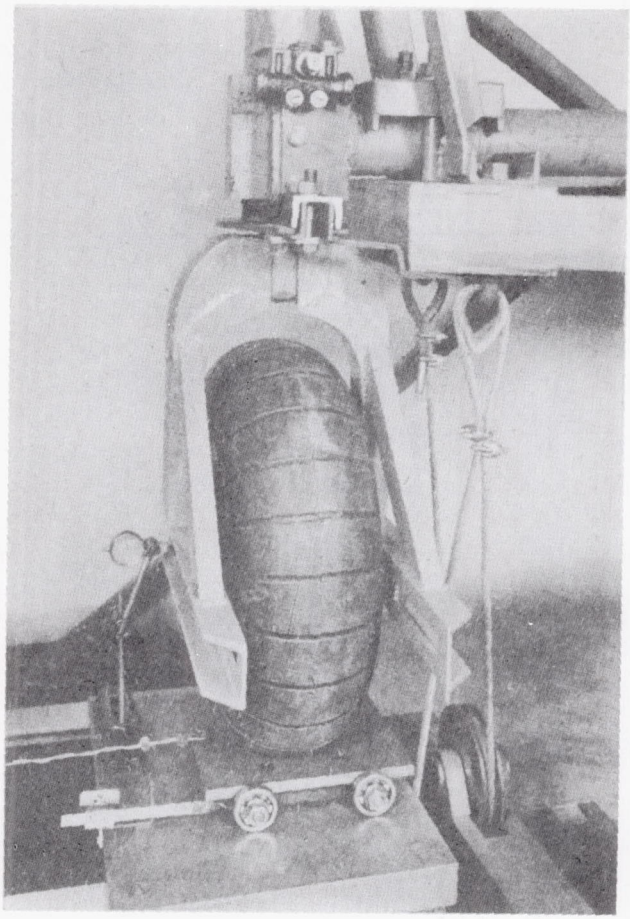

Figure 1.- Measurement of the lateral deformation of airplane tires.

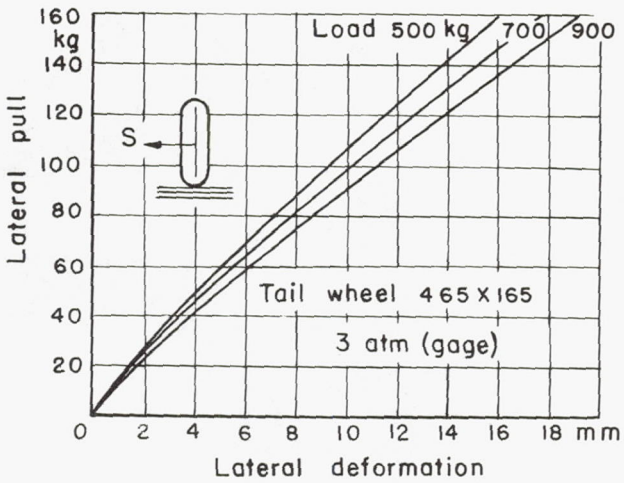

Figure 2.- Lateral deformation of a tire for various wheel loads.

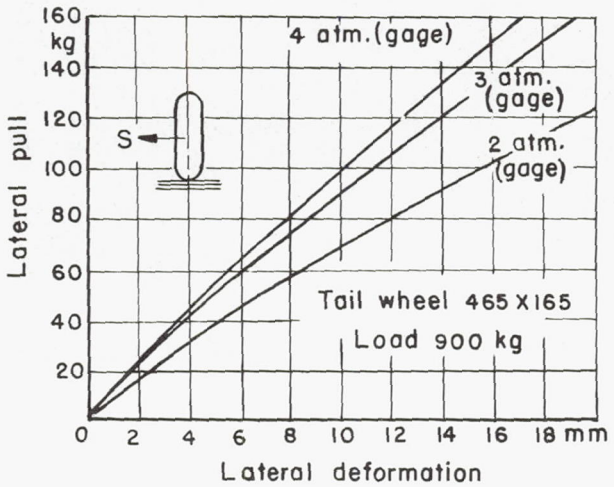

Figure 3.- Lateral deformation of a tire for various tire-inflation pressures.

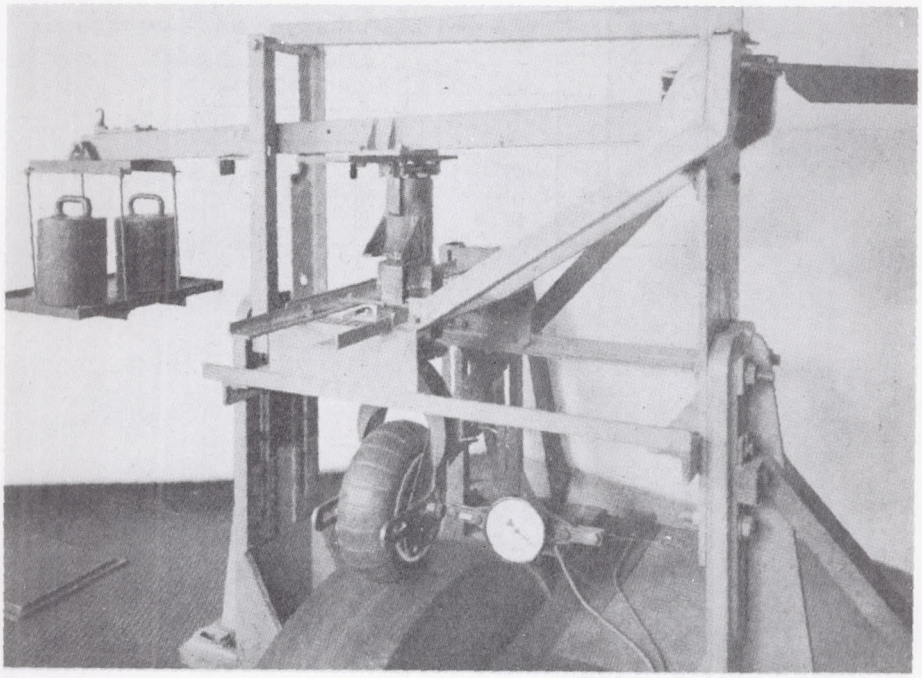

Figure 4.- Measurement of the cornering force of airplane tires.

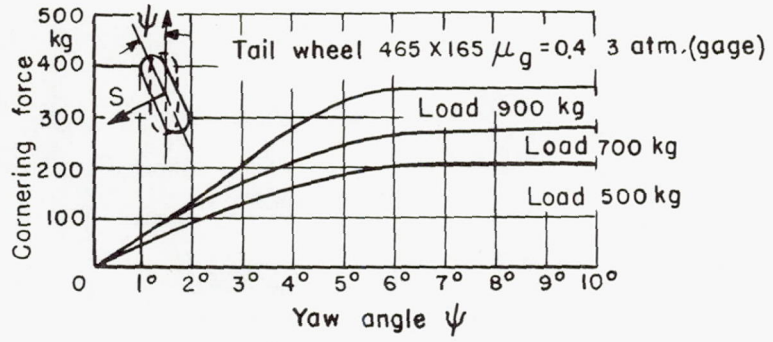

Figure 5.- Cornering force for wheel loads of various magnitudes.

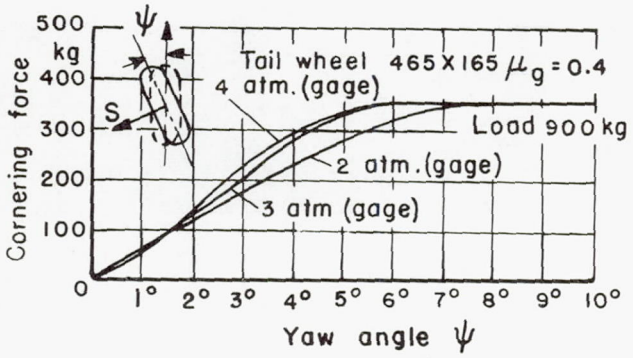

Figure 6.- Cornering force for various tire-inflation pressures.

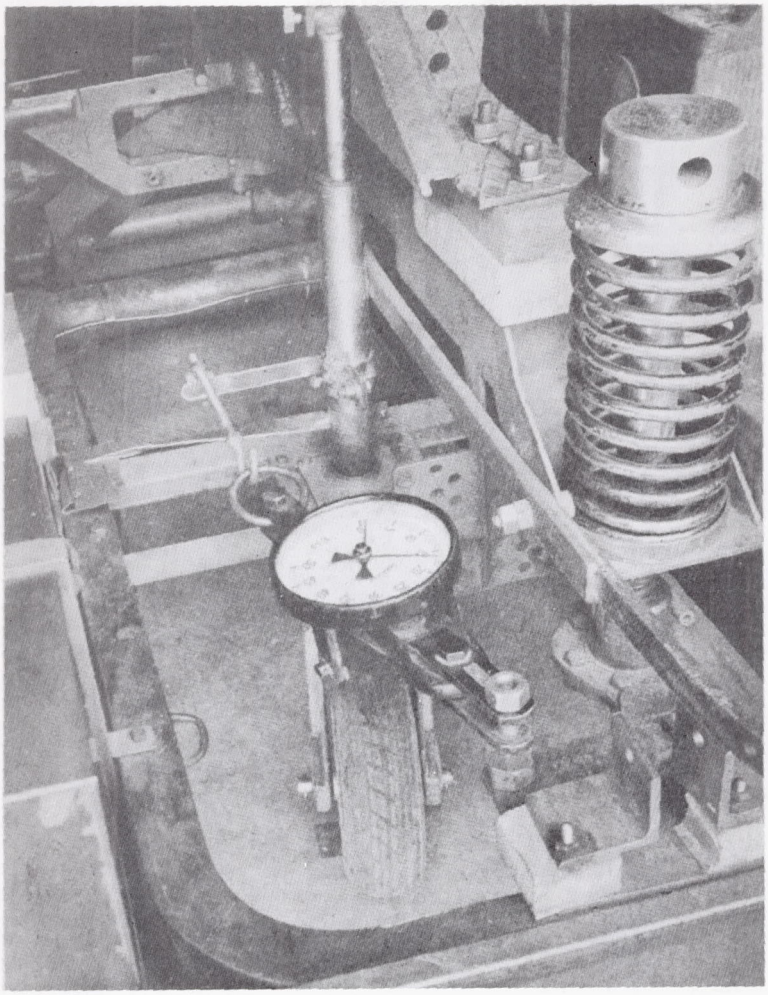

Figure 7.- Measurement of the cornering force of an airplane tire.

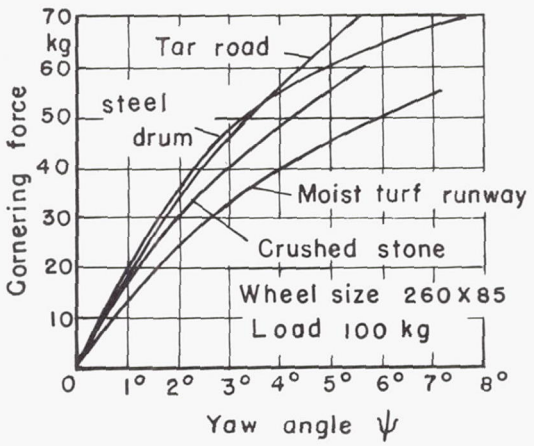

Figure 8.- Cornering force for different road conditions.

STIFFNESSES OF VARIOUS TIRES*

By H. Schrode

ABSTRACT

The rolling behavior of a landing gear with pneumatic tires depends on the elastic characteristics of the tires and may be thus easily influenced by a change in the form of tires. From tests of tires of various form it is shown that, above all, the side stiffness may be increased on the usual tires without an essential increase of the vertical resiliency factor. Wheel shimmy is minimized by the use of wheels of low shimmy tendency.

SUBJECT ARRANGEMENT

1. INTRODUCTION

According to the present investigations and experience the stiffness of the roll body wields a considerable influence upon the rolling stability of a vehicle or airplane[1], and especially on the shimmy behavior of swivellable wheels and steering wheels (ref. 1). Melzer (ref. 2) states, for instance, that in certain arrangements the stability of a tail wheel is especially favored by a great side stiffness

---

*"Steifigkeiten verschiedenartiger Reifen," Bericht 140 der Lilienthal-Gesellschaft, pp. 8-10. (NACA Editor's note: The present translation was based on material included in the 1942 Jahrbuch der deutschen Luftfahrtforschung but the information presented is essentially the same as that presented at the 1941 Stuttgart conference.)

[1]Herein are included the tramping and pitching motions as well as the "floating". Regarding the lateral-guiding or cornering force, important for the side-stability in rolling, it is assumed that tires of different side and torsional stiffnesses in rolling under influence of a given side force have different yaw-angles, so that thus not only the magnitude of the lateral deflection of the resting tire is dependent on the elastic properties of the tire, but the yaw-angle as well.

of the tail wheel. This was confirmed by tests with a tail wheel with a solid roller, the swivel axis of which was rigidly fixed laterally (ref. 3). Changes in shimmy tendencies have been observed already in airplanes with tail wheels due to changes of tire stiffness.

It is, therefore, apparent that the rolling behavior of a landing gear may be influenced favorably in general by the installation of tires of definite stiffnesses. Up until now, however, an improvement of rolling stability has been sought usually by added structures, such as dampers, or by change of the dimensions of the trail, while the spring constant of the tire, similarly to the airplane mass, has been considered as a fixed value.[2]

A change in characteristic values of the conventional balloon tire is basically possible by a change in inflation pressure and the wall thickness, however within certain limits only, since inflation pressure as well as wall thickness are essentially fixed by the required load capacity, the permissible ground pressure, and the demanded low tire weight. It if were necessary for increase of stability to make a great change in stiffness of the tire as compared to that of a balloon tire, one would have to abandon the latter and would have to attempt to achieve the desired stiffness by choosing a different tire form. The possibilities being offered for such shall be shown from tests available on a few experimental tires of various forms.

2. DESCRIPTION OF THE TEST TIRES

Figure 1 shows the various forms of the experimental tires built for general investigations. The tires shown are about equal in load capacity (with a given load they show about the same running period up to rupture). The tires were first designed for a static load of 650 kg; however, during the development the load capacity of the individual tires was raised to about 900 kg. The spherical tire shown is yet in the state of development. One may expect a load capacity of above 1000 kg, a fact which should be considered in the comparison of the separate tires.

The 380 × 150 tire is a standard balloon tail-tire that has been used in Germany since the introduction of tail wheels. Its rotational cross section is very nearly a circle. By widening of the rim a "smooth-contour tire" is obtained, the cross section of which is a part of a vertically placed ellipse. The elliptical 340 × 170 tire represents an attempt

---

[2]In the USA as well as in Russia, according to recent knowledge, however, the streamline tires of greater side stiffness are preferred to balloon tires for nose wheels and tail wheels. It is however not known whether this is done in order to improve the stability.

to build a tire with a specially small outer diameter. Due to the flat curve of its running surface even small spring actions will produce a great force absorption. (In the testing of this tire on a twin-engine airplane, the tail-wheel gear of which was fitted with a balloon tire showing strong shimmy, it was remarkable that, after installing the elliptical tire, the shimmy was considerably reduced.) The spherical tire (K) has very favorable deflection characteristics under load. The roll beads on both sides of the ground-contact surface prevent damage to the side walls during severe impacts and permit rolling after bullet damage. The solid-rubber roll was built for special uses and assembled into a twin roll for stiffness determinations.

3. TESTS AND TEST RESULTS

Moments and forces occur in rolling and in shimmy which cause tire deformations perpendicular to the contact surface and thereby cause (or tend to cause) existing or potential lateral deflections from the vertical axis. Thus, judging tires in respect to their influence on the rolling characteristics of a motor vehicle or an airplane shall be possible only with the knowledge of the course of the tire spring deflections with vertical and side loads as well as of its rotational angle with a rotational moment acting about the vertical axis.

The tests were conducted on a nonrolling tire. The side steering force of the rolling tire is calculated by Fromm (refs. 1 and 5) as $S = K\vartheta$, wherein ϑ is the yaw angle and K is to be determined from the elastic constants of the tire and the load. Insofar as the tests (ref. 6) carried out on airplane tires up to now permit, conclusions as to the dependence of side steering force on the side stiffness are that the side steering force increases with rising sidewall stiffnesses.

Figure 2 shows the spring constant characteristic curves of the various tires for vertical loading at an inflation pressure of 3 atm (gage).[3] The steep rise of the characteristic curve of the spherical tire, beginning with about $4\frac{1}{2}$ cm spring deflection, may be attributed to the participation of the tire beads on the sides. The vertical spring constant, that is, the load related to the unit spring deflection, amounts to about 200 kg/cm on the balloon tire and to about 325 kg/cm on the spherical tire in the lower load ranges.

The measurement of side and torsional stiffness was done with a vertical load of 650 kg and an inflation pressure of 3 atm gage. The side force was not applied at the wheels but was rather applied to the movable base plate, which was mounted on rollers, until a skidding of

[3]The tires were new. After use for some time the vertical spring constant is smaller.

the tires occurred. With each load stage the lateral deflection, or the torsion angle, was measured. The adhesive friction coefficient between the tire and the concrete rolling plate was 0.6 to 0.7.

Figure 3 shows that the deformation of balloon tires under side loads here are found to include two motions: one being a lateral deflection in the direction of the acting force, and one an elevation change of the wheel shaft f_{as} (see fig. 4).

The lateral deflection due to the side force is greatest on the conventional tire; the stiffnesses of the elliptical and wide-rim tires (smooth contour) as well as of the dual solid-rubber roll are about 1.5 times to twice as great as that of the balloon tire; the spherical tire has the greatest form stiffness and has approximately 7 times the stiffness of the balloon tire; it very nearly approaches that of a solid roller.

A change of inflation pressure has a much greater effect on the lateral deformation of the balloon tire than it has on that of the spherical tire.

The lowering of the wheel axle f_{as} of the pneumatic tires are related to each other about in the proportion as the lateral deflections of the tires. The lowering is greatest with the balloon tire and, with a ratio between side force and vertical wheel load of 0.5, amounts to about 5.5 mm. This distance would correspond, under a vertical load, to a force absorption of about 100 kg. With the solid-rubber dual roll a rise of the wheel axle is produced due to tilting of the flattened tire regions.

Figure 5 shows the lateral deflections of the balloon tire at various wheel loads. In increasing the load from 450 kg to 850 kg the lateral springing curves coincide, whereas at a further increase to 1000 kg, even with a slight side force, a buckling of the tire sidewall takes place (fold-formation), which latter causes a greater deflection than with the lower loads.

Numerical table 1 shows the vertical and lateral spring constants of the balloon and spherical tires and a ratio comparison of the two. By means of the choice of a spherical form a very large lateral spring constant, desirable for a good rolling stability (ref. 4), may be attained without an undue increase of the vertical spring constant.

NUMERICAL TABLE 1

	Balloon tire	Spherical tire	
Lateral spring constant	73	533	kg/cm
Vertical spring constant	200	325	kg/cm
RATIO: $\frac{\text{Lateral spring constant}}{\text{Vertical spring constant}}$	$\frac{1}{2.74}$	$\frac{1}{0.61}$	

The deformation of the tire due to a torsional moment about the vertical axis is shown in figure 6. This arrangement corresponds to a tail or nosewheel gear with a vertical swivel axis, the downward continuation of which passes through the middle of the tire ground contact plane; that is, it has no trail. The deformation of the tire resembles that in shimmy with a slight trail and small angular deflection.

The torsional stiffness of the spherical tire in the lower load region is about twice as great as that of the balloon tire (see fig. 7). The smallest resistance to torsion is naturally inherent in the dual roll. With loading increased to about 1000 kg the absorbed torsion moment is larger corresponding to the greater ground-depression area and to the greater normal force.

The elevation change of the wheel axle is very small and is, for instance with the balloon tire, about 3.5 mm until skidding occurs, whereas with the spherical tire it is nearly zero.

At slight turning movements, up to about 3° to 5° rotation angle, the torsion moment is essentially absorbed by the elastic deformation of the tire; that is, upon load release the tire returns to its initial position. With an increasing rotating motion skidding occurs first in the outer regions and gradually within the entire tread-compression area. The balloon tire behaves more elastically over a greater rotation region than does the spherical tire.

4. SUMMARY

Similarly to the design of machine elements, tires may be built to meet specific requirements by selection of a suitable form compared to the conventional balloon tire; above all, the side stiffness could be increased several fold, whereas a torsional stiffness may be attained about double that of the balloon tire.

Of special note is that the great increase in the lateral spring constant may be attained without an essential increase in the vertical spring constant, which fact seemed questionable a few years ago (ref. 1, p. 41).

The investigated tires are model tires. There is no doubt that for most practical cases by a suitable choice of the form and dimensions tires may be built that approach very closely the ideal tire of great softness vertical to the rollpath and yet having a very slight lateral yield.

Shimmy tests with the various tires have shown that the tire form wields a great influence on the shimmy tendency. Compared to the conventional balloon tire, the shimmy region may be considerably narrowed, trail and damping for the complete suppression of shimmy may be held smaller than with the balloon tires.

*Translated by John Perl
Lockheed Aircraft Corporation
Burbank, California (ATI No. 51824)

5. REFERENCES

1. Becker, Fromm, and Maruhn: Schwingungen in Automobillenkungen ("Shimmy"), M. Krayn, Berlin 1931.

2. Melzer, M.: Beitrag zur Theorie des Spornradflatterns, TB 2, 1940.

3. Dietz, O., and Harling, R.: Experimentelle Untersuchungen über das Spornradflattern, FB Nr. 1320.

4. Roberts, E. A.: Development of Wide-Rim Tires for Passenger Cars. S.A.E. Journal (Transactions), vol. 48, no. 4, 1941.

5. Fromm, H.: Sideslip and Guiding Characteristics of the Rolling Wheel. Pp 191 to 215 of present report.

6. Dietz, O., and Harling R.: Seitensteifigkeit und Seitenführung von Flugzeugreifen, FB Nr. 1498. (Available in translation as AAF translation No. ATI 18905)

---

*Note: In order to provide terminology consistent with other papers of this series, this translation has been reworded in many places by the NACA reviewer.

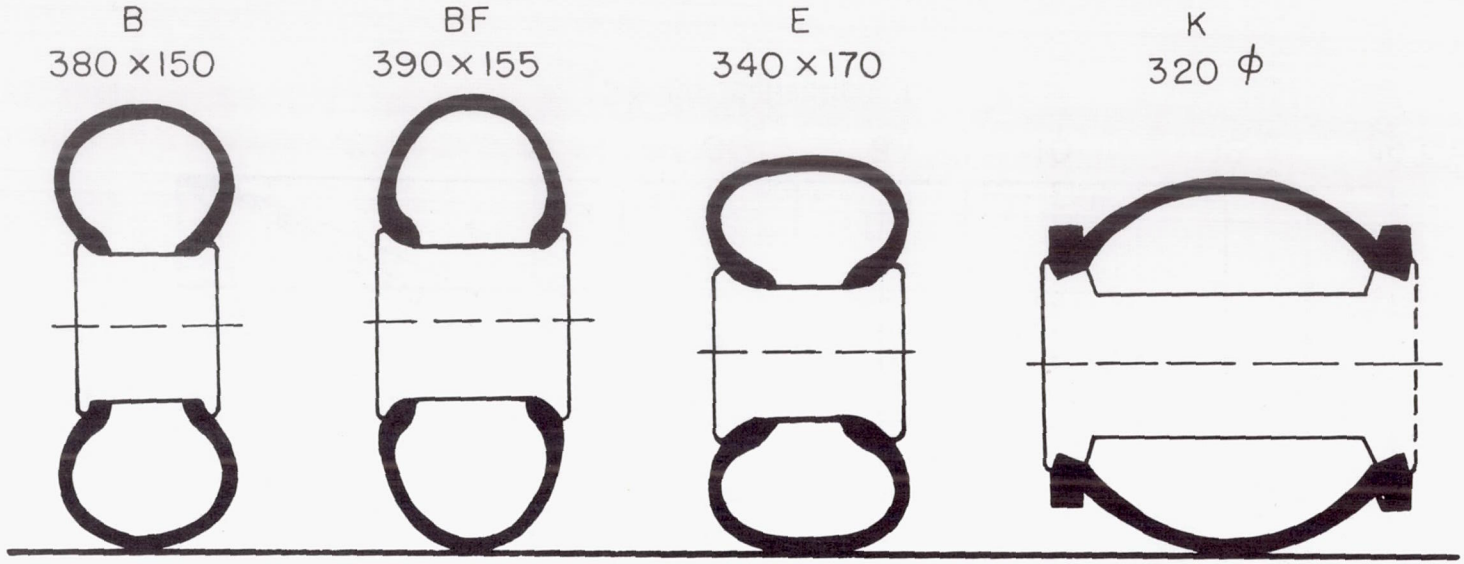

B Balloon tire

BF Wide-rim tire (smooth-contour tire)

E Elliptical tire

K Spherical tire

DV Dual solid-rubber roll

Figure 1.- Various tires of approximately equal load capacity.

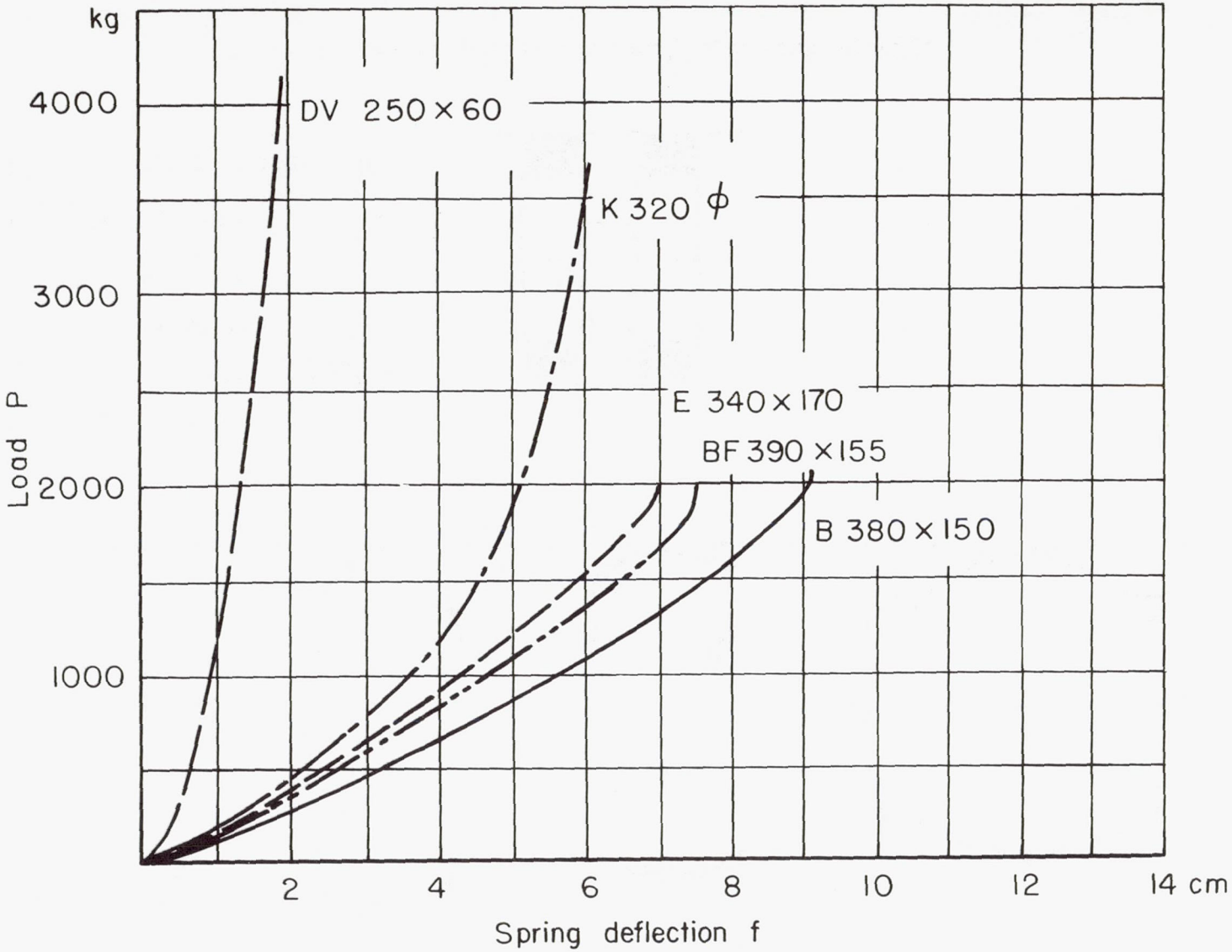

Figure 2.- Spring-constant characteristic curves of various types of tires under vertical loadings.

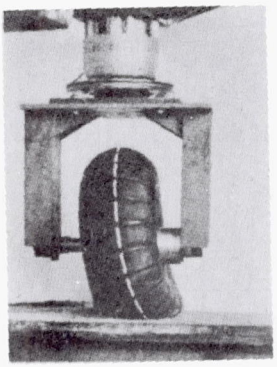

Figure 3.- Deformation of the 380 × 150 balloon tire under side loading.

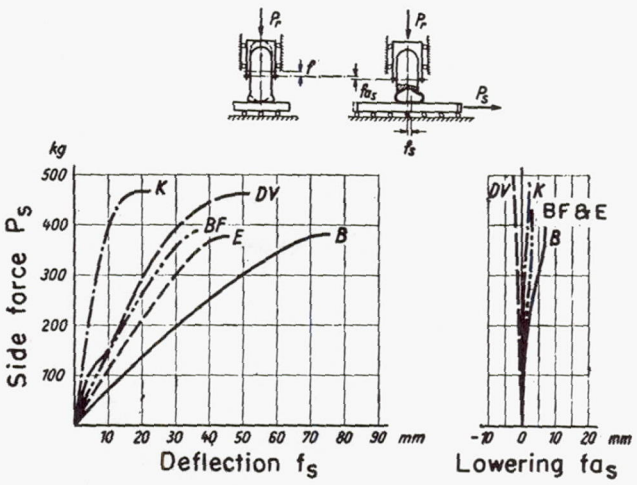

Figure 4.- Tire deformation characteristics under side loading.

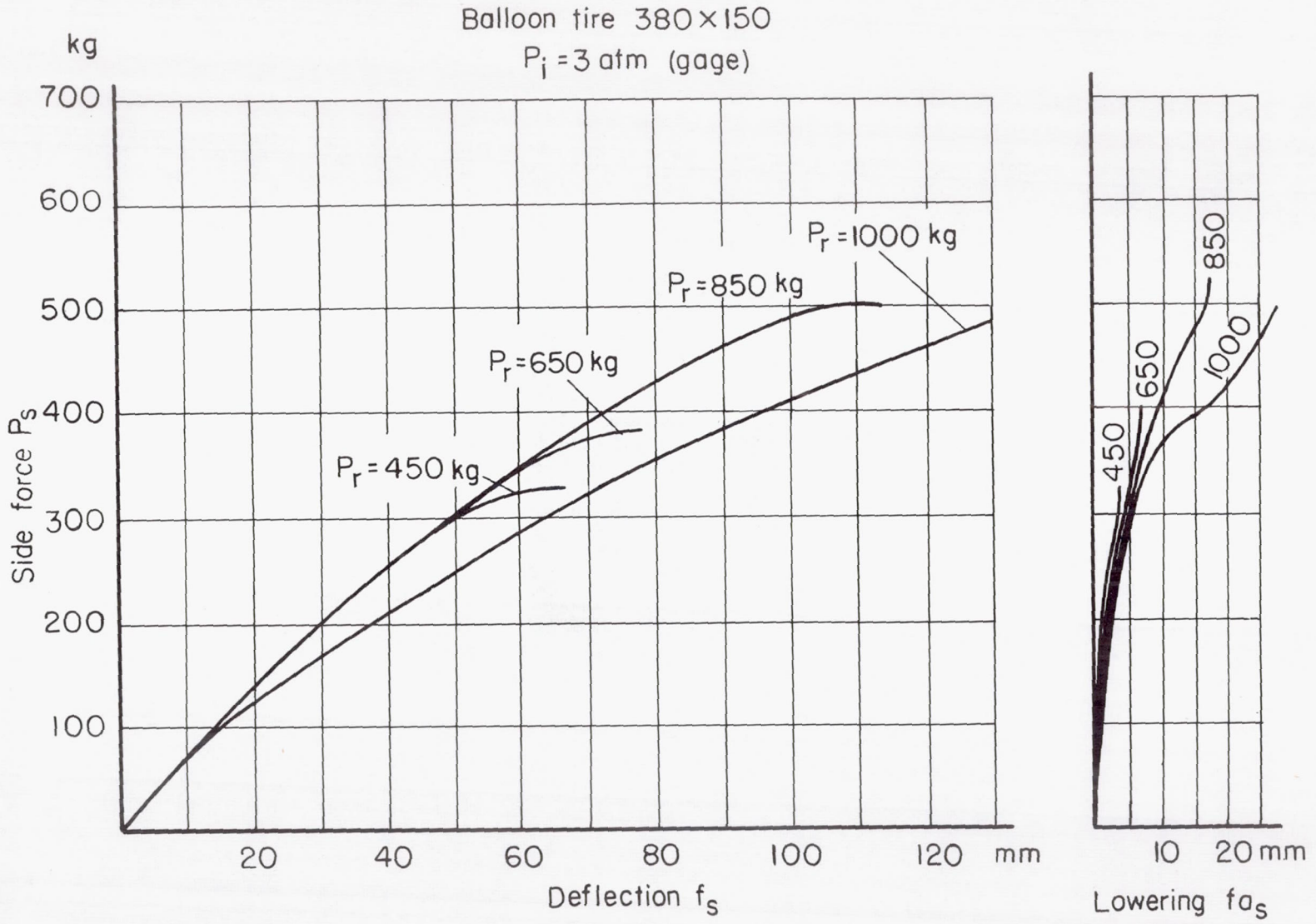

Figure 5.- Side deflection of the balloon tire at several wheel loadings.

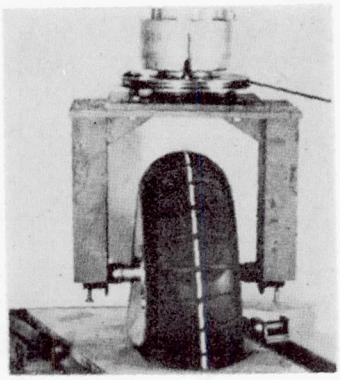

Figure 6.- Deformation of the 380 × 150 balloon tire due to torsion.

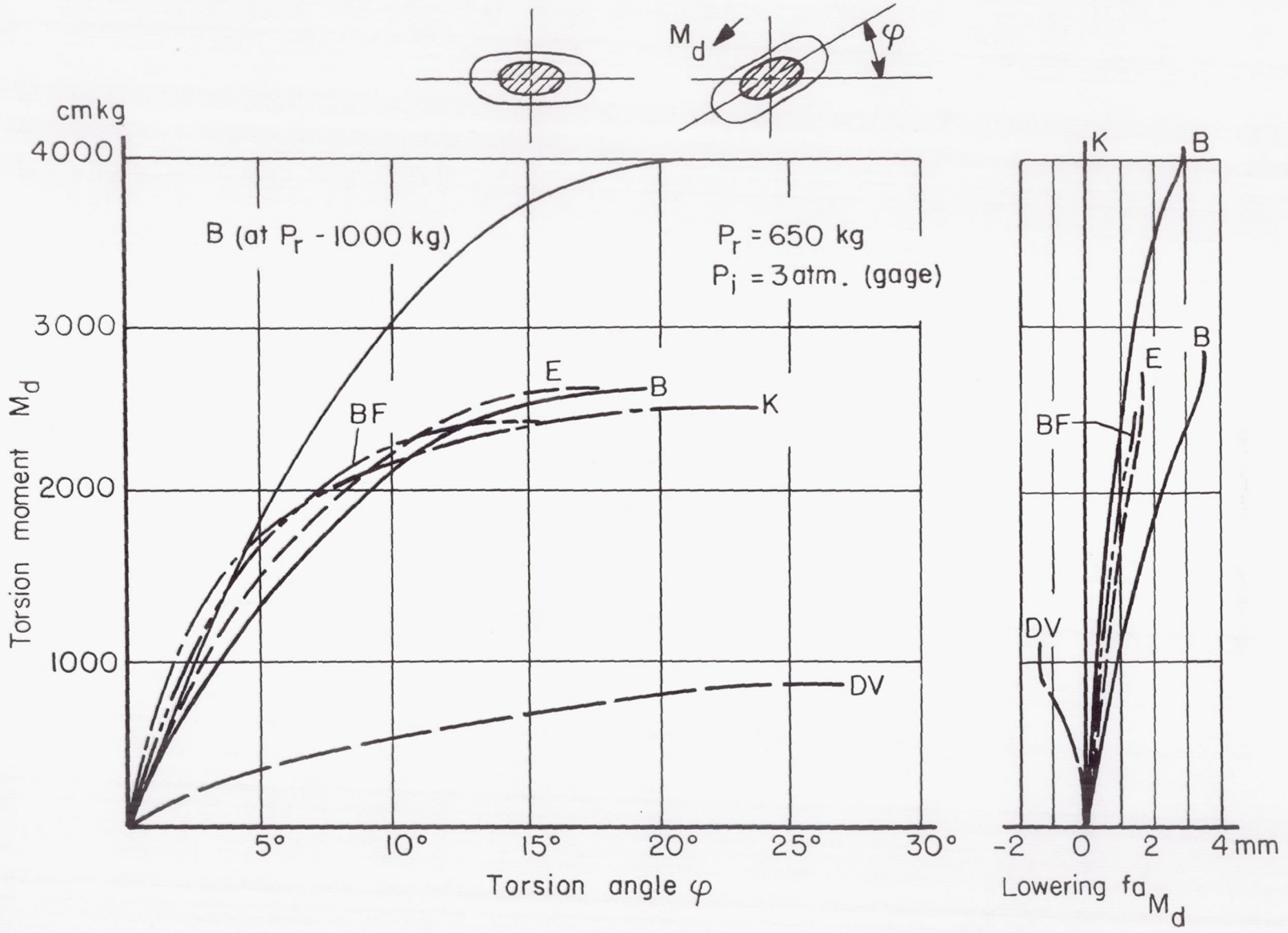

Figure 7.- Characteristic curves for the tire deflection under rotation.

FORCE DISTRIBUTION IN THE CONTACT SURFACE BETWEEN TIRE AND RUNWAY*

By P. Kraft

INTRODUCTION

For clarification of the causes of very heavy and irregular wear on tires of automobiles, an investigation and measurement of the pressure and stress variation in the contact surface between tire and runway on the rolling wheel seemed indicated. Beside measurements on automobile tires[1] measurements on airplane tires could be performed.

1. MEASURING PROCEDURE

The measurements were carried out as single-wheel tests. The wheel guided on rails is rolled over a fixed runway. The runway is interrupted by a table, adjustable over the width of the runway, in which the measuring device is placed. Through an opening in the table top, the plunger of the measuring device protrudes so far into the table top that the plunger surface is exactly flush with the surface of the table (fig. 1).

Each measurement yields the pressure variation in a zone of the contact surface parallel to the direction of travel. The width of the zone is determined by the width of the measuring plunger. By moving the measuring table over the entire width of the contact surface, one obtains the pressure variation in individual adjacent zones, and thus a pattern of the pressure distribution over the contact surface.

2. MEASURING DEVICE

The measuring device (fig. 2) measures the vertical ground pressure and the horizontal shear forces in the contact plane. The shear forces are divided into two components:

1. In or opposite the travel direction (longitudinal direction)

2. Normal to the travel direction (transverse direction)

---

*"Die Kräfteverteilung in der Berührungsfläche zwischen Reifen und Fahrbahn," Bericht 140 der Lilienthal-Gesellschaft, pp. 11-14.

[1]These measurements were carried out within the scope of the research plan of the Reich ministry for communication. A report on the results is published in the Deutschen Kraftfahrtforschung.

A tube dynamometer serves for recording of the normal pressure. The shear forces in the contact surface are resisted by two pairs of spring plates staggered by 90° [2]. The minute spring motions are transferred by means of small mirrors onto a revolving drum provided with light-sensitive paper.

3. NORMAL GROUND PRESSURE

The variation of the normal ground pressure may be seen from figure 3. At the entrance of the rubber particles into the contact surface the pressure in the zone of the tire flattened most rises steeply, takes then an approximately rectilinear course and decreases gradually toward the rear. In the edge zones of the contact surface, the pressure increases to a maximum value, attained approximately below the wheel center, and immediately decreases again.

The variation of the normal ground pressure below the center of the contact surface transversely to the direction of travel, for customary inflation pressure, is approximately a straight line. For diminishing inflation pressure, the ground pressure at the center decreases slightly; the variation becomes saddle-shaped. For very high internal pressure, the highest ground pressure is at the center and decreases toward both sides.

4. TANGENTIAL FORCES IN THE CONTACT SURFACE

Considering the tire cross section, one observes that in the flattening the circular arc of the tire circumference is compressed, and the rubber particles are pushed from the center toward the outside. Thereby, transverse tangential forces originate which, in case of normal wheel position, are directed inward, symmetrically to the longitudinal axis of the contact surface (fig. 4(a)).

Correspondingly, there originate, by the flattening, tangential forces in the longitudinal direction which are symmetrical to the axis of the contact surface which is normal to the direction of travel (fig. 4(b)). The magnitude and direction of the tangential forces on a loaded tire at rest have already been measured by Martin (ref. 1).

In the case of the rolling wheel, the tangential forces stemming from flattening and from rolling are superimposed.

---

[2]The measuring device was developed in cooperation with Prof. Dr.-Ing. A. Thum.

The resultants of the two horizontal components of the tangential forces measured now yield a stress distribution as shown in figure 5.

At the center of the contact surface, the zone of most pronounced flattening, the tangential forces in the longitudinal direction are strongest. The tangential forces in the transverse direction are zero at the center and increase toward the edge. Because of sliding of single rubber particles due to the decrease of the vertical ground pressure shortly before leaving the contact surface, the symmetry of the tangential forces is disturbed.

The stress pattern for a wheel guided rigidly at an angle of yaw is different; it is like that for wheels of automobiles or airplane landing gears running with toe-in. The yaw angle in the present case has been taken as very small; it amounts to slightly more than $1/2^{\circ}$. The distribution of the tangential forces is shown in figure 6.

In entering the runway, the rubber particles maintain the direction of motion of the wheel. Up to far beyond the center of the contact surface the tangential forces are in magnitude and direction equal to those measured for the wheel without yaw angle (fig. 5). However, the tire is deformed. The further to the rear the particles travel in the contact surface, the larger becomes the deformation.

When the road traction produced by the vertical ground pressure is no longer sufficient, the rubber particles are relieved of stress and start sliding. The sliding occurs first at the rear on the contact surface since here the ground pressure has already become smaller, as was shown in figure 3. The larger the toe-in angle, the larger becomes the deformation of the tire and therewith the portion of the sliding area of the entire contact surface.

Due to the fact that the front part of the contact surface still adheres to the ground while the rear part is already relieved of stress, in the case of a large toe-in angle, a kidney-shaped form of the contact surface is produced, as stated before by Fromm (ref. 2).

The tangential forces of figures 5 and 6 have been plotted together in figure 7, for comparison of the tangential forces in case of normal wheel position and of a wheel rolling at a yaw angle. The part which is already sliding is easily recognized.

The variation of the tangential forces for a wheel rolling at a yaw angle also shows that the tire can sustain lateral forces only when an angle of yaw exists, because a dissymmetry of the tangential forces with respect to the longitudinal axis of the contact surface occurs only in case of lateral deformation of the tire, thus of resistance of lateral forces. Deformation of the tire, however, causes the wheel to run at a yaw angle.

The continuously repeated sliding phenomenon at the rear part of the contact surface causes a very heavy wear of the tire. This shows that the zone of maximum ground pressure is not always critical for the wear of the tire, but that wear may occur precisely at the locations of minimum ground pressure because here relative motions between tire and runway are possible.

Translated by Mary L. Mahler
National Advisory Committee
for Aeronautics

5. REFERENCES

1. Martin, H.: Druckverteilung in der Berührungsfläche zwischen Reifen und Fahrbahn. Kraftfahrtechnische Forschungsarbeiten, Heft 2, Berlin 1936.

2. Becker, G., Fromm, H., and Maruhn, H.: Schwingungen in Automobillenkungen. Berlin 1931.

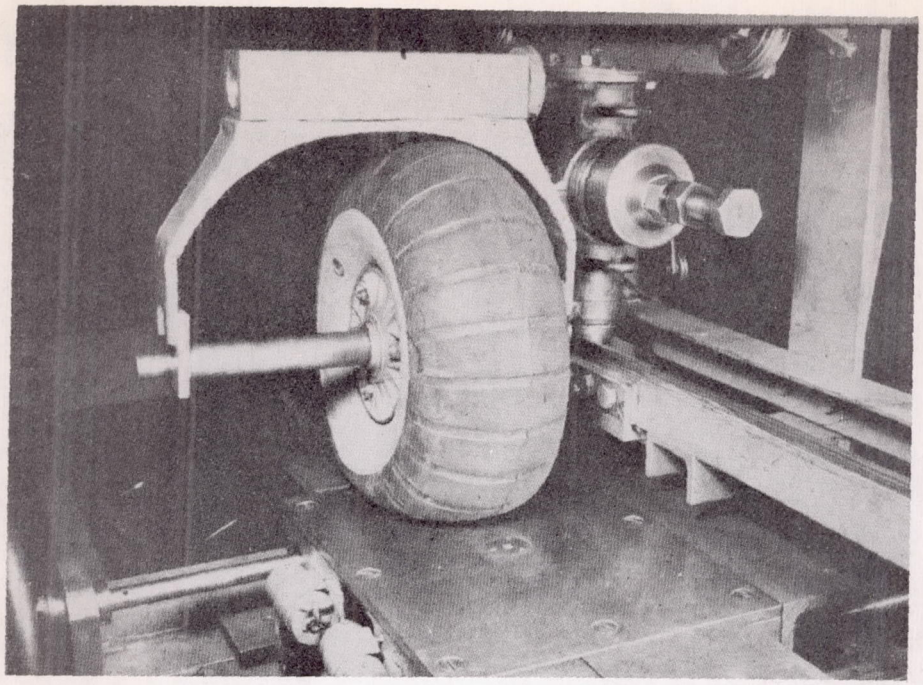

Figure 1.- Wheel with measuring table and plunger of the measuring device.

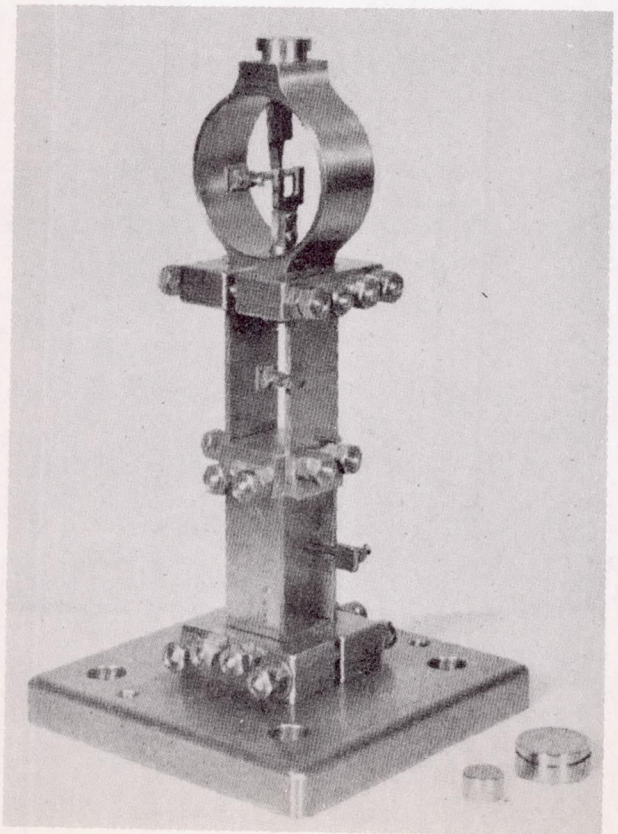

Figure 2.- Measuring device.

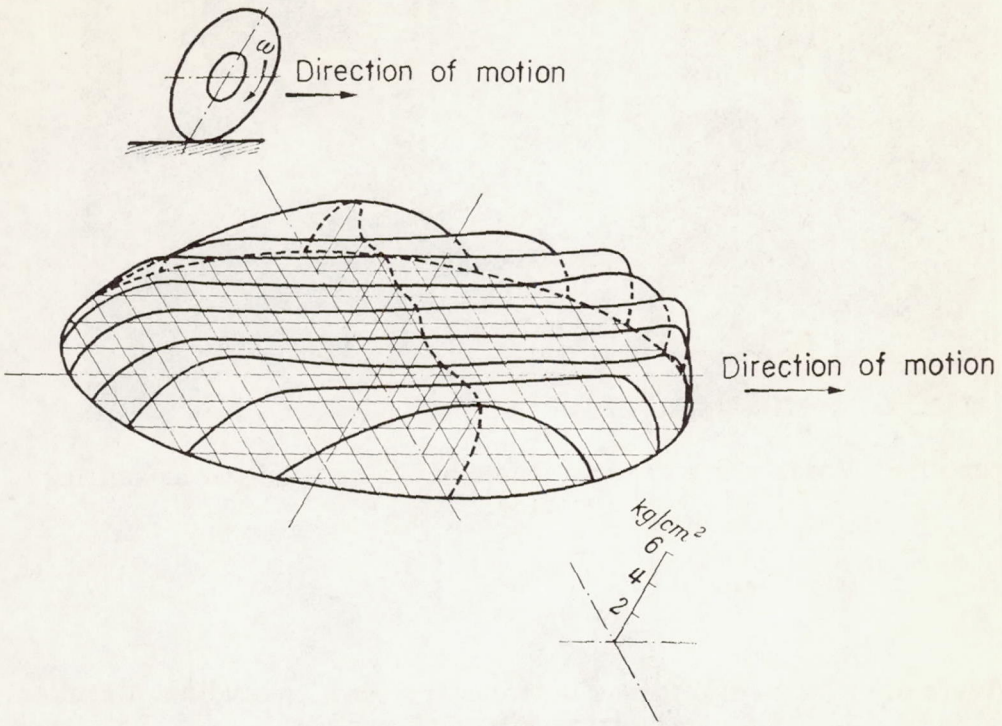

Figure 3.- Variation of the normal ground pressure over the contact surface of a pneumatic tire during motion.

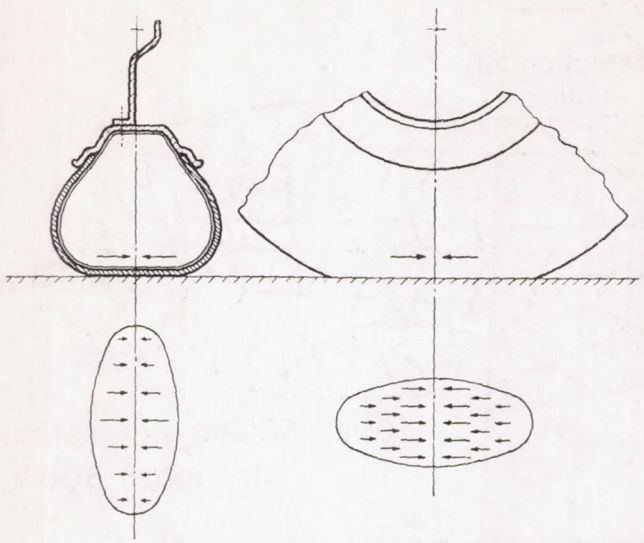

Figure 4.- Tangential forces in transverse and longitudinal direction, stemming from flattening.

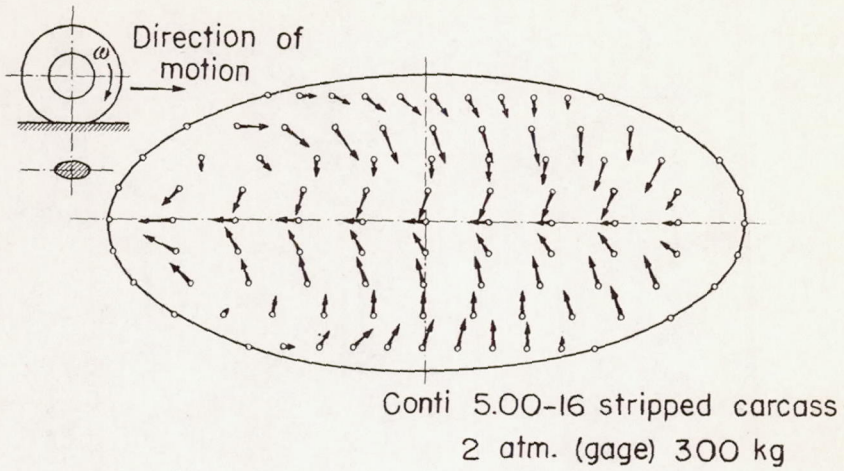

Figure 5.- Tangential forces in the contact surface between wheel and runway on the rolling wheel.

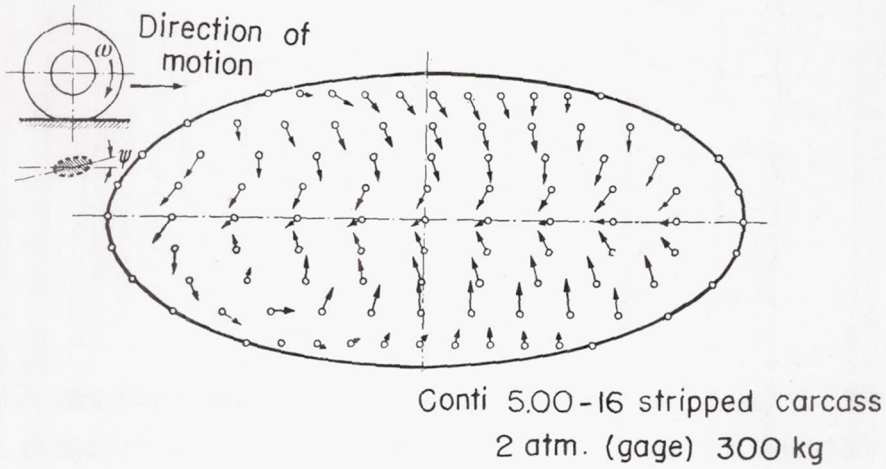

Figure 6.- Tangential forces on the tire with toe-in.

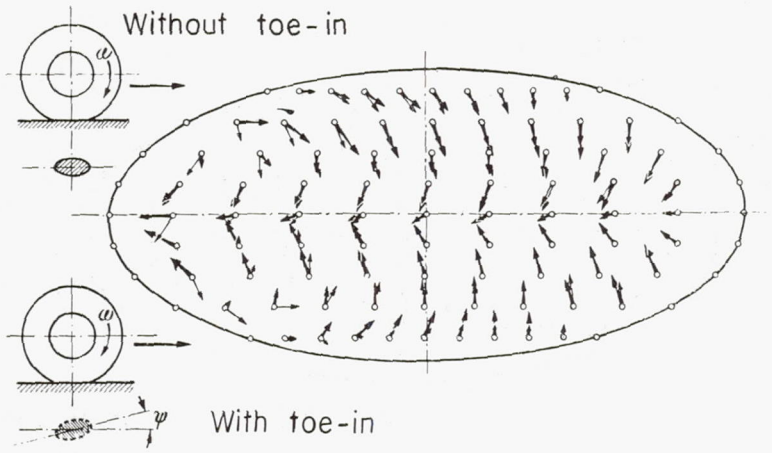

Figure 7.- Comparison of the tangential-force distribution on the tire without (heavily drawn) and with (lightly drawn) toe-in.

VEERING-OFF IN TAKE-OFF AND LANDING*

By F. N. Scheubel

Our present land planes have, as a rule, a landing gear which supports the airplane on three wheels. Two wheels, arranged near the center of gravity symmetrically with respect to the longitudinal axis, carry the main part of the load. Usually these wheels are not swivel-mounted or steerable. A third wheel lying in the plane of symmetry which is always swivel-mounted, although it can occasionally be locked by the pilot, and, in small airplanes, sometimes is steerable as well, forms the third point of support. According to the position of this swiveling wheel, one speaks of a tail-wheel landing gear when the swiveling wheel is placed behind the center of gravity at the airplane tail, of a nose-wheel landing gear when it is placed ahead of the center of gravity at the nose. Here in Germany there exist, aside from single test specimens, only airplanes with tail-wheel landing gear; in the United States, airplanes with nose-wheel landing gear also have been in production for some time. The two categories show fundamental differences in their rolling characteristics.

In airplanes with nose-wheel landing gear, straight-ahead rolling is a stable state of motion; in airplanes with tail-wheel landing gear, it is an unstable one. For reasons of brevity, this stability will be called rolling stability. Rolling instability manifests itself by an aperiodic increase of a disturbance; this is called "veering off."

This veering off may be explained in the simplest manner by a description of the process. Assume an airplane first to roll straight ahead. Due to some disturbance there appears, at first, because of its smallness, unnoticeable for the pilot, a turning away from the initial rolling direction which may increase extremely abruptly and lead to a very violent change in course. Then there appears a very considerable centrifugal acceleration, the reaction to which frequently exceeds the lateral resistance of the wheel tires or of their attachment to the wheel, which may occasionally even lead to lateral overturning and thus to serious damaging of the structure.

Veering-off therefore is a mostly involuntary rolling on a path with increasing path curvature the particular danger of which lies in the fact that the motion once developed can be controlled only with great difficulty or not at all.

---

*"Ausbrechen bei Start und Landung," Bericht 140 der Lilienthal-Gesellschaft, pp. 14-18.

In order to understand the phenomenon, we first consider an airplane rolling at constant speed on a horizontal plane on a slightly curved circular path, touching the ground with all three wheels. For the present, air forces as well as any elastic flexibility are to be disregarded. The airplane is therefore assumed to be rigid.

The motion will be stable if a moment damping the turning appears, thus if $\frac{dM}{d\omega} < 0$. The limiting case of disappearing moment, consideration of which shows all the essential aspects, is the neutral stability. With the assumption that the angular displacement of the swiveling wheel is $\psi \ll 1$, the equation of moments about the main landing-gear axis Zg normal to the ground becomes, with the symbols to be taken from figure 1,

$$M = amv\omega - (l + e)Y_L = 0$$

For establishment of balance of moments, considerable lateral forces must appear on the swiveling wheel, about equal to the centrifugal force $mv\omega$ times the quotient of the distance of the center of gravity from the main landing-gear axis a and the wheel base l. An investigation of the balance of moments of the swiveling wheel about its swivel axis shows the following facts:

The effective moments are (for symbols see fig. 2):

1. The moment of the centrifugal force of the swiveling wheel $s_L m_L v\omega$

2. The moment of the ground reaction Y_L of that component of the centrifugal force of the entire airplane which is resisted by the swiveling wheel $-eY_L$

3. A restoring moment mostly proportional to the angular displacement ψ of the swiveling wheel $M_R = -c\psi$

A balance of moments at the swiveling wheel appears when the sum of these three components disappears:

$$M_L = s_L m_L v\omega - eY_L - c\psi = 0$$

Hence, one can see that balance is possible also without a restoring moment when by pronounced rearward position s_L of the center of gravity of the swiveling wheel, the moment of the centrifugal force of the swiveling wheel is kept sufficiently large and, by small trail e of the swiveling

wheel, the moment of the ground-reaction force Y_L at the swiveling wheel is kept sufficiently small

$$s_L m_L v\omega - e \frac{a}{l + e} mv\omega = 0$$

or

$$\frac{e}{s_L} \frac{a}{l} = \frac{m_L}{m}$$

An estimation shows, however, that this is not possible unless either the trail e of the swiveling wheel is made extremely small or the distance of the center of gravity s_L of the rotatable part of the swiveling wheel assembly from the swivel axis is made extremely large. Reduction of trail would result in a very strong coupling of the swiveling wheel with the airplane and lead to a very unsteady run, particularly on irregular ground, occasionally probably even to complete reversal of direction by 180°. Increase of the distance of the center of gravity of the swiveling wheel could be obtained only at the price of considerable additional weights acting on a long lever arm. Therefore, this method will hardly be usable.

Thus a restoring moment seems indispensable; however, the effect of this moment also is limited. In the equation of moments of the swiveling wheel one may, for stationary rolling, using the kinematic condition that the wheel is to roll without transverse sliding, interchange angular path velocity and angular displacement of the swiveling wheel

$$v_{Ly} = -v\psi - e \frac{d\psi}{dt} - (l + e) \frac{dx}{dt} = 0$$

Therewith one can derive from the equation for the balance of moments of the swiveling wheel that, for stabilizing of the rolling, a restoring process is necessary which is proportional to the mass of the airplane and the square of the rolling velocity

$$\frac{c}{Gl} \geqq \frac{v^2}{gl} \frac{e}{l} \frac{a}{l} \left(1 - \frac{m_L}{m} \frac{s_L}{e} \frac{l}{a} \right)$$

A numerical estimation shows that even for small single-seater airplanes and moderate speeds, about 0.7 of the minimum speed, restraint of the swiveling wheel is needed which makes a steering at low speeds almost

impossible. Thus one is forced to apply considerably less restraint. This means, however, that airplanes with tail-wheel landing gear at speeds above the critical velocity determined by the rearward position of the swiveling wheel must tend to veer off.

A more accurate investigation of the veering-off process is possible by setting up and integrating the equation of motion for small disturbances. It leads to the result that, for the airplane with tail-wheel landing gear, a small disturbance, once initiated, increases as an exponential function of the rolling distance. The exponent which appears as a factor of the rolling distance is practically the distance of the center of gravity from the main landing-gear axis normal to the ground divided by the square of the radius of gyration of the airplane about this axis. For large disturbance amplitudes which present great difficulties to exact calculation, one may state that the airplane with tail-wheel landing gear has the tendency to roll in a loop-shaped curve and in doing so to change its direction of motion so that it continues to roll like an airplane with a nose-wheel landing gear.

Analogous considerations apply to the airplane with nose-wheel landing gear; one only has to insert the corresponding lengths with negative sign. As a result, the airplane with nose-wheel landing gear is shown to have a very high degree of rolling stability.

However, in these considerations, two perhaps essential points have been disregarded: air forces and elasticities. Their influence must therefore be estimated. For reasons of easier visualization, this will again be accomplished by consideration of the balance of forces and moments, although the investigation of the equation of motion is thereby not made superfluous.

It is sufficient to observe the effect of the air forces for still air. Wind results in a particular course angle and thus in further complication of the calculation; this calculation shows that head wind has a stabilizing effect, tail wind an opposite effect. The essentials result from investigation of rolling in still air.

In addition to the mass forces and their ground reactions, there now appear air forces and their moments, essentially a force normal to the plane of symmetry of the airplane and a moment about the vertical axis of the airplane. The main portion of the lateral air force Y_S originates at the vertical tail surface as its lift, so that it is sufficient for an estimation to consider this alone. The lift of the vertical tail surface is proportional to the lift coefficient of the vertical tail surface, the dynamic pressure at the vertical tail surface, and the area of the vertical tail surface (fig. 3):

$$Y_S = c_{a_S} \frac{\rho v_S^2}{2} F_S$$

The lift coefficient, in turn, is approximately proportional to the angle of attack of the vertical tail surface. This angle of attack of the vertical tail surface is, for curvilinear rolling, directly proportional to the angular velocity, inversely proportional to the rolling velocity:

$$a_s \sim \frac{(a + r_s)\omega}{v}$$

Therewith, one obtains for the moment of the vertical tail surface proportionality with the centrifugal acceleration and thus the possibility of taking the influence of the air forces of the vertical tail surface into consideration in the form of a correction term

$$amv\omega\left[1 - \frac{(a + r_s)^2}{as}\frac{\partial c a_s}{\partial a_s}\frac{F_s}{F}\frac{v_s^2}{v^2}\frac{\rho F s}{2m}\right] - (l + e)Y_L = 0$$

An estimation with the numerical values of airplanes customary at present shows that the moment of the air forces of the vertical tail surface reduces the moment of the centrifugal forces only by about 5 to 15 percent. The influence is the lesser, the smaller the airplane and the larger its wing loading. This signifies that the air forces do not bring about an essential reduction of the lateral force to be resisted by the swiveling wheel. The rest of the discussion is the same as that for rolling without air forces, the result practically identical. For airplanes with pronounced rearward position of the swiveling wheel, the critical speed is somewhat, but only insignificantly, increased by the air forces.

A detailed investigation with the aid of the equation of motion which takes into consideration, in addition, a few of the finer characteristics of the air force distribution leads to a similar result.

As was said before, the assumption that the airplane is rigid is not exact. It is, rather, an elastic system; however, the elastic flexibilities are usually small. Only the deformations of the landing gear itself, either of the shock-absorber legs or of the tires, are significant.

In curvilinear rolling, the airplane will be inclined outward. For customary arrangement of the swiveling wheel, this produces additional moments at the swiveling wheel which steer the swiveling wheel of the tail-wheel landing gear into the curve, thus have a destabilizing effect. However, this influence is not large. Besides, it appears with a large

time lag, due to the considerable inertia of the airplane about a longitudinal axis lying in the ground. Under certain assumptions, particularly when sufficient damping in the main landing gear is lacking, a coupled excited oscillation about the longitudinal and vertical axes may appear in a nose-wheel landing gear. However, it will probably never become critical. A larger influence is exerted by the torsional flexibility of the tires and of the structure of the landing gear. As H. Fromm has shown on the occasion of an investigation of the oscillation phenomena in automobile-steering mechanisms, the customary pneumatic tires of automobiles and airplanes must be deformed if they resist lateral forces. This means, however, that such vehicles when loaded by lateral forces do not move in the direction of the wheel planes, but obliquely to that direction, that is, therefore, that they are yawing.

Superimposed on this torsional flexibility of the tires is the always present (but mostly essentially smaller as to amount) torsional flexibility of the structure of the landing gear. According to the static configuration, its sign may be equal or opposite to that of the torsional flexibility of the tires. The sum of both will be designated as torsional flexibility $\frac{\partial \beta_F}{\partial Y_F}$ of the landing gear or $\frac{\partial \beta_L}{\partial Y_L}$ of the swiveling wheel where the considered, elastically or otherwise restrained, swiveling motion is added.

Simultaneously with this torsional flexibility, there appears a kind of bending flexibility which affects the veering-off only slightly.

We shall now consider an airplane with tail-wheel landing gear, the main landing gear and swiveling-wheel gear of which are both torsionally flexible; this airplane is to be loaded by a lateral force such as the centrifugal force which acts at the center of gravity (fig. 4). This force then is distributed, in accordance with the length relationships, between the main landing gear and swiveling gear and twists them. The curvature χ of the path on which the airplane can move is determined by these torsional deformations. For small torsional angles β it is

$$\chi = \frac{1}{R} \sim \frac{\beta_F - \beta_L}{l} = \frac{\frac{\partial \beta_F}{\partial Y_F} Y_F - \frac{\partial \beta_L}{\partial Y_L} Y_L}{l}$$

and with consideration of the distribution of the ground reactions of the lateral force Y prescribed by the dimensions it is

$$\chi = \frac{Y}{l}\left\{\frac{\partial \beta_F}{\partial Y_F}\frac{l - a}{l} - \frac{\partial \beta_L}{\partial Y_L}\frac{a}{l}\right\}$$

It appears forthwith possible to adjust the torsional flexibilities $\frac{\partial \beta_F}{\partial Y_F}$ of the landing gear and $\frac{\partial \beta_L}{\partial Y_L}$ of the swiveling wheel in such a manner that a curvilinear rolling forced in any way diminishes after elimination of the restraints, the airplane therefore attains rolling stability.

No doubt such a landing gear has not yet been intentionally built, but I believe that the large differences in the tendency to veer off of otherwise very similar airplane models can be explained at least in part by very different torsional flexibilities of the landing gears. I hope that, by deliberate application of these findings, a considerable correction of the veering off tendency of airplanes with tail-wheel landing gear is attainable.

A few peculiarities are to be considered for the special phenomena in taking off and landing. I limit myself, where not expressly mentioned otherwise, to airplanes with tail-wheel landing gear.

At the beginning of taking-off, the airplane with tail-wheel landing gear stands, as shown in figure 5, mostly with greatly inclined engine axis. Therefore, a component of the reaction of the engine torque will twist about the vertical axis, according to the direction of propeller rotation here customary, to the right. The component of the reaction of the engine torque, which is parallel to the ground, produces an unequal loading of the wheels of the landing gear; thus, because of the ground friction of the wheels and because of the banking of the airplane caused by the elastic flexibility of the wheels, two small moments are produced about the vertical axis of the airplane and the swivel axis of the swiveling wheel, respectively, which largely compensate each other in their effects. The resulting torque may be counteracted by unsymmetrical braking (which is undesirable) or by rudder deflection, under the assumption that the rudder lies in the propeller slipstream. An estimation shows that when the slipstream is fully effective, even small easily attainable lift coefficients at the vertical tail surface are sufficient

$$c_{a_s} \approx \left(\frac{k_L}{4}\right)^{1/3} \sin a_{st.} \frac{F_{slipstream}}{F_s} \frac{R_{slipstream}}{a + r_s}$$

It is an impediment that the vertical tail surface in static condition mostly obtains not nearly the full dynamic pressure of the slipstream, and that the slipstream itself rotates and is laterally deflected near the ground. However, in a properly functioning plane, this phase of the taking-off will not present any difficulties to an observant pilot.

When the airplane has attained some speed, the dynamic pressure at the horizontal tail surfaces is sufficient for lifting the rear of the fuselage off the ground and for setting the airplane at small angles of attack. Some pilots have the custom or rather the bad habit of doing this very sharply, almost jerkily. With a not very experienced pilot, this may be dangerous. For due to this rotation about the transverse axis, there appear gyroscopic propeller moments which, according to the direction of propeller rotation here customary, tend to turn the airplane to the left and which even in a single-seater may attain amounts of several 100 mkg. Simultaneously, the component of the reaction of the engine torque turning to the right ceases to be effective, and, in addition, the vertical tail surface in most cases comes usually into parts of the slipstream flowing from the left to the right. All three effects add up, and if the pilot, who in the first phase of taxying had deflected the rudder to the left as compensation for the turning to the right, does not immediately apply opposite rudder, dangerous veering off sets in.

But even when the pilot has executed this second phase carefully, a slight rotation may appear. The question is whether the airplane, rolling now, in the third phase, only on the main landing gear, can be made to roll again straight ahead. According to the estimation of the influence of the air forces on the rolling stability given above, it is understandable that the airplane, due to the type of configuration customary at present, will not possess rolling stability. The moment of the centrifugal forces which tends to rotate the airplane into the turn is so large that the damping moment of the vertical tail surface cannot begin to compensate for it.

There arises the question whether the vertical tail surface is at all capable of preventing veering-off. The air forces of the vertical tail surface are limited by the maximum lift coefficients attainable; by substitution into the equation of moments, one realizes that there exists a lower limit for the permissible path radius at which the vertical tail surface can barely balance the centrifugal-force moment (fig. 6)

$$amv\omega \leqq c_{a_s} \frac{\rho v_s^2}{2} F_s(a + r_s)$$

and hence

$$R_{min} \geqq \frac{1}{c_{a_s}} \frac{a}{a + r_s} \frac{F}{F_s} \frac{v^2}{v_s^2} \frac{2G}{\gamma F}$$

At the wing loadings customary at present, these critical path radii lie mostly above 300 m. Here a certain influence of the size of the airplane

becomes manifest. For equal path curvature, a smaller airplane has smaller dynamic angles of attack of the vertical tail surface than a large airplane. Consequently, the attainable lift coefficient c_{a_s} for a smaller airplane will be smaller than for a large airplane, and thus the critical path radius will increase. If the vertical tail surface is shielded by structural parts lying in front of it, rolling even on a less curved path can no longer be controlled solely by means of the rudder.

Once the veering-off in taxying has exceeded this limit, there remains as a last expedient only unsymmetrical braking or, for multi-engined airplanes with side engines, the application of unsymmetrical power. Both are expedients which at least prolong taxying, and are very dangerous in formation take-off.

It is sufficient to consider the case of unsymmetrical braking. Thereby external moments may be produced which are proportional to the friction coefficient, to the unsymmetrical wheel loading, in the phase of the take-off here considered practically half the flying weight, and to half the track width s_F of the main landing gear. A consideration of the balance of moments permits the conclusion that the centrifugal acceleration measured in units of the acceleration of gravity may attain a definite limit if veering-off is still to be checked by unsymmetrical braking

$$\frac{v\omega}{g} = \mu \frac{s_F}{2a}$$

For the friction coefficients attainable on dry ground, this limiting load factor of the centrifugal force may increase up to the order of magnitude of 1. Since even considerably smaller centrifugal-force load factors are clearly perceptible, there still remains, therefore, as a last resort against a veering-off motion, the unsymmetrical braking. A similar effect, although usually not quite as strong, is obtained by application of unsymmetrical power in the case of multiengined airplanes. Whether these measures are still successful depends largely on the speed of reaction of the pilot.

The question remains to be answered how the airplane with torsionally flexible main landing gear, described above as possessing rolling stability, behaves during take-off.

In the two first phases of taxying, no great difference is obvious between this airplane and the airplane with conventional landing gear. In the third phase (the one of longest duration), the rolling with horizontal engine axis, in contrast, the airplane may become stable beginning with a certain rolling speed. Even below this speed, the tendency toward veering-off is considerably decreased. I shall here not go into details.

The take-off of an airplane with nose-wheel landing gear does not offer any problems with respect to veering off since such an airplane possesses rolling stability also when the nose wheel is lifted off.

For observation of the taxying in landing, the relations derived above in the investigation of rolling are almost completely sufficient. Under the assumption that the airplane has a torsionally rigid main landing gear and a swiveling wheel at a rearward position, as is true today almost exclusively, rolling at small speeds up to critical speed (which depends on the rearward position of the swiveling wheel) will, according to these relations, be stable. Beyond this speed, the airplane becomes unstable, more so with growing speed.

Since, however, these relations derived above apply only to rolling at constant speed, it remains to be investigated what influence is exerted by the braking applied after the landing to shorten the landing run. Therein, one must distinguish whether the restoring action of the swiveling wheel depends on its loading (as in case of inclination or wedge-roller traversing of the swivel axis) or whether elastic members constrain the swiveling wheel in center position.

Braking causes an unloading of the swiveling wheel lying behind the main landing gear; thus, in airplanes in which the restoring action of the swiveling wheel is proportional to its loading, a reduction of the restoring forces and, therewith, a decrease in stability or increase in instability. Very strong braking which is so great as to practically unload the swiveling wheel makes it impossible for the swiveling wheel to resist lateral forces. Then one will obtain, for the landing run after the landing, relations similar to those for the taxying to take-off, even slightly more unfavorable ones because the center of gravity lies further to the rear and because the slipstream with its increased velocity at the vertical tail surface is lacking. In an airplane with elastic constraint of the swiveling wheel, the rolling behavior would not be affected in case of moderate unloading of the swiveling wheel by braking. Thus it would be stable or unstable according to the rolling speed. However, a high degree of unloading of the swiveling wheel may lead here also to instability. Other acceleration effects occurring due to braking are insignificant. Likewise, braking at the swiveling wheel has little effect.

In airplanes which have been made to attain rolling stability by torsionally flexible main landing gear, the landing run without application of brakes is stable; however, in these cases also a reduction of stability occurs when there is a restoring action of the swiveling wheel which is dependent on the load and when the brakes are applied during the landing run. Obviously they will also decrease in stability if very strong braking is applied which completely unloads the swiveling wheel. Relations similar to those in taxying during take-off are then valid.

The veering-off in landing can begin for various reasons. Dissymmetries in the landing gear as occasionally appear in operation may impart a bank to the airplane and, therewith, by means of lateral components of the weight reaction, deflections to the swiveling wheel which steer the plane into a curved path. One-wheel impacts or slight sideslipping, which are not always with certainty avoidable, produce rotational shocks. Likewise, irregularities of the ground which reach one half of the landing gear may be the starting point. Landing transversely to the gradient of a slightly sloping airfield leads in airplanes with tail-wheel landing gear to a rotation in the direction toward the slope. It is also conceivable that the flow at the wing separates unsymmetrically and thereby produces as a result of the unsymmetrically acting drag a rotational moment turning about the vertical axis.

The possibility of checking veering-off motions has to be investigated in a similar manner as for the case of take-off. However, there exists a basic difference. In the low-speed regime where checking of veering-off by means of the rudder mostly would not be possible, the airplane can be made stable by sufficiently large restoring moments of the swiveling wheel. It is conceivable to fix this limiting speed rather high, and, on the other hand, the speed for which sufficient rudder effect exists so low that the two regimes overlap. One then has an airplane which possesses rolling stability at low speeds; at high speeds it will be unstable, but its veering-off motions will be controllable by means of the rudder alone. The amount of this limiting speed for the rudder effect depends, as explained above in the investigation of take-off, on the path curvature which the pilot is sure to perceive. It will vary individually; however, I believe that it will be possible to give a value which an unexperienced pilot, too, can perceive with certainty. Probably this limiting value will depend on the rolling speed, in such a manner that the perceptible path curvature decreases with increasing speed. Hence, one could draw a conclusion as to a greater danger of veering-off at lower speeds.

It would be conceivable to make the braking forces at the main landing gear in landing proportional to the normal loads on the individual wheels. Due to the different load in curvilinear rolling, one could thus attain rolling stability for strong braking.

For the airplane with nose-wheel landing gear, there exists no veering-off tendency in landing.

Summarizing, one might say: Today's airplane with tail-wheel landing gear does, in contrast to the airplane with nose-wheel landing gear, not possess rolling stability, has therefore by nature the tendency to veer off. The designer must endeavor to keep this tendency as small

as possible, the pilot must take it into consideration. How far special measures will make it possible to attain rolling stability can be decided only by practical tests.

Translated by Mary L. Mahler
National Advisory Committee
for Aeronautics

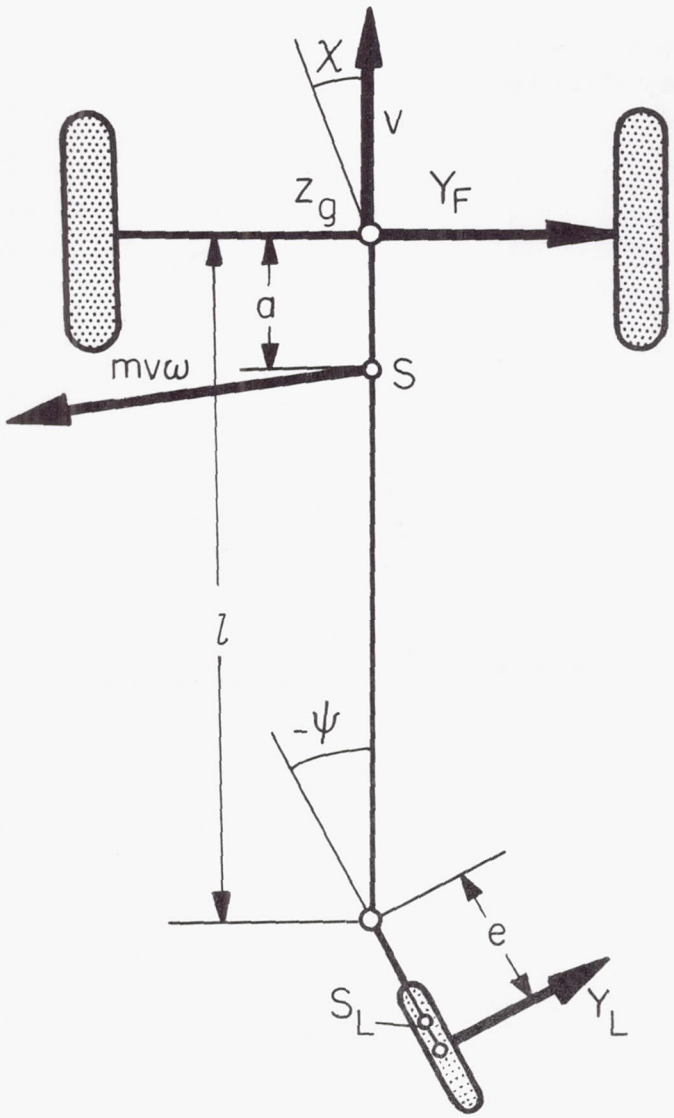

Figure 1.- Equilibrium of a neutrally stable airplane in curvilinear rolling.

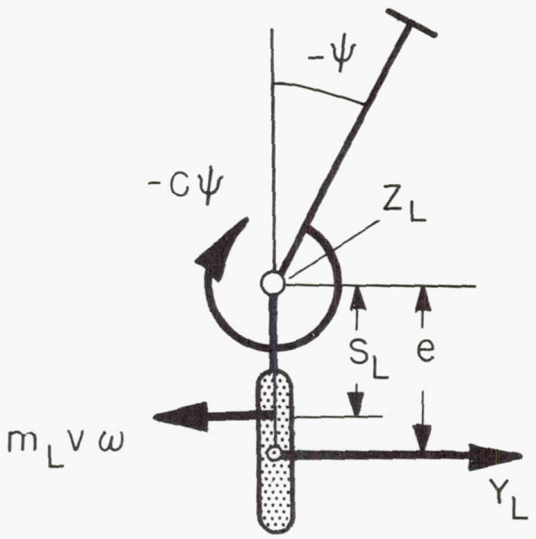

Figure 2.- Forces and moments on the swiveling-wheel gear.

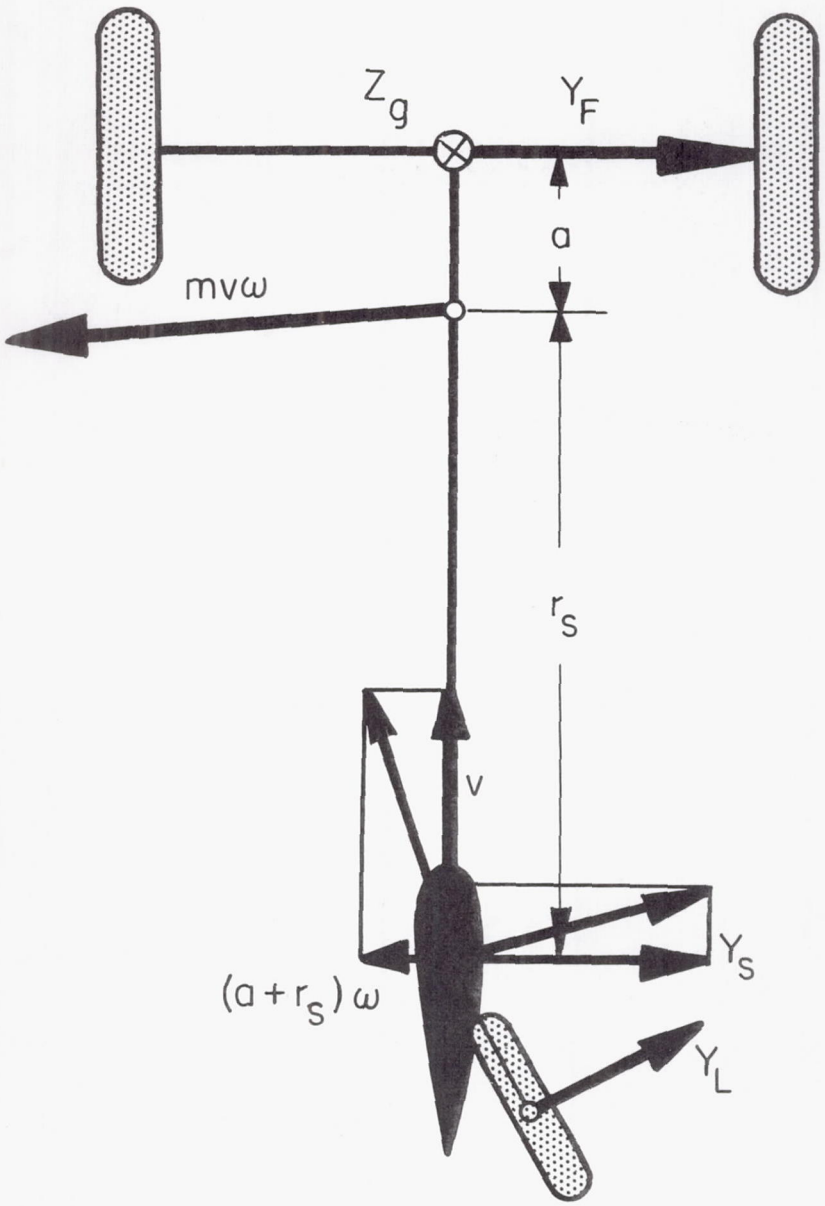

Figure 3.- Influence of the air forces on the rolling stability.

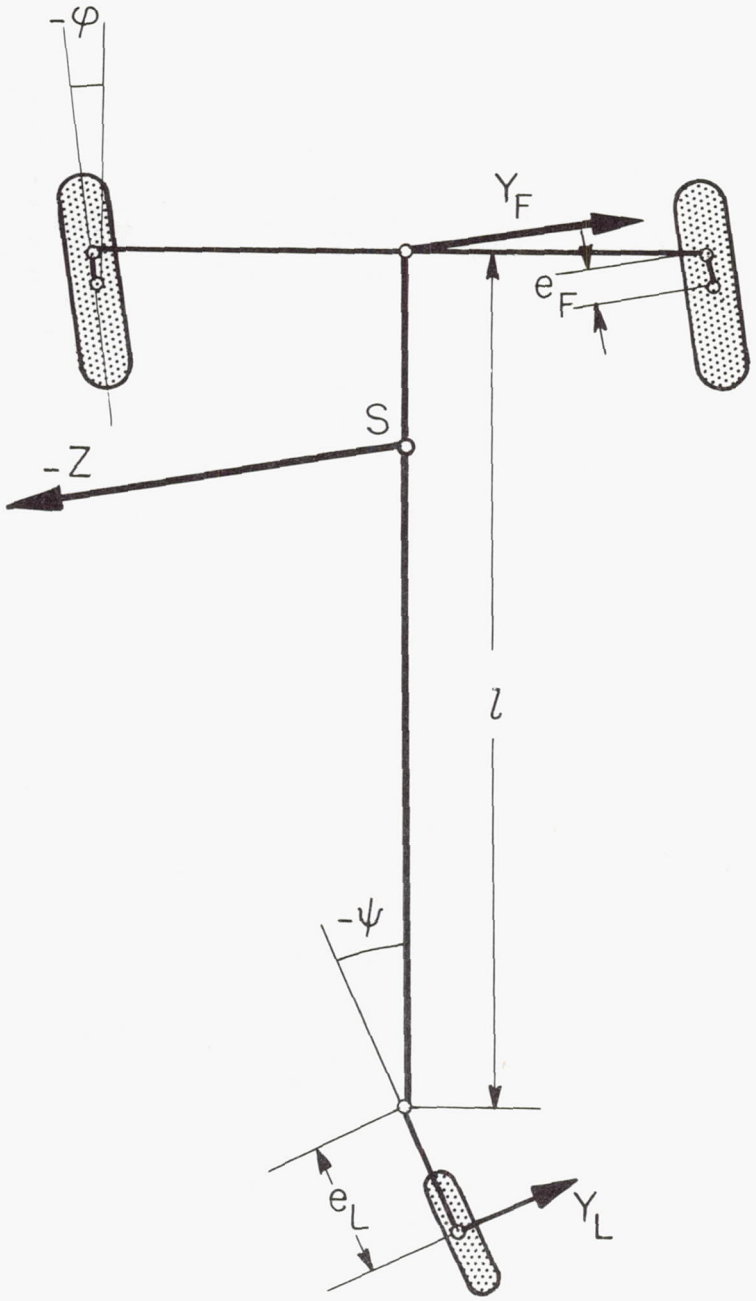

Figure 4.- The airplane with torsionally flexible landing gear.

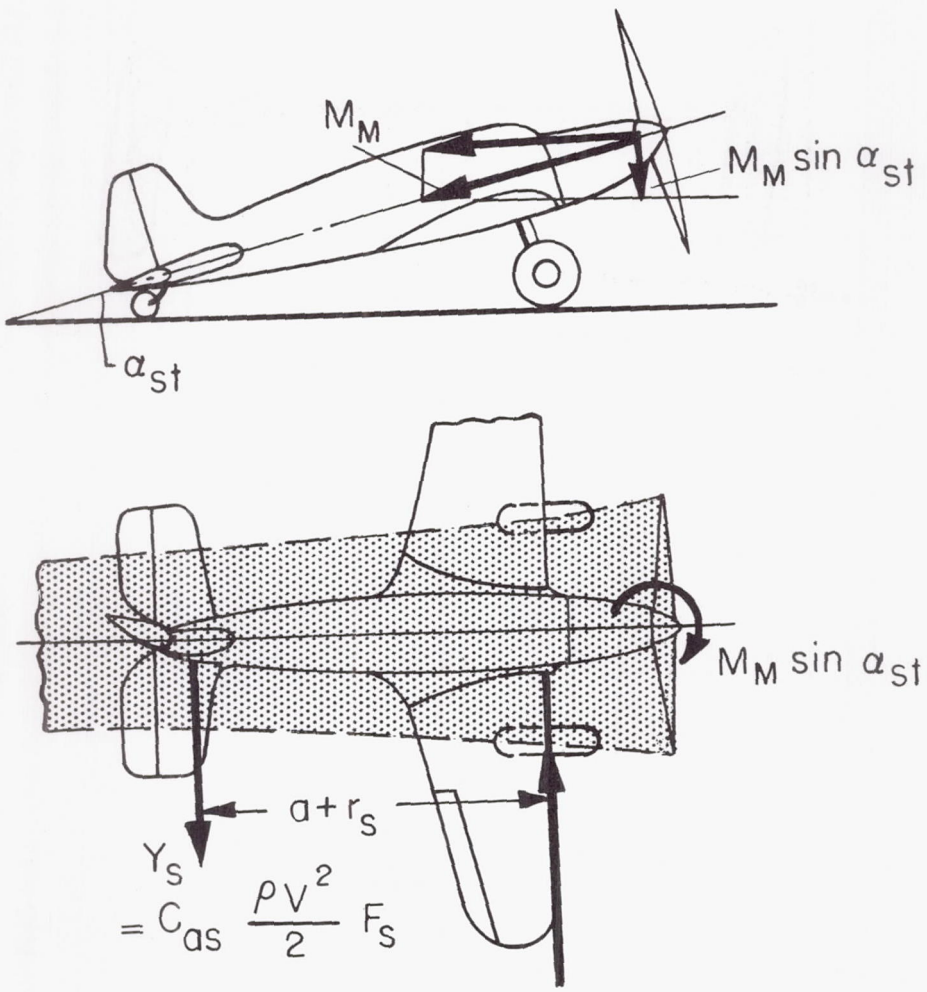

Figure 5.- Moments at beginning of take-off.

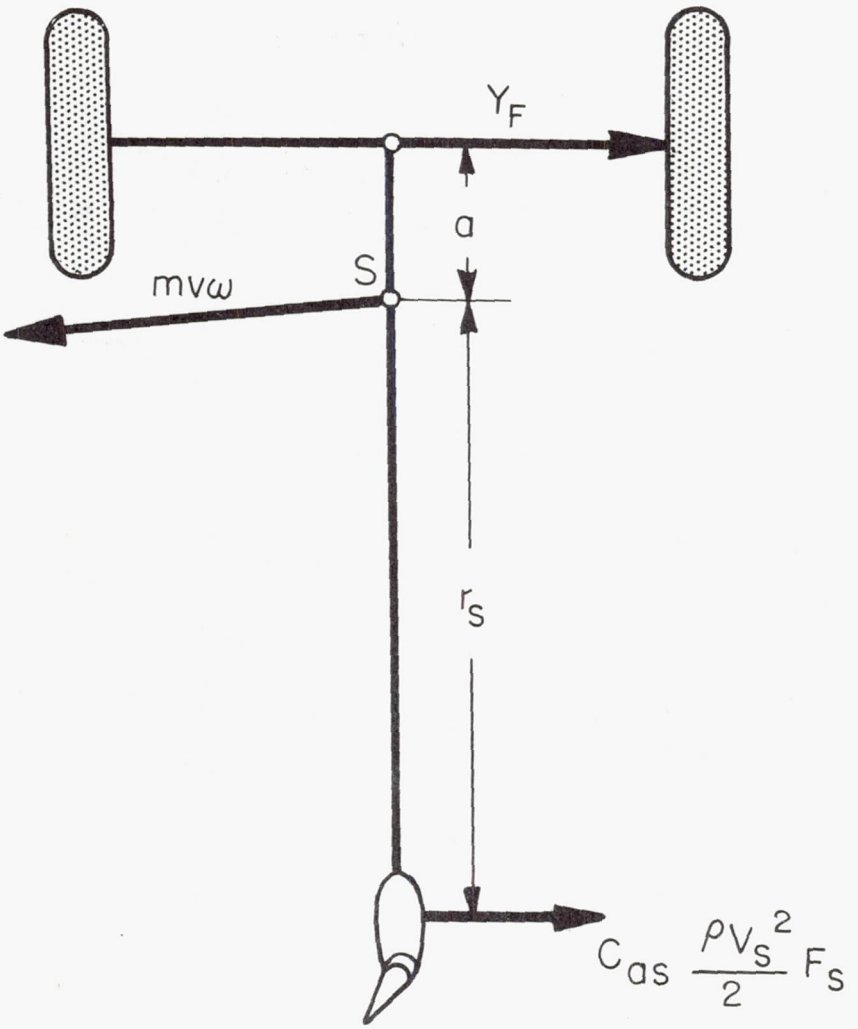

Figure 6.- Vertical-tail-surface effect in rolling with elevated swiveling wheel.

VEERING-OFF (GROUND LOOPING) OF AIRCRAFT EQUIPPED WITH TAIL-WHEEL LANDING GEARS*

By E. Maier

INTRODUCTION

Accident statistics of recent years[1] usually show a large percentage of taxiing mishaps which were caused by veering off (ground looping) of aircraft equipped with tail-wheel landing gears. Consequently, the factors governing such a veering off process had to be investigated. All available data (ref. 1) were mainly of a qualitative nature and were based on evaluations by pilots which naturally do not always agree.

The main reason for the unstable behavior of a tail-wheel landing gear is the fact that the center of gravity is located behind the main landing gear. If the tail wheel does not have a sufficient restoring force, the slightest sidewise deviation of the aircraft will produce a moment from the lateral ground forces at the main landing gear and from the mass inertia. This moment will increase the sideslip angle between longitudinal axis of the aircraft and the direction of motion. That means, it has an unstabilizing effect.

The following investigations cover the most important influences by a theoretical process and disregard a number of viewpoints which may be of importance for the problem.

SYMBOLS

x	originally existing direction of motion
y	horizontal coordinate, perpendicular to x
φ	angle between aircraft longitudinal axis and x-direction
v	taxiing speed
SP	center of gravity

---

*"Das Ausbrechen von Spornradflugzeugen," Bericht 140 der Lilienthal-Gesellschaft, pp. 19-23.

[1]See also the article by Hofmann on pages 1 to 5.

m	aircraft mass
$\Theta = mk^2$	inertia moment about the normal axis
$S_H = C_H\psi$	lateral guiding (cornering) force on both main wheels together
c_H	lateral-guiding characteristic (cornering power)
ψ	yaw angle of tire
P_H	load on the main landing gear
G	gross weight
A	lift
F	wing area
$N = K_N v^2 \tau$	cross-wind force
τ	angle of relative wind with respect to the aircraft longitudinal axis
$M_D = K_D v\dot{\varphi}$	air moment about the normal axis
a	horizontal distance between main landing gear and center of gravity
n	horizontal distance between center of gravity and center of pressure of air
$e^{\lambda t}$	assumed form of solution of the differential equations
λ_1	divergence constant for veering-off
$\chi_N = \frac{K_N k}{m}$	
$\chi_D = \frac{K_D}{mk}$	

ASSUMPTIONS FOR THE CALCULATION

Before establishing the equations of motion, the assumptions made in the calculation must be defined:

1. It is assumed that the aircraft remains undisturbed during the process of motion, i.e., it is not influenced by any deflection of control surfaces or by one-sided braking or by changing engine power. This corresponds to reality inasofar as a certain time always elapses until the pilot notices a change from rectilinear motion and operates the corresponding control device. The time until the control device actually responds also requires a certain length. In the meantime, the veering-off motions can have progressed so far that the airplane can no longer be kept in its original taxiing direction.

2. To produce linear differential equations, the aircraft is assumed to taxi straight ahead in the direction of its longitudinal axis. The velocity of the center of gravity normal to this direction is assumed to be low in comparison to the taxiing speed. The sideslip angles between longitudinal axis and direction of motion are rather low.

3. Any vertical motion of the center of gravity and any rotations about the lateral axis are disregarded.

4. Rotational velocities about the longitudinal axis and thus the elastic or damping effect of the landing-gear struts complicate the calculation considerably and are therefore neglected. A later investigation will have to determine the effect on the veering-off process.

5. The brakes are not used. The veering-off tendency is calculated as a function of the taxiing speed which itself may be regarded as constant during the short time under observation.

6. The propeller thrust has no directional effect since the propeller axis turns with the aircraft longitudinal axis. Consequently, this thrust and the air drag are both disregarded. Any influence on aircraft by the propeller slipstream, the reaction moment of the propeller, or the centrifugal effect of the rotating masses is neglected.

7. The tail wheel is considered to be off the ground or, if it touches the ground, it is assumed to be free of mass and free to swivel, so that no lateral force from the ground is transmitted to the wheel.

8. Calm air is assumed.

9. The equations of motion are established without consideration of any camber or toe-in of the wheels. However, the influence of the toe-in will be given in an example later in the text.

10. Any variations in toe-in during the veering-off process due to elasticity of the wheel suspension are disregarded.

EQUATIONS OF MOTION WITHOUT CAMBER OR TOE-IN OF THE MAIN WHEELS

The motion process is described by a lateral deviation y of the aircraft center of gravity SP from the original center-of-gravity path x (existing at the beginning of the time period under test) and by the angle φ of the aircraft longitudinal axis with the x-direction (fig. 1).

It is assumed that ground forces and air forces act on the aircraft. In a yawed main wheel, side forces are created which can be combined into a force S_H. Since according to the assumptions made, $\dot{y}$ and φ and also the yaw angle ψ remain low, S_H can be assumed to be proportional to ψ which means that

$$S_H = c_H\psi \quad \text{where} \quad \psi = \frac{\dot{y} + a\dot{\varphi}}{v} - \varphi \tag{1}$$

Figure 2 shows the curve of c_H plotted against the load P_H on the main landing gear. When the tail is off the ground, P_H is equal to the gross weight reduced by the lift and, in the case of the skid touching the ground, P_H is equal to the gross weight reduced by the load on the skid.

The resistance to rolling is neglected. If the aircraft is exposed to an airflow inclined with respect to its longitudinal direction by an angle of τ, a lateral air force

$$N = K_N v^2 \tau \tag{2}$$

will be produced which acts at a distance n behind the center of gravity. The rotational velocity $\dot{\varphi}$ changes the sideslip angle along the aircraft. It can be demonstrated that the angle which occurs at the aerodynamic center of pressure should be inserted into the above equation. Consequently,

$$\tau = \frac{\dot{y} - n\dot{\varphi}}{v} - \varphi \tag{3}$$

As soon as a rotational velocity $\dot{\varphi}$ is in existence, an aerodynamic damping moment M_D will result which is due to the fact that one wing has a higher sideslip velocity and thus a higher air drag than the other wing and also by the fact that the sideslip angles are different along the aircraft longitudinal axis. At low sideslip angles and at low rotational velocities, this moment can be represented in the following form:

$$M_D = K_D v\dot{\varphi} \tag{4}$$

Together with the mass force $m\ddot{y}$ and the mass moment $\Theta\ddot{\varphi}$ about the normal axis, the condition of equilibrium of forces in the y-direction and the condition of equilibrium of moments about the normal axis will produce the equations

$$\left.\begin{aligned} m\ddot{y} + S_H + N &= 0 \\ \Theta\ddot{\varphi} + S_H a - Nn + M_D &= 0 \end{aligned}\right\} \tag{5}$$

Using equations (1) to (4), the two coupled linear and homogeneous differential equations

$$\left.\begin{aligned} m\ddot{y} + \frac{1}{v}\left(c_H + K_N v^2\right)\dot{y} + \left(\frac{c_H a}{v} - K_N vn\right)\dot{\varphi} - \left(c_H + K_N v^2\right)\varphi &= 0 \\ ma\ddot{y} + K_N v(a + n)\dot{y} - \Theta\ddot{\varphi} - \left[K_N n(a + n) + K_D\right]v\dot{\varphi} - K_N v^2(a + n)\varphi &= 0 \end{aligned}\right\} \tag{6}$$

are obtained. The assumed solution

$$y = Ae^{\lambda t}, \qquad \varphi = Be^{\lambda t}$$

produces a characteristic equation of the fourth degree for determining λ in which the linear and the absolute term are missing. Consequently, two roots λ are equal to zero while the two other roots are obtained from the dimensionless value

$$\mu = \frac{k}{v}\lambda \tag{7}$$

where k denotes the radius of gyration of the aircraft about the normal axis, obtained from the quadratic equation

$$\mu^2 + \beta_1\mu + \beta_2 = 0 \tag{8}$$

In this case, the following values apply:

$$\left.\begin{aligned} \beta_1 &= \zeta\left(1 + \alpha^2\right) + \chi_N\left(1 + \nu^2\right) + \chi_D \\ \beta_2 &= \zeta\left[-\alpha + \chi_N(\alpha + \nu)^2 + \chi_D\right] + \chi_N(\chi_D + \nu) \end{aligned}\right\} \tag{9}$$

with the dimensionless quantities

$$\alpha = \frac{a}{k} \quad , \quad \nu = \frac{n}{k} \quad , \quad \zeta = \frac{c_H k}{mv^2} \quad , \quad \chi_N = \frac{K_N k}{m} \quad , \quad \chi_D = \frac{K_D}{mk} \tag{10}$$

Stability exists only if β_1 and β_2 are positive. While β_1 always satisfies this condition, the value β_2 may become negative because of the first term $-\alpha$ in the bracket. The center-of-gravity rear position, as mentioned above, is therefore the only reason for the instability of the motion. The air damping always has a stabilizing effect since the terms related to χ_N and χ_D in the equation for β_2 all are positive.

It is readily demonstrated that for taxiing speeds between zero and a critical value v_g one root λ_1 will be positive and the other one negative. Consequently, within this range the aircraft will be unstable, and, at higher velocities, it will again be stable. Numerical calculation shows that the critical velocity v_g is located very near the velocity of take-off, so that the range of stable taxiing becomes practically negligible.

The general integral of the differential equations (6) has the following form for $\lambda_1 \neq \lambda_2 \neq 0$.

$$\left.\begin{aligned} y &= A_1 e^{\lambda_1 t} + A_2 e^{\lambda_2 t} + A_3 + A_4 t \\ \varphi &= \alpha_1 A_1 e^{\lambda_1 t} + \alpha_2 A_2 e^{\lambda_2 t} + \alpha_3 A_4 \end{aligned}\right\} \tag{11}$$

with the constants A_1 to A_4 and α_1 to α_3.

As long as λ_1 remains positive and does not reach too low a value, the first term in equation (11) will dominate after a very short time. The constants A_1 and α_1 depend on the aircraft characteristics and A_1 depends in addition on the initial perturbation. For example, if it is assumed that the angle φ has an initial value of φ_0 at $t = 0$ without presence of a rotational velocity $\dot{\varphi}$, A_1 will be proportional to φ_0.

One of the main problems to be solved is how the veering-off sensitivity should be defined. This tendency for veering off could possibly be defined (under the above initial conditions) as the ratio φ/φ_0 for the aircraft yaw after a definite time at the beginning of the process. However, the mathematical approach is much simpler and produces a similar view for comparisons if the positive value λ_1 (divergence) is used as a criterion for the tendency for veering off. This method was used in the following calculation.

In addition, the numerical value λ_1 representing the limit between permissible and dangerous veering off of an aircraft was to be defined if that is at all possible for any aircraft size in such a definite form.

This problem can be solved only after accurate calculation of a number of aircraft prototypes and cannot be solved at present. However, the influence of various characteristics of the aircraft on the tendency for veering off can be investigated, which is done below in an example. In addition, the tendency for veering off of two aircraft will be compared.

NUMERICAL EVALUATION

For a given prototype which is denoted by A in the following, the tendency for veering-off was calculated according to the above method. The result is shown in figure 3 in which the divergence λ_1 is plotted against the taxiing speed. This diagram shows the relatively rapid increase of this instability during take-off which increases to a maximum value at a medium taxiing speed and then drops to zero at the critical speed v_g. Two attitudes of the aircraft were calculated, namely the attitude with a horizontal fuselage longitudinal axis and an attitude with a large angle of attack in which the tail practically touches the ground. The curves are for constant attitude.

In figure 3, the results with consideration of the aerodynamic damping are compared with the values obtained by disregarding the aerodynamic moment M_D (i.e., at $\chi_D = 0$) or by disregarding the aerodynamic moment and the aerodynamic lateral force $(\chi_D = \chi_N = 0)$. This diagram shows that the aerodynamic moment M_D decreases the tendency for veering off only very slightly. Since the numerical determination of the quantity χ_D is rather time-consuming, this influence is generally disregarded. The lateral force of the air decreases the tendency for veering off in flight attitude considerably, while its influence at large angles of attack is small. Consequently, in the case of high angles of attack the effect of aerodynamic damping is extremely low. For checking the influence of the various characteristics of the aircraft, the stability at high angles of attack is calculated, disregarding the aerodynamic damping, which is permissible especially since the maximum tendency for veering-off occurs in this attitude.

The curves show that the stability occurring at a sufficiently high velocity is not due (as generally assumed) to the increasing influence of aerodynamic damping but much more (and even exclusively at large angles of attack) to the decrease of load on the main wheel by the increase in lift. Although a larger angle of attack is connected with a higher lift coefficient which has a stabilizing effect, the center of gravity is shifted more toward the rear. Disregarding the aerodynamic damping, the two influences according to figure 3 have such an effect that the maximum value of λ_1 in flight attitude is slightly less than at a large angle of attack. Because of the larger effect of aerodynamic damping in flight attitude, this difference is even increased.

The point of intersection of the curves without aerodynamic damping with the abscissa furnishes the velocity at the moment of becoming airborne (lift equals gross weight). Consequently, the velocity range of stable taxiing is negligibly small at large angles of attack but becomes higher

in the attitude of flight. In the second case, instability rarely ever occurs since the take-off and landing speed are much lower. Large angles of attack are the determining factors for these speeds.

The example shows that taxiing at a low angle of attack will produce the lesser tendency for veering off almost over the entire velocity range. On take-off, a large angle of attack becomes more favorable only shortly before the aircraft becomes airborne when the tail is kept to the ground. Generally speaking, the lift coefficient must be as high as possible and the angle of attack of the fuselage axis as low as possible during taxiing. That means, the flaps must be lowered as far as possible. Any twist of the wing with respect to the fuselage would produce the same effect since the center of gravity will not be shifted farther to the rear by this process.

In figure 4, the tendency for veering off of two aircraft prototypes A and B is compared where the damping moment M_D is neglected. The two aircraft have approximately the same wing area and the same radius of gyration about the vertical axis. The aircraft A has a wing loading of 240 kg/m^2 and the aircraft B a wing loading of 170 kg/m^2. The lift coefficient is lower in the aircraft A at equal attitude, which means that this aircraft is considerably faster than the other. It has a landing speed of 195 km/hr compared to 155 km/hr of the aircraft B. The rearward position of the center of gravity of the type A is 35 to 60 percent larger than that of B and, in addition, A is equipped with larger and more rigid tires.

The tendency for veering off of the type A is considerably higher than that of B. A more accurate check of the various influences showed that the main reason for this phenomenon is the much more rearward position of the center of gravity. An additional but less important influence is produced by the lower lift coefficient and by the more rigid tires, while the higher gross weight has almost no influence whatever.

The planned calculation of additional prototypes will show whether a small aircraft shows more danger of veering off than a large aircraft or whether merely the interfering forces (for example, one-sided contact of the propeller slipstream at the tail unit) has a stronger influence in a smaller aircraft.

To test the influence of the various aircraft characteristics, the initial values were changed for the aircraft A, calculated in figure 3 for the attitude of the tail gear practically touching the ground, disregarding the aerodynamic damping. In figures 5 and 6, the divergence is plotted by changing the initial data individually by 10 percent toward the unfavorable side. The plotted effect of the toe-in is discussed below. The peak value of divergence λ_1 obtained from curves of this type is plotted in figure 7 as the ordinate while the modified size relative to the initial value is used as the abscissa.

The following conclusions can be drawn from figure 7:

1. The magnitude of the radius of gyration has the strongest influence on the tendency for veering off. Unfortunately, because of the flight characteristics of combat aircraft, at least, it will never be possible to decrease the tendency for veering off by increasing the radius of gyration.

2. The effect of any rearward shift in center of gravity behind the main landing gear has a very noticeable influence. This rearward distance consequently must be kept as small as possible.

3. The lateral-load characteristic c_H (cornering power) of the main landing gear can be used for noticeably influencing the tendency for veering-off. The main wheels should have sides as soft as possible which requires a special type of tire.

4. Lift coefficient and wing area affect the tendency for veering-off in a similar manner. As mentioned above, a high value of c_α must not be attempted by increasing the angle of attack of the fuselage longitudinal axis but by lowering the flaps. However, this influence is not too large.

5. The smallest influence is produced by the gross weight. This result was entirely unexpected and is caused to the greatest part by the fact that, at increasing load P_H on the main landing gear, the curve of c_H (P_H) becomes flatter, according to figure 2.

INFLUENCE OF TOE-IN ON THE TENDENCY FOR GROUND LOOPING

Recently, the problem has occurred whether a toe-in could possibly affect the tendency for veering off. For solving this problem, the calculation was extended over this particular case. It seems certain that the rotational motion about the longitudinal axis, thus the elastic and damping effects of the landing-gear struts and main tires, have considerable influence. However, for simplification it is assumed in this case also that no compression exists between tire and shock struts. This assumption can at least be considered a critical case which probably will produce the maximum possible influence of the toe-in on the tendency for veering off.

In figure 8, the aircraft is shown with the main wheels installed at a positive toe-in angle ψ_0. The lateral forces of the left-hand or

right-hand wheel are denoted by S_l or S_r. These forces act perpendicularly to the wheel plane. The process of motion will have to include the difference in loads P_l and P_r of the left and right wheel. Both quantities will differ only slightly from the mean load $\frac{1}{2}(P_l + P_r)$ if the quantities $\dot{y}$ and φ are assumed to be small. Consequently, the accurate curve of the tire characteristics $c_{l,r}$ versus the load $P_{l,r}$ can be replaced by the tangent at the point $\frac{1}{2}(P_l + P_r)$ (fig. 9), thus we can write:

$$c_{l,r} = c_0 + c_1 P_{l,r}$$

In addition to the already considered forces and moments there occurs the moment about the longitudinal axis created by the fact that in a rotary motion about the normal axis one wing will have a greater velocity, i.e., a higher lift than the other wing. This moment has the following form:

$$M_A = K_A v \dot{\varphi}$$

where K_A denotes a constant.

The equilibrium conditions (5) are then replaced by the following three equations in which the condition that equilibrium exists about the longitudinal axis has been added:

$$\left.\begin{aligned} m\ddot{y} + S_l + S_r + N &= 0 \\ \Theta\ddot{\varphi} + (S_l + S_r)(a - j\psi_0) - Nn + M_D &= 0 \\ mh\ddot{y} + Nf + (P_l - P_r)j - M_A &= 0 \end{aligned}\right\}$$

The yaw angle of the two wheels changes by $\pm\psi_0$ with respect to equation (1).

The aircraft A with the tail near the ground will be used exclusively in the calculation. Then, the lateral aerodynamic damping, i.e., the quantities N and M_D, can be neglected. Calculation in the

preceding manner will again produce the quadratic equation (8) for determining the divergence λ_1 by means of equation (7). Equations (9) and (10) are then replaced by the following quantities or abbreviations:

$$\beta_1 = \frac{\zeta}{\delta_h}(1 + \alpha\alpha_h) + \frac{\epsilon\chi_A}{\delta_h} \quad , \quad \beta_2 = -\frac{\zeta}{\delta_h}\alpha_h$$

$$\alpha = \frac{a}{k} \quad , \quad \alpha_h = \frac{a - j\psi_0}{k} \quad , \quad \zeta = \frac{c_H k}{mv^2}$$

$$\delta_h = 1 - c_1\psi_0\frac{h}{j} \quad , \quad \epsilon = c_1\psi_0\frac{a - j\psi_0}{k} \quad , \quad \chi_A = \frac{K_A}{mj}$$

As before, c_H denotes the lateral-load characteristic of the two main wheels together, i.e.,

$$c_H = 2c_0 + c_1(P_l + P_r)$$

For a toe-in of 2°, the divergence for the aircraft A without aerodynamic damping is plotted in figure 6 at a large angle of attack. The result shows that the toe-in at lower velocities improves the tendency for veering off only slightly and that the divergence at higher velocity will even be higher. Since a toe-in of 2° represents an almost impermissible increase in tire wear, no toe-in at all should be used. The influences which have been disregarded so far presumably will not increase the effect of a toe-in by as much as one order of magnitude.

ADDITIONAL INVESTIGATIONS

The effect of rolling friction on the tendency for veering off was checked for the case of aircraft A. The maximum of λ_1 is affected with or without toe-in by only a few percent.

An additional calculation was made for determining the effect of any variation in toe-in by elastic suspension of the main wheels. As soon as the elastic axis is located in front of the contact point between wheel and ground, i.e., if the main wheel is constructed similarly as a tail wheel with a pronounced self-alignment, the flexibility of the suspension will decrease the tendency for veering off. Conversely, the

tendency for veering off increases as soon as the wheel has a negative caster which means as soon as the contact point with the ground is located in front of the elastic axis.

SUMMARY

The tendency for veering off (ground looping) of an aircraft equipped with a tail wheel is created by the fact that the center of gravity is located behind the main landing gear. To keep this tendency as low as possible, the rearward distance of the center of gravity should be kept as small as permissible for reasons of a nose-over hazard. An additional decrease in tendency for veering off is produced by increasing the radius of gyration of the aircraft about the normal axis, which is impossible in practice because of the flight characteristics involved. The lateral-load coefficient (cornering power) of the main tires must be as low as possible. This requires development of tires with soft sides. On take-off, as soon as the tail wheel has left the ground, the fuselage should be brought into flight attitude as soon as possible since the rearward distance of the center of gravity is smaller in this position. Only shortly before becoming airborne, the tail should again be lowered slightly toward the ground.

The lift coefficient must be made as high as possible by lowering the flaps (cornering power), since then the main wheels are unloaded and the lateral forces are decreased. At high angles of attack of the fuselage, the lateral aerodynamic damping, thus also the size of the rudder, has practically no influence, but in flight attitude at a higher taxiing speed the tendency for veering off will be influenced by these factors. On take-off, the tendency for veering off increases with the taxiing speed to approximately one half to two thirds of the take-off speed and then drops again. A stable taxiing is reached only shortly before the aircraft becomes airborne. The curve of the veering off divergence versus the taxiing speed is mainly governed by the increasing unloading of the main wheels. A toe-in of the main wheels does not practically influence the tendency for veering-off and should not be attempted because of the increased tire wear. Main wheels, suspended flexibly at a positive caster, will decrease the tendency for veering-off but such a flexibility will be unfavorable for a negative caster.

*Translated and Edited by
the O. W. Leibiger Research Laboratories, Inc.
Petersburg, N. Y. (ATI No. 32512)

---

*Note: In order to provide terminology consistent with other papers of this series, this translation has been reworded in many places by the NACA reviewer.

REFERENCE

1. Klemin, A.: The Phenomenon of Ground Looping. Aircraft Engineering, vol. 7, 1935, p. 81.

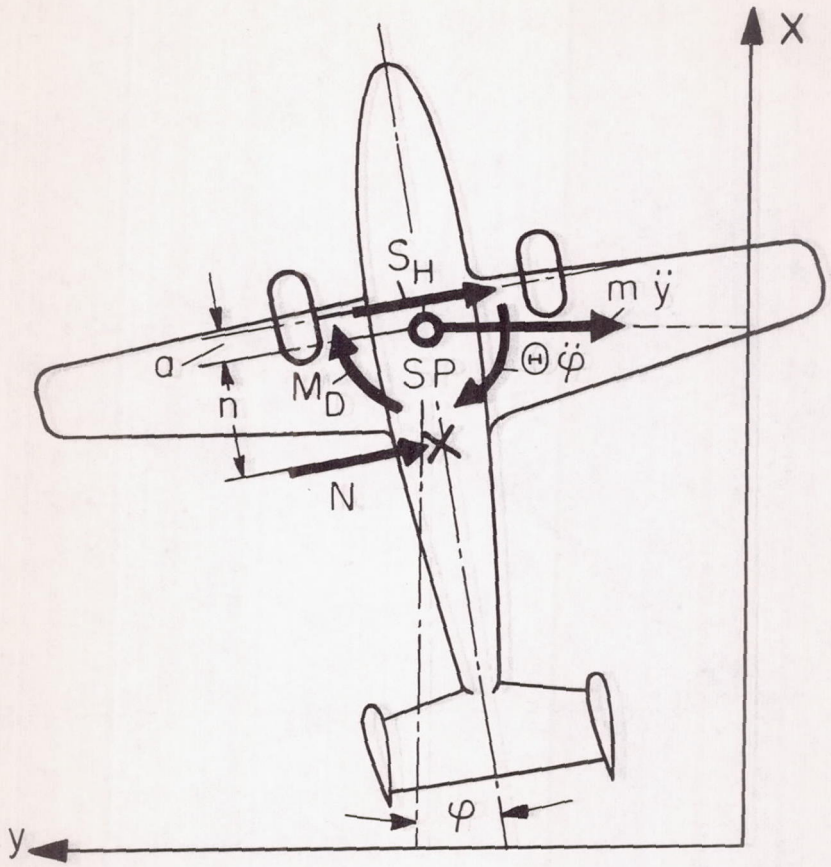

Figure 1.- Forces and moments acting on the aircraft.

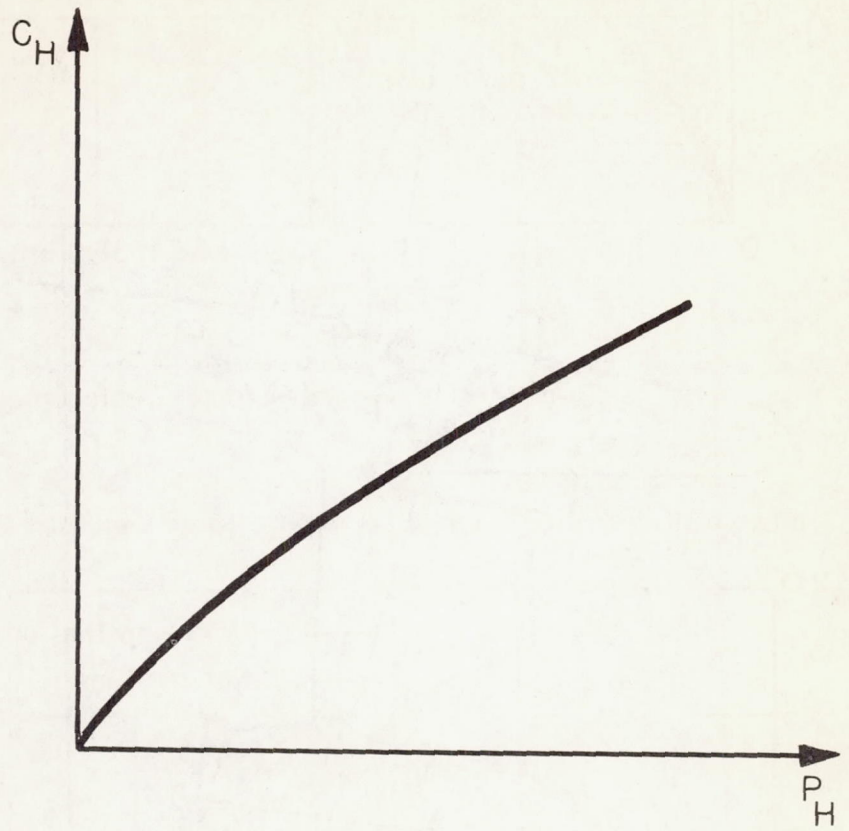

Figure 2.- Lateral-load characteristic c_H (cornering power) plotted against the load P_H of the main landing gear.

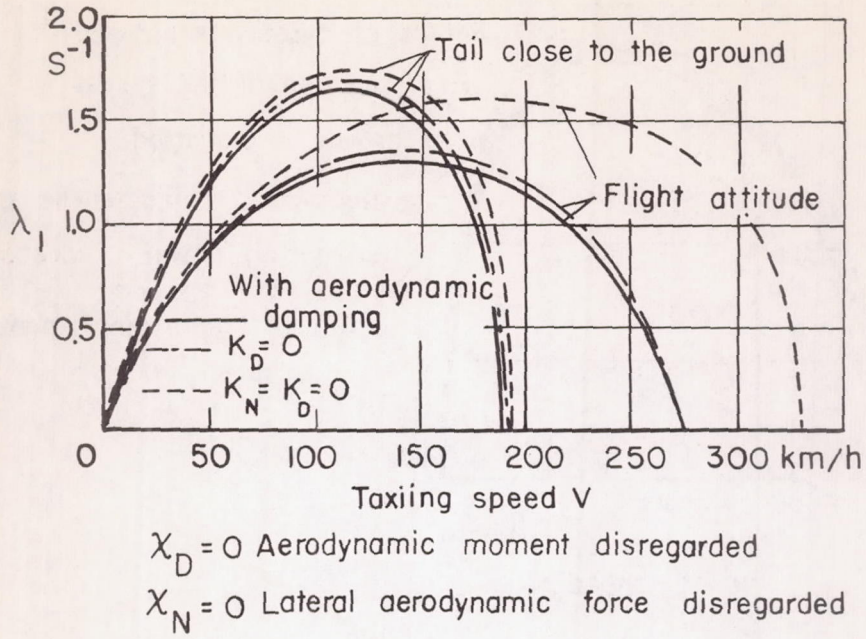

Figure 3.- Tendency for veering-off or divergence λ_1 of the aircraft A in two attitudes with and without aerodynamic damping.

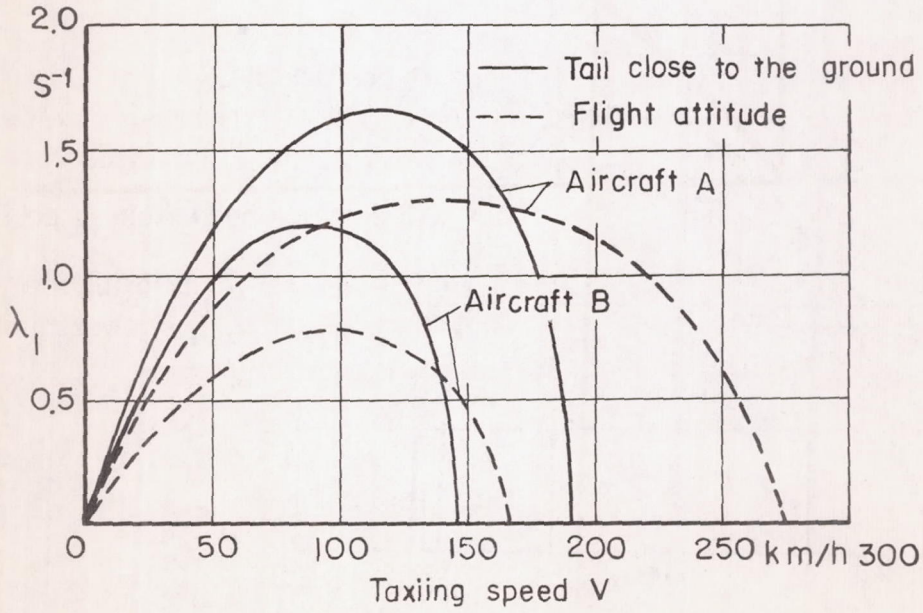

Figure 4.- Comparison of the divergence or tendency for veering-off of two aircraft types.

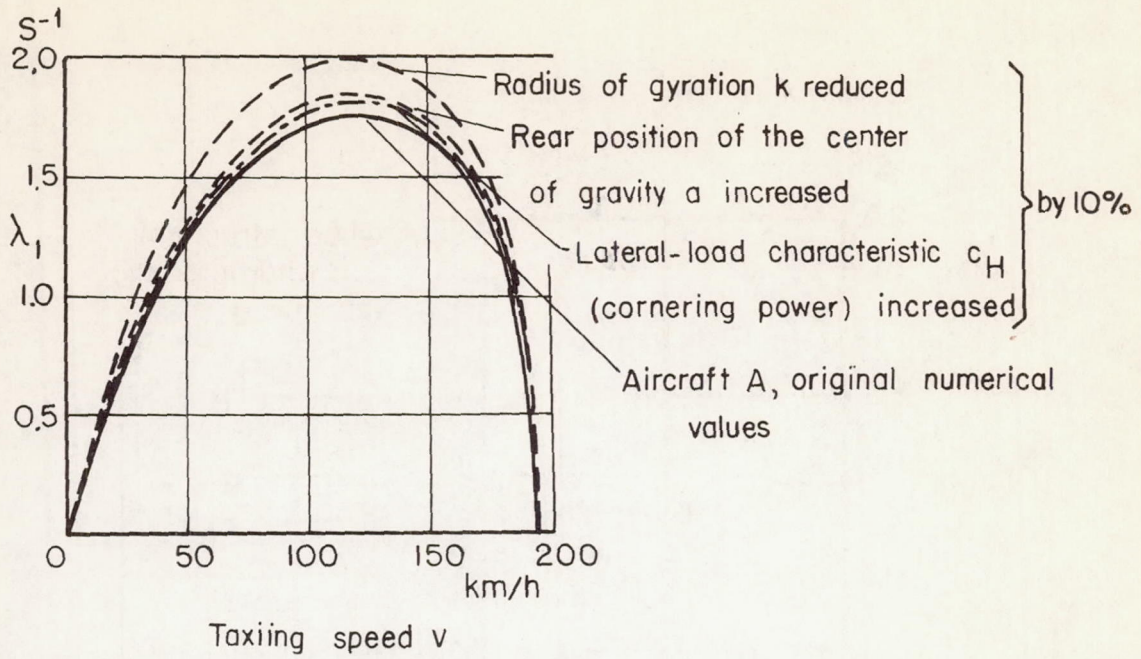

Figure 5.- Effect of a modification of several structural characteristics by 10 percent on the divergence or tendency for veering-off of the aircraft A at large angle of attack.

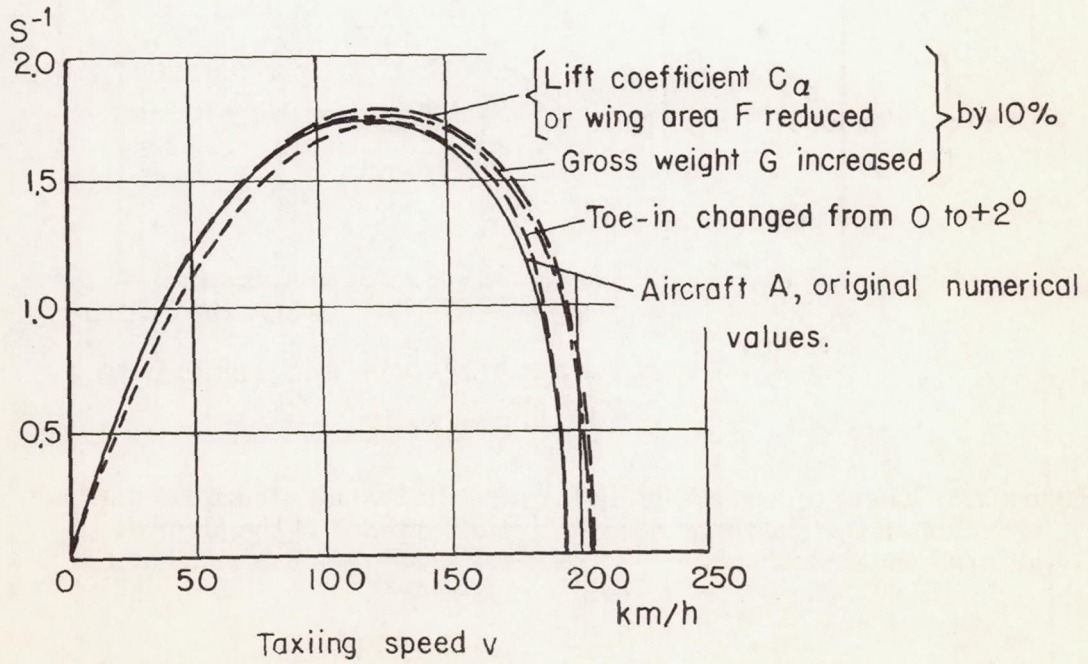

Figure 6.- Effect of the toe-in and of the variation in several structural characteristics by 10 percent on the divergence or tendency for veering-off of the aircraft A at large angle of attack.

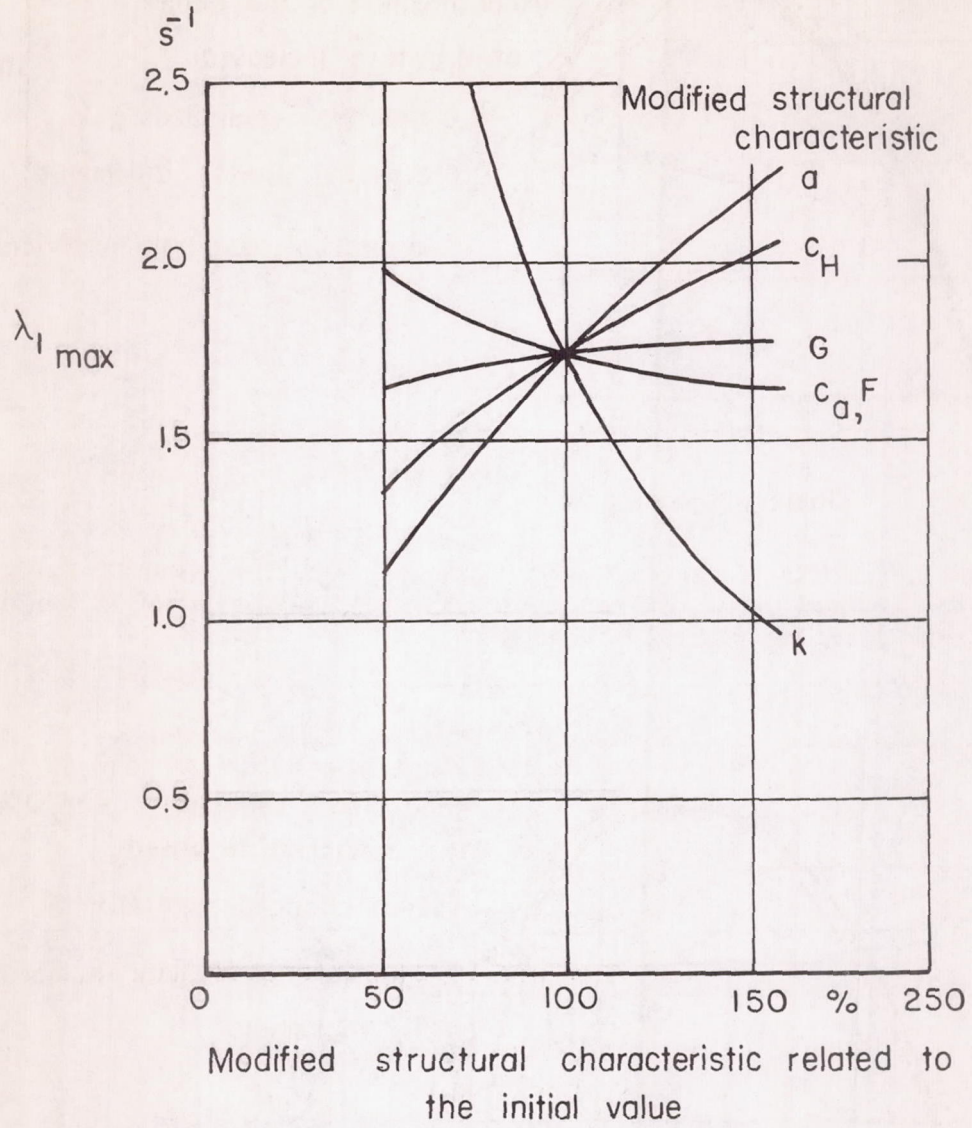

Figure 7.- Effect of a variation in the most important structural characteristics on the maximum value of the divergence of the aircraft A at large angle of attack.

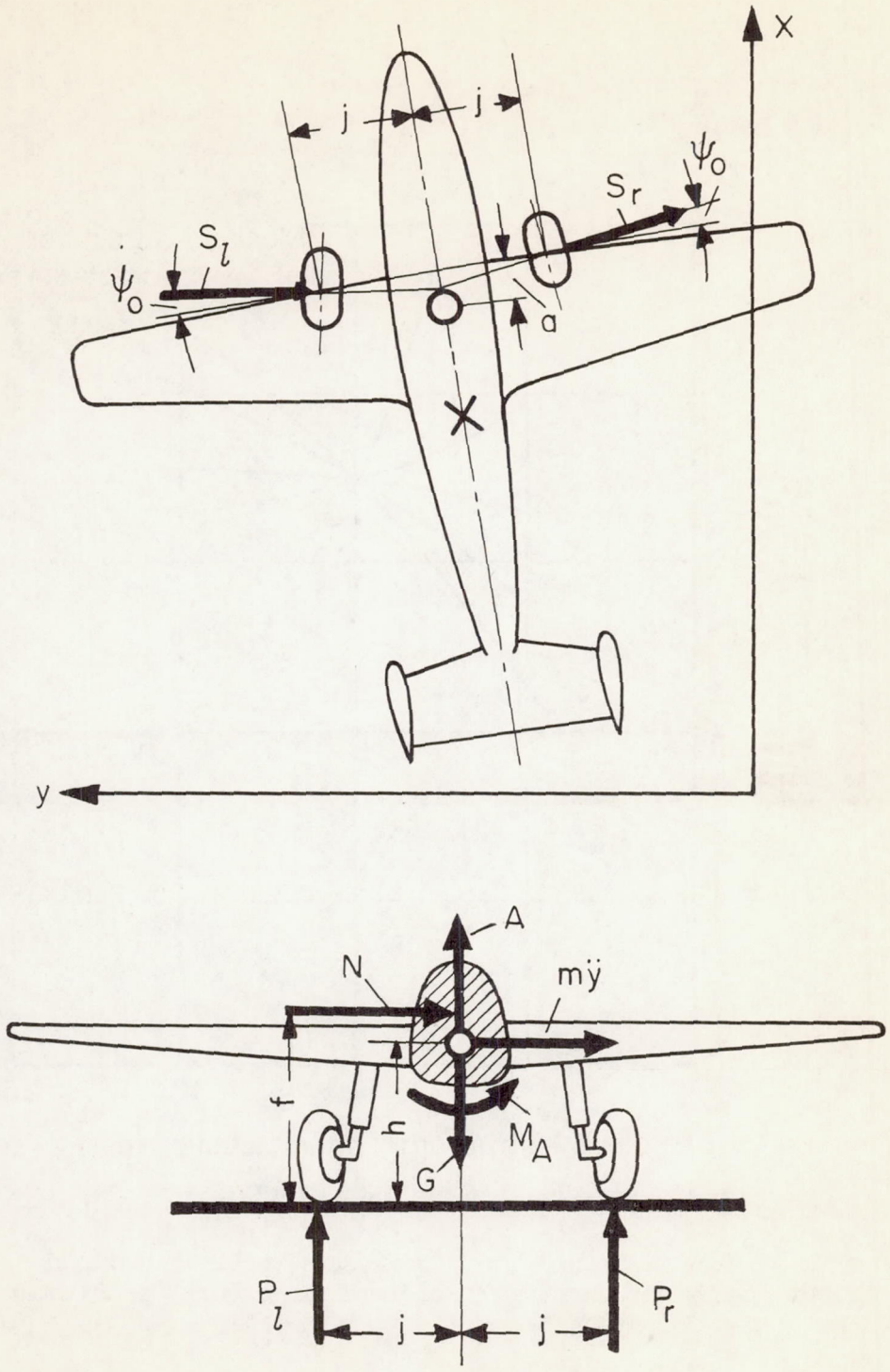

Figure 8.- Forces and moments acting on the aircraft with wheels adjusted to toe-in.

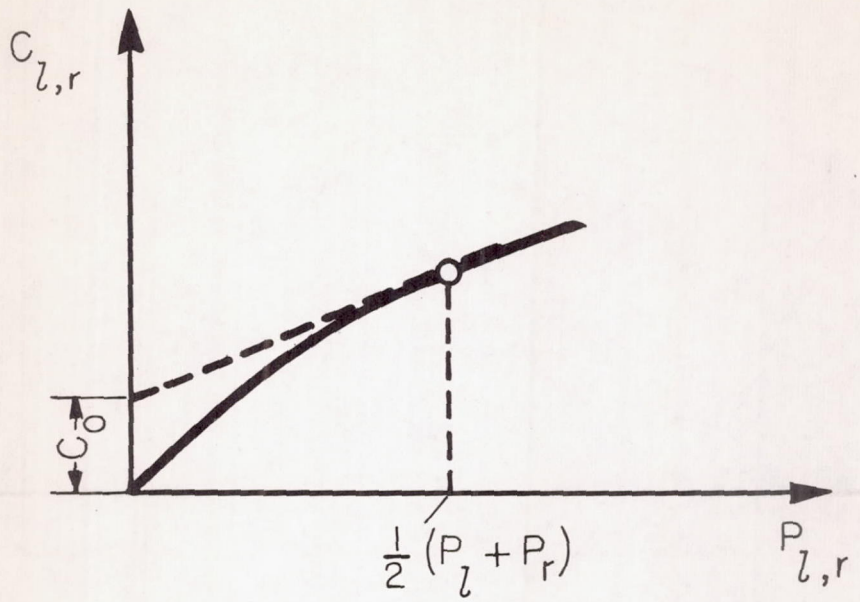

Figure 9.- Lateral-load coefficient c (cornering power) of a wheel versus its load P.

ROLLING STABILITY OF AIRPLANE-LANDING GEARS AND RESULTANT REQUIREMENTS FOR SWIVELING WHEELS

By L. Huber

SYMBOLS AND INTRODUCTION

ψ	Yaw angle of the wheels
P	Wheel load, normal load, taxiing load
S	Lateral guiding (cornering) force
SP	Center of gravity
LP	Center of pressure of the aerodynamic forces
v	Taxiing and flying speed of the aircraft
w_q	Component of the lateral velocity
v_r	Velocity of the resultant relative wind
i	Distance of the center of pressure of the aerodynamic forces from the axis of the leading wheels

The various possibilities of combined effects of air and ground forces on an aircraft produce such different effects on the taxiing behavior that the landing-gear types can be grouped by classes.

Recent data are available for such investigations, which cannot be discussed in detail[1]. Extensive simplifications must be assumed for the discussion given in this paper.

The following investigations assumed a yawed ground contact of the aircraft on a plane runway; thus asymmetrical forces are introduced on the landing gear.

---

*"Die Rollstabilität des Flugzeugfahrwerks und die sich daraus ergebenden Forderungen an das schwenkbare Rad," Bericht 140 der Lilienthal-Gessellschaft, pp. 24-29.

[1]L. Huber, Die Fahrtrichtungsstabilität des schnellfahrenden Kraftwagens. Deutsche Kraftfahrtforschung, Heft 44, Berlin 1940, VDI-Verlag. - P. Riekert und T. E. Schunck, Zur Fahrmechanik des gummibereiften Kraftfahrzeugs. Ing.-Arch., Bd. 11, 1940, S. 210. - E. Sawatzki, Die Luftkräfte und ihre Momente am Kraftwagen. Deutsche Kraftfahrtforschung, Heft 50, Berlin 1941, VDI-Verlag.

It is of no importance for the basic process of veering off or ground looping whether the asymmetrical forces produce a veering toward the right or left.

In addition, the restriction that the pilot does not change the process of motion of the taxiing aircraft is used, which means that the taxiing path is not influenced by any variation in rudder position or by any one-sided braking or accelerating.

AIRCRAFT EQUIPPED WITH TAIL SKID

An aircraft with its center of gravity behind the leading main wheels usually was equipped with a built-in skid for supporting the tail. On yawed ground contact on the runway, lateral forces are created on the elastic main wheels[2] and on the skid which are compensated by an equal mass force acting at the center of gravity SP of the airplane (fig. 1).

The lateral forces may create, in addition to a minor lateral side-slip of the aircraft, a moment even at very low wind, acting from the ground and taking place about the reference point which, for simplicity, is assumed to be located at the center of gravity. In figure 1, v_r corresponds to the geometric sum of all wind velocities resulting from flying speed and from head-wind velocity. The tail skid, which buries itself in the soft turf, obtains a relatively larger lateral guiding force than the main wheels. This returns the airplane into its original taxiing direction.

The result is a restoring ground-force moment which reduces the yaw angle ψ on the wheels. The landing gear is controlled at the front and rear which means it represents a 2-axes system which is stable with respect to the ground.

THE TAIL-WHEEL AIRCRAFT

With introduction of an easily swivelable tail wheel, the lateral guiding or cornering force is eliminated and thus also the restoring

---

[2]This fact was determined and published already by H. Fromm eleven years ago. Cf. G. Becker, H. Fromm, and H. Maruhn, "Schwingungen in Automobillenkungen." Berlin 1931. - For further sources, see list of references in Deutsche Kraftfahrtforschung, Heft 44 and the lectures of the present report by Harling, p. 7, Schrode, p. 17, and Kraft, p. 31.

ground-force moment on the tail skid. At low air forces, i.e., low landing speed or low wing loading, the aircraft is first put transverse to the taxiing direction by the ground-force moment and is then turned by 180° in the form of a spiral.

The landing gear then becomes a single-axis system and is unstable with respect to the ground.

Only if the air forces are sufficiently large (v_r must have a high value), the rudder unit will produce air forces which can be combined at the center of pressure LP of the lateral wind force and which produce a restoring air-force moment. The airplane will then travel mainly in the direction of the resultant air flow. That means, this uniaxial landing gear is then not only unstable with respect to the ground but also sensitive to wind.

The lateral elasticity of the tire affects the veering off process. In tires with hard sides, this veering is much more violent and is rather slow in soft tires, since such tires absorb smaller lateral forces than hard tires on yawed ground contact (see footnote 2).

TAXIING LOAD AND LATERAL-GUIDING FORCE

The lateral guiding or cornering force S (fig. 2) increases with increasing yaw of the wheel (yaw angle ψ). In a wheel with stiff sides, this force, starting from zero, increases suddenly and then remains rather constant with respect to the yaw angle ψ. During this process, any doubling of the wheel load P will produce also a doubling of the lateral guiding force.

In a laterally elastic wheel, the lateral-guiding force increases more slowly with the yaw angle ψ.

At more pronounced yawed positions, a doubling in lateral-guiding force is obtained on doubling the wheel load. However, in the range of small yaw angles, the increase for the higher-loaded wheel remains smaller ($c > d$). This fact is of considerable importance for the following discussion of the behavior of biaxial and multiaxial landing gears.

THE FIXED TAIL WHEEL

A fixed tail wheel equipped with pneumatic tires absorbs a lateral force similarly to the rigid tail skid (fig. 3). According to the variation of lateral force of an elastic wheel in figure 2 in which similar

tires were used, the main wheels, under higher load and located directly in front of the center of gravity, will transfer lower lateral forces per unit of normal load than the less heavily loaded tail wheel tire. Consequently, on a plane hard surface a restoring ground-force moment is created on the biaxial landing gear as long as the tail wheel rolls over the runway at its normal load.

The lateral-guiding force on the wheel can be varied by the type of tire construction, inflation pressure, rim width, and primary dimensions, at least within certain limits.[3] The ground moment may be affected by these values. However, any such influences are disregarded in this report.

The fact that this biaxial landing gear is stable with respect to ground only under certain conditions is of considerable importance.

Under the effect of the resultant air velocity v_r, the landing gear is turned in direction of the resultant air flow by the air forces acting on the rudder unit. Thus the landing gear is still wind sensitive.

THE TAIL-WHEEL AIRCRAFT INSENSITIVE TO CROSS WIND

If it were possible to shift the position of the resultant lateral air force toward the front into the vicinity of the center of gravity until the sum of the lateral air and ground forces and the resulting moments (related in this case to the center of gravity SP) would become zero, a biaxial landing gear would be obtained which is stable with respect to the ground under certain conditions and insensitive to cross wind. The restriction "under certain conditions" means that the landing gear has these characteristics only as long as the tail wheel rolls along the ground at a sufficient load. The aircraft will then no longer attempt any veering off or ground looping and will not run into the wind. The lateral wind forces will be absorbed by a slight yaw of the wheels, i.e., by only slight turning of the aircraft into the wind direction.

For this purpose, the following conditions would have to be satisfied:

1. The rudder surfaces would have to be decreased considerably which means the flight characteristics of the aircraft would become changed (deterioration of the flying stability).

---

[3] Cf. lectures of Harling, p. 7, and Schrode, p. 17, in the present report.

2. The tail wheel would have to be fixed in the direction of the aircraft longitudinal axis.

3. The tail wheel would have to roll along the ground at a sufficient normal load.

THE NOSE-WHEEL AIRCRAFT

The rather difficult conditions for a pilot, given above, are eliminated in a nose-wheel landing gear (fig. 4).

At low air forces, a uniaxial nose-wheel landing gear is always stable with respect to the ground, no matter whether the nose wheel is still in the air or has touched the ground since the freely swivelable nose wheel does not create any lateral forces.

The lateral guiding or cornering forces acting on the main wheels behind the center of gravity will turn the aircraft into the direction of travel.

In a cross wind, the airplane will turn into the direction of the resultant air flow under the effect of the air-force moment.

The position of the center of pressure LP of the lateral wind force behind the center of gravity SP is given by the flight characteristics. Generally, the center of gravity is only sufficiently far in front of the axis of the main wheels that the aircraft can still tilt toward the front without creating too high a load on the nose wheel.

Because of the slight distance of the center of gravity from the main wheels, i.e., because of the short lever arm at which the lateral guiding forces of the wheels act, a relatively small restoring ground-force moment becomes effective. The uniaxial landing gear can be easily turned about the leading main wheels. The aircraft will then turn more readily into the direction of the resultant air flow than the tail-wheel landing gear with a fixed tail wheel touching the ground in which a change from the taxiing direction is possible only by lateral deformation of the tires.

THE NOSE-WHEEL AIRCRAFT INSENSITIVE TO CROSS WIND

The nose wheel will become less sensitive to cross wind if the distance between the transverse forces on the fixed wheels and the center of pressure LP of the lateral wind force are decreased.

If the aircraft characteristics, i.e., the position of the center of gravity with respect to the center of pressure of the air, remains unchanged, the attempt of the air-force moment to turn the aircraft into the resultant wind direction can be eliminated by shifting the axis of the leading main wheels back into the plane going through the center of pressure of the lateral air force.

If one now takes into account the changing wheel load between left and right main wheels, previously neglected in the action of the side force, and the thereby arising small ground-force moment, then one arrives at a final position of the main wheel axis slightly in front of the center of pressure LP.

This uniaxial landing gear is then not only stable with respect to the ground but also insensitive to cross wind. For resisting the cross-wind forces, the aircraft will turn its longitudinal axis slightly yawed to the main taxiing direction by turning slightly into the wind. This may create corresponding guiding forces on the leading main wheels, corresponding to the cross-wind pressure.

Even at sudden cross-wind gusts, the aircraft will continue essentially in its original landing direction.

This backward shift of the main wheels or forward shift of the center of gravity increases the portion of the load on the nose wheel. Consequently, it seems logical that the aircraft designer would prefer different measures for increasing the insensitivity to cross wind.

FIXED NOSE WHEEL

The taxiing behavior of a nose-wheel landing gear with a fixed nose wheel and small wind forces is determined by the side forces on the wheels (fig. 5). Since the center of gravity is located slightly in front of the main wheels, the nose wheel has relatively low load. Its lateral guiding force is therefore relatively larger per unit of normal wheel load (according to fig. 2) than the lateral guiding forces on the main wheels. If it is assumed for simplification that the mass system turns about the center of gravity, then a ground-force moment is created on the biaxial landing gear, which will turn the aircraft from its taxiing direction. The airplane will then become unstable with respect to the ground. The tendency for ground looping increases when the mass forces produce an additional higher load on the nose wheel.

During an additional cross wind, the air-force moment, turning in the same direction, will have an influence, so that the aircraft tends to turn rapidly into the resultant wind direction.

Consequently, a fixed nose wheel will produce a biaxial aircraft which is unstable with respect to the ground and is also wind-sensitive.

SWIVELABLE NOSE WHEEL

The idea of designing a swivelable nose wheel so that the ground and air-force moments will be compensated by yawing of the nose wheel was a logical development. Generally, the required restoring ground moment can be produced by turning the nose wheel.

However, the assumption made above that the taxiing behavior is to be independent of the operation by the pilot must then be abandoned.

The airplane landing gear with a swivelable nose wheel must have the same stability behavior with respect to the ground forces as a biaxial automobile steered at the front.

The center of pressure of the resultant lateral wind force is not located behind but in front of the center of gravity in the case of a motor vehicle. This is due to the fact that the air forces, especially in an aerodynamically-favorable body such as an airship hull from which the fins and rudders were removed, act far at the front of the body.

Consequently, in a cross wind an air force acts on a vehicle in front of the center of gravity, resulting in an air-force moment related to the center of gravity which attempts to push the car transverse to the resultant direction of the air flow.

MOTOR VEHICLE SENSITIVE TO CROSS WIND

The behavior of a high-speed car was clarified by means of model tests along a "running track" (continuous belt). The model vehicle, in the left of figure 6, runs from the bottom to the top at a velocity of 150 km/hr[4] along the center of the track which corresponds to the width of a four-lane highway. In the second part of the photograph, the car is exposed to a gust which strikes the car at a speed of 14 m/sec perpendicular to the vehicle. After half a second, the vehicle has already reached the edge of the track. During this process, it was assumed that the driver had not moved the steering wheel at all.[5]

---

[4]The model values have been converted according to the model rules for the actual vehicle.

[5]The hand of the clock provided at the right in the moving picture revolves once in 0.6s, here contrary to the usual sense of rotation of the clock.

The air forces increase with the square of increasing velocity. At the same time, the time during which the vehicle travels up to the edge of the track is shortened.

Check tests of the Institute on the reasons for the accident of Rosemeyer on the Frankfort racetrack showed that the gust had turned the racing car of Rosemeyer within a period of 0.1 sec and had pushed it to the edge of the track in this time.

However, a well-trained driver expecting such an accident will require approximately 1/2 sec for compensating this motion of the vehicle. An average driver or a person not expecting such a wind gust will need at least 1 sec to release a required ground countermoment by turning his steering wheel. This created the concept "horror moment".

Consequently, the behavior of the vehicle in the example of figure 6 at the left-hand side is dangerous since the vehicle reaches the edge of the track in such a short time that not every driver can compensate the motion by proper steering.

This danger to motor vehicles at high speeds was felt more keenly after the German superhighways had come into use and presented the problem of eliminating this hazard. Wind-tunnel tests, model, and actual highway tests produced the principles for design of a vehicle insensitive to cross wind.

Attachment of fins made it possible to shift the point of action of the air sufficiently far toward the rear (this point usually lies far in front of the center of gravity) that the desired compensation of side forces and moments was produced. However, the fins must be correctly designed and dimensioned. Excessively large fins would make the vehicle yaw toward the wind and would thus cause it to run into the wind.

The effect of correctly designed and dimensioned fins is shown in the right-hand side of figure 6 where the travel of a vehicle insensitive to cross wind is shown. This vehicle travels on the small track at a speed of 150 km/hr and in a cross-wind gust of 14 m/sec velocity without any action by the driver. During this process, the vehicle changes to a sufficiently yawed position with respect to its direction of motion such that the cross-wind forces can be resisted by the lateral guiding forces of the yawed wheels.

The process in a controlled nose-wheel landing gear corresponds accurately to that determined in an ordinary motor vehicle with the exception that the aircraft runs into the wind.

The uncontrolled nose-wheel landing gear with a freely swivelable nose wheel also turns rapidly into the wind as soon as a cross-wind force

is exerted on it and leaves the narrow track (fig. 7, left-hand side). The nose-wheel landing gear insensitive to cross wind behaves exactly as the motor vehicle which also is insensitive to cross wind (fig. 7, right-hand side).

STABILITY CLASSES

The described aircraft-landing gears, together with the motor vehicles, can be grouped in five stability classes.

The most favorable taxiing behavior will be denoted by I and the most unfavorable by V (fig. 8).

The uniaxial controlled tail-wheel airplane which is unstable with respect to the ground and runs into the wind belongs in the stability class V. Such an aircraft requires a circular airfield because of the varying directions of wind.

At a high wing loading, i.e., with small rudder surfaces, the lower limit of possible reaction period is reached. In this case, the taxiing motions are no longer entirely controllable and extensive training of the pilot is required for rapid and correct reactions.

The stability classes II to IV which may be denoted as "safe under certain conditions" follow at a rather large distance.

In class IV, the steerable biaxial nose-wheel landing gear corresponds to the motor vehicle with the load at the rear axle which consequently is unstable with respect to the ground and sensitive to cross wind. The driver of such a vehicle is required to move the car in opposite direction to the veering motion within the reaction time. The racing car of Rosemeyer, discussed above, belongs in this class.

A motor vehicle may be considered safe it it can travel at high speed on a narrow highway with a good grip, i.e., if the driver has sufficiently long reaction times for operating the steering mechanism. If this is not the case, the highways must be made wider, as for example had been the case in the raceway belonging to the Reich superhighway near Dessau.

At higher speeds therefore the tracks for cars or aircraft in this stability class must be at least between 40 to 80 m wide.

The landing gear of a uniaxial aircraft with a freely swivelable nose wheel belongs in the stability class III. This landing gear is stable with respect to the ground but runs into the wind.

The biaxial aircraft with a fixed tail wheel belongs in the stability class IIb. The letter b represents the restriction that this stability degree can be reached only if the compression between wheel and ground is sufficiently high.

The biaxial vehicle which has the main load on the front axle since its center of gravity lies in front of the axis center can be grouped in stability class IIa. This vehicle has the advantage over the aircraft IIb that its stability is definitely maintained by the continuous control of all four wheels. The vehicle is sensitive to cross wind but stable with respect to the ground and therefore will not leave the track as readily during a cross-wind gust. Consequently, the track for class II may be slightly more narrow even at high velocities.

Stability class Ib includes the tail-wheel airplane with a fixed wheel but reduced rudder surface, i.e., with changed flight stability.

If the assumption (indicated by the letter b) that the tail wheel touches the ground is not made, the stability behavior immediately changes into class V.

This restriction does not apply to the biaxial vehicle insensitive to cross wind nor to the uniaxial nose-wheel landing gear insensitive to cross wind, both belonging to class Ia.

The requirement as to width of the runway can be reduced because of the stability conditions in taxiing. A width of 10 m may be sufficient since the controller of the landing gear has longer reaction periods at his disposition.

REQUIREMENTS FOR A SWIVELABLE WHEEL

The requirements made on a swivelable wheel result necessarily from the desired stability conditions:

1. The nose wheel must be freely movable for any slow swivel motion of the aircraft and any necessary damping must be adapted to this condition.

2. The tail wheel of an airplane must be fixed during landing or take-off and be freely movable only for a slow rolling motion.

In contrast to the motor vehicle, the nose-wheel landing gear which is insensitive to cross wind has no wheel control. At high speed, the necessary moments for a desired variation of the taxiing direction can be produced by air forces acting on the rudder or, in slow taxiing, by

a one-sided braking or racing of the engines. The pilot will then notice that the landing gear which is stable with respect to the ground will not change its taxiing direction as readily as the conventional unstable tail-wheel landing gear.

Naturally, an additional steering mechanism can be installed in the nose-wheel suspension but this is for exerting a steering force only in slow taxiing.

GENERAL DEVELOPMENT TREND

The progress made by changing from the stability class V of the tail-wheel aircraft to the stability class III of the conventional nose-wheel landing gear has been felt to be so considerable that, at the moment, class I stability for aircraft has not yet been demanded.

The time at which a solution for a cross-wind-insensitive nose-wheel landing gear will be demanded depends only on the extent of possible increases in the wing loading of aircraft and on the desire or necessity of building more narrow runways. The taxiing behavior of aircraft will most probably approach more and more that of a motor vehicle at higher speed; never will it differ from it more than now.

Research on automobiles was stimulated to strive for class I stability by the construction of German superhighways and the general increase in automobile speeds.

The resultant data, which could be obtained only after decades of research in the development of the earth-bound motor vehicle, can now be used judiciously for further development of aircraft.

HYPOTHESES FOR A LANDING GEAR STABLE IN ROLLING

In the literature in the U. S., a nose-wheel landing gear generally is known under the designation of tricycle landing gear. The concepts of nose-wheel landing gear or tricycle landing gear however may not completely cover the existing problem.

Several examples (fig. 9) show that the favorable effect of a ground-stable landing gear in combination with insensitivity to cross wind can be obtained also by different arrangements of swivelable and fixed wheels.

The main presupposition is location of the center of gravity in front of the main wheels. In addition, the resultant of the guiding forces on

the main wheels must act shortly in front of the center of pressure of the resultant lateral air force and the swivelable wheels must be attached in front of the center of gravity of the system.

The classification of landing gears according to their stability behavior and establishment of requirements on the swivelable wheel were made here on the basis of visual considerations.

The theoretical and experimental results, as well as a film[6] of the model tests, confirm these statements.[7]

*Translated and Edited by
the O. W. Leibiger Research Laboratories, Inc.
Petersburg, N. Y. (ATI No. 32171)

---

[6]"Das Verhalten des Flugzeugs auf dem Rollfeld bei Seitenwind." Research film 2 of the ZWB.

[7]Cf. in present report the lectures of Scheubel, p. 41, E. Maier, p. 59, and T. E. Schunck, p. 103.

*Note: In order to provide terminology consistent with other papers of this series, this translation has been reworded in many places by the NACA reviewer.

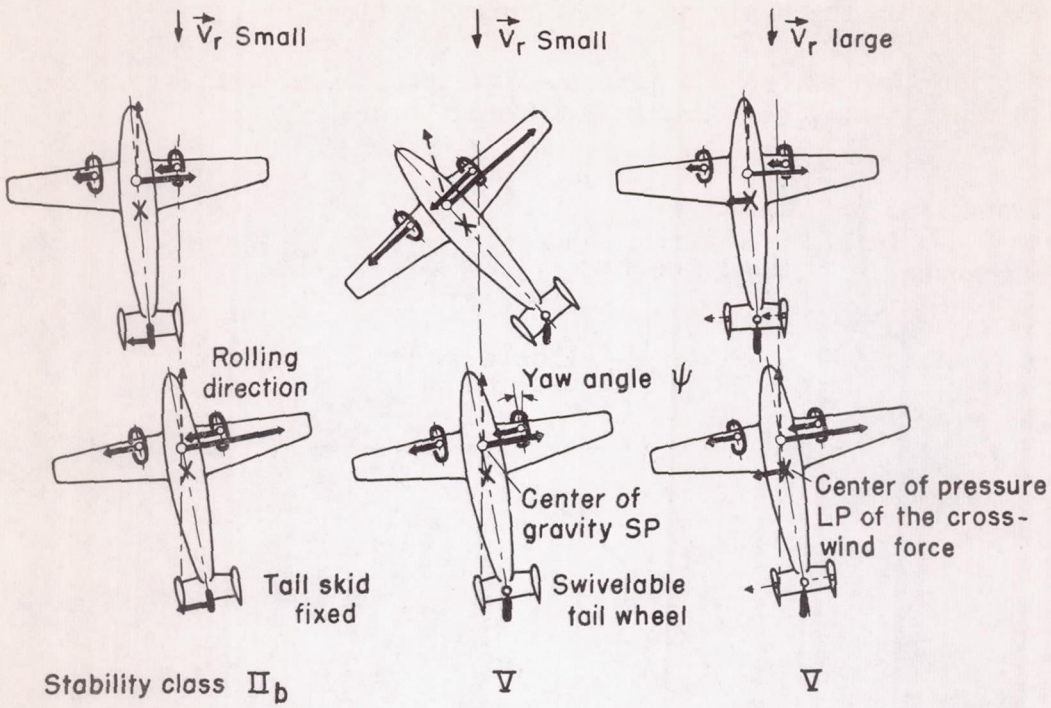

Left-hand side : Fixed tail skid
Center : Freely swivelable tail wheel, low wind velocity
Right-hand side : Freely swivelable tail wheel, high wind velocity, landing in direction of wind

Figure 1.- Taxying behavior of modern tail-skid and tail-wheel landing gears.

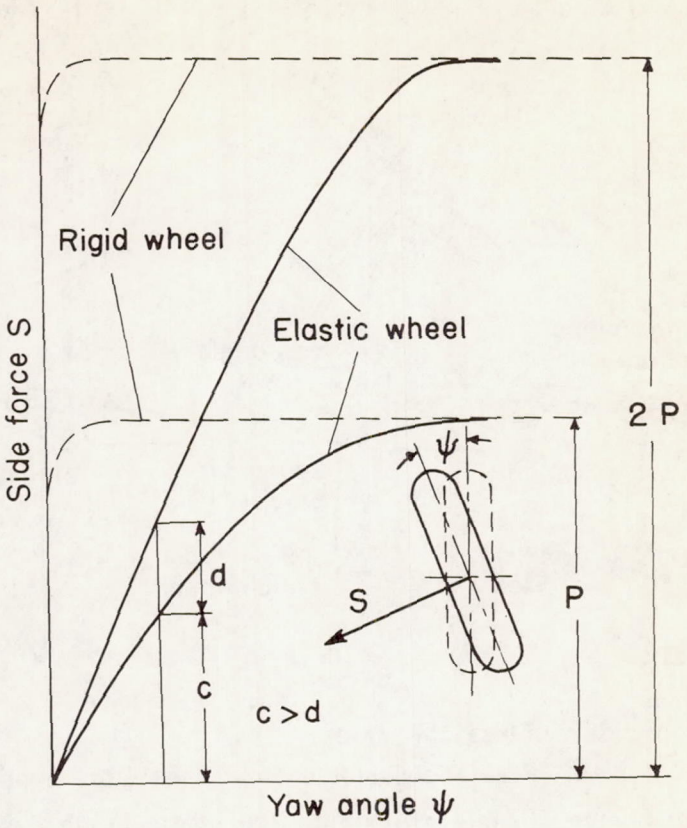

Figure 2.- Taxying load and lateral guiding or cornering force of tires with laterally rigid and elastic wheels.

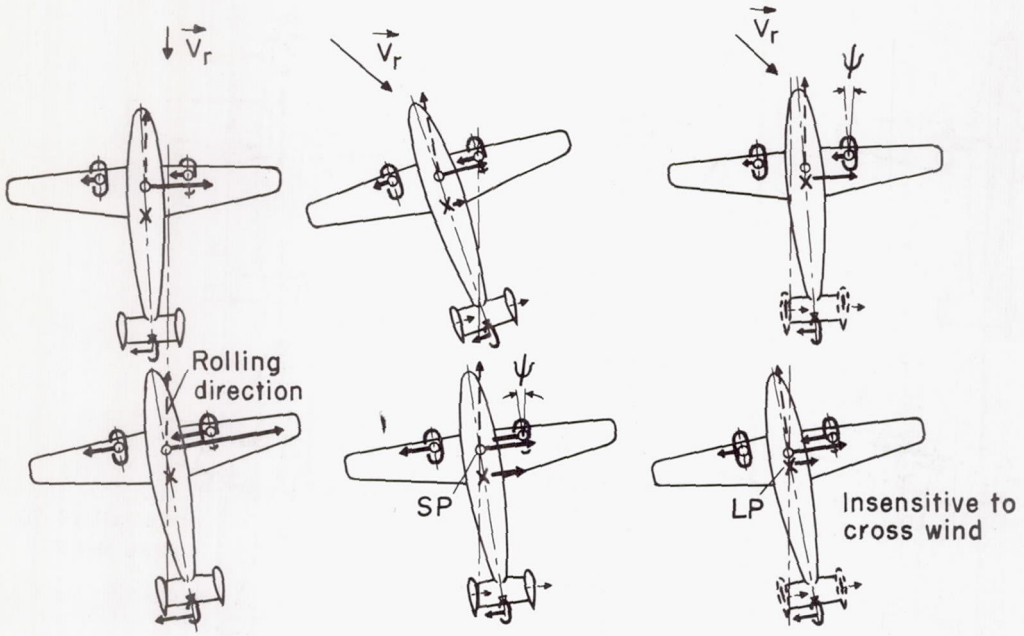

Left-hand side : Fixed tail, low wind velocity

Center : Fixed tail, cross wind

Right-hand side : Fixed tail, cross wind

Reduced rudder area produces a cross-wind-insensitive taxying behavior

Figure 3.- Taxying behavior of an aircraft with fixed tail wheel.

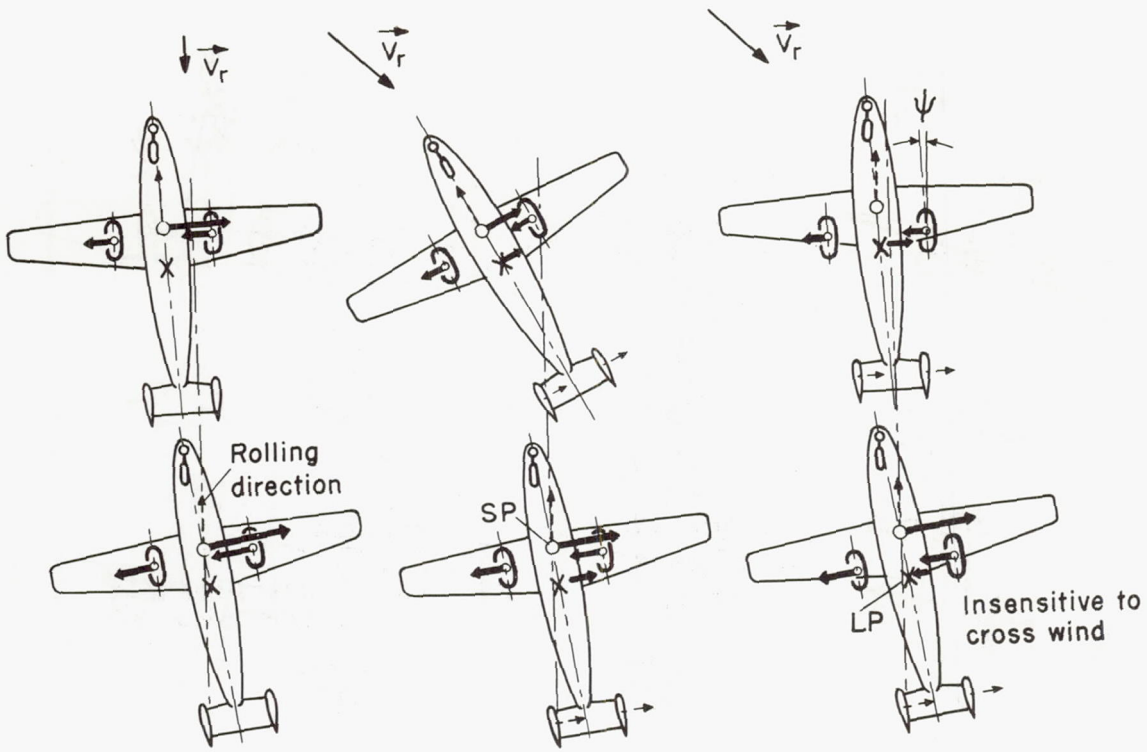

Left-hand side: Freely swivelable nose wheel, low wind velocity

Center: Freely swivelable nose wheel, cross wind

Right-hand side: Freely swivelable nose wheel, cross wind

Axle of the main wheels was shifted backward which produced cross-wind-insensitive taxiing behavior

Figure 4.- Taxying behavior of the nose-wheel landing gear.

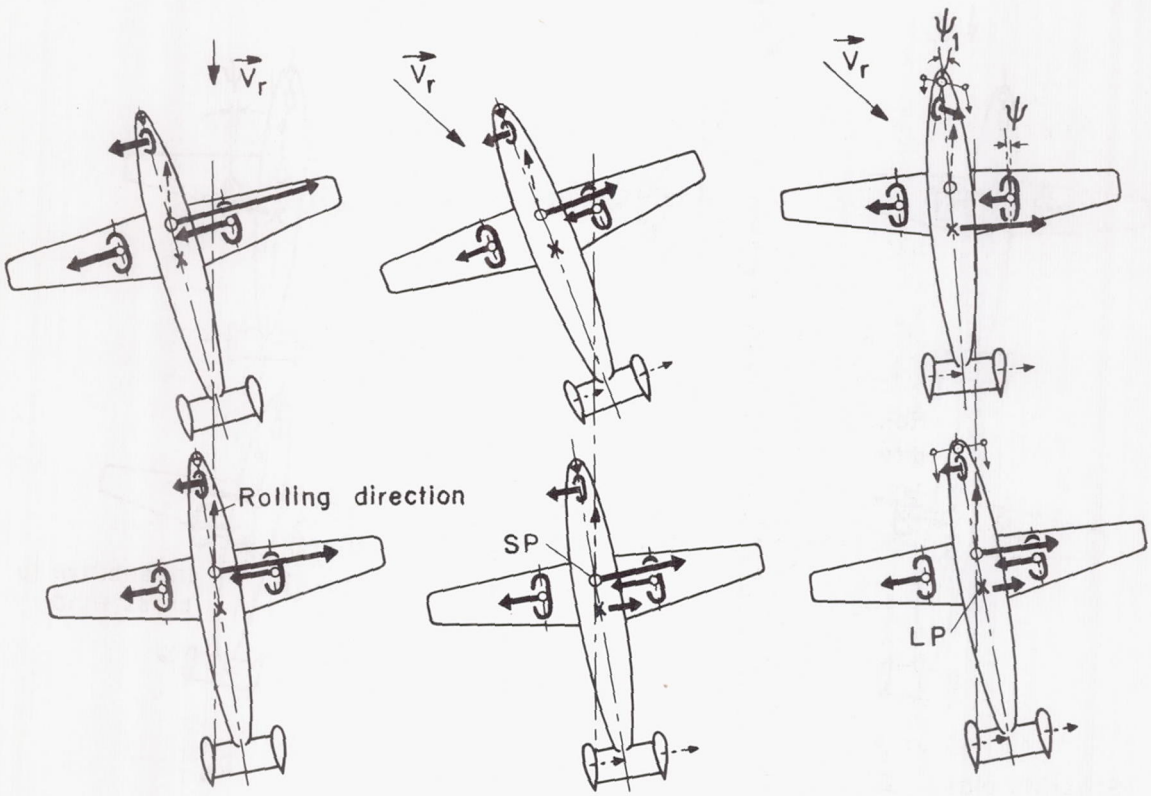

Left-hand side: Fixed nose wheel, low wind velocity

Center : Fixed nose wheel, cross wind

Right-hand side: Controlled nose wheel, cross wind

Figure 5.- Taxying behavior of fixed and steerable nose wheel.

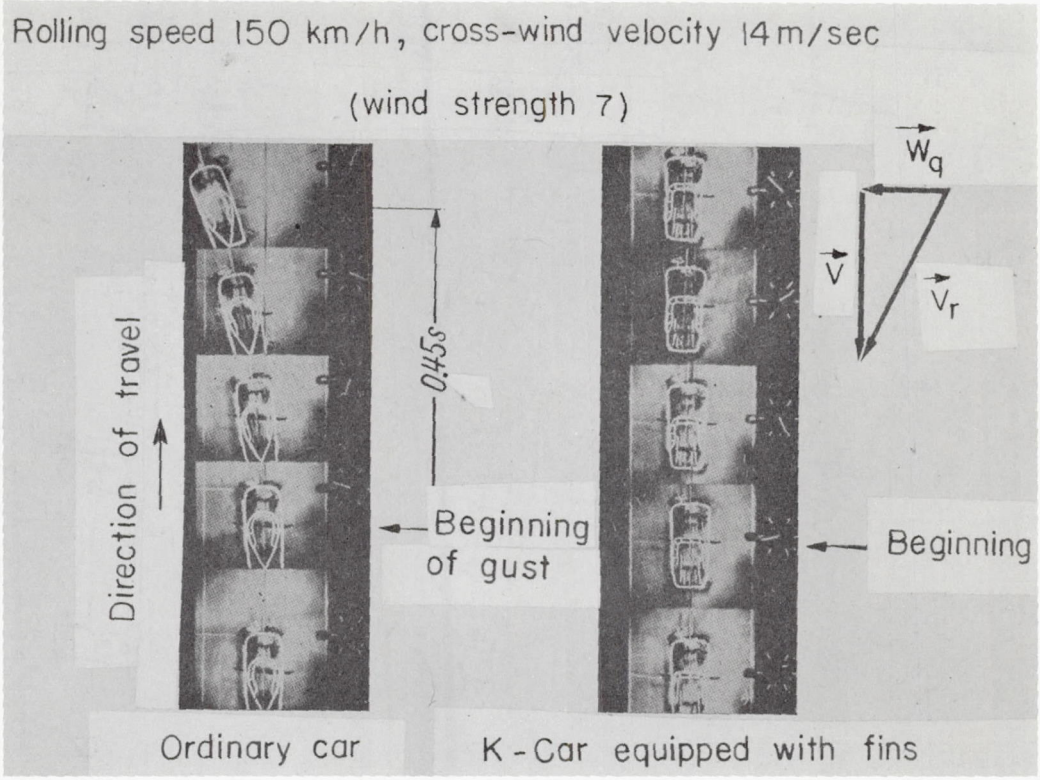

Figure 6.- Traveling motion of two automobiles at sudden cross wind.

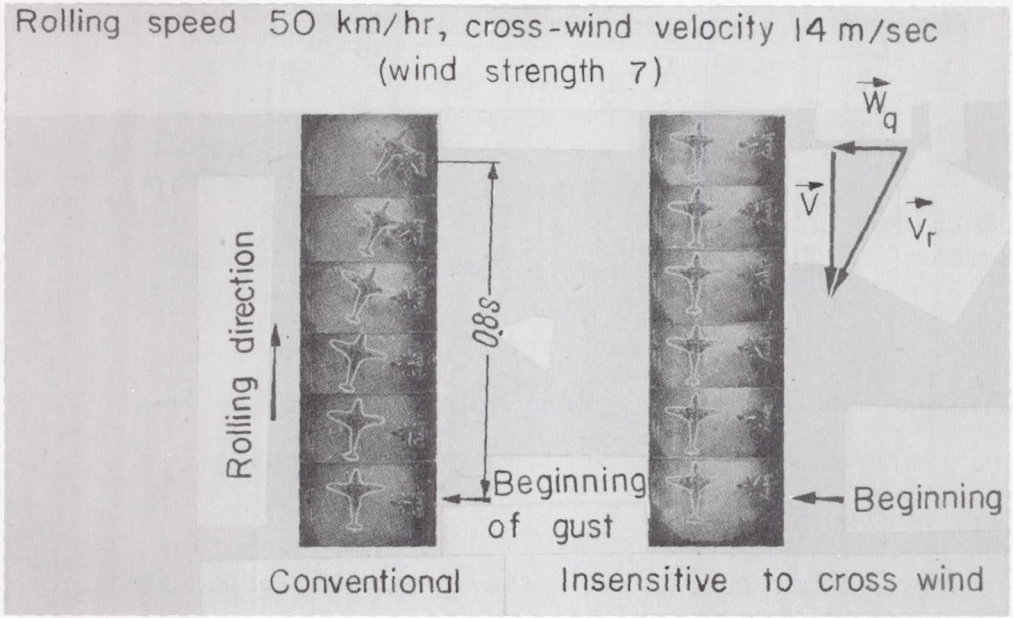

Figure 7.- Taxying motion of two aircraft with nose-wheel landing gear.

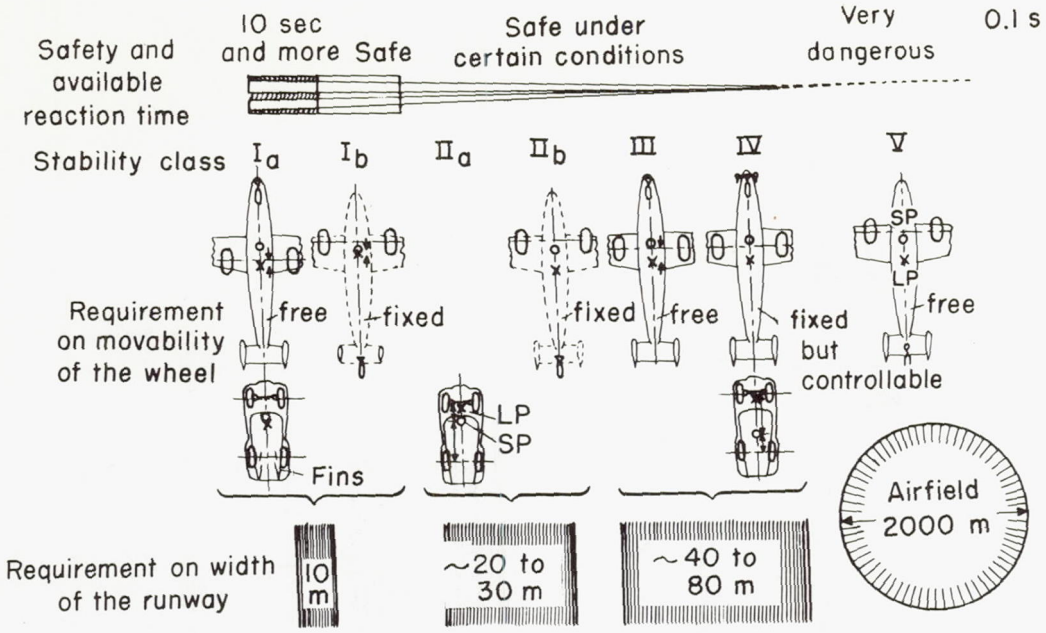

I_a Airplane with freely swivelable nose wheel, axis of the main wheels displaced toward the rear; automobile with regular fins.

I_b Tail-wheel airplane, fixed tail wheel, reduced rudder areas

II_a Motor vehicle with the load at the front axle

II_b Tail-wheel airplane, free tail wheel

III Nose-wheel airplane, free nose wheel

IV Nose-wheel airplane, controlled nose wheel; vehicle with the load at the rear axle

V Tail-wheel airplane, freely swivelable tail wheel

Figure 8.- Rolling stability of landing gears compared to the stability of vehicles and their influence on landing safety with expenditure required for the runway.

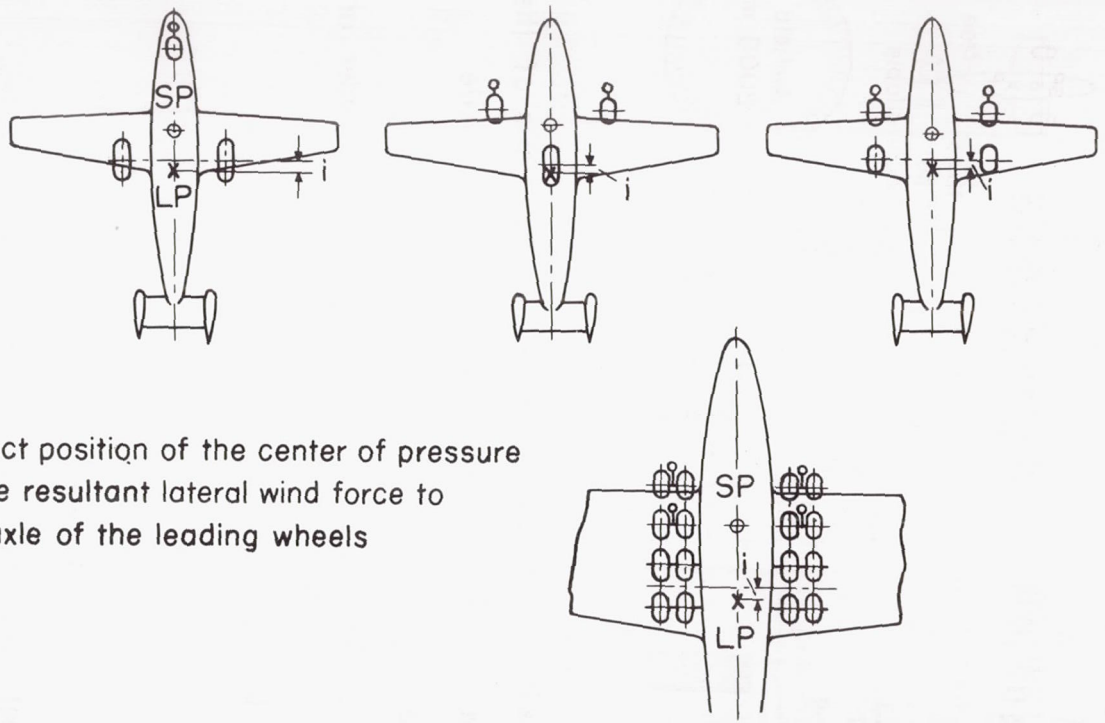

Figure 9.- Possibilities of a landing-gear design with rolling stability and insensitivity to cross wind.

ON THE MECHANICS OF THE ROLLING OF AN AIRPLANE WITH A NOSE-WHEEL LANDING GEAR*

By T. E. Schunck

1. PROBLEM

Scheubel[1] and Huber[2] have mentioned the advantages in taxiing of an aircraft equipped with a nose wheel over that equipped with a tail wheel. This paper furnishes an analysis of the taxiing process during landing of an aircraft equipped with a freely swiveling nose wheel. The main point investigated is the influence of a wind blowing across the landing strip and the conclusions drawn from theoretical calculations on the preferable position of the axle of the main landing gear.

2. SYMBOLS

a	distance of the nose wheel from the center of gravity
b	distance of the main landing gear from the center of gravity
$b^*; b_m; b_z; b_{z_0}; b_a; b_{a_0}; b_{kr}; b_{kr_0}$	special values of b
c_0, c_1	coefficients in the main equations of motion
c_m	coefficient of moment for M_L'
c_n	coefficient of force N'
c_n'	coefficient of force L
c_t	coefficient of force T

---

*"Zur Mechanik des Rollens eines Flugzeugs mit Bugradfahrwerk," Bericht 140 der Lilienthal-Gesellschaft, pp. 30-33.

[1]See paper by Scheubel of present report, p. 41.

[2]See paper by Huber of present report, p. 81.

$$k_m = \frac{FB}{2}\rho\left(\frac{\partial c_m}{\partial \tau}\right)_0$$

$$k_n = \frac{F}{2}\rho\left(\frac{\partial c_n}{\partial \tau}\right)_0$$

$$\bar{k}_t = \frac{F}{2}\rho c_{t_0}$$

} aircraft characteristics

m mass of the aircraft

m' mass of the aircraft increased by the inertia of the wheels

n distance from center of pressure of the resultant air force to the center of gravity

t time

$\vec{v}, v$ taxiing speed

v_g critical velocity for stability

$\vec{v}_h$ velocity of the hub of the fictitious tail wheel with respect to the ground

$\vec{v}_r$ relative velocity of the air with respect to the aircraft

$\vec{v}_v$ velocity of the nose-wheel hub with respect to the ground

$\vec{w}$ wind velocity

$\vec{w}_a; \vec{w}_q$ components of $\vec{w}$

B span

$C_1; C_2$
$D_1; D_2$ } coefficients in the main equations of motion

F wing area

H force in direction of the plane of the rear wheels (main landing gear)

L air force produced by the rudder

M_L air moment

M_L' air moment for negligibly small rudder deflection

N air force normal to the aircraft axis

N' air force N for vanishing rudder deflection

R resultant force acting on the aircraft

S lateral force acting on the rear wheels (main landing gear)

SP center of gravity

T air force in direction of the aircraft axis

V force in direction of the nose-wheel plane

β angle of $\vec{v}_v$ to the aircraft axis

$\beta_k = 1 - \frac{\bar{k}_t}{k_n}$ characteristic dimension for the aircraft

γ hodographic (direction of travel) angle

δ rudder deflection

$\chi_n = \frac{F}{2} \rho \left(\frac{\partial c_n'}{\partial \delta} \right)_0$ characteristic dimension for the aircraft

ρ air density

τ relative-wind angle; $\tau_0 = \tau$ at $\psi = 0$

φ angle of the aircraft axis in space

ψ drift angle of the aircraft

ψ_e drift angle ψ in the state of equilibrium

$\psi_v; \psi_h$ yaw angle of the front or rear wheels

Θ moment of inertia of the aircraft about the normal center-of-gravity axis

3. DIFFERENTIAL EQUATIONS

Figure 1 shows a tricycle landing gear. The center of gravity of the entire aircraft is denoted by SP. This aircraft moves with a velocity $\vec{v}$ which forms an angle γ with a given axis (for example, the landing-strip axis) fixed with respect to space. It is assumed that the aircraft "drifts" by the angle ψ. The nose-wheel, which is assumed freely swivelable and not braked, is oriented with its plane in the direction of the velocity $\vec{v}_v$ of its hub with respect to the ground. This velocity is composed of the center-of-gravity velocity and of the rotational velocity of the wheel hub about the center of gravity. Consequently, no lateral forces can be transmitted to the aircraft. The rolling friction V is negligibly small with respect to the other forces.

The two wheels of the main landing gear located at a distance b behind the center of gravity, as shown by a separate investigation, can be combined into a fictitious tail wheel at the axle center without producing any noticeable error. This assumption is shown in figure 1 as a broken line. The plane of this tail wheel runs yawed at an angle ψ_h with respect to the relative velocity $\vec{v}_h$ of the wheel hub to the ground. This produces a lateral force S, according to investigations made by Harling[3] and Kraft[4]. With respect to the center of gravity, this lateral force has a moment (-Sb). The main landing gear generally is braked in taxiing. The resultant of braking-force and rolling friction is denoted by H.

To these forces exerted by the ground on the aircraft, the air forces must be added. These air forces are produced by the relative velocity of the air with respect to the aircraft, which is composed of the true wind $\vec{w}$ and the negative traveling speed $(-\vec{v})$. This product can be expressed by $\vec{v}_r$ (fig. 2). The relative-wind angle, that is, the angle between this relative velocity and the aircraft axis, is denoted by τ. Generally, the resultant air force does not go through the center of gravity. Consequently, this force is resolved into its components T in direction of the longitudinal axis of the aircraft, N in perpendicular direction to this axis, and into a moment M_L (fig. 2). The effect of a rudder deflection δ is contained in these forces.

---

[3]See paper by Harling of present report, p. 7.

[4]See paper by Kraft of present report, p. 31.

The above-mentioned forces acting on the aircraft and the moments furnish the following equations of motion for the velocity variation.

$$m' \frac{dv}{dt} = -(H + T)\cos \psi - (S + N)\sin \psi - V \cos(\psi - \beta)$$

and for the angle in the direction of travel:

$$mv \frac{d\gamma}{dt} = -(H + T)\sin \psi + (S + N)\cos \psi - V \sin(\psi - \beta)$$

Finally, the equation of motion for the position of the aircraft axis in space reads as follows:

$$\Theta \frac{d^2\varphi}{dt^2} = M_L - Sb + V\alpha \sin \beta$$

where m denotes the mass of the aircraft, m' the mass increased by the inertia of the rotating parts, and Θ the moment of inertia about the vertical axis.

If the resultant forces and moments are known from tests as to their dependence on the determining factors, the equations can be numerically integrated for each individual case. However, for making any general statements the following simplifying assumptions must be made. By means of these assumptions, the equations can be analytically treated:

(a) The yaw angle of the fictitious tail wheel remains so small that the lateral load can be assumed to be proportional to this angle

(b) Only a pure cross wind of a velocity w_q is considered. This velocity, with respect to the taxiing speed v, is so low that the angle between v_r and v can be expressed by

$$\tau_0 = \frac{w_q}{v}$$

(c) The relative-wind angle τ and the rudder deflection δ are assumed to remain within the limits where the aerodynamic side force N and the aerodynamic moment M_L can be set proportional to each of the two values, while the tangential force T remains unaffected.

(d) The entire taxiing process is subdivided into intervals within which the velocity decreased by the brake force H and the resistance D can be replaced by a mean value v_m.

The angle for the direction of taxiing γ and the drift angle ψ can then be expressed by differential equations of the following form:

$$\frac{d}{dt}(\ddot{\gamma} + c_1\dot{\gamma} + c_0\gamma) = D_1\delta + C_1\tau_0$$

$$\ddot{\psi} + c_1\ddot{\psi} + c_0\psi = D_2\delta + C_2\tau_0$$

The coefficients c_0, c_1, C_1, C_2, D_1, and D_2 depend on the aerodynamic and mass-geometric characteristics of the aircraft as well as on the characteristics of the tires and on the mean taxiing speed of the interval in question.

The solutions of these differential equations are composed of the complete integral of the homogeneous equation and of a particular integral of the complete equation. This latter integral produces the mechanical state of equilibrium to which the aircraft adjusts itself. The complete integral of the homogeneous equation which contains the integration constant, shows whether this state of equilibrium can be reached from all initial positions and whether it will be insensitive to slight perturbations.

4. STATE OF EQUILIBRIUM

If the rudder deflection required in the equilibrium state during a cross wind is defined and if the resultant drift angle is plotted as a function of the position of the main landing gear given by the value b, the mean velocity v_m can be represented by functions similar to those shown in figure 3. The distance b of the landing gear refers in this case to the center-of-pressure distance n shown by the air force at vanishing rudder deflection. These functions are then used for plotting the equilibrium positions of the aircraft shown in figure 4.

It is of considerable importance that the required rudder deflection vanishes at the point denoted by b_z which means that the aircraft continues traveling in a straight line even during a cross wind without any rudder deflection at the taxiing speed used in figure 3. In the vicinity of this point, the necessary rudder deflections for a straight motion are rather small. Consequently, the pilot can keep his aircraft easily in the desired straight direction.

However, a critical rear-axle distance b_{kr} exists, at which the required rudder deflections and drift angles obtained from the linearized

theory grow beyond all limits. This creates very complicated taxiing conditions which are difficult to calculate in any practical manner.

In figure 3 which, as mentioned before, applies only for a mean velocity, arrows are drawn at the range limits. These arrows indicate the tendency of the range limits to approach values of b_{z_0} and $b_{\alpha_0} = b_{kr_0}$ at decreasing taxiing speed. These values are valid for vanishing taxiing velocity.

If the critical range is to be avoided in a given aircraft, for which infinite rudder deflections were calculated, the rear axle must either be shifted so far toward the back that $b > b_{kr}$ even at maximum taxiing speed or so far toward the front that $b < b_{kr_0}$. Along with structural reasons, the rear-axle distance b will be selected according to its influence on the stability of the aircraft in taxiing.

5. STABILITY OF THE TAXIING PROCESS

Taxiing of an aircraft will be stable and will permit reaching the equilibrium stage from all initial positions if the solutions of the homogeneous equations do not contain any terms which increase with time. This is the case in an aircraft with a freely swivelable nose wheel above a certain critical velocity v_g, while in the range between $v = 0$ to $v = v_g$, the aircraft is not unstable.

This critical velocity of the stability depends greatly on the rear-axle distance b as shown in figure 5. Consequently, if the range in which the aircraft is unstable is to be kept to a minimum, the rear-axle distance must be kept as low as possible. If the mass of the aircraft m is smaller than a characteristic value k_m (which mainly contains the moment coefficient of the air moment M_L) the function $v_g^2(b)$ will reach a maximum at b_m. If it is impossible to keep b lower than b^* (fig. 5), the zone near b_m must not be used.

The asymptote which is approached by v_g^2 depends mainly on the magnitude of the brake force H. Consequently, the zone of initial instability can be decreased by lowering the brake force at the end of the taxiing process.

6. CONCLUSION

The above discussions represent the general conclusions to be drawn, from a simplified analytical calculation of the taxiing process during a cross wind, in regard to a favorable position of the main landing gear with respect to the center of gravity.

*Translated and Edited by
the O. W. Leibiger Research Laboratories, Inc.
Petersburg, N. Y. (ATI No. 32117)

---

*Note: In order to provide terminology consistent with other papers of this series, this translation has been reworded in many places by the NACA reviewer.

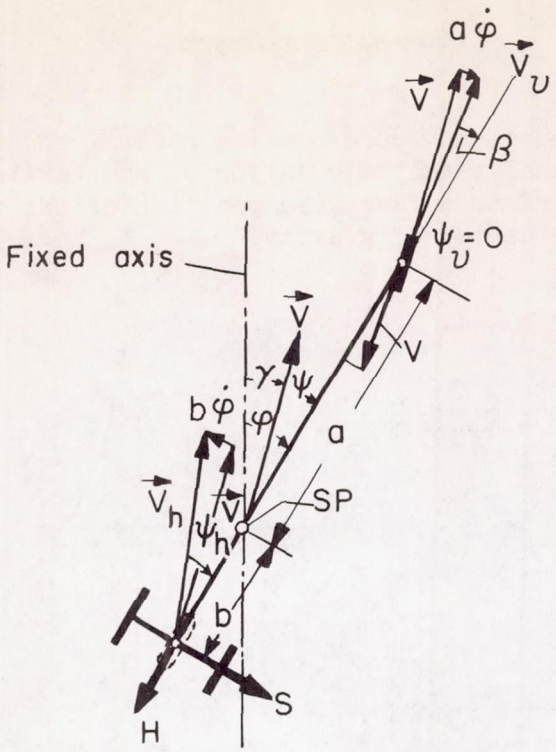

Figure 1.- Nose-wheel landing gear of an aircraft with velocities and ground forces.

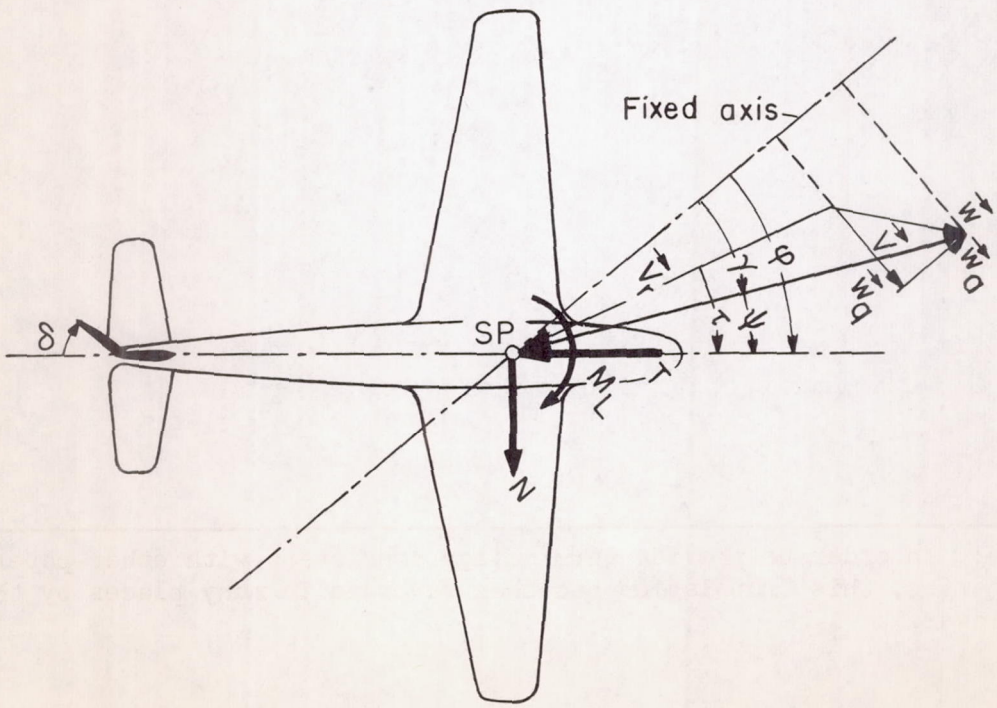

Figure 2.- Aerodynamic forces and velocities in wind.

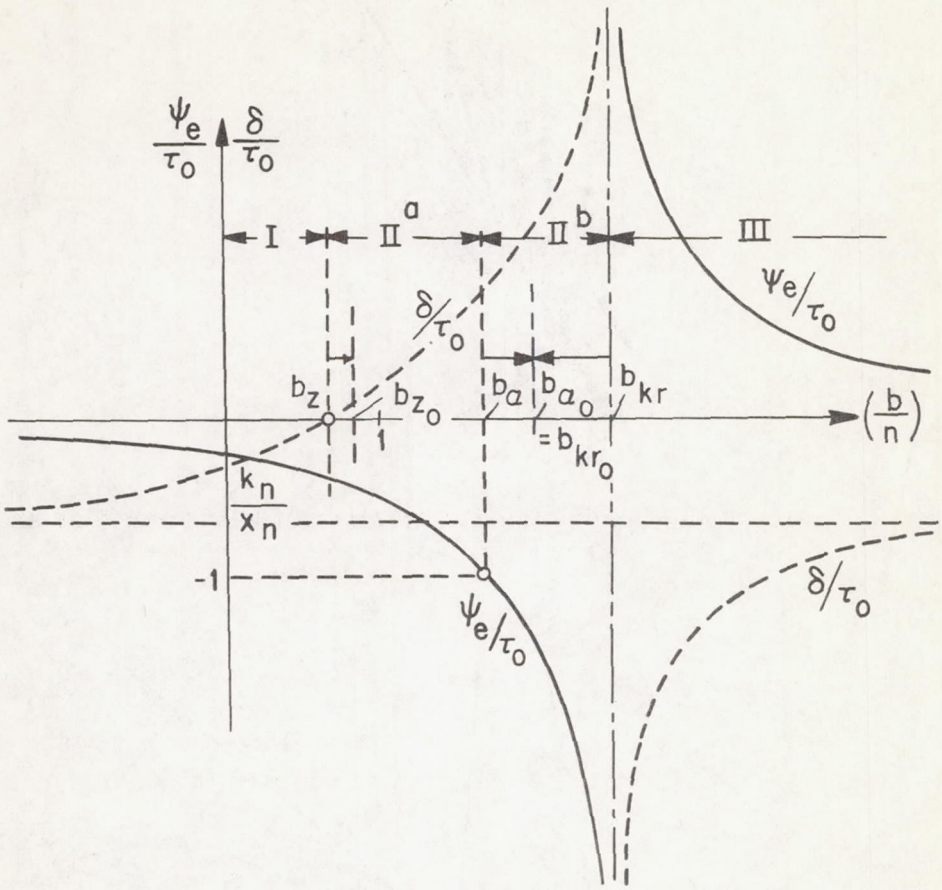

Figure 3.- Relative drift angle $\frac{\psi_e}{\tau_0}$ and relative rudder deflection $\frac{\delta}{\tau_0}$ as a function of the relative rear-axle distance $\frac{b}{n}$.

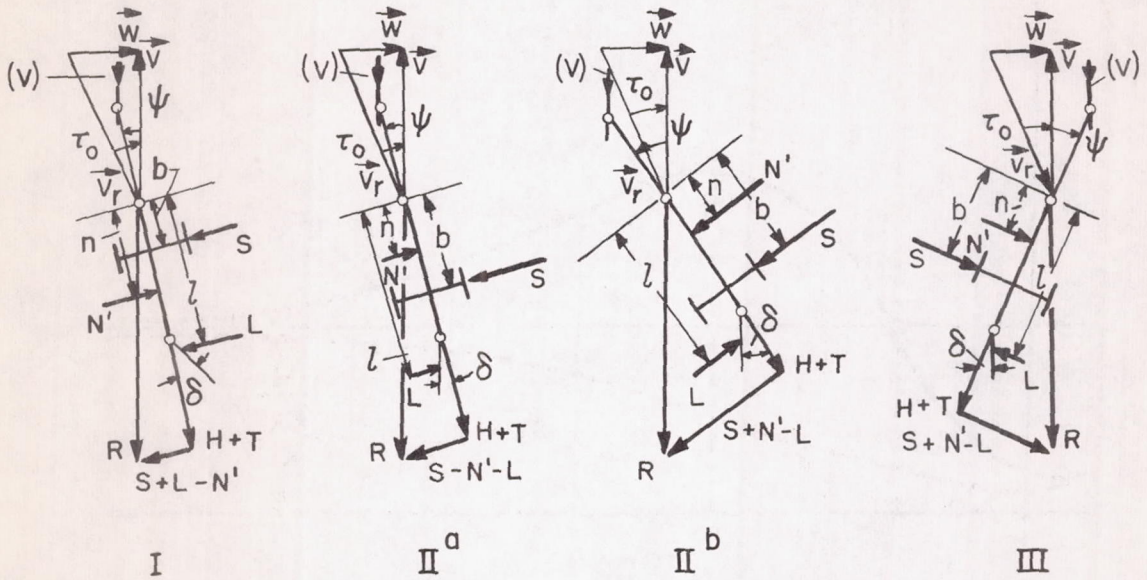

Figure 4.- Positions of the aircraft and forces in taxying.

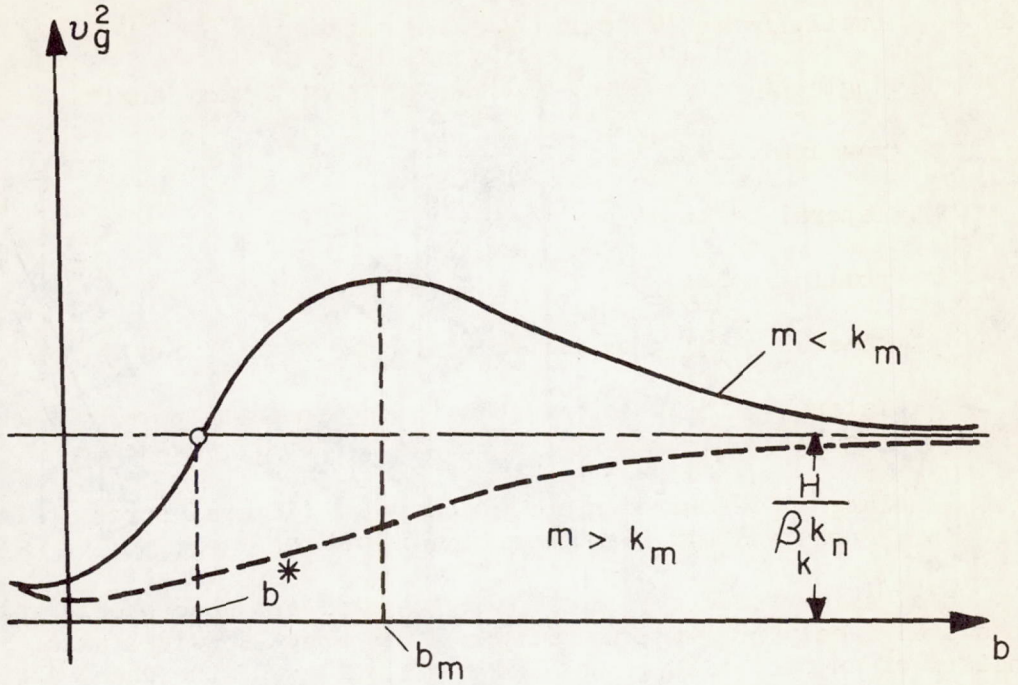

Figure 5.- Critical velocity of the stability v_g as a function of the rear-axle distance b.

FUNDAMENTAL PERCEPTIONS ON WHEEL SHIMMY*

By P. Riekert

SYMBOLS

e	trail
e/d	trail, referred to the wheel diameter d
φ	angle of rotation of the wheel plane (shimmy angle)
ψ	yaw angle
ξ	lateral deformation
v	rolling speed
s	lateral guiding or cornering force
c	lateral guiding characteristic or cornering power (lateral guiding or cornering force in kg for 1^{o} yaw angle)
c_R	lateral-deformation spring constant (lateral force in kg required for 1-cm lateral deformation)

Wheel shimmy occurs predominantly on tail and nose wheels which can swivel freely or with restoring moments about a swivel axis. It consists of an oscillating back and forth motion of the wheel about its swivel axis; the deflections may assume large amounts. Considerable wear on tires, high stresses on wheel support and attachment to the fuselage as well as vibrations of the airplane result. Elimination of shimmy is therefore of essential importance.

Investigations regarding the causes of the phenomena of shimmy and the means to control them have been undertaken in Germany and abroad. A report on the American publications by Wylie (ref. 1) and Kantrowitz (ref. 2) is to be found elsewhere (ref. 3). Melzer (ref. 4) created a clear theory of the phenomenon which is in good agreement with model tests and practice; he extended appropriately the concepts concerning the shimmy of automobile wheels, arrived at before by H. Fromm (ref. 5).

---

*"Grundsätzliche Erkenntnisse über das Radflattern," Bericht 140 der Lilienthal-Gesellschaft, pp. 33-35.

At the Forschungsinstitut für Kraftfahrwesen und Fahrzeugmotoren an der Technischen Hochschule Stuttgart (Research Institute for automobilism and automobile engines at the Technical Academy of Stuttgart), Dietz and Harling (refs. 6 and 7) performed above all practical tests:

1. With model wheels on the "moving roadway"

2. With full-scale wheels of minor dimensions on the revolving drum

3. With full-scale wheels of relatively small dimensions as an undriven wheel in a front-wheel driven motor vehicle

4. With full-scale wheels of relatively large dimensions in a truck trailer

5. With various shimmy dampers on the tail wheel of a Me 110 on hard landing strips and turfs

The essential results were in agreement in all types of tests.

Regarding the phenomenon of shimmy, there arises the fundamental question how the excitation of the system comes about. Since, in practice, a certain damping is always present due to the deformation of the tire and by axle friction, energy must be supplied from the outside for the maintenance or self-reinforcement of the deflections. This is possible because two degrees of freedom exist. On one hand, the wheel plane (fig. 1) forms with the rolling direction the angle φ; on the other, the tire undergoes, under the influence of a lateral guiding or cornering force S, a lateral deformation ξ. With the trail e of the wheel which signifies the distance between the center of the pressure area and the point where the swivel axis penetrates the rolling plane, there results a transverse velocity $w = e\dot{\varphi} + \dot{\xi}$ of the tire-pressure center. This velocity w forms with the rolling velocity v the angle of yaw ψ. The lateral guiding force S is proportional to ξ and to $-\psi$.

The results obtained according to Melzer's theory may be represented in a vector diagram (fig. 1, right) according to E. Maier (ref. 8). The oscillation angle φ is represented by a vector of the length φ. The oscillation vector ξ is shifted by ϵ° and, in contrast, the oscillation vector ψ by 180° since the proportionality of S to ξ and ψ shows inversion of sign. The phase shift ϵ depends kinematically on the condition that the quantities φ, ψ, $\dot{\varphi}$, and $\dot{\xi}$ are coupled according to the relation

$$\psi = \varphi + \frac{e\dot{\varphi} + \dot{\xi}}{v}$$

The velocity vectors $\frac{e}{v}\dot{\varphi}$, $\frac{e}{v}\dot{\psi}$, and $\frac{\dot{\xi}}{v}$ lie perpendicularly to φ, ψ, and ξ, with a phase lead of 90°. The vector w/v is found by geometrical addition of $\frac{e}{v}\dot{\varphi}$ and $\frac{\xi}{v}$. The separate vectors are geometrically dependent on one another corresponding to the plotted circles, as may be mentioned without detailed proof.

If one visualizes the entire vector diagram revolving about the origin of the vectors corresponding to the oscillation frequency, the projection of the individual vector on a fixed axis forms a measure for the momentary magnitude of oscillation. It is essential that energy is supplied to the system when, as plotted, S and w/v form a phase angle $\chi < 90^{\circ}$. The deflections increase and the wheel shimmies. This is the case as long as the vectors $\frac{w}{v}$, $\frac{e}{v}\dot{\psi}$, and, and ψ lie in the particular domains indicated. Outside of them, energy supply is stopped and hence stability established. Then $\frac{\xi}{v} < \frac{e}{v}\dot{\psi}$ or, which is equivalent, $c_R e > c$. For an undamped system, shimmy is possible only when the product of trail e and lateral-deformation spring constant c_R is smaller than the lateral guiding characteristic (cornering power) c.

Figure 2 shows the deformation relations of the tire in the stable and unstable domain as plan view on the shimmying wheel rolling straight ahead. In the stable case, the lateral deformation lags behind the angular rotation of the wheel so that the lateral guiding force S attempts to retard the latter. The inverse is true for the unstable case.

The most important influences on shimmy are shown in the following figures. Partially they may be confirmed also theoretically if a damping term is added in the calculation.

The shimmy deflection shows at a certain velocity (fig. 3) a maximum value. It disappears very rapidly at a lower and an upper velocity limit. Increased ground friction augments the shimmy deflection.

The trail referred to the wheel diameter e/d influences (fig. 4) the maximum shimmy deflection in such a manner that the shimmy deflections almost disappear for small values and entirely for values above an upper limit. By a sufficiently large trail, one can therefore practically stop shimmy. This measure sets, however, higher requirements for the development of the wheel suspension for reasons of strength. A small trail, favorable in itself, results in a veering around its swivel axis of the wheel when landings take place on slightly yielding ground like snow, sand, and water since thereby the trail changes into lead. A wheel, however, which is able to swivel freely or with small restoring moments is statically unstable in case of lead.

Increasing wheel load augments the shimmy tendency since lateral force and energy absorption of the oscillation system increase with it (fig. 4).

Trail and velocity together determine the limits within which shimmy is possible (fig. 5). If the system shows merely its natural damping, this region increases somewhat with growing ground friction. The range of shimmy may be considerably reduced by attachment of a fluid or frictional damping so that relatively small trails are sufficient for complete prevention of shimmy. The condition of highest shimmy tendency is decisive for the dimensioning of the damper.

Increase of the tire inflation pressure has a favorable effect. I want to mention, furthermore, that the frequency of the shimmy oscillations increases with growing rolling speed. Built-in restoring springs have practically no effect on the shimmy phenomena; they merely modify the frequency.

Over-all motions of the entire airplane affect the shimmy oscillations comparatively slightly. Such an influencing is possible only when, for instance, the natural frequency of the airplane about its longitudinal axis exceeds the natural frequency of the swiveling part about the swivel axis (ref. 4). Similar conditions probably prevail for other motions, for instance, about the vertical center-of-gravity axis or about the transverse axis.

Kantrowitz (ref. 2) indicates a peculiar possibility of damping. Axial clearance of the wheel on its axle is to reduce shimmy by decreasing the coupling between the rotary motion of the wheel plane and the lateral deformation of the tire.

Considered, as a whole, the causes for excitation of shimmy phenomena and the means for their elimination have been understood. In practice, there remains the development of fluid dampers in such a manner that their effectiveness is sufficiently large and the wheel may be rotated by a full 360°. The friction damper has the disadvantage of very much impeding curvilinear rolling if heavily tightened for the purpose of providing sufficient energy absorption.

Translated by Mary L. Mahler
National Advisory Committee
for Aeronautics

REFERENCES

1. Wylie, Jean: Dynamic Problems of the Tricycle Alighting Gear. Jour. Aero. Sci., vol. 7, no. 2, Dec. 1939, pp. 56-67.

2. Kantrowitz, Arthur: Stability of Castering Wheels for Aircraft Landing Gears. NACA Rep. 686, 1940.

3. Marquard, E.: Comments on Two American Research Reports. Bericht über zwei amerikanische Arbeiten. Present report, p. 161.

4. Melzer, M.: Beitrag zur Theorie des Spornradflatterns. Dtsch. Luftf.-Forsch., Techn. Bericht 2, 1940.

5. Becker, G., Fromm, H., and Maruhn, H.: Schwingungen in Automobillenkungen. Berlin 1931.

6. Dietz, O., and Harling, R.: Bericht zum Forschungsfilm Nr. 1, Dtsch. Luftf.-Forsch. "Spornradflattern."

7. Dietz, O., and Harling, R.: Experimentelle Untersuchungen über das Spornradflattern. Dtsch. Luftf.-Forsch. FB 1320, 1940. In this report, in contrast to the present lecture, φ denotes the entire shimmy angle between the two limiting positions of the wheel.

8. Maier, E.: (FKFS), not yet published.

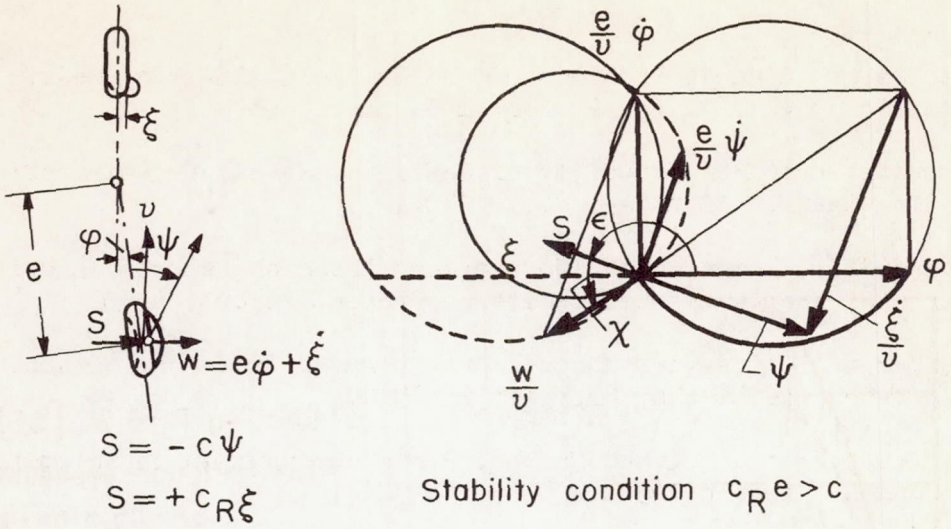

Figure 1.- Vector diagram of the shimmying motion.

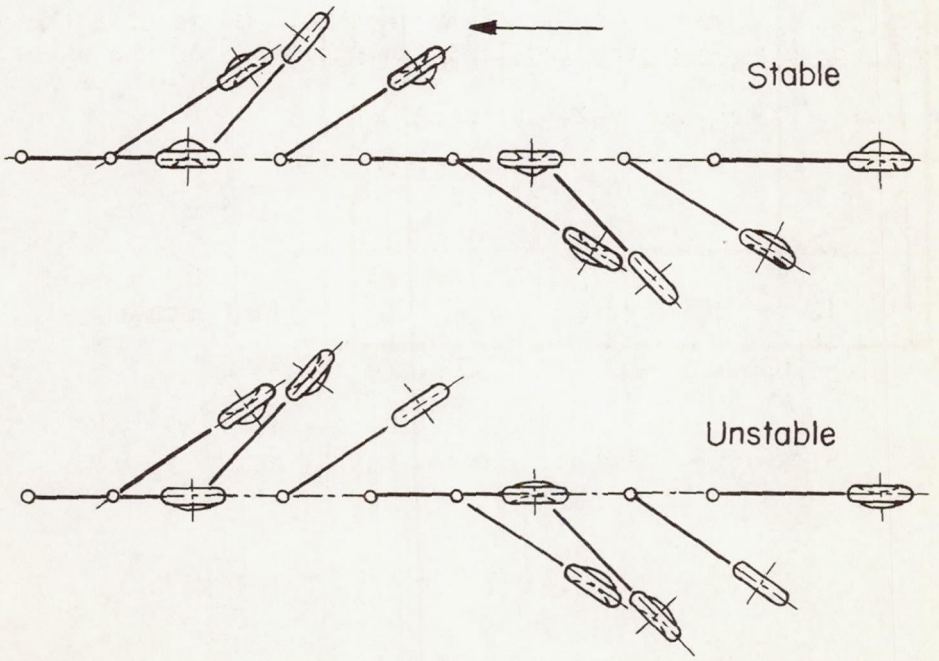

Figure 2.- Tire deformation in the stable and the unstable case.

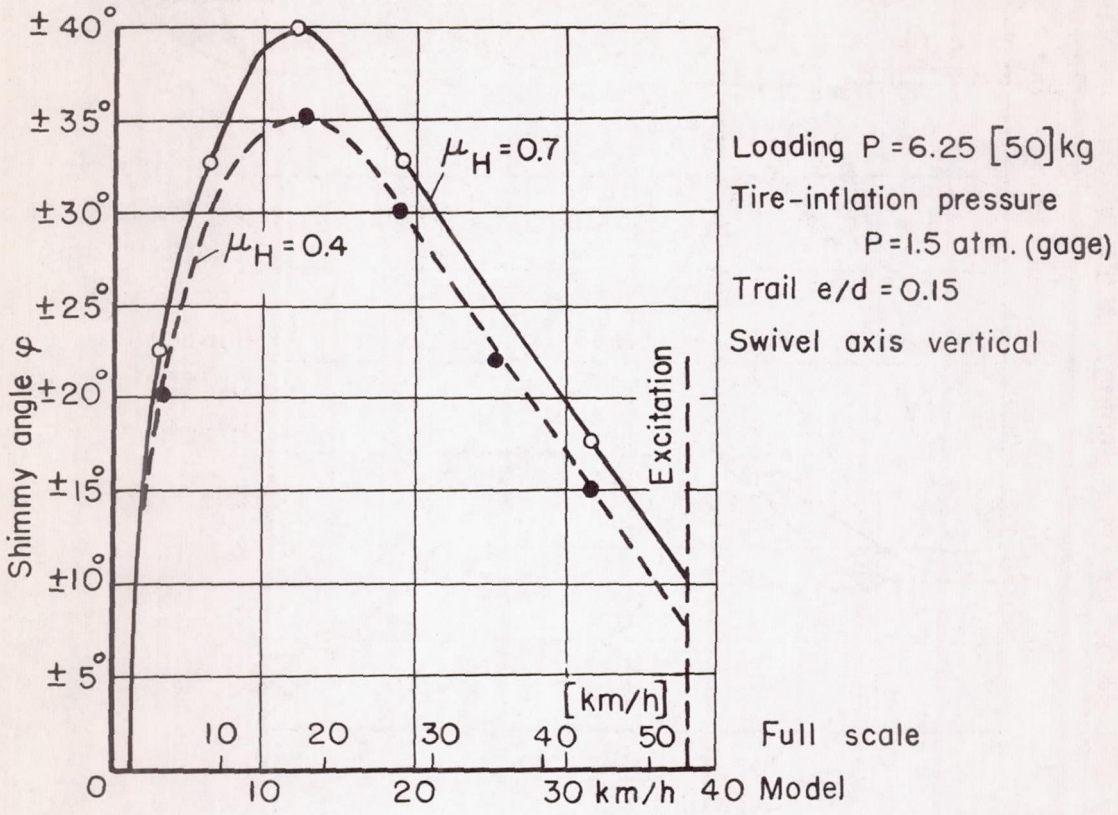

Figure 3.- Influence of speed on shimmy.

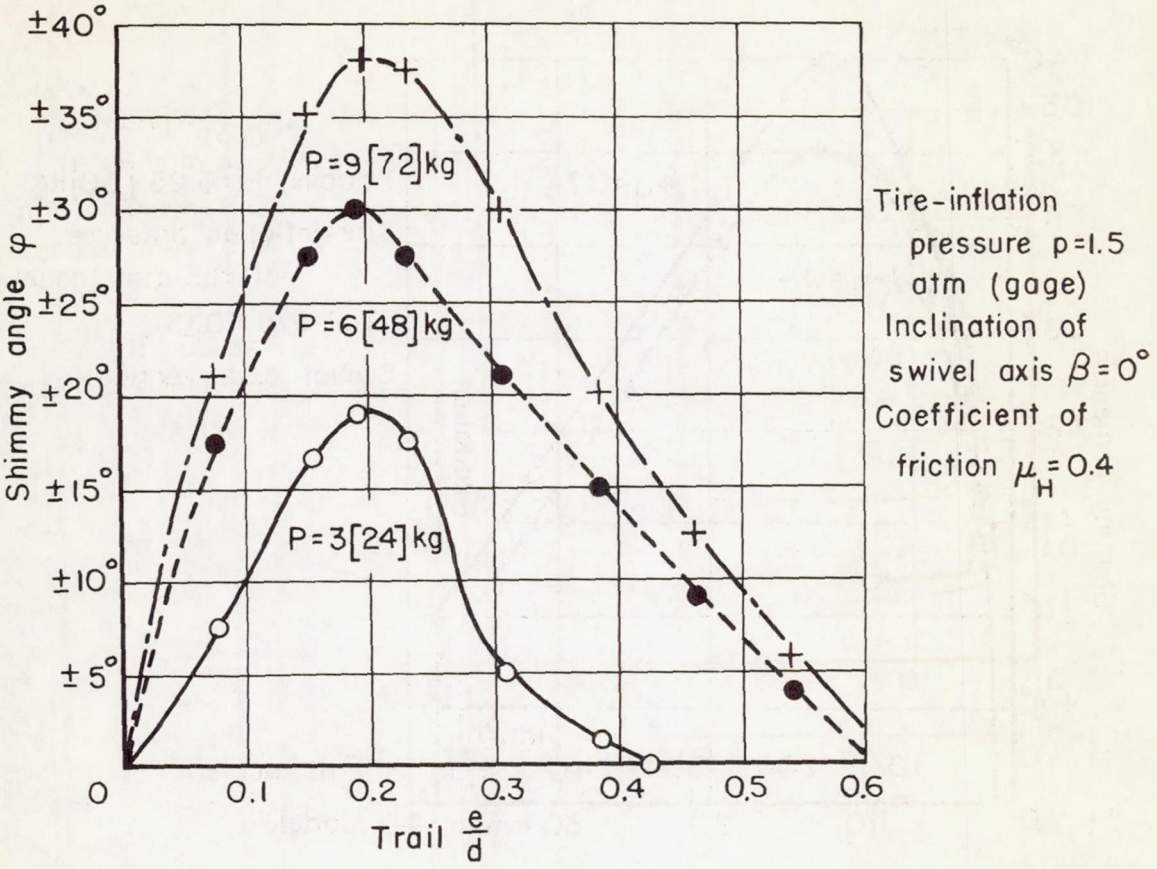

Figure 4.- Influence of trail and load on shimmy.

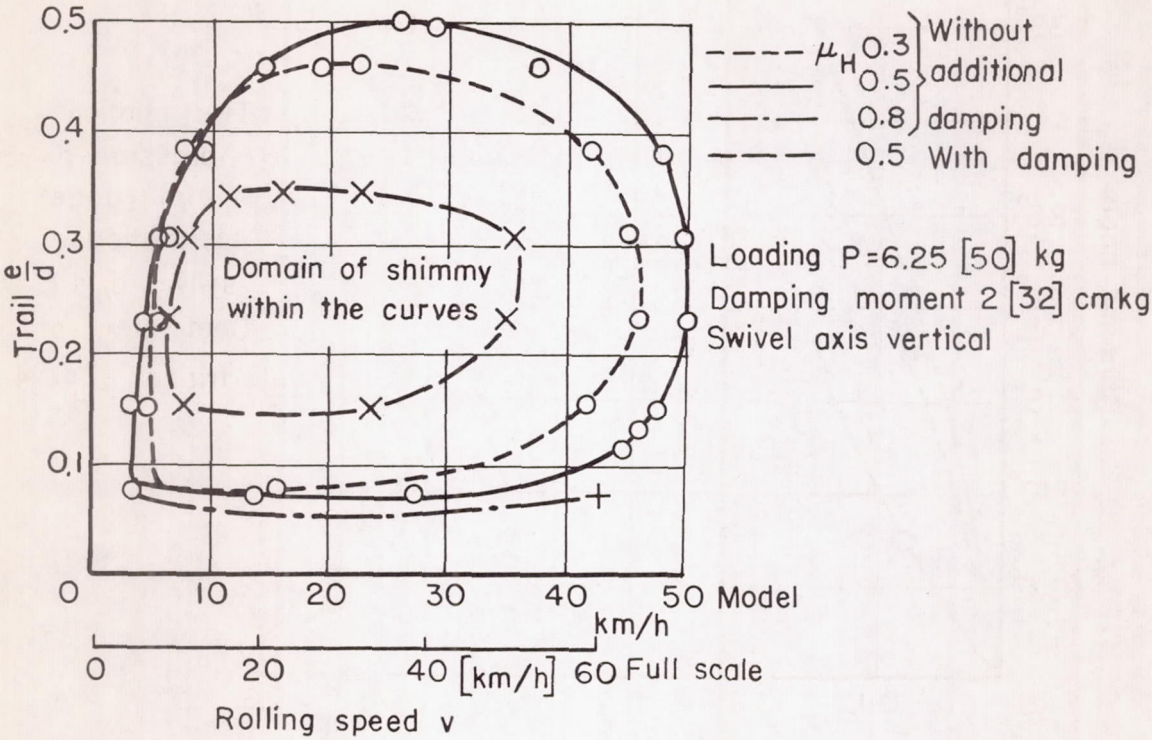

Figure 5.- Shimmy tendency as a function of trail and rolling speed.

SHIMMYING OF A PNEUMATIC WHEEL*[1]

By B. v. Schlippe and R. Dietrich

1. SYMBOLS

A	general integration constant
B	foremost point of ground-contact surface
$C = \frac{1}{c}(cm)$	tire constant
H	rearmost point of ground-contact surface
M(cmkg)	moment of the elastic forces acting on the rim
N(kg)	vertical load on wheel
P(kg)	elastic force acting at the center point
S(cm)	wave length of a sinusoidal oscillation
$U_1(kg\ cm^{-1})$	force coefficient
$U_2(kg)$	moment coefficient
$c\left(\frac{1}{cm}\right)$	tire constant
2h(cm)	length of the ground-contact surface
p(atm)	tire pressure
q(cm)	swivel arm
r(cm)	tire radius
s(cm)	path coordinate (abscissa of the wheel center point)

---

*"Das Flattern eines bepneuten Rades," Bericht 140 der Lilienthal-Gesellschaft, pp. 35-45.

[1]Derivation of fundamental equations and further remarks are presented subsequently in "Supplement for clarification of several remarks in the discussion," p. 217 of the present report.

t(sec)	time
v(cm/sec)	rolling velocity
x(cm)	ordinate of the wheel center point
y(cm)	ordinate of the foremost ground-contact point B
$\overline{y}$(cm)	ordinate of the rearmost ground-contact point H
z(cm)	deflection of point B from the wheel plane
$\overline{z}$(cm)	deflection of point H from the wheel plane
$\alpha\left(\frac{1}{cm}\right)$	path frequency (2π times reciprocal of wave length)
ζ(cm)	lateral deflection
η(cm)	ordinate of the tire points
χ_1(kgcm s/rad)	damping coefficient when damping is proportional to the velocity
χ_2(kgcm s/rad)	damping coefficient when damping is proportional to the deflection
$\lambda\left(\frac{1}{cm}\right)$	root of the characteristic equation
ξ(cm)	circumferential coordinate
ρ	correction factor
σ(kg/cm^2)	elasticity constant
φ(rad)	swivel angle
ω(1/s)	circular frequency

A. TIRE MECHANICS

By B. v. Schlippe

In order to be able to theoretically comprehend the shimmy phenomenon of a wheel it is necessary to make a detailed study of the mechanics of

a pneumatic wheel or tire. By tire mechanics is meant the behavior of a tire on a wheel that is pushed perpendicular to its plane, which behavior is ultimately dependent on the elastic forces and moments. We will first discuss the question how a tire moves perpendicular to its direction of motion, wherein we shall assume that the transverse motion is small compared to the forward rolling motion. It is known that an automobile wheel, especially with a low-pressure tire, can be yawed without skidding on the road. This effect depends on the elasticity of the tire.

If we perform a corresponding test we see that the ground-contact surface shifts from its central position and deforms the tire. In order to arrive at the elastic forces we must know the lateral deflections, that is, the path of the ground-contact surface. The wheel is yawed by the small angle φ with respect to its plane. At the first moment of rolling the tire, held fast to the ground by friction, follows the direction of the wheel plane, likewise at the angle φ to the direction of motion. The spring action of the elastic tire however gradually causes a restoring action and the ground-contact surface gradually changes its direction of motion until it converges with that of the wheel (fig. 1).

First we assume the simplification that the ground-contact area is drawn together into a single point. The path coordinate is designated as s and the lateral deflection as z. At the first instant the tangent to the direction of motion is

$$\left.\frac{dz}{ds}\right|_{s=0} = \varphi$$

The elastic restoring effect will be based on a linear principle, that is, the deviation from the original angle φ shall be proportional to the lateral deflection z. This motion can be expressed by the differential equation:

$$\frac{dz}{ds} = \varphi - cz$$

or

$$\boxed{\frac{dz}{ds} + cz = \varphi} \qquad (1)$$

where c is the proportionality factor which must be determined experimentally. This is the fundamental equation of tire mechanics on which all further derivations are based.

Since c was assumed to be constant, the equation may be integrated as follows:

$$z = Ae^{-cs} + \frac{\varphi}{c}$$

This is an e-function. Since

$$z = 0 \quad \text{at} \quad s = 0$$

then

$$z = \frac{\varphi}{c}\left(1 - e^{-cs}\right)$$

When

$$s = \infty$$

then

$$z_\infty = \frac{\varphi}{c}$$

This theoretical curve can be determined by a simple experiment. The wheel circumference is blackened along the center line and pushed across white paper. This reproduces the characteristics of the function (fig. 2).

One could be tempted to determine the value of c from this track; however, this cannot be done since smudging occurs due to skidding (though this skidding is slight) and the desired constant is thus falsified. The constant c is the reciprocal value of a length which we shall designate by C. Thus

$$C = \frac{1}{c} \tag{2}$$

From the equation

$$z_\infty = \frac{\varphi}{c}$$

we obtain

$$C = \frac{z_\infty}{\varphi}$$

and in the e-curve, C is the segment formed by the point of intersection of the asymptote with the wheel plane at the zero position (fig. 1).

We had assumed, to begin with, that the ground-contact area is a point. Actually this is not the case. Instead, it has a finite expansion, a length 2h, and a width 2b. The width need not be considered at the moment and we will assume that the ground contact is only a line 2h in length (fig. 3).

The next question concerns the path of the foremost ground-contact point B. We will generalize the direction of motion and instead of pushing the wheel at a constant angle φ, will rotate it around the vertical axis while it is moving, and shift the wheel center to the side. As an illustration let us imagine that small pointed nailheads are placed along the wheel circumference and that they alone contact the ground. This will also clarify the concept of absolute adhesion between the tire and the ground from the front point of contact B to the rear point H. The differential equation for the motion of the front point is derived from the fundamental equation with the additional terms for generalized wheel motion, dx/ds (lateral movement of the wheel-center point) and $h\frac{dy}{ds}$ (swivel of the wheel plane).

$$\frac{dz}{ds} + cz = \varphi - h\frac{d\varphi}{ds} - \frac{dx}{ds} \tag{4}$$

where z is again the lateral distance from the tire-contact point B to the rim. The lateral distance of the point from a fixed ground coordinate is:

$$y = x + h\varphi + z \tag{5}$$

as illustrated geometrically in figure 3. Combining the two equations we obtain the differential equation for y:

$$\frac{dy}{ds} + cy = \varphi(1 + ch) + cx \tag{6}$$

where φ and x are arbitrary functions of s.

If we know the motion of the center point and the rotation of the rim around the vertical axis, we can, with this equation, determine the path of the contact point B. The curve formed by the ground-contact line extends from the front point of contact B to the rear point H and can be imagined to be composed of a series of points whose future path is of great interest to us. They cannot, like point B, move forward according to external influences. Rather they are completely dependent upon the course of point B. This important fact is the first cornerstone of our problem. The following fact clearly illustrates how subsequent points depend upon the path taken by point B: Every point on the

tire contacts the ground and adheres until raised from it. Every one begins its life as a front point, becomes a middle point and then a rear point. Throughout this life each point retains its original position with respect to the s-axis (fig. 4).

We can picture the ground-contact curve as a train consisting of a tractor and several trailers. The tractor travels along a certain prescribed path $y(s)$ and all the trailers follow it, but with a certain phase displacement, the amount depending on their distance from the tractor. Likewise, the ground-contact line follows the front-point of contact B, just as the trailers follow the tractor (fig. 5).

If we let ξ be the distance between the tractor and any one of the trailers, whose lateral deflection from a reference line is given by η, then η equals:

$$\boxed{\eta(s,\xi) = y(s - \xi)} \tag{7}$$

This also gives the functional relation for the lateral deflection of the ground-contact points, their life equation so to speak, which is the second cornerstone of this problem. The special equation for the rear point of the ground-contact line becomes:

$$\bar{y} = y(s - 2h) \tag{8}$$

After having established the ground contact curve, we must now consider the parts of the tire before and after the ground-contact line that do not contact the ground.

Our object is to determine the elastic forces and moments acting on the rim during lateral deflection of the bulge. The tire affects the rim not only in the region of the ground contact, but in the surrounding area as well.

It is natural to assume the curve to be an e-function since it has a finite deflection at the point where the ground contact begins and approaches zero asymptotically. This was confirmed experimentally (fig. 6).

If ξ is the circumferential coordinate, the equation of the lateral deflections ζ in regard to the rim is

$$\zeta = ze^{-c\xi} \tag{9}$$

A few remarks about the constant c follow. It turns out to be identical with the one used in the linear formulation of the fundamental equation

$$\frac{dz}{ds} + cz = \varphi$$

This can be concluded by deduction and confirmed experimentally. It is interesting also that the forward part of the tire that does not contact the ground converges with the ground-contact surface without forming an angle. Thus, the front point of contact moves constantly in the tangential direction of the preceding forward part. (On the basis of this fact different fundamental equations can be set up, all of which will arrive at the same result. See "Supplement for Clarification of Several Remarks in the Discussion", by B. v. Schlippe and R. Dietrich on p. 217 of the present report). This is not the case at the rear end of the ground-contact line, where theoretically any angle can be formed between the part of the tire that does not contact the ground and the ground-contact curve. Actually this angle is rounded off because of the bending stiffness of the tire (fig. 7).

We will now consider the forces that act on the wheel. In the beginning all forces act on the ground-contact surface and deflect the tire. It is impossible to evaluate them mathematically and therefore we will measure the elastic forces of the tire acting on the wheel rim by the deformation they cause. Their effect is identical with that of the forces mentioned above. We refer the forces to the center of the ground-contact surface, where we have basically the force P acting perpendicular to the wheel plane and the moment M about the vertical axis (fig. 8).

I would like to omit details and disregard secondary forces and their causes. We will consider only the important elastic forces produced by the deformation ζ wherein we take for the force the expression

$$dP = \sigma\zeta \, d\xi$$

and for the moment

$$dM = \sigma\zeta(h - \xi)d\xi$$

Here, σ is a stiffness constant of the tire. (Despite the units kg/cm^2 it is not a measure of tension).

The last two equations must be integrated for the whole wheel circumference. The e-function of the lateral-deflection curves decreases rapidly and it is immaterial whether we integrate from the beginning of the ground-contact length over the circumference to the end of the contact length, i.e. $(2\pi r - 2h)$ or to $\pm\infty$. It can be shown that the error

is negligible. For simplicity we choose the latter and the following equations result:

$$P = \int dP = \sigma \int_{-\infty}^{\infty} \zeta \, d\xi$$

$$M = \int (h - \xi) dP = \sigma \int_{-\infty}^{\infty} \zeta (h - \xi) d\xi$$

The side areas can be integrated immediately so that

$$P = \sigma \int_{0}^{2h} \zeta \, d\xi + \sigma \frac{z + \bar{z}}{c}$$

and

$$M = \sigma \int_{0}^{2h} \zeta (h - \xi) d\xi + \rho\sigma \frac{\left(h + \frac{1}{c}\right)(z - \bar{z})}{c}$$

where $\bar{z}$ is the lateral deflection of the rear tire point from the rim; ρ is a reduction factor that allows for wheel curvature. One might mention here that σ is somewhat greater in the equation of moments than in the force equation because in case of a tire deflection there occurs simultaneously a circumferential deformation which additionally makes its contribution to the stiffness; this will, however, not be discussed further. In order to integrate the equations for P and M, we must know $\zeta(\xi)$ which in special cases can be obtained from the above working equation of the deformation. Before this is developed further, we will introduce a simplification based on the fact that the ground-contact line never moves in a severely bent curve, as there would be danger of skidding and the equation would then no longer hold true. On the whole we are dealing only with minor deflections and angles and must be careful to stay below the start of skidding. (Nevertheless, even at small deformations near the sides and at the rear of the tire some skidding does take place, yet this is insignificant in view of the amount of elastic force. The fact that damping is increased considerably by friction is important and will be discussed later). The equation may be simplified because the deflection curve has a large radius and can be approximated by a straight line (fig. 9).

The quantities z and $\bar{z}$ can now be substituted for the values of ζ. This gives the two approximations:

$$P = (z + \bar{z})(h + C)\sigma \tag{10}$$

and

$$M = (z - \bar{z})\left[\frac{h^2}{3} + C(h + C)\right]\sigma \tag{11}$$

or, abbreviating:

$$P = U_1(z + \bar{z}) \tag{12}$$

$$M = U_2(z - \bar{z}) \tag{13}$$

The percentage of the error due to this simplification is small in all cases.

As mentioned above, the moment is actually somewhat larger than given in the equation, since an additional moment arises from the increasing width of the ground-contact surface due to the deformation in circumferential direction, thus perpendicularly to z. For greater clarity this additional moment was omitted here, but must certainly be included in the calculation.

The two principal constants of the equation, c and σ, must be determined experimentally. Fortunately, we can perform several experiments that supplement and check each other. For example, c and σ can be obtained from the deformation of the lateral curves. For this purpose the wheel is placed transversely to the direction of the drum to which a force is applied at the circumference (figs. 10 and 11). The displacement of the tire can be measured and the curve calculated to give the value for c. In a balloon tire, 260 × 85mm, c is almost independent of the load and the pressure and equal 0.1 1/cm or

$$C = \frac{1}{c} = 10 \text{ cm}$$

In this experiment we find the values for z and $\bar{z}$, equal in this case, by direct measurement. The value of σ is obtained from the equation

$$P = \sigma(z + \bar{z})(h + C)$$

or

$$\sigma = \frac{P}{(z + \bar{z})(h + C)}$$

The experiment shows that we are actually dealing with an e-function. C can also be determined in the "yawed rolling experiment". This involves rolling the wheel at a small angle to its plane. Let us follow this case in more detail mathematically. In the equation

$$\frac{dz}{ds} + cz = \zeta - h\frac{d\varphi}{ds} - \frac{dx}{ds}$$

the value of φ is constant. Also

$$\frac{d\varphi}{ds} = 0 \quad \text{and} \quad \frac{dx}{ds} = 0$$

Therefore

$$\frac{dz}{ds} + cz = \varphi$$

Integrated, the equation is:

$$z = Ae^{-cs} + \frac{\varphi}{c}$$

With

$$y = z + h\varphi + x$$

we obtain

$$y = Ae^{-cs} + \varphi(h + C)$$

and with

$$\overline{y} = y(s - 2h)$$

$$\overline{y} = Ae^{-c(s-2h)} + \varphi(h + C)$$

Furthermore, with

$$\overline{z} = \overline{y} + h\varphi - x$$

$$\overline{z} = Ae^{-c(s-2h)} + \varphi(2h + C)$$

After a sufficiently long period of rolling, the e-functions disappear and we have

$$z_\infty = \frac{\varphi}{c}$$

$$\overline{z}_\infty = \varphi(2h + C)$$

and

$$y_\infty = \overline{y}_\infty = \varphi(h + C)$$

From the last equation we see that

$$y_\infty = \overline{y}_\infty$$

that is, that the tire track runs parallel to the s-axis. It forms a straight line with the distance of $\varphi(h + C)$ from the s-axis. Knowing φ and h, we are able to find C by measurement of y. The test results were in good agreement with those of the first determination. In this test we can again find σ as well by substituting the values for z in the equation for P:

$$P = \sigma\left[\varphi C + \varphi(2h + C)\right](h + C)$$

$$P = 2\sigma\varphi(h + C)^2$$

Measuring the force P, for example by the deformation of the fork, will enable us to calculate σ from the equation. Similarly, the constant for the moment M can be determined by several tests.

I have purposely avoided discussing deformation of the circumference until now, since it is of minor importance in shimmy. However, it is mentioned rather briefly for the sake of completeness.

The ground-contact surface has a finite lateral expansion. In a curve the outer part of the tire ground-contact surface describes a greater curve than the inner part. To compensate, some skidding or a constant deformation of the circumference must result. The latter occurs when the curves have a large radius. To measure deformation and the resulting force, the following test is performed (fig. 12). The wheel is rolled in a circular path. The above equations show that the tire track also describes a circle, concentric with the circular path but having a slightly larger radius. A force P develops which passes

through the wheel-center point toward the outside. The lateral deformation does not create a moment because of symmetry. Since

$$\overline{z} = z$$

therefore

$$z - \overline{z} = 0$$

Only the moment produced by change in the length remains and can be measured. The equation, whose derivation is similar to the ones shown above, will be omitted for the sake of brevity.

Likewise I can only briefly consider similarity considerations. The values for c and σ vary with the different tire parameters, that is, diameter $2r$, width B, pressure p, and the load N as well as the construction of the tire. For a series of similar tires there appears to be the following conformity:

The values C/r and σ/p depend only upon the magnitudes of the two quantities N/prB and B/r. Figures 13 and 14 show the test results.

The variation in the values is very great with different loads and pressures of the wheel. As long as there is no particular regularity, one might almost conclude that C/r and σ/p are independent of N/rpB, that is, they are constant when B/r is constant. For example, when $B/r = 0.65$, approximately

$$C = 0.8r(\text{cm}) \tag{14}$$

and

$$\cdot\ \sigma = 0.9p(\text{kg/cm}^2) \tag{15}$$

Yet I do not want to generalize from a few experimental values. Much needs to be done before reliable numerical constants can be reported.

Finally, and as an introduction to the subject of shimmying I would like to illustrate the calculation procedure of a wheel rolling on a sine curve. Let us assume that the wheel is attached to a fork on a swivel axis. The center point of the wheel is made to travel along the sine curve (fig. 15). The swivel angle is

$$\varphi = \varphi_o \cos \alpha s$$

where α can best be called the path frequency. It is the reciprocal of the wave length S:

$$\alpha = \frac{2\pi}{S} \tag{16}$$

Figure 15 shows further that:

$$x = q\varphi = q\varphi_o \cos \alpha s$$

This expression inserted in the differential equation for y results in:

$$y = \varphi_o \frac{1 + ch + cq}{c^2 + \alpha^2}\left[c \cos \alpha s + \alpha \sin \alpha s\right]$$

and for $\bar{y}$:

$$\bar{y} = y(s - 2h) = \varphi_o \frac{1 + ch + cq}{c^2 + \alpha^2}\left[c \cos \alpha(s - 2h) + \alpha \sin \alpha(s - 2h)\right]$$

We find z and $\bar{z}$ by substituting y and $\bar{y}$ into the equations:

$$z = y - x - h\varphi$$

$$\bar{z} = \bar{y} - x + h\varphi$$

Considering that

$$P = U_1(z + \bar{z})$$

$$M = U_2(z - \bar{z})$$

we obtain finally

$$P = U_1\varphi_o\left\{\frac{1 + ch + cq}{c^2 + \alpha^2}\left[c(\cos \alpha s + \cos \alpha(s - 2h)) + \right.\right.$$

$$\left.\left.\alpha(\sin \alpha s + \sin \alpha(s - 2h))\right] - 2(q + h)\cos \alpha s\right\}$$

and

$$M = U_2\varphi_o\left\{\frac{1 + ch + cq}{c^2 + \alpha^2}\left[c(\cos \alpha s - \cos \alpha(s - 2h)) + \alpha(\sin \alpha s - \sin \alpha(s - 2h))\right] - 2h \cos \alpha s\right\}$$

Both the ground-contact-line lateral deflection and the forces are pure trigonometric functions.

Now I would like to conclude the discussion of tire mechanics and, as an introduction to wheel shimmying, give a short physical description of the phenomena involved.

We assume that the swivel axis is perpendicular and passes through the wheel center point. The wheel plane forms an angle φ with the s-axis and the wheel has moved forward a short distance. The ground contact line shifts to the side and takes the position shown in figure 16, phase 1. The force area is somewhat greater behind the center point than in front of it, so that an inward rotating moment develops. As the wheel continues to move, the moment causes the rim to rotate (phase 2 and 3). The elastic moment continues in the same direction so that the rim turns over completely and forms a negative angle in regard to the s-axis (phase 4). In phase 5 the rim reaches the opposite maximum value of φ because the moment is now negative. Then the elastic forces return it to the original position. We must take into consideration that the path of the front point of the ground-contact line always follows, tangentially to the e-function, the forward tire center line that does not contact the ground and whose asymptote is the rim.

There is a continuous play between the rim which is turned by the elastic moment and the ground-contact line, whose path is determined by the current position of the wheel plane. This reciprocal effect explains the occurrence of free oscillations.

In addition it is to be noted that equilibrium of the moments around the swivel axis can be maintained by damping.

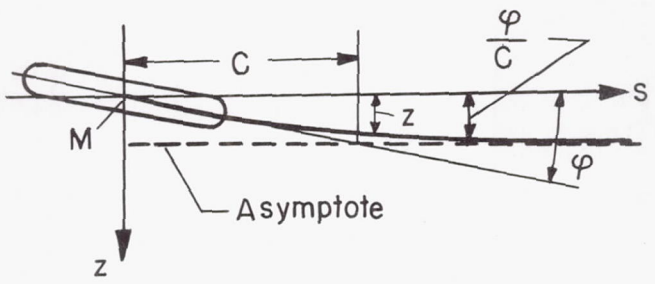

Figure 1

Figure 2

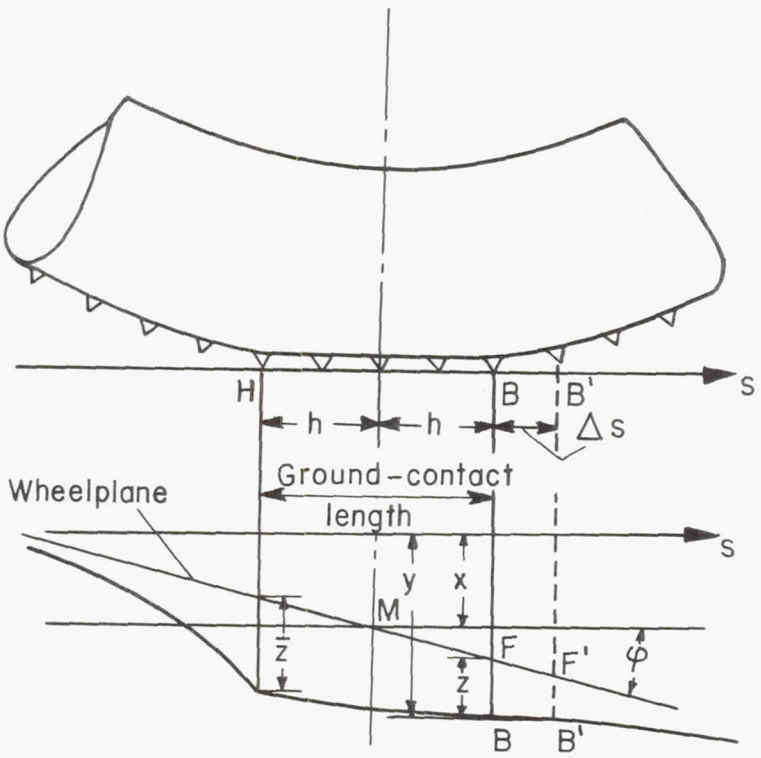

Figure 3

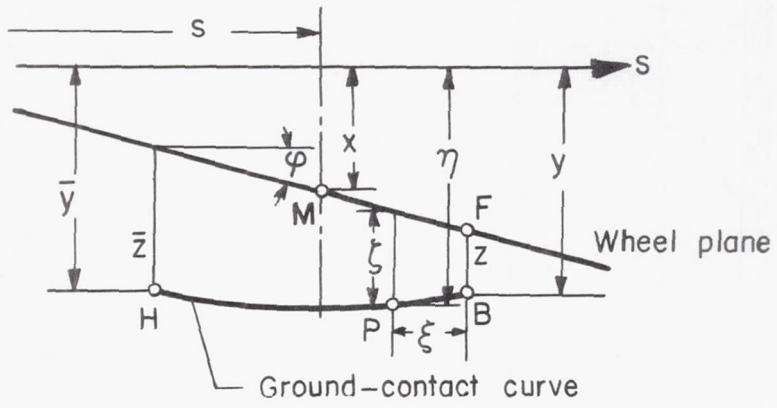

Figure 4

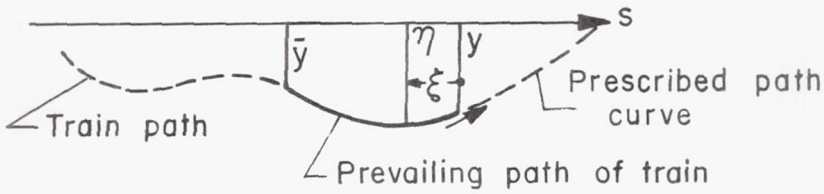

Figure 5

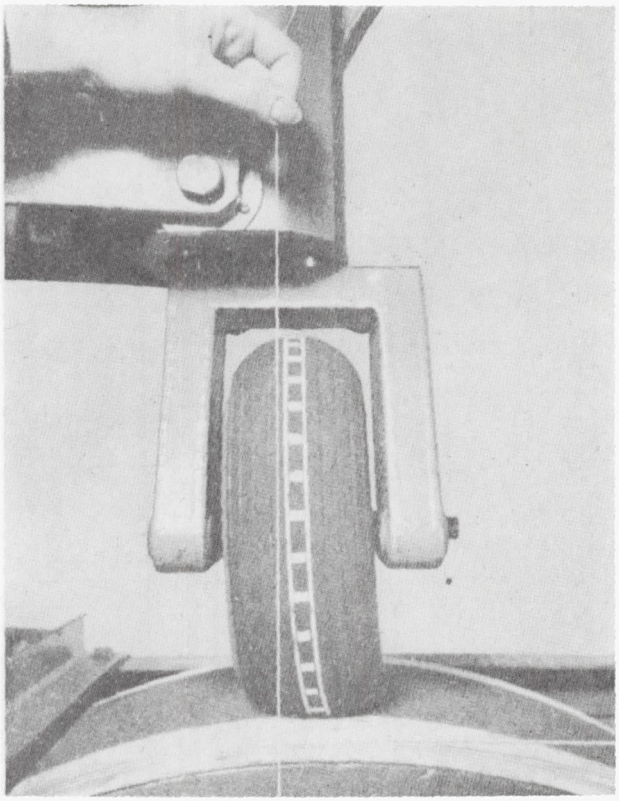

Figure 6

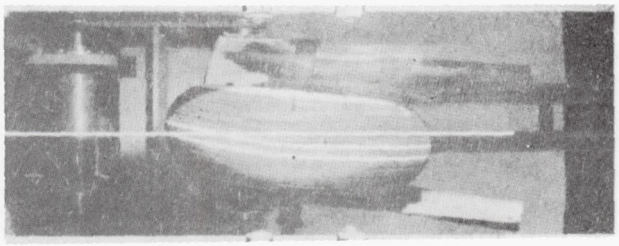

Figure 7

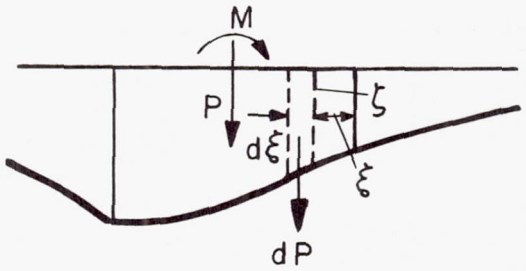

Figure 8

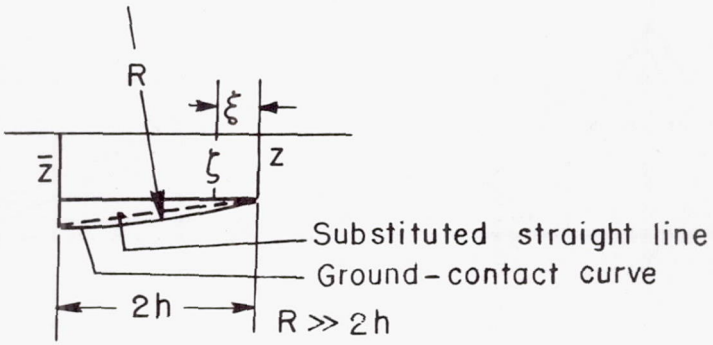

Figure 9

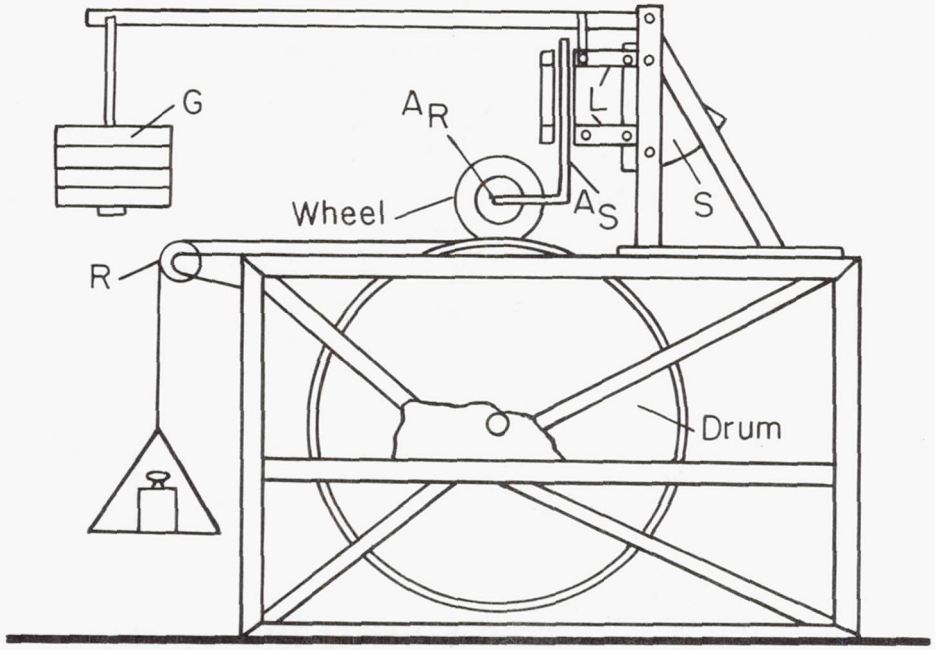

Figure 10

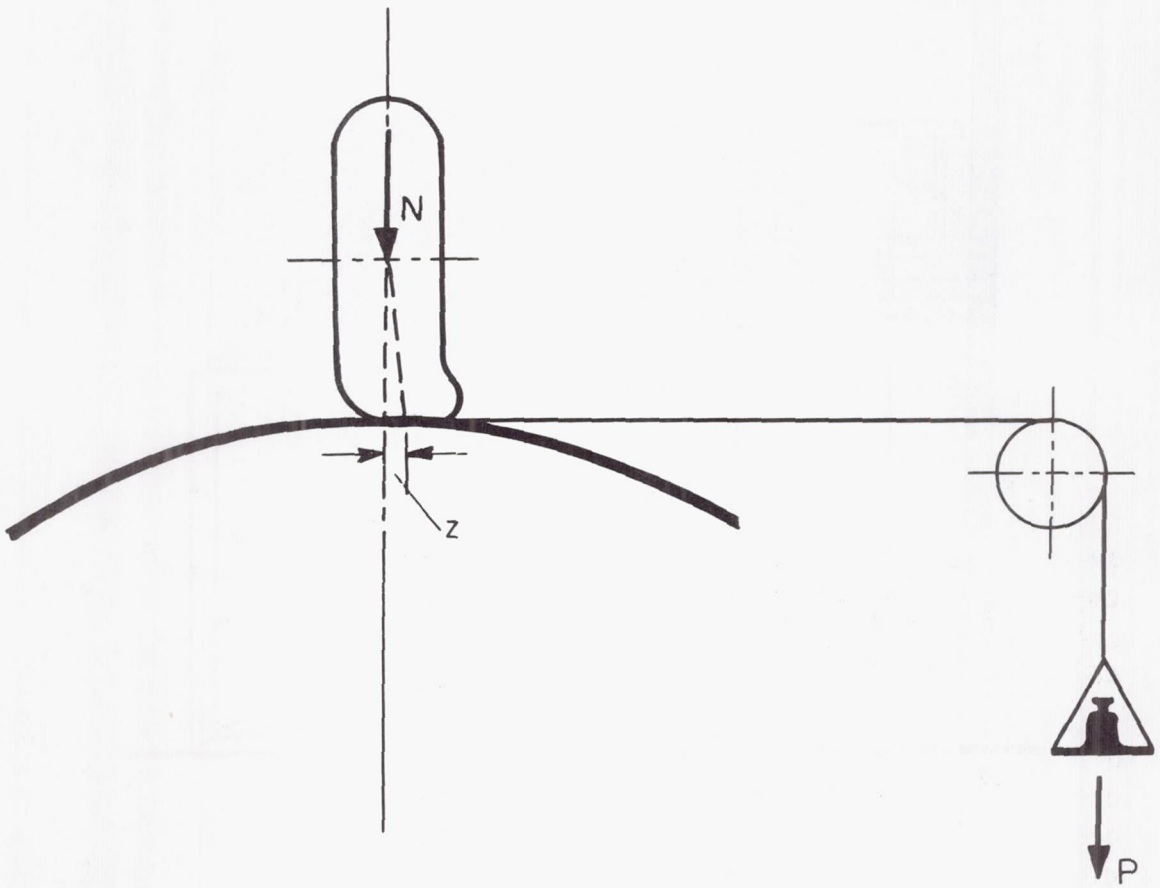

Figure 11

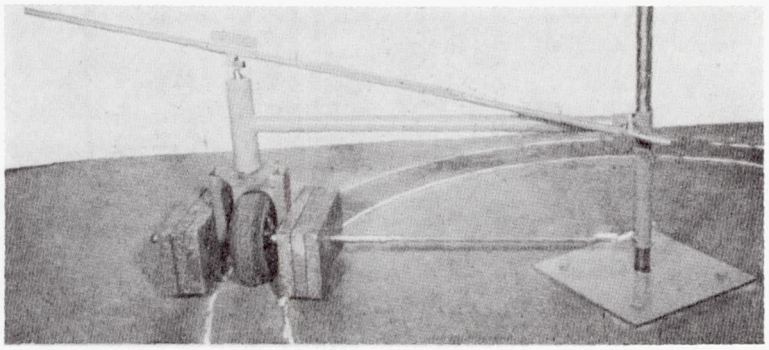

Figure 12

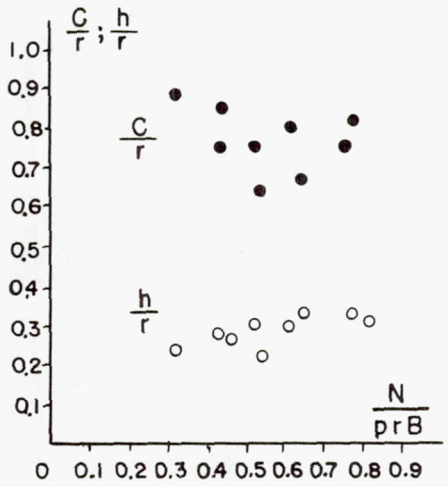

Figure 13

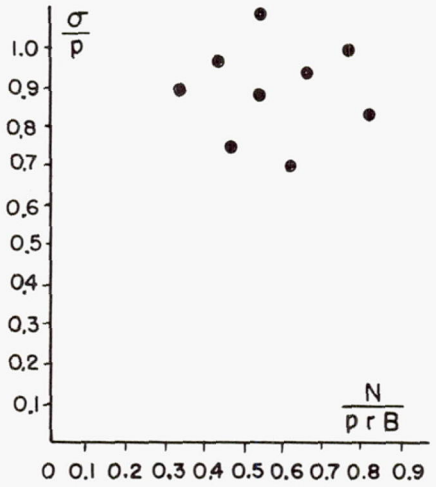

Figure 14

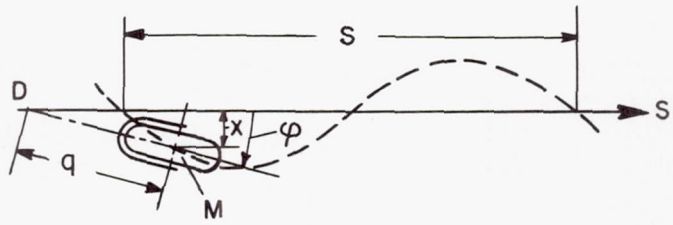

Figure 15

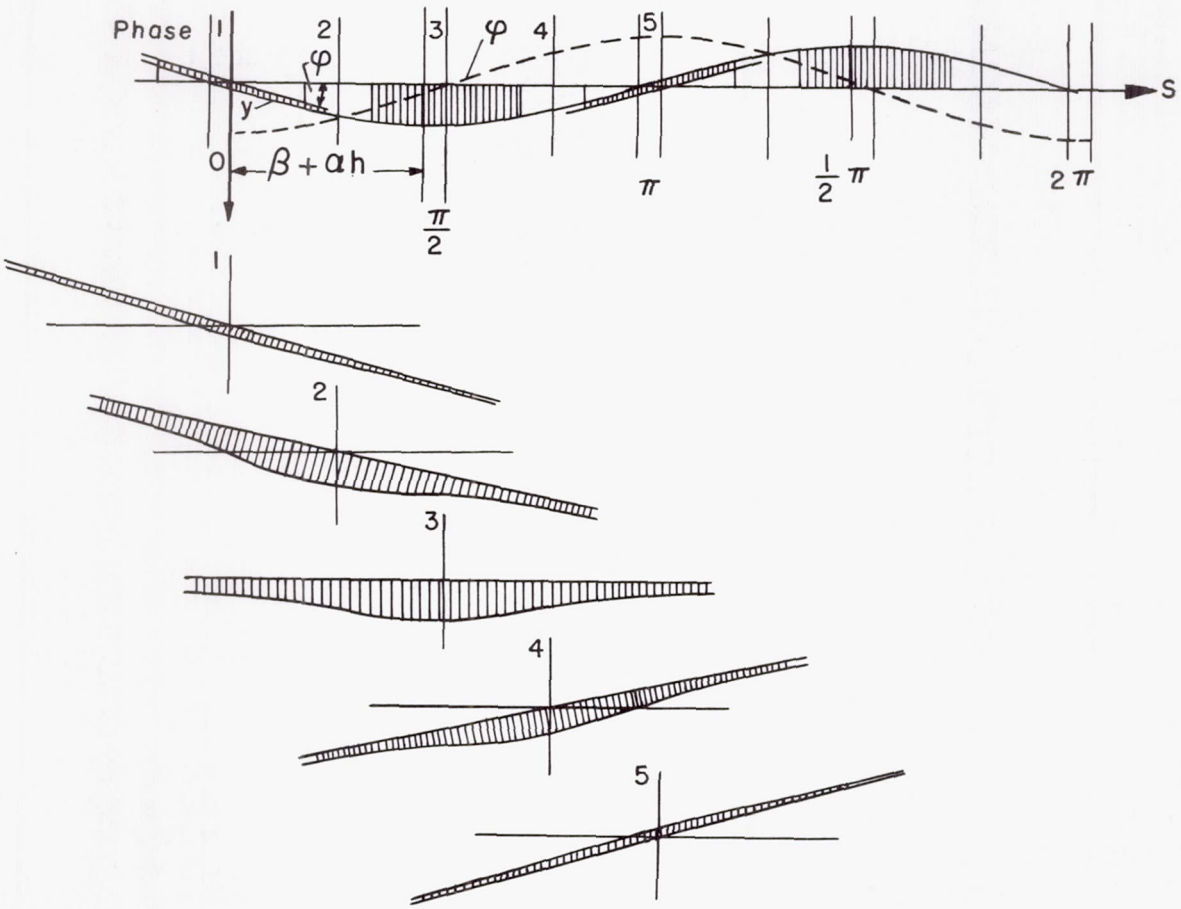

Figure 16

B. WHEEL SHIMMY

by R. Dietrich

The preceding paper by v. Schlippe describes the characteristics, the deformations and resulting forces of a rolling tire. The theoretical investigation of wheel shimmy, based on his results, will now be discussed in detail. First I shall repeat some of the known equations.

1. The equation of motion of the foremost ground-contact point (see fig. 1):

$$y' + cy = \varphi(l + ch) + cx \tag{1}$$

2. The equation of motion of the rearmost ground-contact point:

$$\bar{y} = y(s - 2h) \tag{2}$$

3. The lateral deflection of the foremost and rearmost ground-contact points from the wheel plane:

$$z = y - x - h\varphi \tag{3}$$

$$\bar{z} = \bar{y} - x + h\varphi \tag{4}$$

4. The resulting elastic forces

$$P = U_1(z + \bar{z}) \tag{5}$$

$$M = U_2(z - \bar{z}) \tag{6}$$

The wheel rolls with a constant velocity v in the direction of the s-axis. The swivel axis, assumed to be perpendicular to the ground in the beginning, always remains in the vertical plane which passes through the s-axis, whereas the wheel itself can swivel on the lever arm q. The lever arm q shall be called the lead $(+q)$ whenever the center ground contact point precedes the projection of the swivel axis on the ground plane. In general when the swivel axis inclines, the lead q is understood to be the distance from the center ground contact point to the point of intersection of the swivel axis with the ground plane (see fig. 2).

The ordinate of the rim-center point is

$$x = q\varphi \tag{7}$$

Next we will set up the equation of motion. The equilibrium of moments around the swivel axis is given as

$$J\ddot{\varphi} - qP - M + \mu\varphi + \chi_1\dot{\varphi} + \frac{\chi_2}{\omega}\dot{\varphi} = 0 \tag{8}$$

$J\ddot{\varphi}$ moment of inertia times angular acceleration

$qP + M$ elastic moment of the tire

$\mu\varphi$ restoring moment, produced by springs or by inclination of the swivel axis; in the latter case,

$$\mu = N\beta q$$

$\chi_1\dot{\varphi} + \frac{\chi_2}{\omega}\dot{\varphi}$ outer and inner damping moment

The damping moment $\chi_1\dot{\varphi}$ stands for true velocity damping, as produced, for example, by a liquid-type damper attached to the swivel axis. Aside from this, the system already has heavy inner damping, especially damping produced by the material of the tire. The inner damping is assumed to be proportional to the swivel amplitude, but independent of the frequency. The total inner damping must be in the form of an integral, whose value is also proportional to $\dot{\varphi}$. If the expression χ/ω [1] is substituted for the constant χ, we obtain a type of damping that is independent of the frequency ω (circular frequency). In the periodic formulation $\varphi = \varphi_o \sin \omega t$, the damping moment becomes

$$\frac{\chi}{\omega}\dot{\varphi} = \frac{\chi}{\omega}\varphi_o\omega \cos \omega t = \chi\varphi_o \cos \omega t$$

whose maximum value, and that alone is the deciding factor, is actually independent of the frequency. The equation of motion therefore includes the additional damping moment $\frac{\chi_2}{\omega}\dot{\varphi}$. The term is meant to summarize only ideal conditions of inner damping. Actually this is probably much more complicated. Let us consider the equation of motion (8) first. For the first time we are dealing with time t; again we will take the path s

---

[1] See v. Schlippe: "Die innere Dämpfung," Ingenieur-Archiv, Bd VI, p. 127, 1935.

as the independent variable and substitute:

$$\dot{\varphi} = \frac{d\varphi}{dt} = \frac{d\varphi}{ds}\frac{ds}{dt} = \varphi' v$$

$$\ddot{\varphi} = \frac{d^2\varphi}{dt^2} = \frac{d^2\varphi}{ds^2}\left(\frac{ds}{dt}\right)^2 = \varphi'' v^2$$

For the circular frequency ω we introduce a "path frequency" α, as follows. If for a periodical swinging the deflection φ is plotted against the path coordinate s (fig. 3) then the wave length is:

$$S = v\frac{2\pi}{\omega}$$

accordingly there follows as "path frequency":

$$\frac{\omega}{v} = \frac{2\pi}{S} = \alpha \tag{9}$$

With these substitutions the equation of motion (8) becomes

$$Jv^2\varphi'' - qP - M + \mu\varphi + \chi_1 v\varphi' + \frac{\chi_2}{\alpha}\varphi' = 0 \tag{10}$$

Equation (10) and equations (1) to (7) are sufficient for the solution of our problem. By assuming a solution of the form

$$\varphi = \varphi_o e^{\lambda s} \tag{11}$$

for this system of equations, one obtains a characteristic equation for λ.

The calculation is carried out as follows. From the assumed solution (11):

$$\varphi = \varphi_o e^{\lambda s}$$

according to equation (7)

$$\chi = q\varphi = q\varphi_o e^{\lambda s}$$

and substituting in equation (1) gives

$$y' + cy = \varphi_o e^{\lambda s}(1 + ch) + cq\varphi_o e^{\lambda s} = (1 + ch + cq)\varphi_o e^{\lambda s}$$

Solving for y (using only the particular integral of the nonhomogeneous equation) gives

$$y = \varphi_o \frac{1 + ch + cq}{\lambda + c} e^{\lambda s}$$

According to equation (2) then

$$\bar{y} = y(s - 2h) = \varphi_o \frac{1 + ch + cq}{\lambda + c} e^{\lambda(s-2h)}$$

Equations (3) and (4) become

$$z = y - x - h\varphi = \varphi_o e^{\lambda s}\left(\frac{1 + ch + cq}{\lambda + c} - q - h\right)$$

$$\bar{z} = \bar{y} - x + h\varphi = \varphi_o e^{\lambda s}\left(\frac{1 + ch + cq}{\lambda + c} e^{-\lambda 2h} - q + h\right)$$

The forces created by the tire according to (5) and (6) are

$$P = U_1(z + \bar{z}) = U_1\varphi_o e^{\lambda s}\left[\frac{1 + ch + cq}{\lambda + c}\left(1 + e^{-\lambda 2h}\right) - 2q\right]$$

$$M = U_2(z - \bar{z}) = U_2\varphi_o e^{\lambda s}\left[\frac{1 + ch + cq}{\lambda + c}\left(1 - e^{-\lambda 2h}\right) - 2h\right]$$

Finally these expressions, all of which contain the factor $\varphi_o e^{\lambda s}$ because of homogeneity, are substituted into the equation of motion (10).

The factor $\varphi_o e^{\lambda s}$ can be divided out, leaving an equation for λ, which is transcendental because of equation (2):

$$c_o + \left(c_1 + \frac{c_1'}{\alpha}\right)\lambda + \left(c_2 + \frac{c_2'}{\alpha}\right)\lambda^2 + c_3\lambda^3 + c_4 e^{-\lambda 2h} = 0 \qquad (12)$$

Its roots are

$$\lambda = \delta + i\alpha$$

The sign of the real part δ determines the stability of the respective oscillations; $\delta > 0$ means divergence, $\delta < 0$ means convergence. We are interested in the critical values for q and v, that is, those that involve neither increase nor decrease of oscillations, or where

$$\delta = 0$$

The transcendental equation for $\lambda = i\alpha$ can be broken down into two real equations by making the real and the imaginary parts equal to zero. The calculation itself will be omitted for brevity and only the result will be given. The two equations can be expressed in the form

$$X_1 v + \frac{X_2}{\alpha} = -\frac{1 + ch + cq}{c^2 + \alpha^2}\left[U_1 K_1 q + U_2\left(2 - K_1\right)\right] \qquad (13)$$

$$J v^2 \alpha^2 = 2\left(U_1 q^2 + U_2 h\right) - \frac{1 + ch + cq}{c^2 + \alpha^2}\left(U_1 K_2 q + U_2\left(2c - K_2\right)\right) + \mu \qquad (14)$$

where the following abbreviations are used

$$K_1 = 1 + \cos \alpha 2h + \frac{c}{\alpha} \sin \alpha 2h$$

$$K_2 = c\left(1 + \cos \alpha 2h - \frac{\alpha}{c} \sin \alpha 2h\right)$$

We will discuss equations (13) and (14) in more detail. First when damping is not proportional to speed, X_1 must equal 0. The equation (13) can then be written

$$\chi_2 = -\frac{\alpha(1 + ch + cq)}{c^2 + \alpha^2}\left[U_1 K_1 q + U_2(2 - K_1)\right] \qquad (13a)$$

For a given value of χ_2, q is a double-valued function of α. When $\chi_2 = 0$ the equation falls into three parts:

1. $\alpha = 0$ $\qquad$ q arbitrary

2. $1 + ch + cq = 0$ $\qquad$ $q = -\frac{1 + ch}{c}$

3. $U_1 K_1 q + U_2(2 - K_1) = 0$ $\qquad$ $q = -\frac{U_2}{U_1}\frac{2 - K_1}{K_1}$ function of α.

The curves of q against α corresponding to the three curve branches 1, 2, and 3 are plotted in figure 4. Equation (3) has further curve branches because of the trigonometric functions of K_1. From the point of view of physics only the drawn lines are of interest, namely the heavily lined "triangle", along with lines 1 and 2. The lower corner of the "triangle," that is, when 1 and 3 are solved simultaneously, corresponds to the transition to static indifference, since $\alpha = 0$. If the lead is greater than $\frac{U_2}{U_1}\frac{ch}{1 + ch}$, the wheel will deflect aperiodically. This is just within the limit of validity of the formulated inner damping, because for the above a true oscillation (frequency ω) is necessary. If the damping constant χ_2 assumes a small positive value, the "triangle" becomes a closed curve with a continuous tangent throughout. The corners round off. The greater the value for χ_2, the smaller the closed curve becomes until it finally reduces to a point. This is the case when the discriminant of the quadratic equation for q (13a) has a maximum value of 0. Then only one real point (α, q) remains of the family of curves and χ_2 has a finite value. If χ_2 is given a still greater value, oscillations with a constant amplitude are no longer possible; that is, they always decrease.

It is striking that each α value corresponds to two q values and that there are two α values for every q value.

With equation (14) we can calculate the critical speeds that correspond to a given lead q. Since there are two α values, we have in general two critical speeds. Thus the v-, q-curves also will be closed.

Next we will again consider the special case $\chi_2 = 0$ and the series of different cases mentioned above. The restoring moment μ is also zero.

1. $\alpha = 0$

(a) q arbitrary

$v = \infty$, see figure 5.

(b) $q = \frac{U_2}{U_1} \frac{ch}{1 + ch}$ (Point of intersection 1/3 in the v, q plane)

Substitution in equation (14) results in

$$Jv^2\alpha^2 = 0$$

Regardless of the value chosen for v, the equation is always satisfied when $\alpha = 0$, thus we obtain the straight line 1/3 in the v, q plane (fig. 5).

2. $q = -\frac{1 + ch}{c}$

q is independent of α; i.e., v can be given any value. Thus we obtain the straight line 2.

3. $q = -\frac{U_2}{U_1} \frac{2 - K_1}{K_1}$

results in the curve branch 3. v^2 becomes negative before q attains the value $\frac{U_2}{U_1} \frac{ch}{1 + ch}$, that is, v becomes imaginary.

When χ_2 does not equal zero but has a positive value, the resulting curves are finite; as χ_2 increases, the curves close although the first of the family of curves is open on the left just like the initial curve. With proper χ_2 value they reduce to a point, like the curves in the α, q plane, when the χ_2 values are equal. For the points v, q that lie within the curve for the chosen χ_2 value, there is an increased wheel oscillation (a decrease outside of the curve); it is obvious from the standpoint of physics that with increased damping the range of shimmy must decrease. Figures 6 and 7 show the α, q and v, q curves calculated for an experimental wheel.

Closed curves of this type occur also in the formulation for damping that is proportional to speed only. This is not as obvious at first as for the type of damping that is proportional to the amplitude and independent of the frequency. In place of (13a) we have

$$\chi_1 = -\frac{1 + ch + cq}{v\left(c^2 + \alpha^2\right)}\left(U_1 K_1 q + U_2\left(2 - K_1\right)\right) \tag{13b}$$

whereas equation (14) remains unchanged. Equation (13b) includes q as well as v. The following can be said at first glance:

When $\chi_1 = 0$, either

1. $v = \infty$

or

2. $1 + ch + cq = 0$

or

3. $U_1 K_1 q + U_2\left(2 - K_1\right) = 0$

} as before

For case 1, because of equation (14),

$$\alpha = 0 \quad \text{and} \quad q \quad \text{arbitrary}$$

Thus the "triangle" already shown in figure 4 is formed. The same closed curve that reaches infinity is formed in the v, q-plane.

The point of intersection 1/3 is given by

$$\alpha = 0 \quad \text{and} \quad q = \frac{U_2}{U_1}\frac{ch}{1 + ch}$$

Equation (14) is satisfied for every v; thus, the straight line 1/3 is formed again.

If χ_1 does not equal 0, closed curves result once more. They are not as easily calculated, however, because now both (13b) and (14) contain v and q. By eliminating v, the equation for q is of the sixth degree (since J can be set up as a quadratic function of q), whose coefficients include the parameter α whereas in the first case this was a quadratic equation, namely (13a) itself.

In general both types of damping are found. It is obvious then that closed v,q curves will result.

These closed curves already appeared in Professor Kamm's experiments, with which you are undoubtedly familiar.

Since our experiments and calculations have not been completed, I can give only partial results. At the lower critical speeds the experimental values were in good agreement with the theoretical curves. The damping constant χ_2 could be determined by a simple deflection experiment with a stationary wheel. After a small deflection the damping produced by the tire forces returns the loaded wheel to the original position. The q,α and v,q curves were calculated from the resulting damping value χ_2, and, as shown in figures 8 and 9, they agree somewhat with the experimental values. There was no artificial damping.

The principal part of the theory of wheel shimmy is completed with the development of closed curves. Nevertheless, there are many other important problems that must be solved experimentally and mathematically, especially those that will give better understanding of the skid effect at large angles of deflection which probably will affect the damping forces primarily. It is hardly expected that the theory needs to be changed even when applied to larger deflections; the same is often the case with other oscillation phenomena. Another important aim is to find simple formulas (general-purpose formulas) that will aid in the practical construction of a non-shimmy wheel (nose or tail wheel) and do not involve numerous complicated calculations and experiments.

*Translated and edited for the AAF by:
Charles A. Meyer & Company
25 Vanderbilt Avenue
New York, 17, New York
July 7, 1947 (ATI No. 18920)

*Note: In order to provide terminology consistent with other papers of this series, this translation has been reworded in many places by the NACA reviewer.

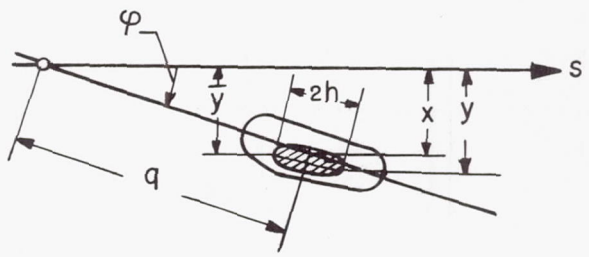

Figure 1

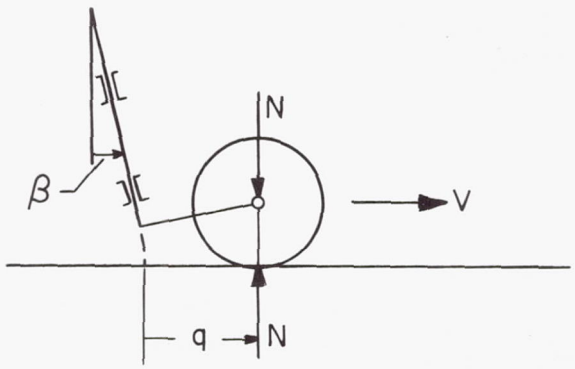

Figure 2

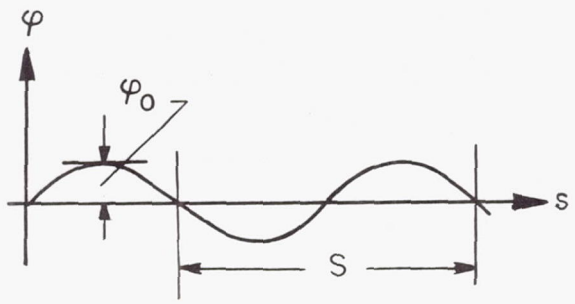

Figure 3

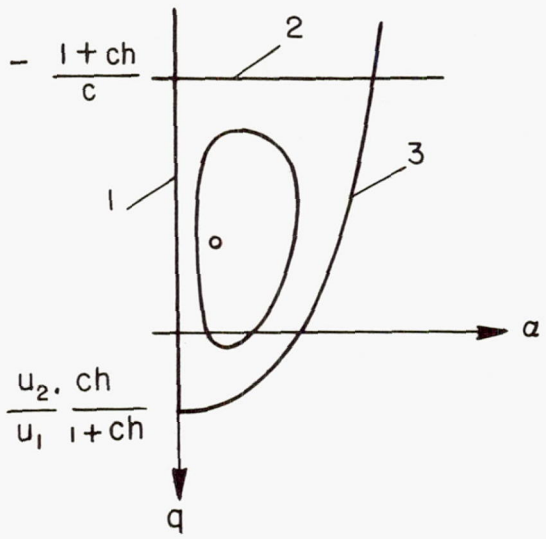

Figure 4

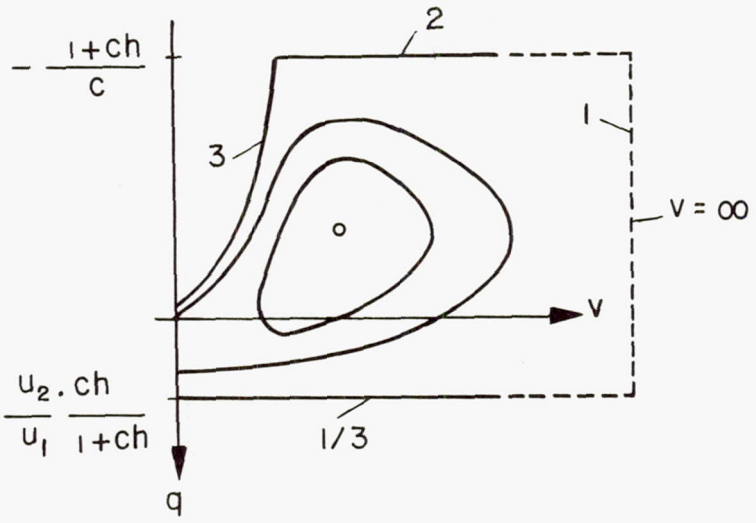

Figure 5

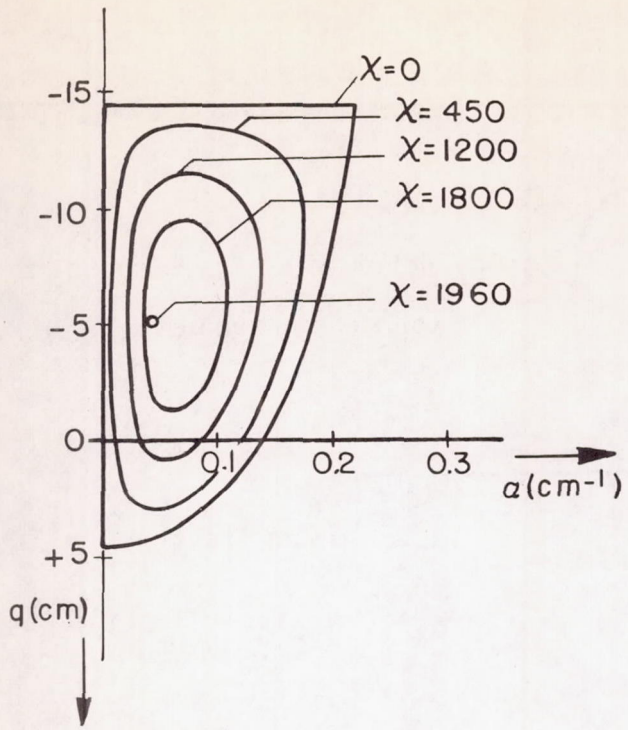

Figure 6

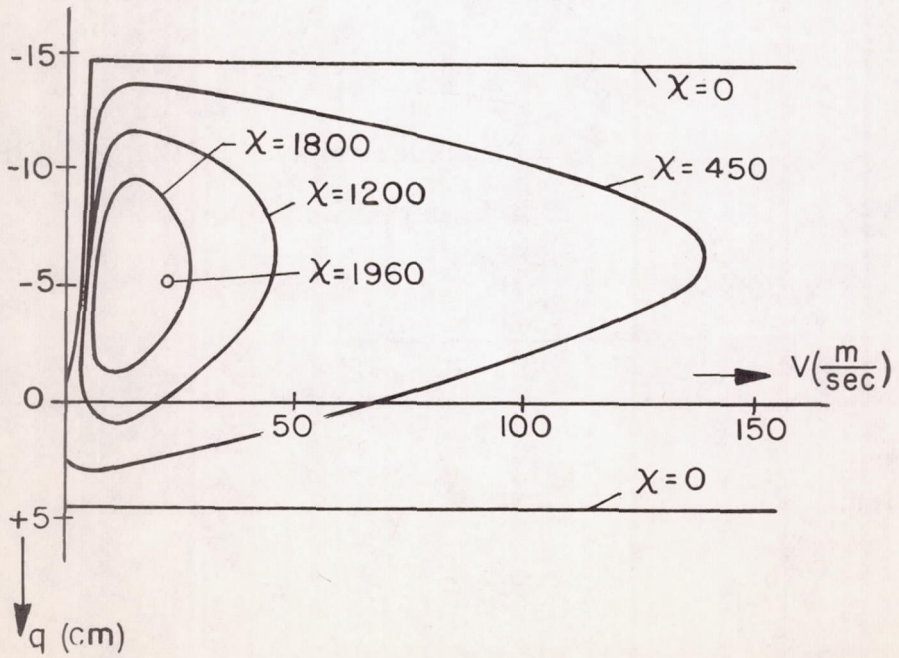

Figure 7

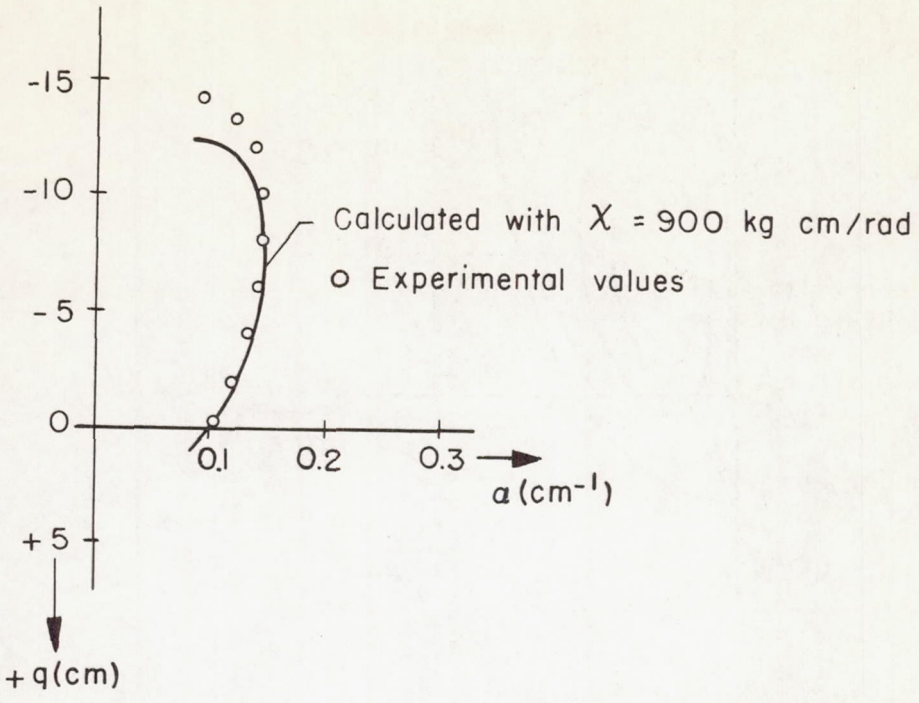

Figure 8

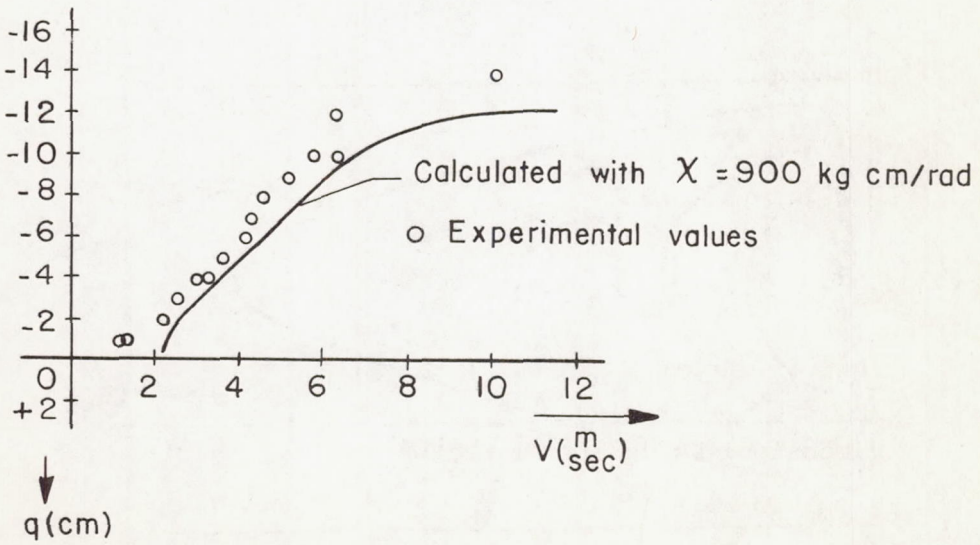

Figure 9

COMMENTS ON TWO AMERICAN RESEARCH REPORTS*

By E. Marquard

OUTLINE

Brief Summary

1. Kantrowitz, Arthur: Stability of Castering Wheels for Aircraft Landing Gears. NACA Rep. 686, 1940.

2. Wylie: Dynamic Problems of the Tricycle Landing Gear. Journal of the Aeronautical Sciences, vol. 7, no. 2, Dec. 1939.

On the Theory of Wheel Shimmy

Results

SYMBOLS

Θ swivel angle of the wheel

r wheel radius

t trail

J moment of inertia about the swivel axis

v rolling speed

K damping factor

$C_l \approx \epsilon r \frac{W_s}{J}$

W_s lateral spring constant of the tire

ϵ dimensionless numerical factor

$$\left(\epsilon = \begin{cases} 0.69 \text{ for } 5^\circ \text{ trail} \\ 1.0 \text{ for } 20^\circ \text{ trail} \end{cases} \right)$$

---

*"Bericht über zwei amerikanische Forschungsarbeiten," Bericht 140 der Lilienthal-Gesellschaft, pp. 46-48.

BRIEF SUMMARY

The report of Kantrowitz gives a theory of tail-wheel shimmy based on the phenomenon of so-called kinematic shimmy. The coefficients of the equations that had been set up and the confirmation of the theory are obtained from the results of three test series.

The first test series was made on a tail-wheel model with low-pressure tires of about 5 cm radius on a running continuous rubber belt. Damping could be installed at the swivel axis of the model wheel. The structural support of the swivel axis was rigidly fixed in the test setup. Since a shimmying airplane wheel causes a reaction on the motion of the entire airplane, a second test series was made for investigation of this influence, with use of a free-rolling catapulted airplane model, the movements of which were photographed in intermittent light. Various tires, model masses, and trail angles (5° and 20°) were investigated.

A third measuring series was performed on an airplane of the type W-1A. The shimmying was filmed for various measured magnitudes of the friction damping.

Following the development of the theory, avoidance of shimmy by hydraulic and frictional dampers is discussed. A further possibility for suppression of shimmy is the introduction of an additional degree of freedom, namely, the lateral freedom of the wheel on the axle. Two types of design, lateral play in the bearings and suspension of the wheel in a double spindle, are briefly mentioned. In an appendix, the effect of a third degree of freedom is estimated numerically. It manifests itself as an additional damping term.

The report of Wylie deals with the problems resulting in case of application of tricycle landing gears. After a short representation of the development of this research, at the Douglas Aircraft Company, the following problems are stressed as most important:

(a) Shimmying of the nose wheel as the main problem

(b) Investigation of the pitching (pitching of the engine) vibrations of the rolling airplane

(c) The maneuverability of the rolling airplane with tricycle landing gears

The last problem is only briefly touched upon. The vibration equations for the lifting and pitching vibrations of the airplane are set up and discussed.

There results a homogeneous linear differential equation of the fifth order which is further discussed with the aid of the Routh[1] discriminant.

Result:

1. Nose-wheel load as large as possible

2. Arrangement of the main wheels always behind the center of gravity, even for farthest rearward position of the center of gravity and lowest tail position

3. The airplane must be statically longitudinally stable and must have sufficient tail-surface volume for damping

4. The position of the main landing gear with respect to the wing must satisfy an equation given in the text.

The calculation method is applied to the airplane type Douglas DC-4. By numerical calculation, two types of pitching vibrations are found which are both harmless due to the long period of vibration and the large damping. These vibration periods are

$$T_1 = 4.06\text{s} \quad \text{and} \quad T_2 = 49.2\text{s} \quad \text{for} \quad V = 91 \text{ km/h}$$

The theory of wheel shimmy is completely taken over from the former report and merely formally somewhat extended. The damping moment required for the suppression of shimmy and the shimmy frequency are calculated for the airplane models OA-4A and DC-4. The calculation values are compared with actual conditions. Also, the effect of combined oil and friction damping, as well as the influence of restoring devices are shown in graphical representations.

CONCERNING THE THEORY OF WHEEL SHIMMY

The method for derivation of the vibration equation applied by the two American authors does not use the customary classical formulations[2]; we feel this method to have the character of a rough calculation with somewhat daring assumptions.

---

[1]E. I. Routh: A Treatise on the Stability of a Given State of Motion (London 1877) German edition: Die Dynamik der Systeme starrer Körper, vol. II, (Leipzig 1898).

[2]Compare, Melzer (Fw): Beitrag zur Theorie des Spornradflatterns. Technische Berichte 2, 1940.

The development of the entire derivations would lead here too far. We shall therefore represent only the expression for the so-called "kinematic shimmy" graphically (fig. 1) without defining our own attitude.

The kinematic shimmy is to take place after an initial deflection of the wheel by the angle Θ against the direction of motion under the following presuppositions:

(a) Slow motion, thus no mass forces

(b) Center line of the deflected surface of contact of the tire bent in the form of a circular arc with the tire diameter as chord

(c) No rolling forces, thus symmetrical stress distribution in the surface of contact

(d) No sliding of any element of the surface of contact

(e) No lead or trail

From figure 1, there result the two relations:

1. $\frac{d\lambda}{ds} = -\Theta$ and

2. $\frac{d\Theta}{ds} = \frac{1}{R} = \frac{2}{r^2}\lambda$ or $\lambda - \frac{r^2}{2}\frac{d\Theta}{ds} = 0$

and

$$\frac{d^2\Theta}{ds^2} = -\frac{2}{r^2}\Theta \quad \text{or} \quad \frac{d^2\Theta}{dt^2} = -\frac{2v^2}{r^2}\Theta$$

frequency $\omega = \frac{v}{r}\sqrt{2}$; wave length corresponding to path

$$S = \frac{2\pi r}{\sqrt{2/r^2}} = \pi r\sqrt{2} \approx 0.7 \quad \text{Circumference}$$

Consideration of the dynamic shimmy, after giving up the simplifying assumptions a, c, and e and after addition of a damping, leads to the equation

$$\frac{d^3\Theta}{ds^3} + \frac{d^2\Theta}{ds^2}\underbrace{\left\{\frac{1}{r} + \frac{r^2}{2}\frac{c_1}{v^2} + \frac{K}{vJ}\right\}}_{A} + \frac{d\Theta}{ds}\underbrace{\left\{2t\,\frac{c_1}{v^2} + \frac{K}{rvJ}\right\}}_{B} + \underbrace{\frac{c_1}{v^2}\left(1 + 2\,\frac{t}{r}\right)}_{C}\Theta = 0$$

Hence, the frequency of the shimmy vibration is

$$\omega = \sqrt{2t\,\frac{c_1}{v^2} + c_2\,\frac{K}{vJ}}$$

The coefficients of the equation are all positive. The Routh discriminant[3] yields the critical minimum damping value from $C = AB$.

It is assumed that critical deflections occur when the tire in shimmying starts skidding. Then one has with a static-friction coefficient μ

$$\mu P = W_s \lambda$$

Hydraulic and frictional dampers are regarded as equivalent when they consume for a whole vibration the same energy quantity

$$\underline{A} = \pi\omega K v \Theta^2_{max}$$

Hence, there results that the maximum damping moment of a hydraulic damper, for the maximum swiveling angular velocity $\dot{\Theta}_{max} = -\omega v \Theta_{max}$,,

must have the magnitude

$$\underline{M}_{max} = -\omega K v \Theta_{max} = \frac{4}{\pi}\,\underline{M}_{friction} = 1.273\underline{M}_{friction}$$

---

[3]Compare, Hurwitz, Mathematische Annalen, vol. 46, 1895, p. 273.

In the further discussion, the influence of the trail is investigated by means of partial differentiation with respect to t; furthermore, the influence of a restoring force $-f\Theta$, finally also the effect of the gyroscopic forces of the rotating wheel.

RESULTS

The character of the shimmy vibrations becomes evident from figure 2 which represents the phase shift between wheel swiveling Θ and lateral deformation λ of the tire, the frequency of the shimmy vibration, and the "excitation" that is a measure for the increment of the subsequent compared to the previous deflection as a function of the rolling speed.

For low rolling speeds, the vibration frequency increases approximately linearly with the velocity; the wheel passes through the zero position with approximately the largest lateral deflection of the tire, the deflections increase rapidly with the velocity. For high rolling speeds, the frequency of vibrations is almost constant, the deflections and the phase shift between wheel swiveling and tire deflection decrease with the velocity.

Both authors calculate the required damping for various airplane models and show the usability of their calculation methods by comparison with the values of full-scale landing gears. The decisive point therein always is determination of the rolling speed v for the maximum excitation (compare fig. 2) and calculation of the required damping. Under the conditions mentioned, the damping factor becomes approximated by

$$K_{max} = 0.43r\sqrt{JW_s}\left[\frac{\text{lb-ft}}{\text{radians/sec}}\right] \quad \text{or} \quad \left[\frac{\text{kgm}}{\text{radian/s}}\right]$$

With the aid of unpublished measurements of tire constants, the further simplification

$$K_{max} = \text{Constant } r\sqrt{J}$$

is made. Therein, one obtains: constant = 16 - 32 when r is inserted in $[\text{ft}]$, J in $[\text{slugs}]$, and K_{max} in $\left[\frac{\text{lb-ft}}{\text{radians/sec}}\right]$, or one obtains: constant = 19.5 - 39.0 when r is inserted in $[\text{m}]$, J in $[\text{kgms}^2]$, and K_{max} in $[\text{kgms}]$.

The velocity of maximum excitation is

$$V_0 = 0.59r^2\sqrt{\frac{W_s}{J}}\left[\text{ft/sec}\right] \quad \text{or} \quad \left[\text{m/s}\right]$$

For model W-1A, one obtains $v_0 = 39$ ft/sec = 12 m/s = 43 km/h and $K_{max} = 4.67\left[\frac{\text{lb-ft}}{\text{radian/sec}}\right] = 0.645\left[\frac{\text{kgm}}{\text{radians/sec}}\right]$. With $\mu = 0.55$ there is

$$\underline{M}_{max} = 19 \text{ lb-ft} = 2.62 \text{ mkg}$$

for $P = 310$ lbs = 140 kg wheel load.

For model Hammond V one obtains $v_0 = 46$ ft/sec = 14 m/s = 50.5 km/h and

$$K_{max} = 13.2\left[\frac{\text{lb-ft sec}}{\text{radians}}\right] = 1.825\left[\frac{\text{kgm}}{\text{radians/sec}}\right]$$

With $\mu = 0.55$ there is

$$\underline{M}_{max} = 44 \text{ lb-ft} = 6.1 \text{ mkg}$$

for $P = 570$ lbs = 258 kg wheel load.

From the calculations for various models, one may indicate the required minimum moment of the frictional damping generally for geometrically similar airplanes and in case of proportionality of nose-wheel load P_F and total weight P_{total}. For $\mu = 0.55$, one has

$$\underline{M}_R = \gamma P_F\left[\text{in-lbs}\right] \qquad \gamma = 0.01\sqrt{P_{total}}$$

$$\underline{M}_R = 0.01P_F\sqrt{P_{total}}\ \left[\text{in-lbs}\right]$$

$$= 0.377 \times 10^{-3}P_F\sqrt{P_{total}}\ \left[\text{mkg}\right]$$

With $P_F = \beta P_{total}$, $\underline{M}_R$ is

$$\underline{M}_R = \text{Constant } \beta P_{total}^{3/2}$$

or with a characteristic length L

$$\delta L^3 = P_{total} \qquad \underline{M}_R = \text{Constant } \delta L^{9/2}$$

Translated by Mary L. Mahler
National Advisory
Committee for Aeronautics

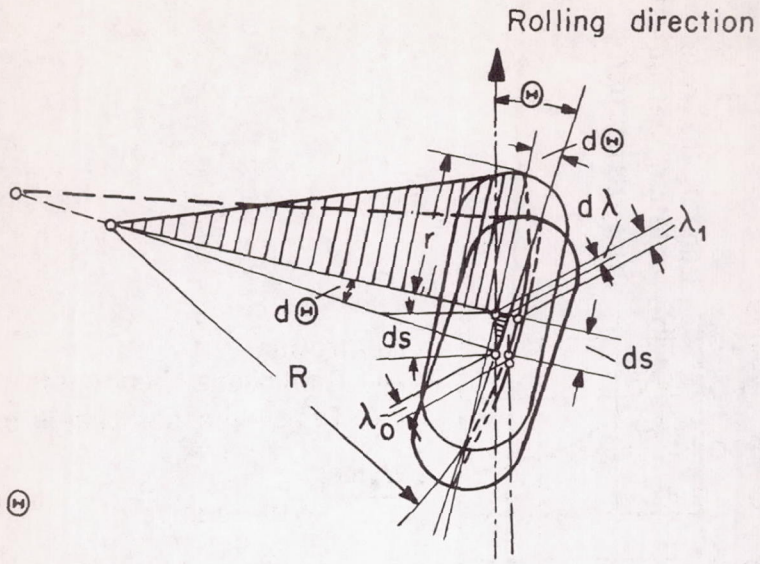

$$\frac{ds}{R} = d\Theta$$

$$\frac{d\lambda}{ds} = -\Theta$$

$$R^2 = r^2 + (R-\lambda)^2 = r^2 + R^2 - 2R\lambda + \lambda^2$$

$$r^2 \approx 2R\lambda \; ; \; R \approx \frac{r^2}{2\lambda}$$

Figure 1.- Derivation of the vibration equation for kinematic shimmy from the geometry of motion. (This figure is not contained in the American original reports.)

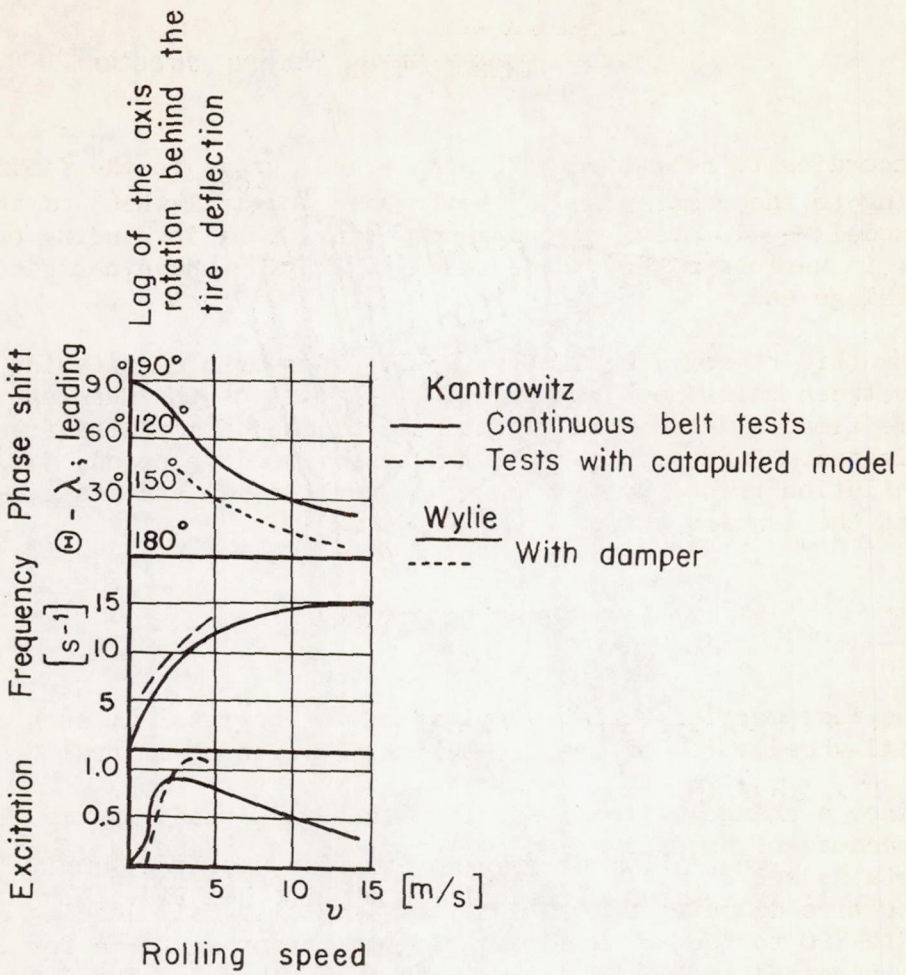

Figure 2.- Fundamental results of the laboratory tests on tail-wheel shimmy (redrawn from the American original figures).

INVESTIGATION OF TAIL-WHEEL SHIMMY ON THE MODEL Me 110*

By M. Renz

INTRODUCTION

According to recent reports from armed forces in the field and according to the compilation by Hoffmann,[1] the tail wheel of the airplane model Me 110 shows strong shimmy vibrations in landing on concrete strips; in various cases, these shimmy vibrations have caused damage on the fuselage end.

For this reason, the Institute was ordered to clarify the connections between tail-wheel shimmy and vibrations of the fuselage end. At the same time, all essential influences on the shimmy itself were to be investigated. Such influences are: trail, rolling speed, tail loading, tire-inflation pressure, damping, tail-gear design and state, and character of the landing strip.

TEST CONDITIONS

The test carrier was an airplane of the series E 1; such airplanes have tail-wheel tires of the size 465 × 165 with 68-mm trail.

Since a change of trail for the aircraft already in use is not possible because of excessive expenditure, such a change was foregone in the tests as well. All tests were therefore performed with a ratio of trail to tire diameter of 0.146, with the static tail loading amounting mostly to 720 to 780 kg, according to fuel reserve; for a few landings, it was increased to 820 to 850 kg with cement bombs. The investigations were made with a quite new tail gear and with one that had been used for some time, with customary self-centering action, furthermore with a tail gear with increased self-centering action. The moment due to deflection from the zero position, for a jacked-up machine, thus in an unloaded condition, was about 4.4 mkg for the new tail gear, about 3.4 mkg for the used tail gear of customary design, and about 8.5 mkg for the tail gear with increased self-centering action; these values are greatly dependent on the loading.

---

*"Untersuchung des Spornradflatterns am Baumuster Me 110," Bericht 140 der Lilienthal-Gesellschaft, pp. 48-51.

[1]Compare the present conference report, p. 1.

Figure 1 shows the arrangement of the tail gear on the airplane with added fluid damping. The latter consists of an automobile shock absorber the damper arm of which is deflected by a cam plate. The cam plate is connected with the swivel-mounted parts of the tail gear by transmission levers. The swivel range is limited; it is $\pm 90^{\circ}$. The airplane tail cone had to be taken off because of the fluid damping.

In figure 2, a friction damper is attached; it consists of two friction disks, more or less pressed together by springs; it is therefore adjustable. Figure 2 shows further the measuring device for shimmy vibrations which works according to the principle of the Wheatstone bridge on the oscillograph placed in the cockpit. The transfer of the tail-wheel rotation to the shimmy transducer is made by a thin cord rolling over the tail skid and the transducer wheel.

For determination of the influence of shimmy on the fuselage, the bending vibrations of the rear of the fuselage about the vertical axis of the airplane, and its torsional vibrations about the longitudinal axis were measured. The measuring device for the bending vibrations, acting inductively by way of an amplifier on the oscillograph, is installed in the fuselage directly ahead of the tail gear, as indicated in figure 3. It consists of a mass (suspended movable transversely to the longitudinal airplane axis) with a magnet in the field of which a coil rigidly connected with the airplane is moved. The natural vibration frequency of this device is 4.3 cycles per second.

The torsional vibration indicator which is likewise dynamic has a fundamentally similar construction; it is placed in the fuselage end ahead of the bending vibration indicator in such a manner that its axis of rotation coincides with the longitudinal axis of the fuselage. (See fig. 4.) Its natural vibration frequency lies at 4.2 cycles per second.

The rolling speed was determined with the aid of a speed indicator in several landings.

For the tests, the tail-wheel tire inflation pressure of 3.25 atm gage pressure customary for E-machines was varied between 2.5 and 5 atm gage pressure.

Altogether, approximately 70 test landings were performed, 80 percent on a concrete strip, 10 percent on a tar-macadam strip, the remaining 10 percent on turf.

TEST RESULTS

Of the great number of oscillograms recorded, we shall show only three stages of a test landing on concrete with high tail-gear load, prescribed tire pressure, and undamped tail gear.

In figure 5, about 2 seconds have elapsed since the first contact with the ground of the airplane. On the uppermost top, one may see the time trace; from timing mark to mark there elapses 0.2 second. Underneath, the shimmy vibrations are plotted; one sees clearly the ground contact of the tail gear, a few still somewhat irregular vibrations, and again lifting off. The bending vibrations of the fuselage end are plotted in the middle, the torsional vibrations which increase greatly with the shimmy vibrations at the bottom.

In figure 6, 20 seconds after the first ground contact, the shimmy angle has increased to its maximum value of about ±20°; the frequency is 12.4 cycles per second. The bending and torsion vibrations of the fuselage end also have increased still more. In the torsional vibrations, the fundamental frequency is exactly synchronous with the shimmy frequency. One deals here with strong forced vibrations since the fundamental frequencies of the natural vibrations of the fuselage lie below these values; higher-harmonic vibrations lie at 19 to 20 cycles per second and at 75 cycles per second.

Figure 7 shows the ending of shimmy. After the shimmying has stopped, bending and torsional vibrations of the fuselage become small. The rolling speed here is about 25 km/h. The frequency has decreased to 11.9 cycles per second. Stopping of shimmy has always been observed at a lower-limit speed which lay between 20 and 30 km/h.

Shimmy in taxying, that is, at increasing speed, was found only in one single case of particular arrangement; the airplane was rolling to the take-off on concrete, with very high tail-gear load (870 to 880 kg), and retracted landing flaps. Shimmy started at about 80 km/h. For normal take-off, the tail gear did not shimmy.

Evaluation of the oscillograms resulted fundamentally in the curves plotted in figure 8. A landing on concrete, under normal conditions, is represented. The duration of the landing run in seconds is plotted on the abscissa, starting with the first ground contact of the airplane. The three curves are the rolling speed in km/h, the shimmy frequency in cycles per second, and the shimmy angle in degrees. The velocity variation corresponds to the behavior in case of a landing run without braking. The landing speed is 134 km/h. The frequency somewhat decreases with increasing duration of the landing run whereas the shimmy angle first increases to a maximum value and then very rapidly decreases to zero. By plotting frequency and shimmy angle against the rolling speed, one obtains figure 9; the landing proceeds from the right to the left. The variation of the shimmy angle agrees very well with the results given in Riekert's lecture[2], obtained by model and drum tests.

---

[2]Compare conference report on this meeting, p. 115.

CONCLUSIONS

The investigation of the parameters affecting the shimmy of the undamped tail skid led to the following findings:

An increase in tail-gear load and in tire pressure causes an increase in frequency. The condition of the tail gear also is of importance. If the guiding grooves of the self-alining cam plates are greatly deformed so that, in zero position, large clearance exists, the shimmy frequency will also increase as in the former case. The maximum value of the shimmy angle fluctuated about $\pm 20^{\circ}$ for the tail gear without damping.

Of decisive importance is the condition of the landing strip, that is, the state of its surface and the coefficient of friction between strip and tire. Shimmy was never found on turf. Comparison of shimmy on concrete and tar-macadam showed only slight differences with respect to frequency (on concrete the frequency was a little higher) but large differences with respect to wear on the tires; these results were more favorable for the tar-macadam strip. In this connection, I should like to point out the importance of propelling the main wheels commensurate with the landing speed. Work on this problem is being carried out at various places[3].

In the investigation of fluid damping, which unfortunately is not adjustable, violent shimmy occurred every time on concrete and tar-macadam, with the frequencies still somewhat higher than for the undamped tail skid, whereas the shimmy deflections decreased a little. Too little damping had therefore been applied. Thus, the opposite of the desired effect was obtained since the forces acting on the fuselage increased. According to the statement of the pilot, the machine also showed greater than usual tendency to veer off. The curvilinear rolling within the prescribed swivel range was not reduced by the damping.

The adjustable friction damping permitted the adjustment in every case of a damping moment ensuring suppression of shimmy. It is true that this moment varied rather widely in the individual cases. For the new tail skid, 5 to 5.5 mkg[4] were sufficient under normal conditions;

---

[3] A report on the findings obtained at the Research Institute for Automobilism and Vehicle Engines at the Technical Academy, Stuttgart, will be distributed shortly by the Zentrale für wissenschaftliches Berichtswersen über Luftfahrtforschung des Generalluftzeugmeisters Berlin-Adlershof.

[4] This value and the following ones contain the friction moment of the damping and the self-alinement for unloaded tail gear.

for the used tail gear, about 6 mkg were needed. This value was increased to 7 mkg by increase of the load. For the tail gear with intensified self-alinement, which without damping shimmied at increased frequency, even 12 mkg were required. An increase in tire pressure somewhat reduced the tendency to shimmy.

These values were obtained by perfect landings, without noticeable cross wind, and on a completely plane strip. The shimmy tendency, and thus the damping moment for its elimination, is considerably increased in landings at an angle of yaw due to cross wind or slant of the strip.

The curvilinear rolling was rather reduced since the tail gear was no longer deflected on turf for 6 mkg damping moment. On concrete, this value lay between 9 and 10 mkg.

Lately, the friction brake has been installed in all machines of the series B, D, and E with the direction to adjust a moment of 8.8 to 9 mkg. In most cases, this moment guarantees safety from shimmy; it must, however, be denoted as slightly too large with respect to the rolling in curves.

The best solution probably would be a larger dimensioned adjustable fluid damping which would permit a free swiveling range of $\pm 180^{\circ}$ and could be installed in the machine in such a manner that no essential change of the tail cone would be required.

Translated by Mary L. Mahler
National Advisory Committee
for Aeronautics

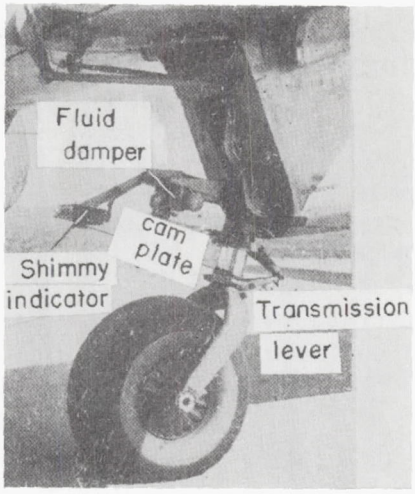

Figure 1.- Tail gear with fluid damper.

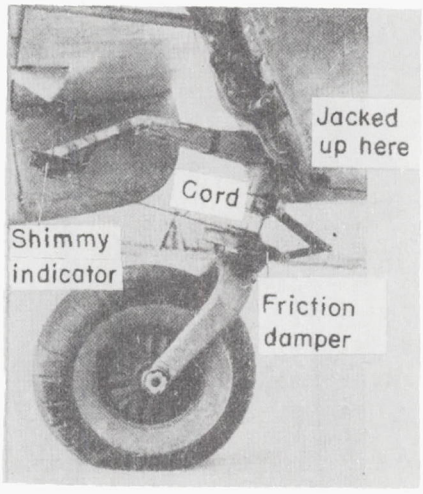

Figure 2.- Tail gear with friction damper.

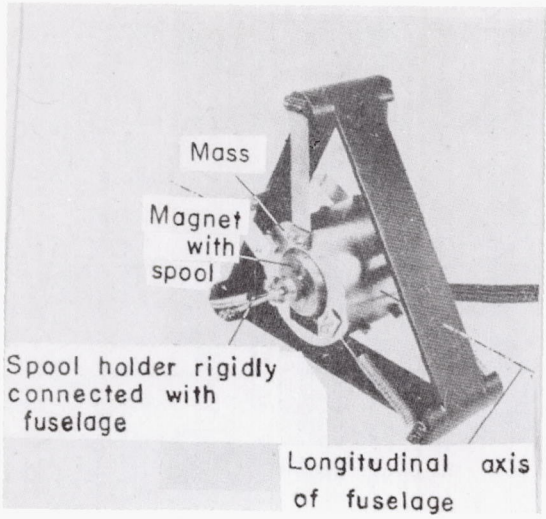

Figure 3.- Bending-vibration indicator.

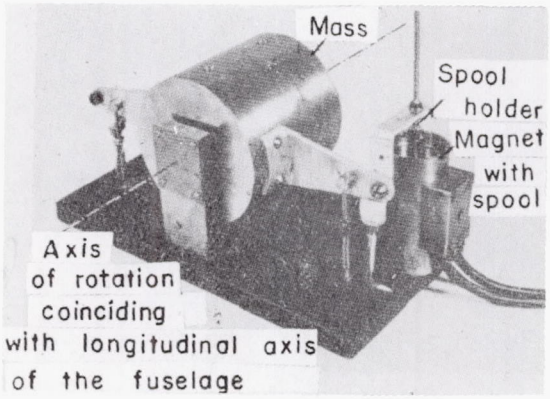

Figure 4.- Torsional-vibration indicator.

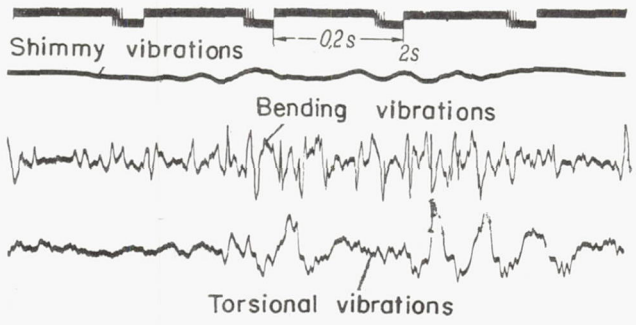

Figure 5.- Oscillogram at ground contact of the tail wheel.

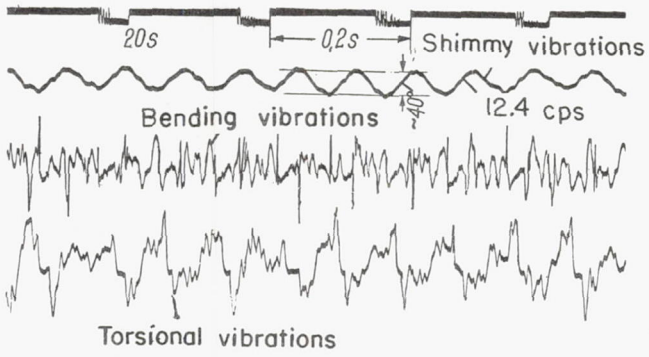

Figure 6.- Oscillogram at the location of the maximum shimmy angle.

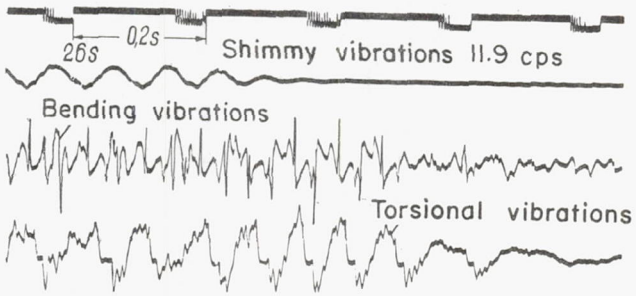

Figure 7.- Oscillogram at the ending of shimmy.

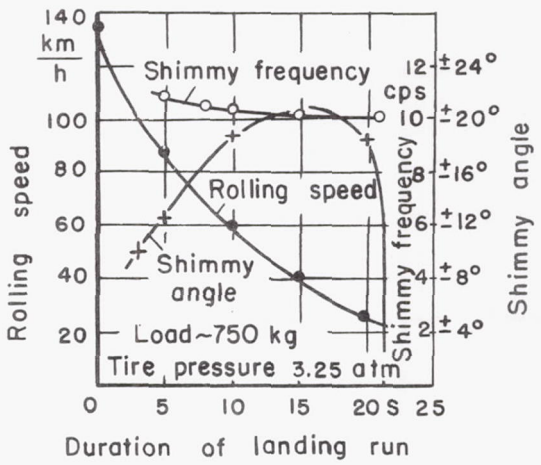

Figure 8.- Shimmy and rolling speed plotted against the duration of landing run.

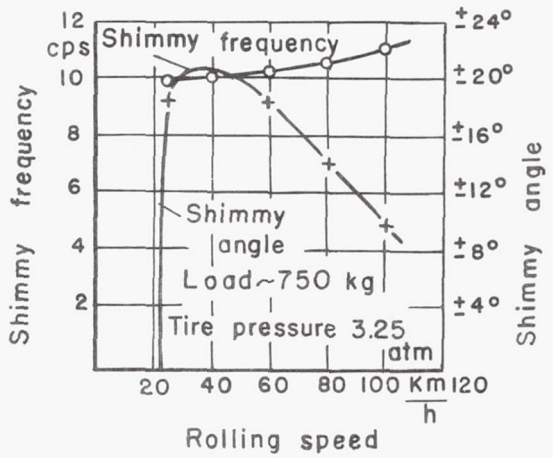

Figure 9.- Shimmy as a function of the rolling speed.

APPENDIX

BRIEF REPORT ON THE HISTORY OF THE THEORY OF WHEEL SHIMMY*

By H. Fromm

The oldest investigation on wheel shimmy known to me is a French report by Sensaud de Lavaud (ref. 1). De Lavaud considers the front axle of an automobile with the wheels as a system with two degrees of freedom: Rotation of the whole about the longitudinal axis of the vehicle (tramping) against the spring suspension toward the frame, and rotation of the wheels about the swivel axis (shimmy) against the spring suspension of the elasticity of the steering linkage. Due to the coupling of these two motions by the gyroscopic effect of the revolving wheels, the problem is identical with Schlick's theory for ship gyros.

At this state of knowledge, the investigations in Berlin (ref. 2) were started in 1927. De Lavaud's formulation bypassed the problem because it disregarded any effect of the ground forces on the wheels. The introduction of this effect led me to note the following points:

(a) As the first parameter, I took into account the vertical elasticity of the tires since I recognized that this elasticity makes the main contribution to the vertical springing; in comparison, the frame springing is almost negligible so that torsional oscillations of the frame are almost without influence. In this respect, conditions are different for the supporting struts of airplane landing gears which have comparatively high bending rigidity; all further effects, however, retain the same significance for the airplane landing gear, too, so that they must be discussed.

(b) The second important finding was that, in case of a shimmy oscillation of the wheel, the vehicle must move in a meandering curve, and that, for this transverse motion of masses, forces are required which can take effect on the wheels only from the runway. Thus, the lateral force acting on the wheels was introduced and therewith the following cycle of the coupling recognized: A shimmy oscillation causes, through the meandering oscillating, lateral forces; the moment of those forces about the longitudinal axis of the vehicle causes a tramping oscillation, and this last one again affects, by gyro effect, the shimmy oscillation. According to the phase shift there occurs, therefore, either damping or build-up of the first disturbance.

---

*"Kurzer Bericht über die Geschichte der Theorie des Radflatterns," Bericht 140 der Lilienthal-Gesellschaft, pp. 53-56.

(c) Furthermore, I was able to prove clearly, by analysis of observed oscillations, that, aside from forced oscillations with typical resonance regions, self-exciting oscillations occurred as a particular danger, and that one dealt, therefore, with a case of typical excitation. The necessary energy must be provided for a vehicle on the road by the driving motor or the kinetic energy of the vehicle, for the vehicle on the drum test stand by its engine. However, the explanation was to be found in the effect of forces between wheel and road.

(d) For rigid tires, one could only point out that the system is rheonomous. However, I recognized as the decisive factor the elasticity of the tires under the effect of lateral forces observed in two phenomena which must be distinguished from one another. One is the lateral elasticity of the tires (which is possible also on the wheel at rest); for small oscillations, it can be represented by

$$S = c_s \xi_e \tag{1}$$

(S = lateral force, ξ_e = elastic side deflection, c_s = spring constant, see fig. 1.)

(e) My previous detailed investigations on the rolling slip of deformable wheels (ref. 3) led me, on my search for the cause of excitation, to corresponding considerations regarding the effect of the lateral forces; I found that under the effect of lateral forces a sideslip (yaw) must appear on the rolling wheel which is in unique connection with the lateral force: the sideslip is expressed solely by the fact that the direction of motion does not coincide with the track of the wheel plane but forms with it an angle ϑ which I named the "angle of sideslip" (yaw angle). The law of sideslip $S = f(\vartheta)$ must therefore be formulated; the first[1] measurements for small ϑ resulted in the proportionality

$$S = K\vartheta \tag{2}$$

K (originally named "sideslip factor") is called guiding characteristic or cornering power at present.

(f) If the wheel plane forms momentarily a swivel angle of φ (shimmy angle) with a stationary axis (for instance the main direction of motion s), the track forms with the latter the angle $(\varphi + \vartheta)$ (see

---

[1]Made by the author together with B. Förster, compare reference 2.

fig.); the track velocity thus has a side component in the direction ξ of the magnitude

$$\dot{\xi}_s = v(\varphi + \vartheta) \tag{3}$$

wherein v is the speed of motion and φ, ϑ are assumed to be small. The masses attached to the wheel axle, however, perform a larger side motion ξ, by the amount ξ_e according to equation (1), by $a\varphi$ (with a signifying the length of the trail), and by $h\lambda$ if the wheel performs at the same time a tramping motion λ with positive inclination to the right (h = height of center of gravity above ground). Thus, there follows from the kinematic condition $\xi = \xi_s + \xi_e + a\varphi + h\lambda$ for small angles φ, λ and γ with equations (1), (2), and (3) the equation

$$\dot{\xi} = v\left(\varphi + \frac{S}{K}\right) + \frac{\dot{S}}{c_s} + a\dot{\varphi} + h\dot{\lambda} \tag{4}$$

which correlates the essential new findings with the customary dynamic equations, and yields the exciting phase shift. Since equation (4) is a true differential equation of the first order ($\dot{S}$ beside S), the characteristic equation of the oscillation system is always of an odd order.

(g) There are, furthermore, the dynamic equations which connect the inertia resistances with the restoring forces and moments. Among them are the spring forces as well as the moments of the three ground forces acting on the wheel (supporting force N, lateral force S, rolling resistance W). N in particular yields moments dependent on φ and λ if the swivel axis is not perpendicular where lifting motions appear in shimmy. Finally, the finding that the lateral force S acts through a lever arm ρ_0 behind the wheel center (whereby the trail a appears increased to $\rho_0 + a$) gives for the moment of S and W about the swivel axis in the sense of growing φ

$$M_0 = S(\rho_0 + a)\cos\gamma - W\cos\gamma\xi_e$$

$$= \left(\rho_0 - \frac{W}{c_s} + a\right)\cos\gamma S = a_0 S \tag{5}$$

a_0 therein may be termed "dynamic trail."

The calculation for the automobile was performed with use of these bases (ref. 2); due to the small trail (lead), the moment of equation (5) is, in first approximation, negligible compared to the strong spring-restoring moment. For free-swiveling airplane wheels, however, equation (5) is essential.

(h) A further moment of an order of magnitude similar to that of equation (5) was, although its existence was recognized, not taken into consideration because of the difficulty in expressing it quantitatively; this in turn would be questionable for free-swiveling wheels. One deals here with a slip moment created on the rolling wheel if the wheel plane is rotated, and the path therefore curvilinear. One may put in first approximation

$$M_S = -m_1 \frac{d\varphi}{ds} - m_2 \frac{d\vartheta}{ds} \tag{6}$$

wherein m_1 and m_2 are constants. Equations (5) and (6) together form, therefore, the moment about the swivel axis:

$$M_A = a_0 S - m_1 \frac{d\varphi}{ds} - \frac{m_2}{K} \frac{dS}{ds} \tag{7}$$

These first findings are the basis for all other work in this field as well; thus, the reports published meanwhile may be surveyed quickly. This summary is given separated into two parts: investigations regarding the elastic and slip characteristics of the rolling wheel with lateral force, and investigations regarding the shimmy oscillations themselves.

A. THE ELASTIC AND SLIP CHARACTERISTICS OF THE ROLLING WHEEL

Adjoining the first common measurements which resulted in equation (2), B. Förster (ref. 4) investigated the entire course of the function $S = f(\vartheta)$ by measurements under all sorts of conditions (type and state of tires, type and state of roads, operating conditions, weather conditions). There followed investigations of the same kind in the Forschungsinstitut für Kraftfahrwesen und Fahrzeugmotoren an der Technischen Hochschule Stuttgart (research institute for automobilism and vehicle engines at the Technical Academy at Stuttgart) under the direction of W. Kamm; among them, the tests on model wheels (ref. 5) and the measurements on airplane tires (ref. 6) should be stressed particularly.

I myself was able to present a calculation of the function $S = f(\vartheta)$ from the elastic properties of the tire profiles (ref. 7) which shows especially the influence of the shape of the pressure surface and of the pressure distribution in that surface and confirms, among other facts, that the guiding characteristic (cornering power) K (in the eq. (2) valid for small ϑ) is independent of the friction coefficient μ.

The lectures of v. Schlippe and Dietrich (ref. 8) mark an essential progress; here the simplifying limitation to the steady state was lifted. Not only the yaw angle ϑ but also the swivel angle φ are assumed to be arbitrarily variable with time, that is, with the path. Consequently, the contact points of the wheel circumference, even in the range of adhesion, no longer are impressed rectilinearly in one track direction but must follow the track direction of the motion which is now curvilinear (called by v. Schlippe "law of heredity"). The simplifying concept of the tire as a thin band with lateral elasticity leads to expressions for the lateral force and the moment in e-functions, the first approximation of which will probably agree with the equations (1), (2), and (7). Also, the Schlippe formulation $z' + cz = \varphi - h_1\varphi' - x'$ shows in the rearrangement $x' = (\varphi - cz) - z' - h_1\varphi'$ its identity with the previous equation (4), where aside from $\lambda = 0$ obviously $h_1 = -a$ and, according to equation (2) $z = -\xi_e = -\frac{S}{c_s}$ and c signifies $c = \frac{c_s}{K}$.

It should be stressed in this connection, that the slip moment (6) appears only in rolling $\left(\frac{d\varphi}{ds}, \frac{d\vartheta}{ds}\right)$, thus, must be distinguished from an elastic restoring moment as equation (2) from equation (1) for the lateral force. Introduction of such a spring-back moment of the tires would require a change of the equations (4) and (6), and yield a second differential equation analogous to equation (4). Furthermore, equation (6) is no damping moment in the customary sense.

A damping of oscillations due to imperfect elasticity or to slipping in the pressure surface must be formulated separately. It must be noted that the damping for a rolling wheel cannot attain the values measured in measurements on a stationary wheel (for instance by free-damped lateral oscillations). What matters here is the ratio n of the wave length λ of the oscillation on the runway to the wheel circumference U, or in other words, the ratio of the rotational frequency of the wheel ω to the frequency of the oscillation α, thus $n = \frac{\lambda}{U} = \frac{\omega}{\alpha}$. For a stationary wheel ($n = 0$) the damping is at its largest; it decreases steadily with increasing n and disappears completely for very slow oscillations during rapid motion. This may be understood by visualizing these changes as variations of a steady state of rolling where the varied state must always be newly produced on parts newly flowing into the deformed region.

Thus, the larger n, the greater the number of parts to which the variation is distributed, and the more this variation vanishes in the deformation process of the steady state. The necessary energy, which is therefore utilized to the greatest part as deformation work, is supplied by the engine or the kinetic energy of the vehicle, and only the remainder becomes effective in damping out of the oscillations.

Even for $n = 1$ one oscillation runs around the entire wheel, thus over more than 10 pressure-surface lengths. Therefrom resulted an oscillation damping already very slight in comparison with the wheel at rest, for all types of springing (normal, lateral, and torsional). This fact was confirmed by observations on the test stand. For shimmy oscillations values of $n = 0.5$ to 3 occur; thus, it will never be possible to count on a considerable damping resulting from the tires as far as such a damping does not follow from the slip parameters formulated in equations (2) and (6).

B. THE SHIMMY OSCILLATIONS

The shimmy oscillations of swiveling wheels depend (among other factors) on the lead or trail position a of the wheel. This position is affected by two parameters: the inclination of the swivel axis toward the direction of motion (γ) and the distance of the wheel axle from the swivel axis (q). For automobiles $q \approx 0$; for bicycles both influences exist; for nose and tail wheels of airplanes occasionally $\gamma \approx 0$. An inclination of the swivel axis causes a double complication of the relations (compare section g): First, the ground pressure, that is the main force of the wheel, obtains thereby a lever arm about the swivel axis proportional to the shimmy deflection; thus, there originates for the shimmy oscillation, according to the sign, a restoring or diverging moment which intensifies or attenuates any occurring springing action possibly up to instability. Second, lifting oscillations of double the frequency are coupled to the shimmy oscillation.

The resulting stability conditions, also for elastic lateral spring action of the supporting leg, have been thoroughly investigated by E. Maier (ref. 9) on the basis of the findings (a) to (g). However, he disregards the elastic lateral spring action, thus the term $\dot{S}/c_s$ in equation (4), and thereby suppresses a condition for excited shimmy.

This condition is taken into consideration by M. Melzer (ref. 10) who in turn limits himself to a perpendicular swivel axis ($\gamma = 0$). Melzer obtains the stamping motion λ by assuming a torsional elasticity of the airplane fuselage; he neglects, however, the moment effect of the ground pressure and the gyro effect of the wheels so that the stability condition found by him is valid only for corrected torsional elasticity of the fuselage and for small speed of motion. The reason

that he himself does not find a condition given by Maier, although he includes precisely the condition suppressed by Maier, is the fact that he does not make full use of the stability criteria contained in his argument $\left(D_4 = A_5 D_3 > 0;\ \text{that is,}\ A_5 > 0;\ \text{thus}\ a > -\frac{c_\varphi}{K}\ \text{wherein}\ c_\varphi\right.$ signifies the constant of a restoring spring action of the shimmy deflection $\left.\varphi.\right)$

Kantrowitz (ref. 11) introduces a shimmy oscillation designated as "kinematic shimmy" which he proves by model tests; his (qualitative) theoretical considerations, however, are not intelligible. Thus the considerations of "dynamic shimmy" (including the forces of inertia) based on them and the connected report by Jean Wylie (ref. 12) do not offer any theoretical gain.

"Kinematic shimmy" probably is essentially the shimmy oscillation at which v. Schlippe (ref. 9) arrives in his investigation of the tire on a curved track (for lacking inertia and elastic restoring moments about the swivel axis as well). The transcendent form is not essential since the result follows also from the approximate formulation (7). The moment about the swivel axis disappears with the inertia and elastic restoring moments $\left(M_A = 0\right)$; on the other hand, the lateral motion of the swivel axis $(\xi = 0)$ and its stamping rotation $(\lambda = 0)$ disappear with very large airplane mass or rigidity. Thus equations (4) and (7) yield the two differential equations of the first order

$$\varphi + a\frac{d\varphi}{ds} + \frac{S}{K} + \frac{1}{c_s}\frac{dS}{ds} = 0$$

$$m_1\frac{d\varphi}{ds} - a_0 S + \frac{m_2}{K}\frac{dS}{ds} = 0$$

when $a_0 = \left(a + \rho_0 - \frac{W}{c_s}\right)\cos\gamma$ is the "dynamic trail". Hence results a shimmy oscillation $\varphi = \Phi_e^{\delta s}\ \sin\left(2\pi\frac{s}{\lambda}\right)$ of the wave length

$$\lambda = \frac{4\pi(k_c - \eta a)}{\sqrt{4k_m(k_c - \eta a)a_0 - \left(1 + k_m a a_0 - \eta a\right)^2}}$$

wherein we had put for abbreviation $k_c = \frac{K}{c_s}$; $k_m = \frac{K}{m_1}$; $\eta = \frac{m_2}{m_1}$. The

frequency is therefore proportional to the speed of motion as long as the forces of inertia are negligible. The excitation amounts to

$$\delta = \frac{1 + k_m a a_0 - \eta a}{2(\eta a - k_s)}$$

An excited oscillation of this type is therefore possible only for sufficiently large $\eta = \frac{m_2}{m_1}$ in the region of a not-too-large trail a.

The evaluation of v. Schlippe's argument was made by Dietrich (ref. 13) by taking into consideration the forces of inertia. He introduced as damping the torsional damping on the wheel at rest without taking its reduction due to the rolling of the wheel into consideration. Thereby the comparison between calculation and test shifts its proportions.

Translated by Mary L. Mahler
National Advisory Committee
for Aeronautics

REFERENCES

1. Sensaud de Lavaud, D.: Comptes rendus, Bd. 185, 1927, I, p. 1636, II, p. 254.

2. Fromm, H.: Verh. 3. Intern. Kongr. f. techn. Mech., Stockholm 1930, Bd. III, p. 278; Becker, G., Fromm, H., and Maruhn, H.: Schwingungen in Automobillenkungen (M. Krayn), Berlin 1931.

3. Fromm, H.: Z. angew. Math. u. Mech., Bd. 7, 1927, p. 27; Fromm, H.: Z. techn. Phys., Bd. 9, 1928, p. 299.

4. Förster, B.: Deutsche Kraftfahrtforschung, Zwischenbericht Nr. 22.

5. Huber, L., and Dietz, O.: Einradmodellversuche, FKFS-Bericht Nr. 58, 1934.

6. Harling, R.: p. 7 of the present report.

7. Fromm, H.: Führungskraft des rollenden Rades und Schiebebewegung des Fahrzeugs, Vortrag auf der Tagung der Ges. f. angew. Math. u. Mech. in Braunschweig am 4. Mai 1940. Z. angew. Math. u. Mech., Bd. 20, 1940, p. 184. Extract on p. 191 of the present report.

8. Schlippe, B. v., and Dietrich, R.: p. 125 of the present report.

9. Maier, E.: Deutsche Luftfahrtforschung, Forschungsbericht Nr. 1166, 1940.

10. Melzer, M.: TB 2/1940.

11. Kantrowitz, A.: NACA-Report No. 686, 1937.

12. Wylie, Jean: Journ. of the Aeronautical Sciences, Vol. 7, 1939, p. 56.

13. Dietrich, R.: p. 148 of the present report.

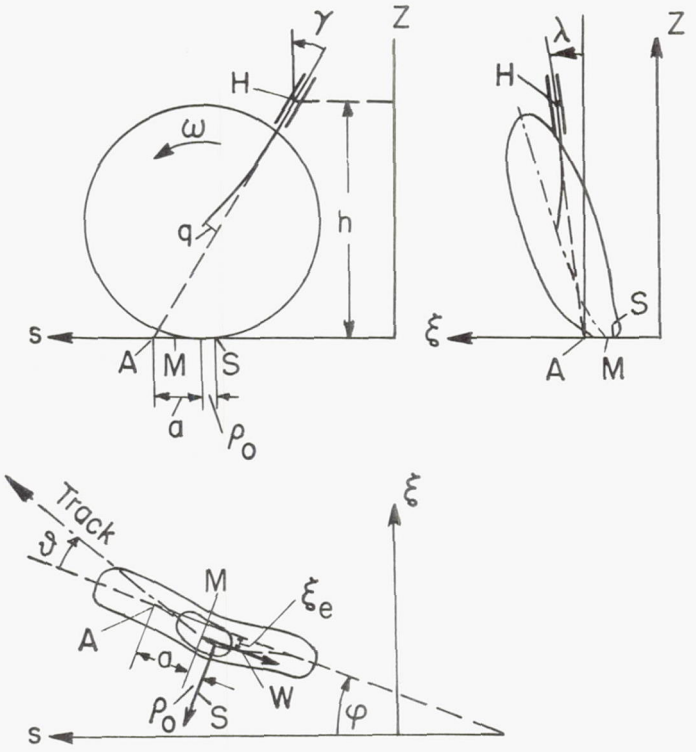

Figure 1

SIDESLIP AND GUIDING CHARACTERISTICS OF THE ROLLING WHEEL*[1]

By H. Fromm

1. INTRODUCTION

The forces between the rolling wheel and the runway frequently have been the subject of thorough investigations. They are indeed of great importance in evaluating the stress on wheel and runway, the slip and the wear it causes, the attainable driving and braking effect, and the directional stability of the vehicle.

O. Reynolds (ref. 1) recognized, probably as the first, by means of tests with rubber models, that local expansions and compressions of the wheel circumference take place and that, in a part of the common pressure surface between wheel and runway, adhesion (that is, pure rolling-off) occurs; whereas in the remaining part, sliding motions appear. Developing this concept, the author then showed in reference 2 that the slip is completely determined by the difference of the expansions of wheel circumference and runway in the domain of adhesion, and that, in the sliding region of the pressure surface, the total slip may be represented as the sum of such an expansion slip and a sliding slip with only the sliding slip affecting the wear. For pure rolling, which need not be free from slip, the region of adhesion covers the entire pressure surface; with increasing circumferential force (driving or braking force), the region of adhesion gradually decreases in size while the sliding region appears beside it, increases, and finally covers the entire pressure surface when the circumferential force reaches the friction limit; simultaneously the slip increases.

Exact calculation of these relations (ref. 2) yielded simultaneously, as an extension of the well-known Hertz theory of contact, besides the distribution of the compression stresses also that of the tangential stresses over the pressure surface of solid wheels. According to the measurements of the pressure distribution by H. Martin (ref. 3), one may assume that the calculation intended only for small pressure surfaces yields still satisfactory agreement with actual conditions for solid

---

*"Seitenschlupf und Führungswert des rollenden Rades," Bericht 140 der Lilienthal-Gesellschaft, pp. 56-63.

[1]The report was read for the first time at the meeting of the Gesellschaft für angewandte Mathematik und Mechanik on May 4, 1940 in Braunschweig. At the conference, the author briefly reported on it.

rubber tires as well. The fundamental findings, however, hold true also for pneumatic tires; they have been clearly explained for this purpose by R. Schuster and P. Weichsler (ref. 4).

The same concepts may be applied to the rolling wheel pushed out of its path by a lateral force normal to its plane. As the author has shown already in 1930 (ref. 5), the direction of motion deviates, in case of an acting lateral force, from the center plane of the wheel by an angle ϑ which is a function of the characteristics of the tire and of the lateral force S. (See fig. 3.) The smaller the angle ϑ for a prescribed lateral force, the higher the directional stability of the tire which is of great significance for driving safety and for wear.

The "sideslip angle" ϑ appears with a lateral force as unavoidably as an elastic variation in form under a stress. This angle is the cause of all snaking motions of the vehicle. The author was able to show that the sideslip angle is responsible for the occurrence of self-exciting shimmying oscillations of the guided wheels. He pointed out at the same time (ref. 6) that the center of the turning circle shifts with increasing speed of motion because of the appearance of the sideslip angle. The pertinent calculation and the solution of the statically indeterminate problem of the center of the turning circle of triaxial vehicles which form the subject of a further report[2] represent another important application of the findings regarding the sideslip angle.

The author performed measurements concerning the dependence of the sideslip angle ϑ on the lateral force S for the first time within the scope of the shimmy investigations mentioned (refs. 5 and 6) and found for small angles a proportionality $S = K\vartheta$ (fig. 1). His co-worker at the time, B. Förster, meanwhile carried out independently comprehensive tests (ref. 7) on the behavior up to the limit of adhesiveness for all kinds of road conditions. I am greatly obliged to him for putting some of the still unpublished results of these tests at my disposal for comparison.

In keeping with the importance of the appearance of the sideslip angle (to which too little attention has been paid so far), it will be shown below how the phenomenon itself and its numerical implications can be understood so that viewpoints and data for favorable profiling of the tires may result. The parameter K proves to be of fundamental significance for the evaluation of the guiding or cornering ability of the tires.

---

[2]This report, too, has already been read at the conference on May 4, 1940. It will be published in "Deutsche Kraftfahrtforschung."

2. BASES OF THE CALCULATION

(a) Origin of the Sideslip Angle

Under the effect of a lateral force, a wheel at rest undergoes a lateral elastic deflection which is brought about by the changes in form of the wheel disk, the rim, and the tires. A circumferential line U which before action of the force was a circle in a base plane normal to the wheel axle shows a course symmetrical to the vertical section through the wheel axle as represented, for instance, in figures 2(a) to 2(d), with exaggeration of the lateral deflection δ, for the circumferential line of the center plane of the wheel. Correspondingly, the distribution of the lateral force $S = \int s\, dF$ over the pressure surface F is symmetrical as well as that of the pressure force $N = \int p\, dF$, with p indicating the compression stress, s the lateral tangential stress in the surface element dF. For most operating conditions for rubber against road surface, one may use Coulomb's friction law according to which the tangential stress is limited by $s \leqq \mu p$ (μ = friction coefficient); the limiting value of the lateral force $S = \mu N$ is therefore reached, and a "total" sliding, that is skidding, occurs only when the condition $s = \mu p$ has been attained in all surface elements dF.

If one lets the wheel roll a distance (to the left) without permitting a lateral shift of the wheel hub, that is, the wheel center plane, wherein the front contact zone of the pressure surface moves from A to A', the rear contact zone from B to B' (fig. 2(e)), and does not permit a lateral shift of the wheel hub so that the wheel-center plane shifts within itself, all points of the pressure surface at which s remains $<\mu p$ will adhere to the ground. Consequently, there is no reason for points which newly enter into the pressure surface in a circumferential line at the front contact zone (for instance, from A to A') to change their initial lateral displacement δ; in this quasi-rigid rolling-in, the piece AA' remains free from lateral loads s, as it had been before when in equilibrium. At the rear contact zone, in contrast, the points lying between BB' will lose their original lateral load s when leaving the pressure surface. Because of this removal of load, the circumferential line to the right of B' will approach the wheel-center plane and, as a result, lead to an increase of s closely to the left of B'. This increase may cause here, too, skidding in the sense of a reduction of δ as far as s becomes $s = \mu p$; however, this increase does not compensate the loss of s to the right of B' for, on the whole, the circumferential line has moved more closely

toward the wheel center plane, that is, the elastic deflection has become smaller, which is compatible only with a reduction of the total lateral force $S = \int s\, dF$. Moreover, the resultant force S' now lies behind the center M' of the pressure surface which is of importance for the moment of the lateral force about the swiveling pin.

In case of forced rolling straight ahead, an initial lateral force therefore decreases and disappears completely when the state of equilibrium is approached. If, however, after traveling the distance AA' the lateral force is again increased to the former value S, there occurs with the deflection δ increasing again a shifting of the center plane opposite to the direction of S (in direction of the hub force Z). Hence, it follows that for an invariable lateral force S a rolling straight ahead is impossible; rather, the lateral motion (mm") is superimposed on the rolling so that, for instance, the point A immediately moves in the direction $A"$, and B in the direction $B"$ (fig. 2(g)). The lateral motion is not a skidding phenomenon; rather, there remains a region of adhesion in existence where $s < \mu p$, and a rolling free from skidding[3] occurs which makes the wheel progress toward its center plane under a "sideslip angle" ϑ.

As far as adhesion remains in existence to the right of A, the circumferential line retains its position with respect to the former center plane m; the deflections here therefore increase by the amount $mm"$ of the lateral shift of the wheel. To the left of A, too, δ increases corresponding to the advance $A'A"$ so that, for instance, $\delta_{A"} > \delta_{A'}$ approaches δ_A; the asymptote moves with $m"$, likewise to the right of $B"$ where again complete unloading of s occurs. The lateral-force distribution will now, with a pointed terminating region, extend to $A"$ so that S again lies behind $M"$.

Due to the effect of the constant lateral force S, an invariable sideslip angle ϑ develops as the state of equilibrium; as a result, every point entering into the pressure surface through the front contact zone runs in the image of the pressure surface moving with the wheel in a rectilinear course at the angle ϑ as long as it is in the region of adhesion ($s < \mu p$). (Compare fig. 3 which indicates, beside the distribution of S, that of the normal force which takes effect ahead of M in case of imperfect elasticity.) The circumferential line and all circles parallel to it before the force has taken effect therefore take in the region of adhesion of the pressure surface a rectilinear course at the angle ϑ toward the wheel center plane; in the region of sliding,

---

[3]Freedom from skidding does not exclude the occurrence of sliding in a part of the pressure surface, the sliding region.

in contrast, the lateral stress is determined by the limiting value of the sliding friction $s_g = \mu p$. These two findings form the basis of the following calculation.

(b) Formulation for the Lateral Stresses

Determination of the lateral stress distribution s_h in the region of adhesion from the known course of the circumferential line encounters the further difficulty that the deflection δ at any arbitrary point is caused not only by the stress s acting there but depends on the entire distribution of s which is still unknown; for instance, in figure 2(d), the deflection δ does not disappear to the left of A and to the right of B in spite of $s = 0$. This fact has to be taken into consideration, particularly when the contact surface is smooth, as in rubber tires with worn profile or in railroad-steel wheels on steel rails. The solution for this problem may be obtained by setting up an integral equation and will be given at another occasion.

For rubber tires with pronounced tread, on the other hand, a simpler method is possible which will yield results the better, the more finely and deeply cut the "valleys" dividing the tire tread into separate rubber lugs; each of these lugs backs away from the lateral-force component apportioned to it with a deflection δ_p without being considerably affected by the adjacent lugs (figs. 4(a) to (c)). This condition is probably fulfilled satisfactorily in the usual cross-country profiles and nonskid profiles, particularly when the notched "valleys" run crosswise; however, the local bending rigidity probably yields the essential force component also in case of longitudinally running ridges whereas the "wall support" which is weak anyway may be neglected in first approximation, in view of the steady course of the lateral stresses. Thus, it is then permissible to write

$$\frac{\Delta P}{\Delta F} = s = s(\delta_p) = q\delta_p \qquad (1)$$

wherein q is an elastic rigidity constant determined by the shape of the lugs and the E-moduli of the rubber, as far as Hooke's law is valid; ΔF signifies the cross section of the lug including a border strip of half the width of the "valleys" so that the sum $\sum(\Delta F)$ over the pressure surface yields the pressure surface F.

The quantity δ_p is only part of the total elastic lateral displacement δ of the top of the lug from the base plane which as a point of the circumference comes into contact with the ground and therefore in

the region of adhesion lies on the rectilinear part of a circumference line. The lug root, however, undergoes a lateral displacement δ_F as a point of the coherent root surface as elastic deflection of all wheel parts from hub to root surface, and this root point lies on a root line which was before the loading a root circle in the base plane of the pertaining circumference point. (Compare figs. 4(a), (b), and (c).) δ_F is a function of the total distribution of the lateral force as δ for smooth contact surface. The condition of rectilinearity in the region of adhesion at the angle ϑ is valid for the circumference line, thus for the sum $\delta = \delta_F + \delta_P$.

Furthermore, one can see that δ_P must begin at the point of ground contact A with $\delta_P = 0$ since the lug enters the pressure surface undeformed. The amount at that point δ_A is therefore without significance for the entire process of sideslip; it represents a single elastic deflection in bringing about the lateral force which affects the motion of the vehicle only in case of variations of the lateral force. The component which is important for the sideslip motion is to be calculated from the line of reference through A parallel to the ground plane and amounts, at a distance w from A, for a point of the region of adhesion to

$$\delta - \delta_A = \delta_P + \left(\delta_F - \delta_A\right) = w \tan \vartheta \qquad (2)$$

Therein the "height of camber" $\left(\delta_F - \delta_A\right)$ of the root line with respect to the line of reference may be neglected in first approximation compared to δ_P, particularly when the root surface is rigid and the profile little worn.

Combination of the equations (1) and (2) then yields, for the region of adhesion, the lateral stress

$$s_h = qw \tan \vartheta \qquad (3)$$

Even when $\left(\delta_F - \delta_A\right)$ is not negligible, equation (3) may still be applied by assumption of a value of q somewhat smaller than would correspond to the rigidity of the profile lug since, especially near to A, $\left(\delta_F - \delta_A\right) \sim \delta_P$. With nothing neglected and in case of deviations from Hooke's law, $s_h(w)$ will probably take a course according to figure 4(d), for instance.

Figure 4(d) shows, furthermore, a plotted possible course of μp which forms the friction limit for s_h. The point of intersection

with s_h yields the boundary[4] between the region of adhesion and the adjoining region of sliding where

$$s_g = \mu p \tag{4}$$

is valid; therein $\mu = \mu_g$ denotes the sliding-friction coefficient. If the adhesion-friction coefficient μ_h is larger than μ_g, which is frequently the case for good adhesion on a dry road, the boundary between adhesion and sliding region shifts to the right up to the intersection of s_h and $\mu_h p$, and s then jumps back to $s_g = \mu_g p$.

(c) Shape of the Pressure Surface and Distribution of the Compressive Stresses

For further calculation, data on the shape of the pressure surface and the distribution of the compressive stresses p in it are necessary. The pressure surface usually has a shape lying between a rectangle and an ellipse; these two forms are treated as limiting cases.

For performance of the calculation, we presupposed as pressure distribution first an ellipsoidal, then a paraboloidal, and finally a uniform distribution. With these limiting cases, the actual conditions can, to a great extent, be expressed or at least estimated.

For solid rubber tires, probably the ellipsoidal distribution is valid in the range of small variations in form, that is, small normal pressures whereas, for customary loadings, according to measurements by Martin (ref. 3) on solid rubber tires, the distribution approaches the paraboloidal form, a transition which is probably also connected with the elastic compression of the profile lugs.

For pneumatic tires of aircraft, the assumption of uniform pressure distribution represents a limiting case which corresponds to a completely lacking wall rigidity for which the pressure would have to equal the excess pressure of the air in the air tube. On the other hand, high wall rigidity would give an approximation to the conditions of the solid rubber tires which, therefore, represent the other limiting case. Measurements by Martin (ref. 3) on pneumatic tires resulted in a complicated shape which shows the simultaneous effect of flank rigidity, root-surface rigidity, and air pressure. One may regard it, approximately,

---

[4]More accurately, the horizontal stresses s_0 measured by Martin (ref. 3) also would have to be taken into consideration. As far as these stresses have a cross effect, the boundary would be given by $s_0 + s_h = \mu p$; the longitudinal components require geometric addition as in the case of the circumferential force.

as paraboloidal at the edge with an almost uniform longitudinal valley through the middle, and introduce it as such into the calculation.

3. RESULTS OF THE CALCULATION

The calculation was carried out first for $\mu_h = \mu_g = \mu$. A short summary of the results follows.

(a) Ellipsoidal Pressure Distribution

The lateral force S as a function of the sideslip angle ϑ is

$$S = \mu N \frac{1}{\pi}\left[(2\Theta) + \sin(2\Theta)\right] \quad \text{with} \quad \tan\Theta = \frac{\pi}{4} \chi_E \tan\vartheta \tag{5}$$

Therein the guiding or cornering characteristic parameter

$$\chi_E = \frac{qD}{\mu} \frac{m - 1}{mG} f \tag{6}$$

is the characteristic construction constant of the tire in which D denotes the diameter, G the shear modulus of elasticity, m the Poisson constant for rubber, and f a form factor depending on the shape of the tire according to figure 5. This result for an elliptic shape of the pressure surface applies with $f = \frac{2}{\pi}$ also to the rectangular pressure surface $\left(\frac{D}{d} = 0\right)$.

The resistance to skidding μN is a limiting value for the lateral force S. Thus the ratio $\nu = \frac{S}{\mu N}$ gives a clear measure for the utilization of the resistance to skidding by the lateral force. According to previous use of the author (ref. 2), this ratio will be designated as utilization value ν. Thus the result (5) may also be written in the form

$$\text{Utilization value:} \quad \nu = \frac{S}{\mu N} = \frac{1}{\pi}\left[(2\Theta) + \sin(2\Theta)\right]$$

with

$$\tan\Theta = \frac{\pi}{4} \chi_E \tan\vartheta$$

This form shows even more convincingly that $\nu(\vartheta)$ is determined solely by the guiding characteristic parameter χ_E.

Figure 6 represents this relation for various values χ_E and shows an increase of ν with ϑ, at first almost proportional, which, particularly for high values of χ_E, leads even for small values of ϑ closely up to the limit $\nu = 1$. The initial increase is of particular importance; one finds for it from equation (7)

$$\left(\frac{d\nu}{d\vartheta}\right)_{\vartheta=0} = \chi_E \tag{8}$$

This further significance of the guiding characteristic parameter χ_E was the purpose of the adjusting factor $\pi/4$.

According to the amount of the wheel pressure force N, the lateral force is determined by $S = \nu\mu N$. This force, too, increases for small S almost proportionally to ϑ, in agreement with the previous tests of the author. The steeper this increase, the smaller is the angle of sideslip for equal lateral force and the more safe therefore is the guiding of the wheel. The derivative $\frac{dS}{d\vartheta}$ for $\vartheta = 0$ represents, therefore, a suitable measure for the guiding value[5] or cornering power of tires for a given load. Thus, there follows for the guiding value or cornering power

$$\left.\begin{aligned} K = \left(\frac{dS}{d\vartheta}\right)_{\vartheta=0} = \left(\frac{d\nu}{d\vartheta}\right)_{\vartheta=0} \mu N = \chi_E \mu N \\ \text{or inversely} \\ \chi_E = \frac{K}{\mu N} \end{aligned}\right\} \tag{9}$$

that is, the guiding characteristic parameter is the guiding value of the tires referred to the unit of skidding resistance.

Substitution of equation (6) into equation (9) yields

$$K = fqD \frac{m - 1}{mG} N \tag{10}$$

---

[5]This appropriate expression was suggested by B. Förster.

that is, the guiding value is a function of the elastic properties of the tires, and of the load, but not of the friction coefficient μ! This result is generally valid and independent of the special assumptions and neglections of this calculation.

The boundary ξ_g between the region of adhesion and the sliding region also is of interest (fig. 7). It is given by $\xi_g = \cos(2\Theta)$; that is, for $\vartheta = 0$ the entire pressure surface belongs to the region of adhesion, and with increasing ϑ the sliding region increases from the rear contact side ($\xi_g = +1$), beginning over the pressure surface, which it covers ($\xi_g = -1$) when $\vartheta = \frac{\pi}{2}$ is reached - that is, when the wheel slides laterally without having to roll further.

(b) Paraboloidal Pressure Distribution

Here, the guiding characteristic parameter becomes

$$\chi_P = \frac{K}{\mu N} = \frac{4}{3} \frac{qD}{\mu} \frac{m - 1}{mG} f \tag{11}$$

wherein the form factor again has the significance illustrated in figure 5.

For rectangular pressure surface, one thus finds, for rolling with a region of adhesion, the utilization value

$$\nu = \frac{S}{\mu N} = 3T\left(1 - T + \frac{T^2}{3}\right) \quad \text{with} \quad T = \frac{1}{3} \chi_P \tan \vartheta \leqq 1 \tag{12}$$

With $T = 1$, the region of adhesion disappears (compare the "limiting case" in fig. 8(b)), and rolling with skidding occurs where

$$\nu = \frac{S}{\mu N} = 1 \quad \text{with} \quad T > 1, \text{ that is,} \quad \tan \vartheta > \frac{3}{\chi_P} \tag{12a}$$

For elliptic pressure surface, the final formula becomes less convenient; its law, however, hardly deviates from equation (12) so that the law $\nu = f(\vartheta)$ is practically independent of the shape of the pressure surface in the case of paraboloidal pressure distribution as well. The variation for different χ_P is represented in figure 9.

(c) Uniform Pressure Distribution

For uniform pressure distribution p, one must distinguish (see fig. 10):

State 1: For small lateral force, a sliding region does not yet exist.

State 2: Besides the region of adhesion, a sliding region develops.

For a rectangular pressure surface of the width b, the guiding characteristic parameter reads

$$\chi_g = \frac{K}{\mu N} = \frac{qN}{2\mu p^2 b}, \quad \text{thus} \quad K \sim N^2 \tag{13}$$

and the utilization values are

$$\left.\begin{aligned} &\text{for the state 1:} \quad \nu_1 = \frac{S_1}{\mu N} = \chi_g \tan\vartheta \quad \text{for} \quad \tan\vartheta \leqq \frac{1}{2\chi_g} \\ &\text{for the state 2:} \quad \nu_2 = \frac{S_2}{\mu N} = 1 - \frac{1}{4\chi_g \tan\vartheta} \quad \text{for} \quad \tan\vartheta \geqq \frac{1}{2\chi_g} \end{aligned}\right\} \tag{14}$$

The transition from state 1 to state 2 lies at $\nu_1 = \nu_2 = \frac{1}{2}$.

For an elliptic pressure surface, the characteristic parameter becomes

$$\chi_G = \frac{K}{\mu N} = \frac{8}{3\pi} \frac{q}{\mu p} \sqrt[4]{\frac{D}{d}} \sqrt{\frac{N}{\pi p}} \qquad \text{therefore,} \quad K \sim N^{3/2} \tag{15}$$

and again

$$\text{for the state 1:} \quad \nu_1 = \frac{S_1}{\mu N} = \chi_G \tan\vartheta \quad \text{for} \quad \tan\vartheta \leqq \frac{4}{3\pi\chi_G} \tag{16}$$

For the state 2, ν_2 is a complicated function of $(\chi_G \tan\vartheta)$ which, however, again does not essentially deviate from the course in the case of rectangular pressure surface for equal characteristic parameter.

The variation is represented in figure 11, the distribution of region of adhesion and sliding region in figure 12.

(d) Special Influences

The influence of the shape of the pressure surface on the course of the curves of sideslip $\nu = f(\chi,\vartheta)$ is essentially taken into consideration by means of the cornering characteristic parameters.

The influence of the type of pressure distribution is illustrated in figure 13 which shows curves from the figures for equal guiding characteristic parameters $\chi_E = \chi_P = \chi_g = 7.65$.

If the coefficient of adhesive friction μ_h between rubber and roadway lies above the coefficient of sliding friction μ_g, there result curves $\nu(\vartheta)$ such as those in figure 14 (for $\chi = 7.65$). For extraordinary increases of the adhesion friction $\left(\frac{\mu_h}{\mu_g} > 1\right)$, a maximum for $\nu = \frac{S}{\mu_g N}$ occurs. It is of great importance for an estimation of the danger of sideslip to note that the maximum cornering force S_{max} can only slightly exceed the skidding value $\mu_g N$ and must remain far below the limit of adhesiveness $\mu_h N$, particularly for large $\frac{\mu_h}{\mu_g}$. A rolling wheel tends to sideslip much sooner than could be expected from the adhesion friction on the wheel at rest.

4. CONCLUDING REMARK

The results are essentially in accordance with the course of the $S(\vartheta)$ curves found experimentally. The comparison must, above all, produce agreement for the guiding value (cornering power) K and the skidding resistance $\mu_g N$; since the correct pressure distribution and the value of μ_g are not known, this becomes an ambiguous task because the measurements will mostly include only $\vartheta < 30^\circ$. A method of evaluation will be given in a detailed publication in the "Deutschen Kraftfahrtforschung" which contains also the derivation of the above-mentioned results. Furthermore, the effects of additional stresses in transverse and circumferential direction are discussed there. Finally, it is shown there how the entire calculation results for sideslip may be transferred to rolling slip in case of circumferential forces (braking or accelerating). The angle of sideslip then is replaced by "slip," the guiding characteristic parameter by a "traction coefficient," and the guiding value by a "traction characteristic value."

Translated by Mary L. Mahler
National Advisory Committee
for Aeronautics

REFERENCES

1. Reynolds, O.: On Rolling-Friction. Philos. Transact. of the Royal Soc. of London, vol. 166, 1876, p. 155.

2. Fromm, H.: Berechnung des Schlupfes beim Rollen deformierbarer Scheiben. ZAMM, Bd. 7, 1927, p. 27; Schiene und Rad, Z. VDI, Bd. 72, 1928, p. 1899.

3. Martin, H.: Druckverteilung in der Berührungsfläche zwischen Reifen und Fahrbahn, Kraftfahrtechn. Forschungsarbeit des VDI, Heft 2; - ATZ., Bd. 39, 1936, p. 230.

4. Schuster, R., and Weichsler, P.: Der Kraftschluss zwischen Rad und Fahrbahn. ATZ, Bd. 38, 1935, p. 499.

5. Fromm, H.: Schwingungsvorgänge an der Lenkung von Kraftfahrzeugen. Verh. des 3. intern. Kongr. für technische Mechanik, Stockholm 1930, Teil III, p. 278.

6. Becker, G., Fromm, H., and Maruhn, H.: Schwingungen in Automobil-lenkungen. Verlag M. Krayn, Berlin 1931, p. 43.

7. Förster, B.: Versuche zur Feststellung des Haftvermögens von Personenwagen-Bereifungen. Deutsche Kraftfahrtforschung, Zwischenbericht Nr. 22.

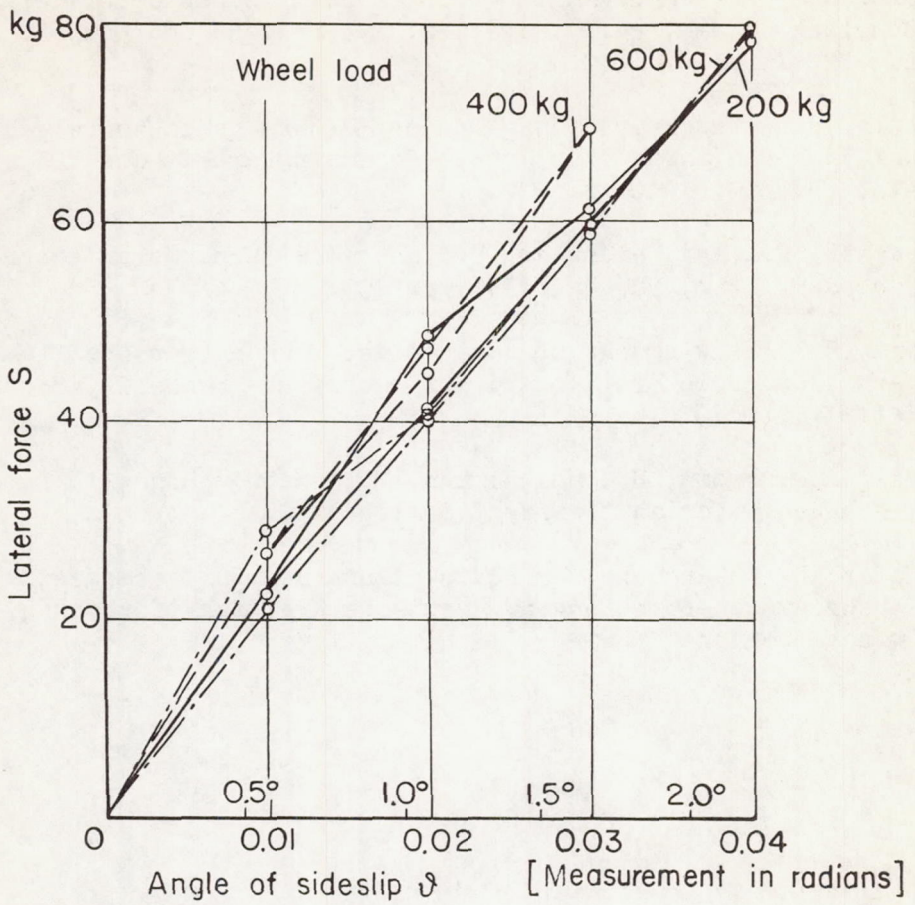

Figure 1.- Lateral force for small angles of sideslip according to tests (taken from "Oscillations in automobile-steering mechanisms (Shimmy)," authors: Gabriel Becker, Hans Fromm, Herbert Maruhn. Publishing house: M. Krayn, Technical Publishers, Berlin 1931).

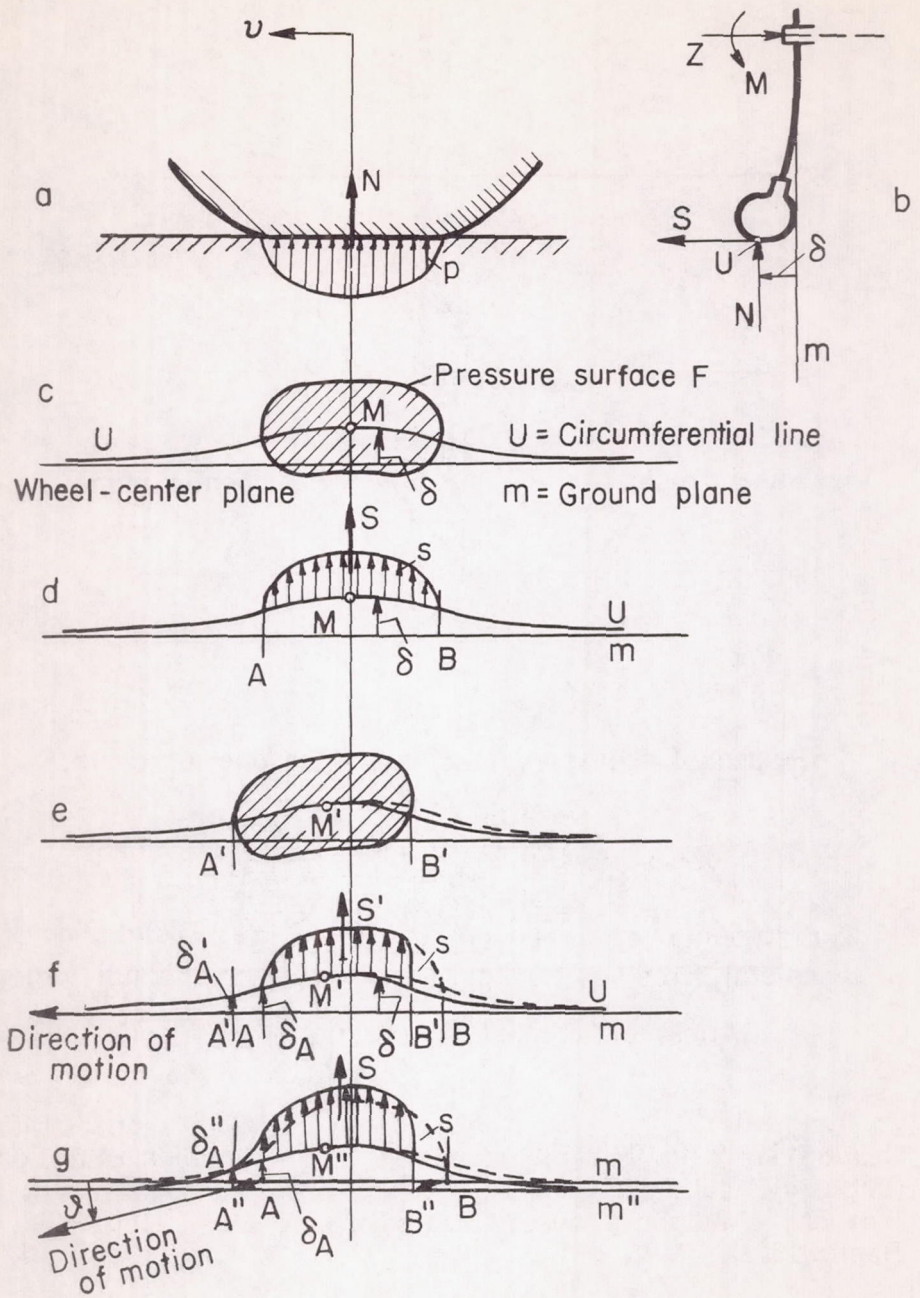

Figure 2(a-g).- Forming of the angle of sideslip.

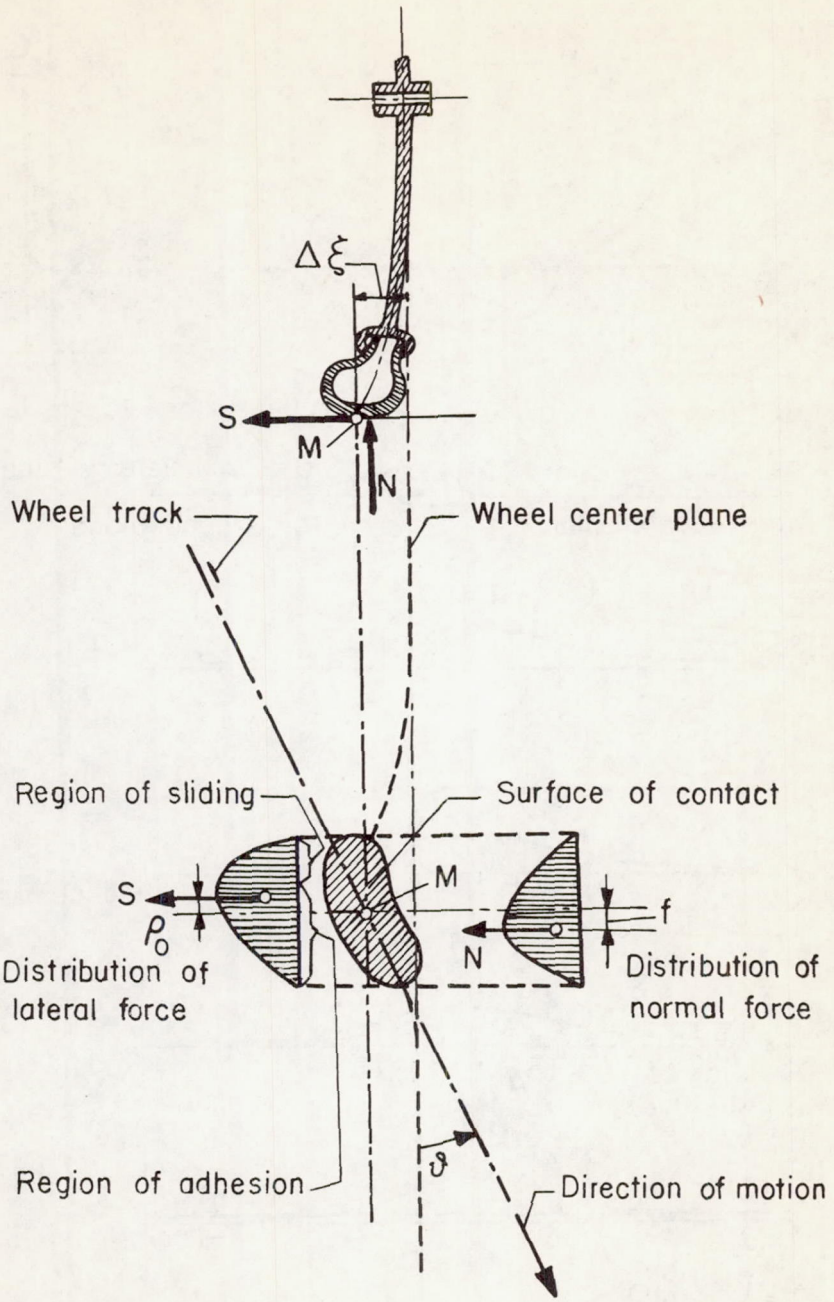

Figure 3.- Steady-state condition in sideslip (taken from "Oscillations in automobile-steering systems (Shimmy)," authors: Gabriel Becker, Hans Fromm, Herbert Maruhn. Publishing house: M. Krayn, Technical Publishers, Berlin 1931).

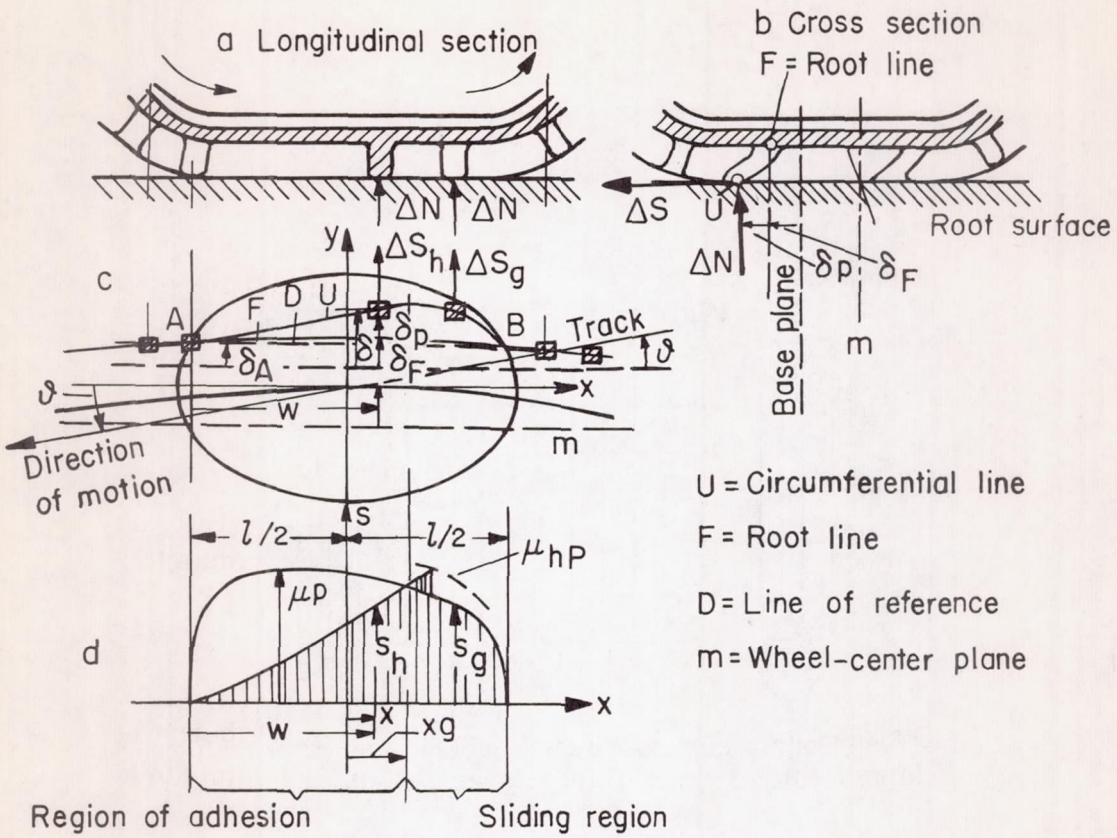

Figure 4(a-d).- Root line and deflection of the profile lugs.

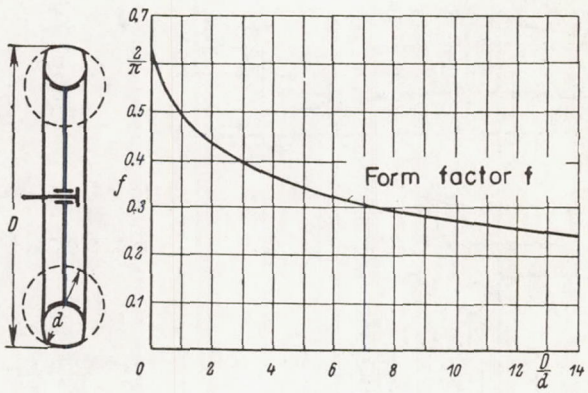

Figure 5.- Doubly curved running surface and its form factor for ellipsoidal or paraboloidal pressure distribution.

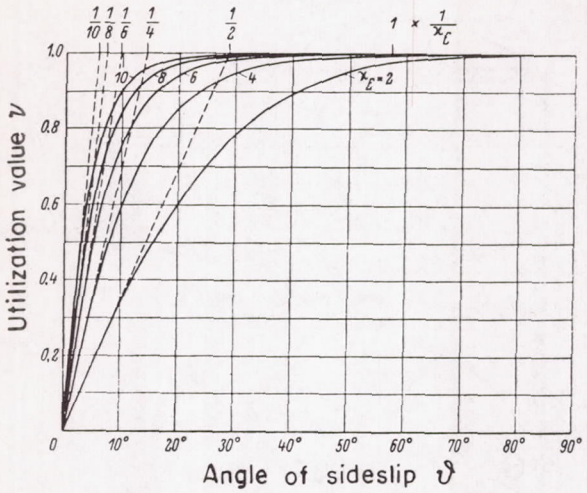

Figure 6.- Guiding-characteristic curves $\nu(\vartheta)$ for ellipsoidal pressure distribution.

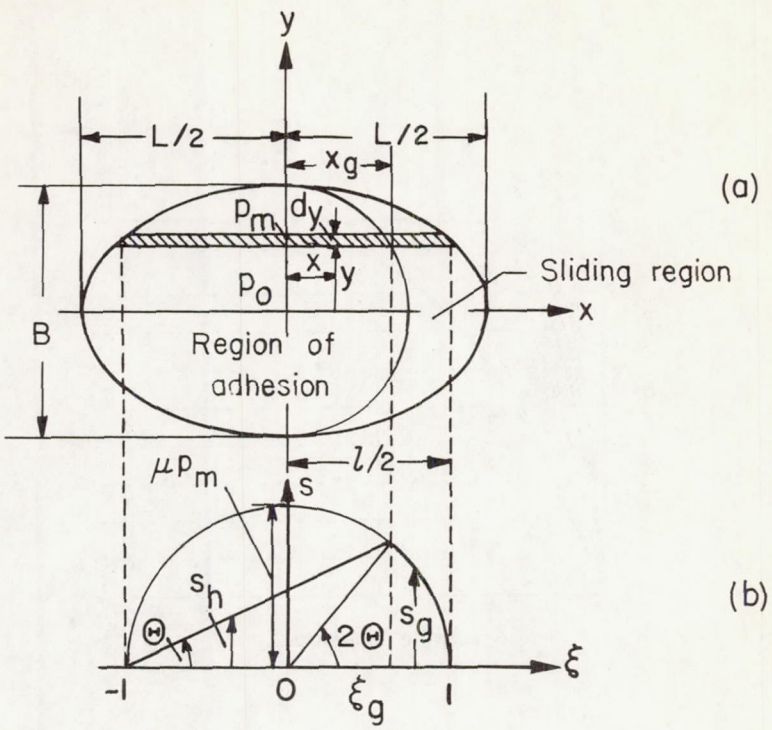

Figure 7.- Lateral stresses in an elliptic pressure surface for ellipsoidal pressure distribution.

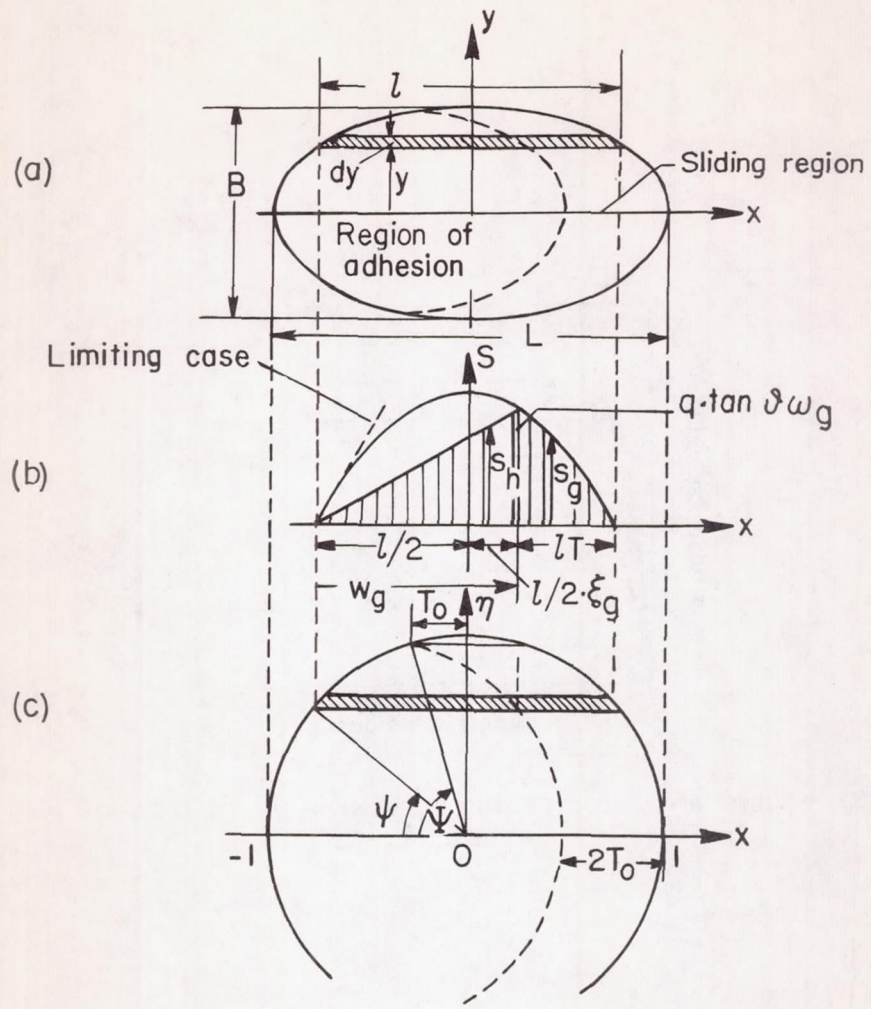

Figure 8(a-c).- Lateral stresses for paraboloidal pressure distribution.

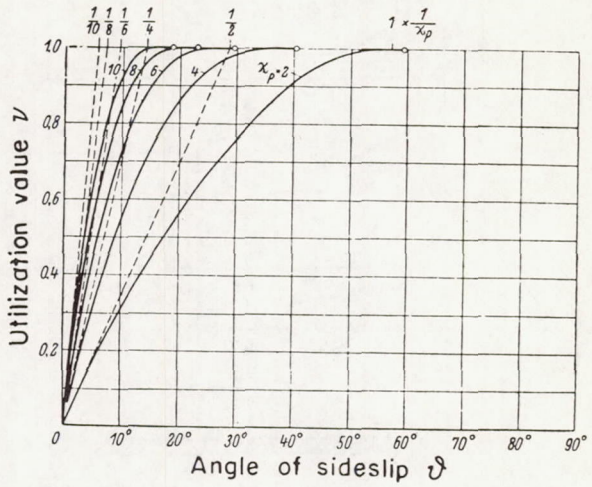

Figure 9.- Guiding-characteristic curves $\nu(\vartheta)$ for paraboloidal pressure distribution.

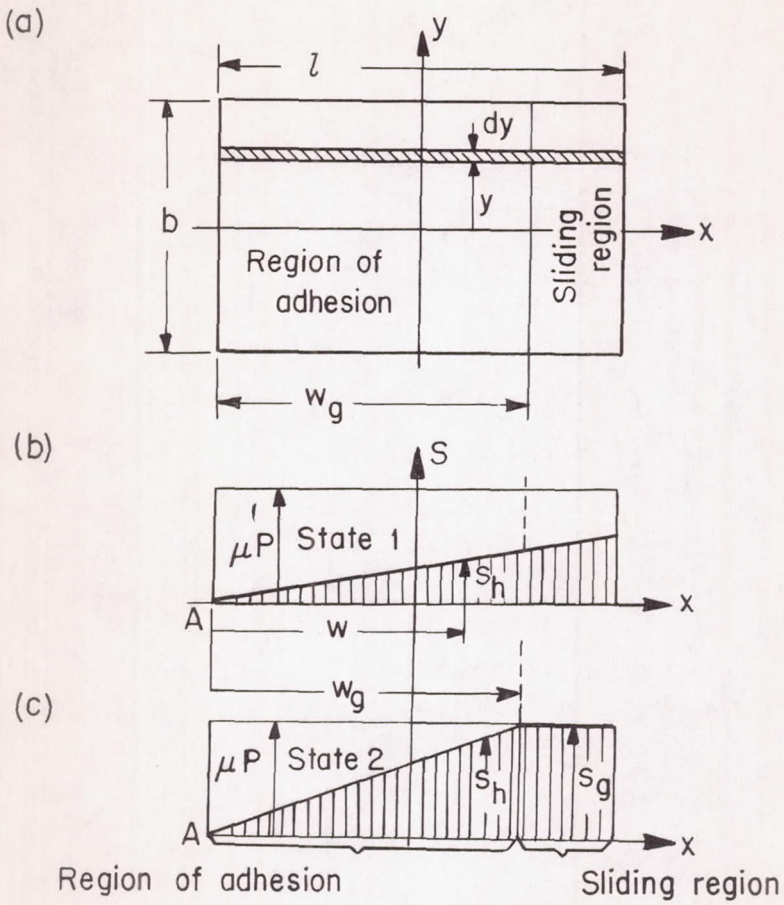

Figure 10(a-c).- Lateral stresses in a rectangular pressure surface for uniform pressure distribution.

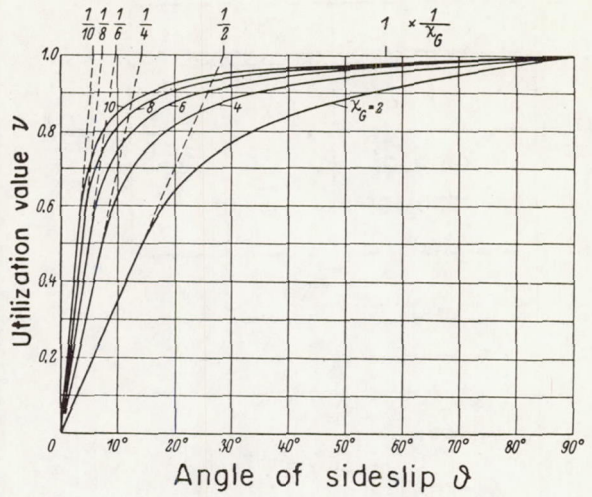

Figure 11.- Guiding-characteristic curves $\nu(\vartheta)$ for uniform pressure distribution.

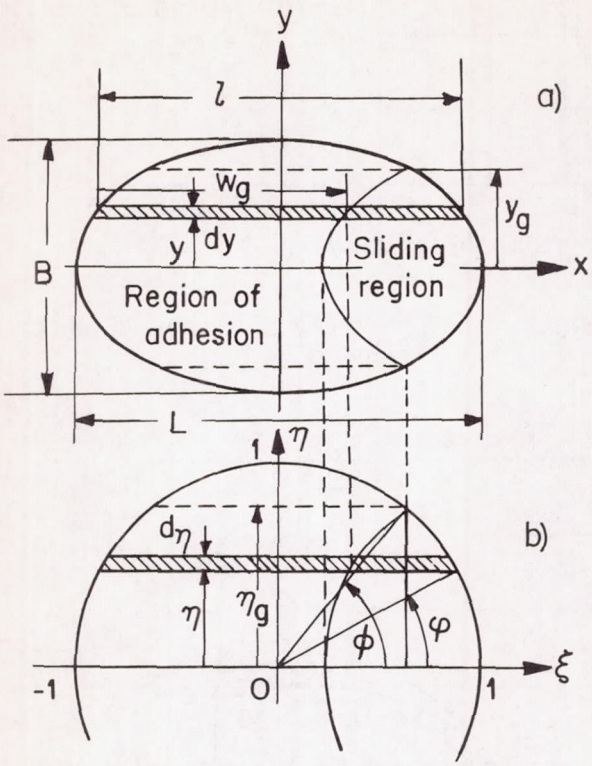

Figure 12(a,b).- Lateral stresses in an elliptic pressure surface for uniform pressure distribution.

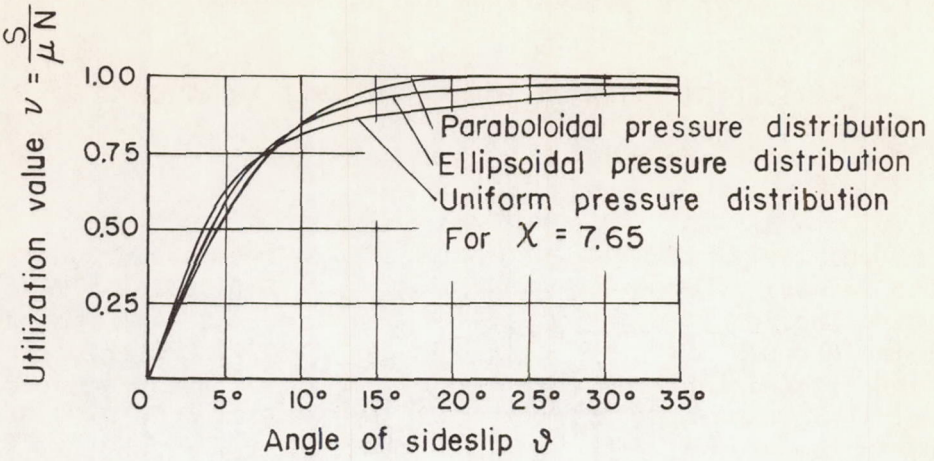

Figure 13.- Influence of the pressure distribution on the lateral-force curves.

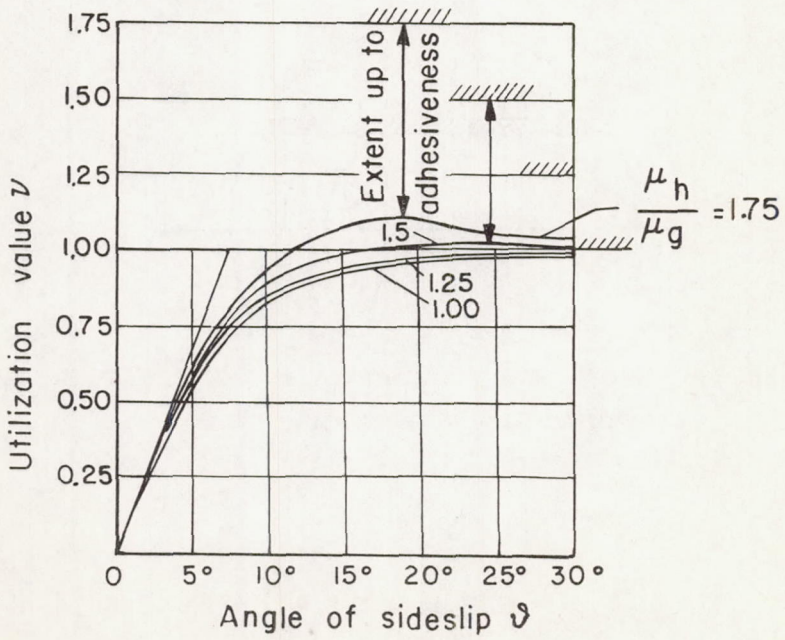

Figure 14.- Influence of extraordinarily increased adhesion-friction.

SUPPLEMENT FOR CLARIFICATION OF SEVERAL REMARKS IN THE DISCUSSION*

By B. v. Schlippe and R. Dietrich

1. DERIVATION OF THE FUNDAMENTAL EQUATION FROM TRACKING CONSIDERATIONS

The fundamental equation of motion of the foremost ground-contact point can be derived from the recognition that this point always travels along the direction taken by the forward part of the tire that does not contact the ground. This fact was observed also by Professor Fromm and can be interpreted geometrically as coincidence of the tangential inclination at the ground-contact point B in the forward free part of the tire and in the ground-contact region (see fig. 1).

The tangential inclination angle with respect to the wheel plane (R.E.) in the forward region at the point B has the value cz. The tracking condition resulting from the sum of the angles reads (see fig. 1):

$$\frac{dy}{ds} + cz = \varphi$$

If the relation valid between z and y

$$y = z + x + h\varphi$$

or

$$z = y - x - h\varphi$$

is introduced, we obtain the fundamental equation for z or y

$$\frac{dz}{ds} + cz = \varphi - h\frac{d\varphi}{ds} - \frac{dx}{ds}$$

or

$$\frac{dy}{ds} + cy = \varphi(1 + ch) + cx$$

---

*"Nachtrag zur Klaerung einiger Diskussionsbemerkungen," Bericht 140 der Lilienthal-Gesellschaft, pp. 63-66. (Supplement to lectures by v. Schlippe, p. 126 and Dietrich p. 148 of this same volume.)

2. ORDER OF MAGNITUDE OF THE MOMENT IN A YAWED WHEEL

In order to give some idea of the order of magnitude of the elastic moment, which is caused by the finite drawing out of the ground-contact region, there will be given measured values made in tests on a yawed wheel.

The following asymptotic values of the lateral force and of the moment were obtained for a 260 × 85 mm balloon tire with a 180 kg load and 2.5 atm (gage) tire pressure:

$$P_\infty = 690 \text{ kg/rad} \qquad M_\infty = 2270 \text{ cmkg/rad}$$

If the ground-contact region were drawn together to a loading point, it would have to lie behind the center of the ground-contact area by a distance of

$$q = \frac{2270}{690} = 3.3 \text{ cm} = \frac{1}{4} r$$

Since this value is significant in comparison with the usual size of lead or trail, the concept of a loading point must be discarded.

3. KINEMATIC SHIMMY

The experimentally established fact that the wheel is capable of shimmying at a trail $q = 0$, even at the lowest speeds (theoretically at $v = 0$), is due to the elastic moment created by the finite drawing out of the ground-contact region. The equation of motion for this phenomenon of kinematic shimmy is formed by taking v and q in the general equation of motion equal to zero (section B, eq. (10)). Thus:

$$M - \frac{\chi_2}{\alpha} \varphi' = 0$$

We will again consider the special case of oscillations with a constant amplitude, that is for $\lambda = i\alpha$. The following equations are derived:

$$\chi_2 = -\frac{\alpha(1 + ch)}{c^2 + \alpha^2} U_2(2 - K_1)$$

$$0 = 2h \frac{1 + ch}{c^2 + \alpha^2}(2c - K_2)$$

or, in more detail,

$$\chi_2 = U_2\alpha \frac{(1 + ch)}{c^2 + \alpha^2}\left(\cos \alpha 2h + \frac{c}{\alpha} \sin \alpha 2h - 1\right)$$

$$2h + \frac{1 + ch}{c^2 + \alpha^2}(c \cos \alpha 2h - \alpha \sin \alpha 2h - c) = 0$$

The first equation gives the necessary damping constant and the second one determines the path frequency α.

The following experimental values were obtained with a 260 × 85 mm test tire at a load of 180 kg and 2.5 atm (gage) pressure.

$$c = 0.1 \text{ cm}^{-1}$$

$$h = 4.5 \text{ cm}$$

$$U_1 = 22.5 \text{ kg cm}^{-1}$$

$$U_2 = 325 \text{ kg}$$

With these values substituted in the second equation, the path frequency becomes:

$$\alpha = 0.108 \text{ cm}^{-1}$$

that is, the wave length

$$S = \frac{2\pi}{\alpha} = 58 \text{ cm}$$

This value was confirmed by a direct shimmy test. The damping constant, obtained from the first equation, is

$$\chi_2 = 775 \text{ kg cm/rad}$$

a value that definitely falls within the order of magnitude of the value of 900 kg cm/rad which was obtained from a deflection test with the loaded wheel at rest.

4. DAMPING OF OSCILLATING WHEELS THAT ROLL AT THE SAME TIME

Symbols

A(cm kg/sec)	damping work during one period
E(kg/cm^2)	elastic modulus
P(kg)	periodic wheel load
T(sec)	period of oscillation
a_n	Fourier coefficients
b_n	Fourier coefficients
c_n	coefficients
f	function of $\omega t + \varphi$
g	function of λt
p	constant
n	integers
t(sec)	time
y(cm)	oscillation displacement of the force P
ϵ	elastic extension
φ(rad)	circumferential coordinate
λ(1/sec)	frequency of the vertical oscillation
ω(1/sec)	angular velocity of the rolling wheel
σ(kg/cm^2)	normal stress
τ(kg/cm^2)	shear stress
Γ(kg sec/cm^2)	damping modulus

Object of the Discussion

An oscillation test was made with a wheel at rest in order to determine the damping constant χ_2 for shimmy, and χ_2 was found to equal 900 cmkg/rad. In the opinion of some, this test is inconclusive because tire damping varies with the rolling speed. We claim, however, that the material damping is independent of the rolling speed. Only the additional friction between the edges of the ground-contact region and the rolling surface is subject to change. On an adhesive surface (sandpaper, in our case) this factor is very much reduced, so that this type of test is justified for the purpose of approximation.

Evidence that Damping is Independent of the Rolling Speed

A loaded wheel rolls at an angular speed ω and oscillates perpendicularly to the ground with a circular frequency λ (fig. 2).

It will be shown next that the damping work A (and thus χ_2) for one period

$$T = \frac{2\pi}{\lambda} \tag{1}$$

is completely independent of ω.

Aside from the space-fixed system of coordinates x,y, we will also introduce a wheel-fixed system a, b that rotates during the time t by ωt as compared to x, y. Any section cd through the tire is to be found at the same time at $\omega t + \varphi$, where φ is the circumferential coordinate.

In rolling with a constant or a changeable load, the material in each section is deformed, thus consuming energy which is transformed partly into ground resistance and partly into oscillation damping of the force P (in the direction of y). Each element is subject to a complicated stress condition (fig. 3) which represents a function of ωt, as well as λt.

In order to determine the component of damping due only to the force P or rather to prove that it is independent of ω, we must take the damping work of P into consideration. It is:

$$A = \int P \, dy = \int_0^T P\dot{y} \, dt \tag{2}$$

where y is the displacement coordinate of the oscillation (perpendicular to the rolling direction). The force P results from the equilibrium of inner forces or stresses. For this purpose we have sketched a section of the circumference in which the effect of the normal and shear stresses are shown (fig. 4).

The equilibrium is expressed by

$$P = \int_0^{2\pi} \left[\sigma \cos(\omega t + \varphi) + \tau \sin(\omega t + \varphi)\right] d\varphi \tag{3}$$

where for brevity all tire constants, such as wall thickness, etc. are omitted or taken equal to one. In the beginning we will consider only the component of normal stress:

$$P_\sigma = \int_0^{2\pi} \sigma \cos(\omega t + \varphi) d\varphi \tag{4}$$

The second component P_τ is analogous.

The stress σ consists of both an elastic and a damping component,

$$\sigma = E\epsilon + \Gamma\dot{\epsilon} \tag{5}$$

where ϵ is the elastic extension, E the elastic modulus, and Γ the damping modulus. (It seems impossible to calculate the amount of damping unless we assume that it is proportional to the speed). The only thing that we need to know about the deformation ϵ is that it is a periodic function of the angle $\omega t + \varphi$ and λt, and, furthermore, that it is proportional to both functions. The general formulation is in the form of a product:

$$\epsilon = f(\omega t + \varphi)g(\lambda t) = f(\omega t + 2\pi\varphi)g(\lambda t + 2\pi) \tag{6}$$

For example, when $t = 0$, it has the form shown in figure 5(a). Although it can also vary, the derivation is still valid (fig. 5).

From equation (6) it follows that:

$$\dot{\epsilon} = \frac{df(\omega t + \varphi)}{d(\omega t + \varphi)} \omega g(\lambda t) + f(\omega t + \varphi) \frac{dg(\lambda t)}{dt}$$

With

$$\frac{df(\omega t + \varphi)}{d\varphi} = \frac{df(\omega t + \varphi)}{d(\omega t + \varphi)}$$

then

$$\dot{\epsilon} = \frac{df}{d\varphi}\omega g + f\frac{dg}{dt} \tag{7}$$

If equations (6) and (7) are inserted in (5) we obtain:

$$\sigma = Efg + \Gamma\left(\frac{df}{d\varphi}\omega g + f\frac{dg}{dt}\right) \tag{8}$$

A Fourier series can be substituted for the function $f(\omega t + \varphi)$

$$f(\omega t + \varphi) = \sum a_n \cos n(\omega t + \varphi) + \sum b_n \sin n(\omega t + \varphi) \tag{9}$$

where a_n and b_n are the Fourier coefficients. Thus equation (8) becomes:

$$\sigma = Eg\sum a_n \cos n(\omega t + \varphi) - \Gamma\omega g\sum a_n n \sin n(\omega t + \varphi) +$$

$$Eg\sum b_n \sin n(\omega t + \varphi) + \Gamma\omega g\sum b_n n \cos n(\omega t + \varphi) +$$

$$\Gamma\frac{dg}{dt}\sum a_n \cos n(\omega t + \varphi) + \Gamma\frac{dg}{dt}\sum b_n \sin n(\omega t + \varphi) \tag{10}$$

Inserted in equation (4), this gives:

$$P_\sigma = Eg\int_0^{2\pi} \cos(\omega t + \varphi)\left[\sum a_n \cos n(\omega t + \varphi) + \sum b_n \sin n(\omega t + \varphi)\right]d\varphi -$$

$$\Gamma\omega g\int_0^{2\pi} \cos(\omega t + \varphi)\left[\sum a_n n \sin n(\omega t + \varphi) - \sum b_n \cos n(\omega t + \varphi)\right]d\varphi +$$

$$\Gamma\frac{dg}{dt}\int_0^{2\pi} \cos(\omega t + \varphi)\left[\sum a_n \cos n(\omega t + \varphi) + \sum b_n \sin n(\omega t + \varphi)\right]d\varphi$$

The integration, carried out, results in

$$P_\sigma = E\pi a_1 g(\lambda t) + \pi a_1 \frac{dg(\lambda t)}{dt} \tag{11}$$

The contribution of the shear stresses can be expressed by a similar equation and the sum of both gives the force P in the following form:

$$P_\sigma = pEg(\lambda t) + p\Gamma \frac{dg(\lambda t)}{dt} \tag{12}$$

where p is a constant.

Equation (12) is a function independent of ω, whose form is like that of equation (6).

In equation (2) there appears the time derivative of the oscillation displacement $\dot{y}$ which is also a function of λt. Between y and ϵ there exists a geometrical relation. Usually it is linear, that is

$$y \sim \epsilon$$

Since the ground-contact area increases when the wheel is lowered, the linear relation will not persist. Therefore we will use the expanded formulation of a power series

$$y \sim \sum c_n \epsilon^n$$

with c_n as coefficients, which can, for example, have the variation shown in figure 6.

The quantity y must naturally be independent of $(\omega t + \varphi)$ because it is a function of not one but all ϵ-values, so that it must be expressed only by the component $g(\lambda t)$ of the ϵ-function in equation (6). Thus:

$$y = \sum c_n g^n(\lambda t) \tag{13}$$

and

$$\dot{y} = \sum c_n n g^{n-1} \dot{g} \tag{14}$$

If equations (12) and (14) are inserted in equation (2), we obtain:

$$A = pE \int_0^{2\pi} g \sum c_n n g^{n-1} \dot{g}\, dt + p\Gamma \int_0^{2\pi} \dot{g} \sum c_n n g^{n-1} \dot{g}\, dt \tag{15}$$

The elastic component involving E cancels out as was to be expected. This can be proven as follows:

$$\int_0^{2\pi} g \sum c_n n g^{n-1} \dot{g}\, dt = \sum c_n n \int_0^{2\pi} g^n \dot{g}\, dt$$

By integration by parts we obtain:

$$\int_0^{2\pi} g^n \dot{g}\, dt = g^{n+1} \Big|_0^{2\pi} - n \int_0^{2\pi} g^n \dot{g}\, dt$$

According to the hypothesis

$$g(\lambda t) = g(\lambda t + 2\pi)$$

it follows that

$$g^{n+1} \Big|_0^{2\pi} = 0$$

and that

$$(n + 1) \int_0^{2\pi} g^n \dot{g}\, dt = 0$$

There remains thus only the damping component

$$A = p\Gamma \sum c_n n \int_0^{2\pi} g^{n-1} \dot{g}^2\, dt \qquad (16)$$

This equation shows that damping work is definitely independent of the rolling speed ω because, aside from the constant magnitudes, there appear only the functions of λt, namely $g(\lambda t)$ and $\dot{g}(\lambda t)$; thus the proof is furnished in an entirely general form.

*Translated and edited for the AAF by:
Charles A. Meyer & Company
25 Vanderbilt Avenue
New York 17, New York
July 7, 1947 (ATI No. 18920)

---

*Note: In order to provide terminology consistent with other papers of this series, this translation has been reworded in many places by the NACA reviewer.

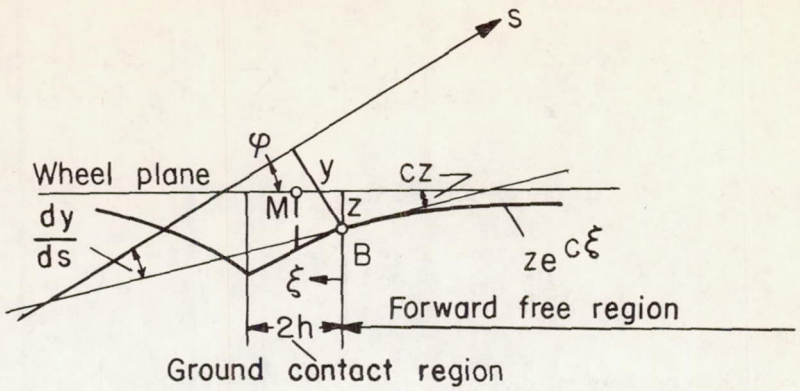

Figure 1

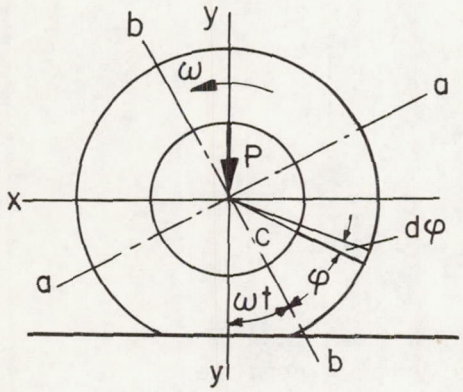

Figure 2

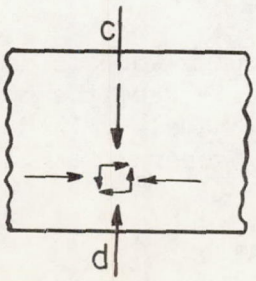

Section cd

Figure 3

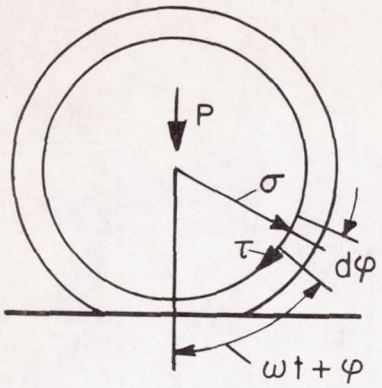

Figure 4

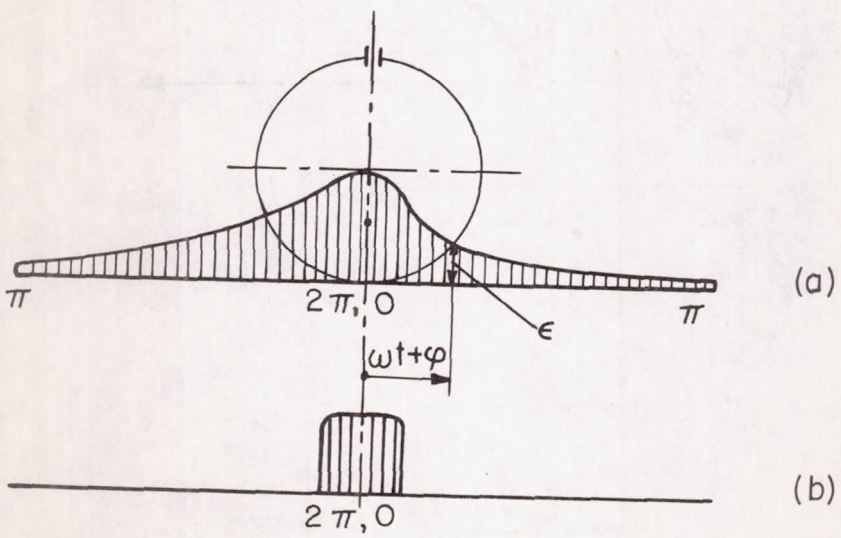

Figure 5

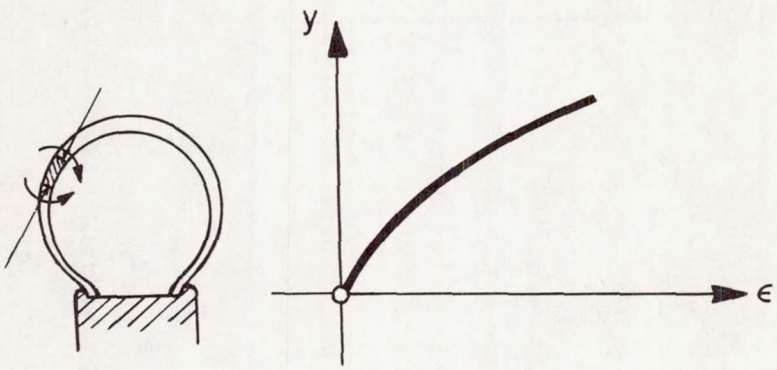

Figure 6

OSCILLATION DAMPING ON THE ROLLING WHEEL*[1]

By H. Fromm

My assertion that the oscillation damping in the tires on the rolling wheel decreases with increasing speed of motion was contradicted by Mr. von Schlippe; he substantiated his opinion subsequently by a calculation. One can show without entering into the details of this calculation that his result is based on the assumption of Newtonian stress damping (that is, stress damping proportional to the velocity). Stress damping due to imperfect elasticity (hysteresis), in contrast, is above all independent of the velocity and, hence, follows my assertion that the oscillation damping on the rolling wheel decreases with increasing speed of the vehicle. Proof, in the most simplified form, may be presented as follows:

1. Kinematics: The deformation of an elastic wheel on a rigid roadway (see fig. 1(a)) is

$$y = y_0 - \frac{x^2}{2r}$$

The time rate of deformation therefore is

$$\dot{y} = \dot{y}_0 - \frac{x}{r}\frac{dx}{dt} = \dot{y}_0 - \omega x$$

when $\frac{dx}{dx} = r\omega$ signifies the speed of motion and $\dot{y}_0$ the vertical velocity of the wheel center. (See fig. 1(b).) $\dot{y}_0$ is the oscillation velocity of the vertical oscillation to be considered.

2. Loads: In case of perfect elasticity, the pressure p_v is symmetrically with y distributed over the pressure surface F (fig. 1(c)) and results in a wheel pressure force $P_v = \int p_v \, dF$. In case of imperfect elasticity, p becomes (in first approximation) $p = p_v + g(\dot{y})$, thus unsymmetrical (see fig. 1(d)); the wheel pressure force is $P = P_v + \int g(\dot{y})dF$ and lies ahead of the center of the pressure surface.

---

*"Schwingungsdämpfung am rollenden Rade," Bericht 140 der Lilienthal-Gesellschaft, pp. 66-67.

[1]Sent in by Prof. Fromm as a reply to the supplement of Messrs. von Schlippe and Dietrich, p. 217.

3. The damping force is therefore:

$$P_D = P - P_v = \int g(\dot{y})dF = \int g(\dot{y}_0 - \omega x)dF$$

Let us assume for the damping law: $g(\dot{y}) = \pm k|\dot{y}|^n$ for $\dot{y} \gtrless 0$. Then there is, if one equates in the case of a rectangular pressure surface $dF = b\,dx$:

$$\text{for } |\dot{y}_0| \leqq \omega l: \quad P_D = kb\left[\int_{-l}^{\dot{y}_0/\omega} |\dot{y}_0 - \omega x|^n dx - \int_{\dot{y}_0/\omega}^{l} |\dot{y}_0 - \omega x|^n dx\right]$$

$$= \frac{kb}{\omega(n+1)}\left[(\omega l + \dot{y}_0)^{n+1} - (\omega l - \dot{y}_0)^{n+1}\right]$$

$$\text{for } |\dot{y}_0| \geqq \omega l: \quad P_D = kb\int_{-l}^{l} (\dot{y}_0 - \omega x)^n dx$$

$$= \frac{kb}{\omega(n+1)}\left[|\dot{y}_0 + \omega l|^{n+1} - |\dot{y}_0 - \omega l|^{n+1}\right]$$

4. The evaluation for three different damping laws (n = 0, 1, 2) yields (with $2bl = F$ = pressure area):

For damping law according to:	Coulomb n = 0	Newton n = 1	Quadratic n = 2
for $\dot{y}_0 \leqq \omega l$: PD =	$kF\frac{\dot{y}_0}{\omega l}$	$kF\dot{y}_0$	$kF\frac{\dot{y}_0}{\omega l}\left[(\omega l)^2 + \frac{\dot{y}_0^2}{3}\right]$
for $\dot{y}_0 \geqq \omega l$: PD =	kFl	$kF\dot{y}_0$	$kF\left[\dot{y}_0^2 + \frac{(\omega l)^2}{3}\right]$

For sinusoidal oscillations

$$s = a\sin(\alpha t) \quad \text{there is} \quad \dot{y}_0 = \frac{ds}{dt} = a\alpha\cos(\alpha t)$$

Thus for small oscillation, $\alpha a < \omega l$ becomes

$$P_D = \left| \begin{matrix} kF \frac{\alpha a}{\omega l} \cdot \\ \cdot \cos(\alpha t) \end{matrix} \right| \left| \begin{matrix} kF\alpha a \cdot \\ \cdot \cos(\alpha t) \end{matrix} \right| kF\alpha a \cdot \omega l \cos(\alpha t)$$

5. Conclusions: In case of damping by imperfect elasticity (hysteresis) of the springy material for which Coulomb's law holds true most closely (with $k = k_0 a$, particularly for small oscillations, proportional to the amplitude but independent of the frequency) there results the noteworthy relation that nevertheless on the rolling wheel the damping force

$$P_D = k_0 F \frac{a^2}{l} \frac{\alpha}{\omega} \cos(\alpha t)$$

is to be put proportional to the oscillation frequency α, but also inversely proportional to the rotational frequency of the wheel ω, thus proportional to the ratio $\frac{\alpha}{\omega}$. Therewith the influence of the speed of motion on the oscillation damping on the rolling wheel appears in the manner I described in my remark in the discussion.[2]

Newtonian damping (n = 1) in itself does not result in an influence of the speed of motion as Von Schlippe stressed. However, in material damping, a hysteresis effect is probably always of some importance, if not predominant, so that the damping in the sense of Coulomb's law decreases with increasing speed of motion. In addition, the ground friction is essentially according to Coulomb.

The great importance of introducing the correct damping law is shown by the example of quadratic damping (n = 2). For this damping, the damping force even would increase; however, this law probably widely differs from actual conditions.

6. Correction: If the first approximation under 2 is replaced by the correct influences on the damping force, the result becomes still more complicated. The essential finding that the form of the damping law is of great influence and that, in particular, the oscillation damping is a function of the rolling speed is not affected thereby.

---

[2]See Fromm "Brief Report on the History of the Theory of Wheel Shimmy," last paragraph of Section A on p. 186 of the present report.

Reply of Messrs, B. von Schlippe and R. Dietrich

to the Above Contribution[3]

Our attitude regarding the statements of Prof. Fromm on the dependence of damping on the rolling speed is as follows:

Basically, we have become convinced that Prof. Fromm is essentially right, that therefore in the case of the introduction of Coulomb's law a relationship as described by him exists; we found this fact confirmed by very carefully repeated tests. We think, however, that a division into the two regions indicated by Prof. Fromm, $\dot{y}_0 < \omega l$ and $\dot{y}_0 > \omega l$ does not exist but that the damping further increases with decreasing ω. We believe we can give the following reasons for the deviation of our calculation results from Prof. Fromm's:

Prof. Fromm considers as the damping part only the tire-impression length; actually this does not hold true since the pneumatic tire is deformed long before contact with the ground and the unloading also lasts for a long time after leaving the ground. Furthermore, there is still some uncertainty involved in assuming Coulomb's law since actually the material damping is, although not proportional to the speed, proportional to the amplitude whereas the friction damping does not show any dependence on the deflection.

Translated by Mary L. Mahler
National Advisory Committee
for Aeronautics

---

[3]With this reply, as the final remark of the lecturers, the discussion for the present report will be discontinued although Prof. Fromm and Mr. von Schlippe told us that a factually complete agreement has not yet been reached.

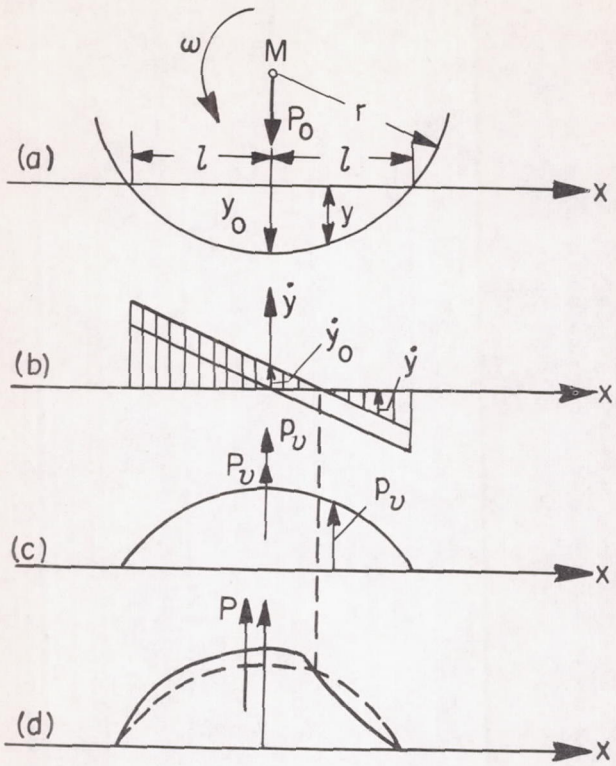

Figure 1